Springer Geography

Balai Chandra Das
Sandipan Ghosh
Aznarul Islam
Md Ismail *Editors*

Neo-Thinking on Ganges–Brahmaputra Basin Geomorphology

Springer

Springer Geography

The Springer Geography series seeks to publish a broad portfolio of scientific books, aiming at researchers, students, and everyone interested in geographical research. The series includes peer-reviewed monographs, edited volumes, textbooks, and conference proceedings. It covers the entire research area of geography including, but not limited to, Economic Geography, Physical Geography, Quantitative Geography, and Regional/Urban Planning.

More information about this series at http://www.springer.com/series/10180

Balai Chandra Das · Sandipan Ghosh
Aznarul Islam · Md Ismail
Editors

Neo-Thinking on Ganges–Brahmaputra Basin Geomorphology

Springer

Editors
Balai Chandra Das
Department of Geography
Krishnagar Government College
Krishnagar
India

Aznarul Islam
Department of Geography
Barasat Government College
Barasat
India

Sandipan Ghosh
Department of Geography
Chandrapur College
Bardhaman
India

Md Ismail
Kalinagar Mahavidyalaya
Kalinagar
India

ISSN 2194-315X ISSN 2194-3168 (electronic)
Springer Geography
ISBN 978-3-319-26442-4 ISBN 978-3-319-26443-1 (eBook)
DOI 10.1007/978-3-319-26443-1

Library of Congress Control Number: 2015955883

Printed on acid-free paper

This Springer imprint is published by SpringerNature
The registered company is Springer International Publishing AG Switzerland

Our oblation
To our teacher
Professor Sandip Kumar Chaudhury

Foreword

Only having a common interest can make more than one person walk together; for the editors of this volume it was love for the physical geography of the Ganga–Brahmaputra Basin where they live. Even being personally unknown to each other, we came closer to organize valuable contributions of different scholars who were also in love with the landscape, ecology, and environment of the region concerned. Being likeminded we felt the problems of scholars who devoted themselves to studying the interaction between landforms and the geomorphic processes that shaped them and the grief of people having no scholarly volume containing all these informations regarding the Ganga–Brahmaputra Basin within only two cover pages. And we tried to materialise it with the existence of this volume.

The initiative came from Aznarul Islam, the only person who is personally known to all three editors and perhaps to every contributing scholar as well. During mid-2014, mail inviting scholarly works on the concerned topic was circulated and the responses gathered up to mid-2015 totalled more than 50. It was a great task to select 11 and we did it out of all of these. We acknowledge spontaneous responses from competent scholars all over India. We are also grateful to Springer for its association with us in giving its most reputed pages for these valuable research works. We hope the volume will be a worthy asset to students and researchers in the field.

July 2015

Balai Chandra Das
Sandipan Ghosh
Aznarul Islam
Md Ismail

Preface

Neo-Thinking on Geomorphology of the Ganges–Brahmaputra Basin is not in a true sense the geomorphology of the Ganges–Brahmaputra Basin but the study of sample forms and processes and events operating in this huge basin through the newer lorgnette.

Chapter 1 deals with the cause–effect relationship between controlling the variable climate and adjustable variables of the alluvial stratigraphy (Charlton 2008) of the Damodar River Basin of West Bengal, a subsystem of the Ganges–Brahmaputra system as tools for inference about the controlling variables of climate of the past geological epoch. Chapter 2 set its specs over typical forms of badlands of Bankura district of West Bengal and the processes responsible for their origin.

Fundamental theoretical bases are the backbone of the study of geomorphology as with all natural sciences. Chapters 3–5 are newer contributions to the theoretical base of fluvial geomorphology. River channel shapes are measured and formulated from different angles. Channel asymmetry is one such measure which was formulated and studied as a self-sufficient topic in fluvial geomorphology by Knighton (1981). But no knowledge in the world within the limited wisdom of mankind is final and so a newer avenue of knowledge opens that is nearer to the ultimate truth. Chapter 3 opens a newer pane to analyse the cross-sectional asymmetry of river channel. Different channel dimensions along with geomatics create hybrid tools in the study of fluvial geomorphic study. Chapter 4 categorizes alluvial channel reaches using these hybrid tools. Epitomizing His creatures is an instinct in human beings and scientists do it for better understanding His forms and processes. Chapter 5 tries to set His unmatchable unique forms into some gathering of geometric shapes which may knock on the newer door of geomorphic, hydraulics, and hydrologic studies.

The most influential external controlling variable interfering with fluvial forms and processes is humans. Through arrogant and callous attitudes towards land use, humans deform and disturb His pure, orderly, esthetic fluvial forms and processes which in turn conflict with human activities. Chapters 6 and 7 are concerned with the interaction between humans and rivers. In Chap. 6 longitudinal disconnection

on road–stream crossings endorses significant changes on in-stream fluvial processes, for example, in-stream bar dynamics, thalweg wandering, and channel avulsion. These in turn impose threats to the bridge stability associated with severe bank erosion. Flood makes deltas possible. Therefore deltas and floods are inseparable no matter what. But when humans perceive it as a hazard, it does matter. Why and how a natural phenomenon became a hazard is a matter of serious concern for today's scientists. But Chap. 7 saw the phenomenon and its causes through the newer lorgnette of victims.

Not only surface water but also subsurface water plays an influential role in earth surface forms and processes. That is why Chaps. 8 and 9 are concerned with groundwater. Applying established methods devised by Thornthwaite and Mather, the water balance of a microregion of this basin is studied in Chap. 8. Chapter 9 opens another newer pane raising the question of whether a dug-well water level can be treated as a groundwater level.

Applied geomorphology perhaps reaches the ultimate as it deals with the use of geomorphological knowledge with the goal of human wellbeing. Chapters 10 and 11 shed a newer spectrum of light on the mining of energy and water and its consequences.

Neo-Thinking on Geomorphology of the Ganges–Brahmaputra Basin has a diverse concern within the sphere of geomorphology ranging from insight into the fundamentals of river science, geology, forms and processes, groundwater, and ecology. Therefore the volume is a useful tool for geologists, geographers, hydrologists, landscape-ecologists, environmentalists, engineers, planners, and policy makers as well.

Balai Chandra Das
Sandipan Ghosh
Aznarul Islam
Md Ismail

References

Charlton R (2008) Fundamentals of fluvial geomorphology, Rutledge, New York, pp 4–7
Knighton AD (1981) Asymmetry of river channel cross-sections: Part I. Quantitative indices. Earth Surf Proc Land 6:581–588

Contents

About the Editors

Balai Chandra Das born in 1970, he began teaching geography at Acharya Prafulla Chandra College, New Barrackpore, North 24 Parganas. Thereafter he joined WBES and served Darjeeling Government College and Krishnagar Govt. College of West Bengal gathering 20 years of teaching experience in the schools at the under-graduate and post-graduate levels. After earning his bachelor's degree (1992) and master's degree (1994) in geography from the University of Burdwan he was awarded his PhD degree in geography from the University of Calcutta. Dr. Das has published about 20 research articles in national and international journals, proceedings, and edited volumes. He has reviewed manuscripts for the *International Earth Science Journal*. At present he is passing his hours with students and rivers and lakes.

Sandipan Ghosh is an Applied Geographer with post-graduate and M.Phil. degrees in geography from The University of Burdwan. He has published more than 25 international and national research papers in various renowned geography and geoscience journals. He has authored a book entitled *Flood Hydrology and Risk Assessment: Flood Study in a Dam-Controlled River of India.* He is one of editors of the *Asian Journal of Spatial Science* (published by the Geographical Society, Dibrugarh University). Alongside he has performed as a reviewer of many international geoscience journals of Taylor & Francis, Springer, and the International Water Association (IWM). Mr. Ghosh is a lifetime member of The International Association of Hydrological Sciences (IAHS), Eastern Geographical Society (EGS), and Indian Geographical Foundation (IGF).

His principal research fields are various dimensions of fluvial geomorphology, flood geomorphology, Quaternary geology, and laterite study. Currently he has worked on the gully geomorphology and soil erosion on the lateritic terrain of West Bengal and the Quaternary geology and active tectonics of the Lower Damodar Basin, West Bengal. At present he is an Assistant Professor at the Department of Geography, Chandrapur College, Bardhaman.

Aznarul Islam is an Applied Fluvial Geomorphologist with his M.Sc. degree in geography from Kalyani University, West Bengal and MPhil in geography from the University of Burdwan, West Bengal. He is currently engaged as an Assistant Professor (WBES) in the Department of Geography, Barasat Government College, West Bengal. Previously he was engaged in teaching and research at the Department of Geography, Aliah University, Kolkata. Mr. Islam has already published 22 research papers in different journals, proceedings, and edited volumes of national and international repute. He has presented papers in more than 15 national and international seminars and conferences. In addition he has also delivered several invited lectures and special lectures in different national and regional programmes. He has reviewed manuscripts for the *International Earth Science Journal*. Mr. Islam is a life member of the Indian Geographical Foundation (IGF), Kolkata, and National Association of Geographers, India (NAGI), New Delhi. To date he has successfully supervised seven dissertations on various topics of geomorphology at the Master's level. His principal area of research includes channel shifting and riverbank erosion. Currently he is deeply engaged in the analysis of channel shifting and bank erosion of the River Bhagirathi, West Bengal, and its impact on society and the economy.

Md Ismail is a geographer associated with the Department of Geography, Aliah University and his field of specialization is agricultural geography and population geography. He also taught contemporary issues, statistics, environmental geography, biogeography, and social geography. He did his post-graduate work and received his MPhil from Aligarh Muslim University. He has published one edited book entitled *Life and Living Through Newer Spectrum of Geography* and more than 20 research papers in various international and national journals, as well as seminars and proceedings and has written chapters in edited volumes. Md Ismail has attended over 12 international and national seminars, conferences, and workshops.

Chapter 1
Quaternary Alluvial Stratigraphy and Palaeoclimatic Reconstruction in the Damodar River Basin of West Bengal

Sandipan Ghosh and Aznarul Islam

Abstract The Quaternary (starting from ~2.6 million years ago) climate changes have progressively triggered abrupt changes in the fluvial system and the resultant signatures are captured in the fluvial archives which are used as climate proxies to detect the palaeoclimate. In this chapter, the stratigraphic exposures, sediment characteristics, and dating information have been utilised to reconstruct the palaeoclimate in the alluvial valley of the Damodar River, West Bengal. This study has identified four distinct Quaternary geological units of the lower Damodar River Basin (DRB)—Lalgarh, Sijua, Chuchura, and Hooghly—morphostratigraphic units which belong to the northwestern part of the Bengal Basin. Analysing the architectures of different lithofacies, approximately six to seven climate changes (semi-arid to warm–humid) occurred in the study area from ~14 and 6 kiloannum (ka). Alongside these climate changes (from Late Pleistocene to Late Holocene) were directly linked the variability of the southwest monsoon (SWM) in two forms: (1) the semi-arid climate (i.e. the onset of low-strength SWM, associated with caliches, pond, and backswamp deposits of waning low-energy floods), and (2) the warm–humid climate (i.e., the onset of high-strength SWM, bearing imprints of sandy bedforms, valley fills, slack water deposits (SWD) of extreme floods, and ferruginous nodules).

Keywords Morphostratigraphical unit · Fluvial archives · Climate proxies · Palaeoclimate · Quaternary · Damodar river

S. Ghosh (✉)
Department of Geography, Chandrapur College, Chandrapur, Bardhaman 713 145, West Bengal, India
e-mail: sandipanghosh19@gmail.com

A. Islam
Department of Geography, Barasat Government College, Barasat, Kolkata 700 124, West Bengal, India
e-mail: aznarulislam@gmail.com

B.C. Das et al. (eds.), *Neo-Thinking on Ganges-Brahmaputra Basin Geomorphology*, Springer Geography, DOI 10.1007/978-3-319-26443-1_1

1.1 Introduction

Climate change refers to a significant shift from the longer term average weather conditions at a place or a region due to natural or anthropogenic causes (Singhvi and Kale 2009). The quest to understand climate change has become more intense in recent times largely on account of anticipated global warming scenarios, which may affect the climate patterns and hence, the biodiversity, food production, and lifestyles of people. But modern scientific research on climate change severally highlights an issue regarding the past climate, that is, palaeoclimate, which validates that our ancient climates were continually changed several times and these are not new phenomena to our planet. To address this issue recourse is taken to reconstruct the past climates of various regions and use the information on the past changes to provide the necessary baseline data of climatic variability. In this case, many researchers select the major river basins of India (as the study unit) to reconstruct the palaeoclimate because these river basins are considered an important repository of Quaternary climate changes (Rajaguru et al. 1993; Kale et al. 2004, 2010; Sridhar 2008; Singhvi and Kale 2009; Sinha and Sarkar 2009). Fluvial systems of drainage basins have been found to be most sensitive elements of the earth's surface and any shift in climate and environmental conditions instigates a rapid response from the fluvial systems (Sridhar 2008; Ghosh and Guchhait 2014). Therefore, it is reasonable to assume that major rivers of West Bengal might have responded to the climate changes of the Pleistocene and Holocene epochs almost in the same way that can be analysed by sedimentology and palaeoclimatology. The Damodar River of India has great potentiality for palaeoclimatic research, because of its existence since the formation of the Bengal Basin (since the Miocene) and it is much older than the Bhagirathi–Hooghly River of West Bengal. The principal aim of this study is to unearth the alluvial history of Quaternary morphostratigraphic units and to correlate Quaternary climate changes with the alterations of fluvial regimes and pedogenesis in the Damodar River floodplain. So to reach that aim, the following major objectives of research are set forth.

(1) Recognizing different morphostratigraphic lithosections from Early Quaternary to Recent
(2) Characterizing the facies of each lithosection from the perspective of palaeogeomorphic origin
(3) Identifying the climate proxies and palaeoclimatic condition since the Early Quaternary

1.2 Study Area

The Damodar River Basin (DRB) is an important peninsular tributary basin of the Bhagirathi–Hooghly River system in West Bengal. Its funnel-shaped basin area is about 23,370 km^2, having latitudinal extension of 22°30′ to 23°40′N and

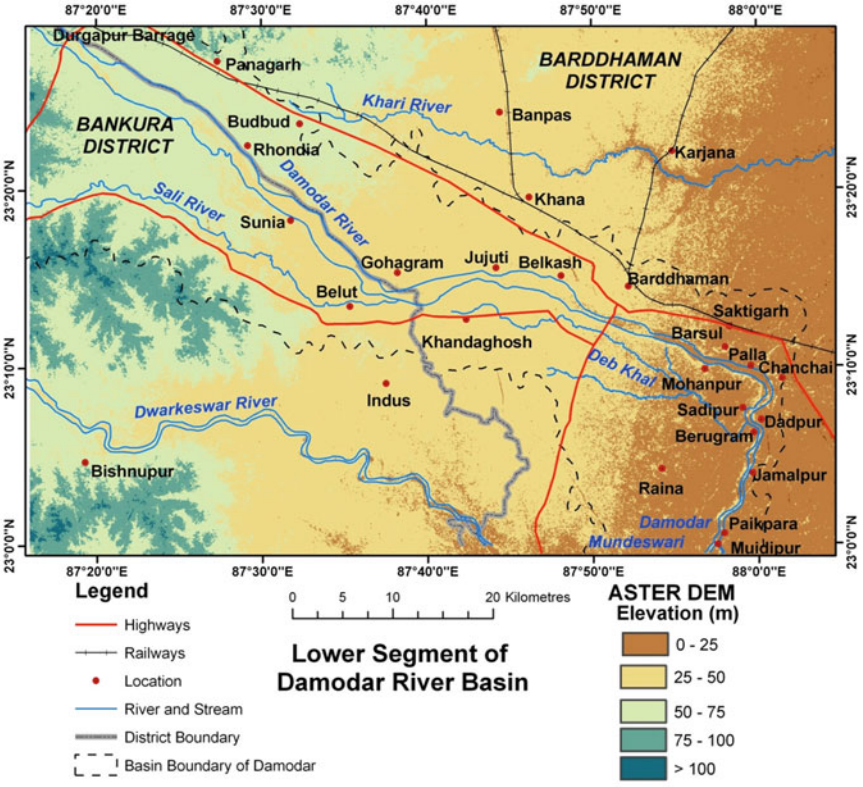

Fig. 1.1 Advanced space borne thermal emission and radiometer (ASTER) elevation map of study area, depicting the west–east slope, river system, and important locations in the lower Damodar River Basin

longitudinal extension of 84°45′ to 88°10′E (covering the states of Jharkhand and West Bengal). For detailed field investigation, the lower course of the Damodar (23°00′ to 23°22′N and 87°28′ to 88°01′E), in between Rhondia and Paikpara, was selected (Fig. 1.1). Topographically, the middle and lower parts of the DRB (specifically in Bardhaman district) can be categorized in five geomorphic units: (1) Ajay–Damodar–Barakar Interfluve (Gondwana part), (2) Kanksa–Ketugram Plain (*Rarh* Plain), (3) Bardhaman Plain, (4) Damodar–Bhagirathi Plain, and (5) Khandoghosh Plain. The lithostratigraphic study has been carried out on the left bank floodplain of the Damodar (from Belkash to Barsul, covering Bardhaman Plain) where ample Quaternary landforms, viz., alluvial terraces, avulsion, palaeochannels, mature point bars, uplifted older terraces, backswamp, levees, and so on are found. A separate laterite lithosection of *Rarh* Plain has been investigated in the region of Durgapur to Panagarh.

Away from the basaltic outcrops in the Rajmahal Hills of Jharkhand (Early Cretaceous), many lava flows have been encountered in a number of deep wells

within the western Bengal Basin which acts as the basement of Pliocene–Miocene sedimentation along the middle to lower Damodar River (Alam et al. 2003; Kuehl et al. 2005; Das Gupta and Mukherjee 2006; Bandyopadhyay 2007). The thickness of sediments overlying the Rajmahal basalt in the wells at Bardhaman and Galsi are, respectively, 2515 and 1273 m from the surface (Kumar et al. 2004). The Damodar River is one of the important peninsular rivers which contributed to fill up the western part of the Bengal Basin through alluvial fan to fan-deltaic sedimentation since the Neogene. From that period, Late Palaeogene, the sedimentation of the western shelf of the Bengal Basin was tectonically influenced due to the Chotanagpur Foothill Fault, Pingla Fault, Garhmayna–Khandaghosh Fault, and Damodar Fault (Singh et al. 1998). The growth of the Damodar floodplain is directly influenced by occasional reactivation of these basement faults, climate changes of the last glacial maxima (LGM), and the marine transgression–regression, forming variable morphostratigraphic units as the fan-delta formations. These fluvial archives provide us ample palaeogeographic information on the western shelf of the Bengal Basin since the Early Quaternary.

1.3 Materials and Methods

Over the last four decades, fluvial sedimentology has progressed towards understanding how fluvial systems develop and change over time as a response to tectonism, climate, and sea-level change (Jain and Tandon 2003). A river can exist close to a threshold condition where a small shift in flow or sediment character, possibly induced by climate, can produce a dramatic change in the style of fluvial deposits (Jain and Tandon 2003; Jain et al. 2004; Sinha et al. 2005; Babar et al. 2012; Babar and Snehal 2014). Floodplain stratigraphy (Bridge 2003; Nichols 2009) provides the timeframe that allows us to interpret sedimentary deposits in terms of dynamic evolving environments. The main focus of methodology is concentrated on the identification of physical, chemical, and biological conditions of Quaternary sediments that existed at the time of sedimentation and the postdepositional environment.

The term *facies* is used here to refer to the individual characteristics of each sedimentary unit or lithosection and through recognizing association of facies or lithofacies (Maill 2006, 2014) it is possible to establish the combination of fluvial processes that were dominant. The term *morphostratigraphic unit* is used here to recognize the similar stratigraphic association of unique lithofacies in a particular region with distinct fluvial depositional style, similar morphology of section, associated landforms, and geomorphic evolution. The main approach of this study is concentrated on the interpretation of lithofacies by which the sediments in terms of the physical, chemical, and ecological conditions at the time of deposition (or post-deposition) enable us to reconstruct our palaeoenvironments. Fundamentally the methodology is adopted from the great works of Kale and Rajaguru (1987), Joshi and Kale (1997), Singh et al. (1998), Rajaguru et al. (1994, 2011), Sinha et al.

(2005), Sridhar (2008) and Kale et al. (2010) etc. The stratigraphical studies were carried out at the selected sites of Attagarh (23°14′28″N, 87°58′25″E), Beldanga (23°23′28″N, 87°56′04″E), Birpur (23°17′09″N, 87°50′32″E), Krishnapur (23°15′37″N, 87°51′18″E), Kamnara (23°17′47″N, 87°51′03″E), Vita (23°17′28″N, 87°54′43″E), Nandra (23°14′55″N, 87°54′39″E), Amarun (23°21′37″N, 87°56′21″E), Nari (23°14′12″N, 87°53′48″E), Kandorsona (23°12′46″N, 87°56′18″E), Balamhat (23°13′34″N, 87°50′37″ E), Bam (23°13′15″N and 87°54′29″E), Kala Nabagram (23°10′42″N, 87°59′54″E), Pamra (23°12′37″ N, 87°54′43″E), Sadhanpur (23°14′51″N, 87°53′04″E), and Baikunthapur (23°17′19″N, 87°50′27″E) having 9.0 m subsurface lithologues. Alongside these, the lithosections of the *Rarh* Plain were investigated around the north of Durgapur City and along the Panagarh–Illambazar Road. The reliable database of deep boreholes was collected from the unpublished reports of the Geological Survey of India (GSI; Eastern Region, Kolkata). Near-surface sediment characters of lithofacies were analysed in the selected sections of levee, bank, backswamp, abandoned channel, and point bar. The facies architecture classification was done using the Miall model (1985, 2006, 2014) to identify the fluvial depositional character (Ghosh 2014). Miall's architectural elements of fluvial deposits, viz., Gcm, Gmg, Gm, Gt. Sp, Sm, Fm, and so on, were applied here to annotate the Quaternary lithofacies (Table 1.1). The graphic sedimentary logs (1:100 scale) were prepared following Tucker (1996) formats and the symbols with abbreviations (Nichols 2009) were used to recognize each facies. Additionally the chemical analysis of climate proxies (i.e. caliches and Fe-nodules) was done. Other secondary spatial information was collected from the Survey of India (SOI) topographical sheets of 73 M/15 and M/16 (1:50,000 scale; 1969–1974), district resource map of Bardhaman from GSI (2001), ASTER DEM data (2011) from United States Geological Survey (USGS; Earth Explorer), and Landsat TM image (2006) from USGS and Google Map.

1.4 Results and Discussion

1.4.1 Quaternary Morphostratigraphical Units of Damodar Floodplain

Geologically the floodplain of the study area belongs to the western part of the Bengal Basin and geomorphologically it is a mature fan-delta of the Damodar River sloping towards the east to southeast. The western part of the study area is associated with the typical lateritic *Rarh* Plain (Acharyya and Shah 2007). Understanding the regional stratigraphy, four major Quaternary to Recent morphostratigraphic units were identified and these reflect a different history of evolution related to palaeoclimate, neotectonic activity, and floodplain processes. These sedimentary units (the names of units are recognized by GSI) are described

Table 1.1 Details of fluvial facies used in the analysis (modified from Miall 1985, 2006, 2014)

Facies code	Sedimentary structure	Interpretation
Gmg	Matrix-supported massive gravels; inverse to normal grading	Pseudoplastic debris flow (low-strength, viscous)
Gcm	Clast-supported massive gravel; out-sized clasts	Pseudoplastic debris flow (inertial bedload, turbulent flow)
Gh	Clast-supported, crudely bedded gravel; imbrications	longitudinal bedforms, lag deposits, sieve deposits
Gt	Gravel stratified; trough cross-beds	Minor channel fills
Gm	Massive poorly sorted gravels	Point bar deposits
Sm	Sand, fine to coarse; massive or faint wavy lamination	Sediment-gravity flow deposits
Sp	Planar cross-bedded sand	Traction and intermittent suspension, forming ripples
St	Trough cross-bedded sand	Migration of dunes with lag deposits
Sh	Horizontally bedded sand	Transition from subcritical to supercritical flow, deposits of flash deposits
Ss	Scour-fill sand	Rapid deposition of poor sand, coarse bed load, basin fills
Fm	Mud, silt; massive, desiccation cracks	Overbank or waning flood deposits
Ft	Laminated sand, silt, and mud	Deposition from suspension and from weak traction currents
Fsm	Finely laminated silt and clay	Floodplain deposits, more distal relative to clastic sources such as nearby fluvial channels

below with important sediment characteristics and landform assemblages (Table 1.2 and Fig. 1.2).

1.4.1.1 Lalgarh Morphostratigraphical Unit

The lateritic or ferruginous lithosections around the Durgapur–Panagarh belt (a part of *Rarh* Plain) is actually the weathering product of ex situ lateritization of debris flow–fluvial deposits during the Neogene to Late Pleistocene. This ferruginous formation is quite comparable to the Lalgarh Morphostratigraphical Unit (LMU) which is analogous to secondary laterites of *Rarh* (Biswas 1987). LMU appears as a conglomerate reworked ferricrete and Gmg fluvial facies (i.e. inverse to normal matrix-supported gravels). The matrix or ground-mass is highly cemented by ferruginous cement (mainly limonite and goethite) which makes it very indurated duricrust. Below the duricrust the pebble horizon is characterized by lag deposits (fan-delta formation) constituted of pisoids, quartz pebbles, and petrified

Table 1.2 Quaternary alluvial morphostratigraphic units of Damodar River Basin

Sedimentary units	Landforms (lithology)	Relative age
1. Lalgarh morphostratigraphical unit (LMU)	Ferruginous hard crust and badlands (lateritic deposits with gravels, oxidized coarse sands and kaolin)	Middle pleistocene to late pleistocene
2. Sijua morphostratigraphical unit (SMU)	Undulatory surface with terraces and older alluvium (fairly oxidized clay-slit with alternate caliches and ferruginous nodules)	Late pleistocene to early holocene
3. Chuchura morphostratigraphical unit (CMU)	Levee, backswamp, mature point bar, sloughs, and palaeochannel (sparsely oxidized clay, silt, and sand, with fining upward sequence)	Early holocene to late holocene
4. Hooghly morphostratigraphical unit (HMU)	Mid-channel bar, point bar, valley fill, and few abandoned channels (bed deposits, fine to coarse sand, slit, and occasional clay)	Late holocene to recent

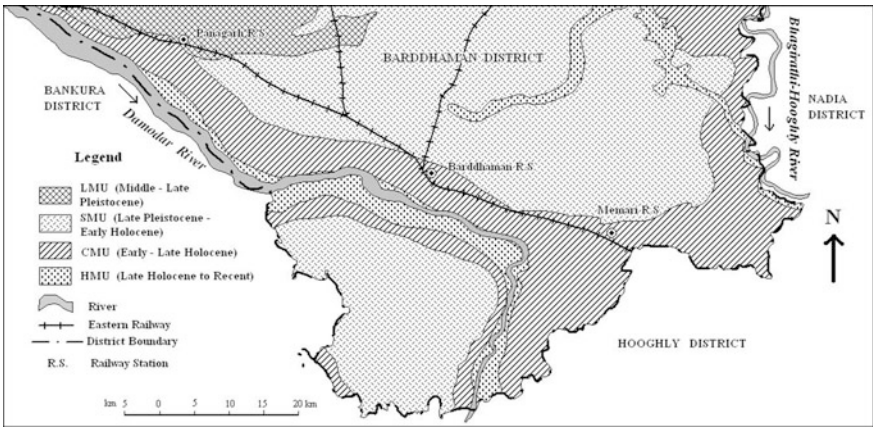

Fig. 1.2 Quaternary morphostratigraphic map of Damodar floodplain, Bardhaman district

woods of varying sizes set in a ferruginized matrix of sands. A well-preserved lithosection of LMU is found at Hetodoba (23°26′45″N and 87°32′07″E), north of Durgapur City, Bardhaman District (Table 1.3).

These lateritic sediments were deposited as valley deposits in the tectonic shelf of the Bengal Basin in between the Chotanagpur Foothill Fault and Pingla Fault. Up to the Late Pleistocene these ferruginous sediments were relateritized under a tropical wet–dry climate to form a lateritic hard crust. Due to neotectonic uplifts, resistant crust formation, and erosion, the former valley floors became inverted relief (McFarlane 1976; Ollier and Sheth 2008) rather than the adjacent valley slopes of the Holocene. The optically stimulated luminescence (OSL) dating of these ferruginous hard crusts suggests that the age of sedimentation or time of cut-off from the sunlight for the hard crust ranges from ~ 96 to 35 ka (Middle–Late

Table 1.3 Development of ferruginous sediments (LMU) on Neogene gravels and pebbles at Hetodoba, north of Durgapur City

Profile depth (m)	Lithological description
0–0.15	Ferruginized gravels and pebbles, cementation of hematite nodules (Gmg), affected by erosion
0.15–0.72	Murram with gravels, hard crust, Gmg facies
0.72–1.20	Ferruginized clay bands, hard on exposure (Fm)
1.20–3.10	Mottle zone with upward fining pebbles and gravels (Gcm)
3.10–4.15	Yellowish white kaolinite ochre with upward fining pebbles with dicotylendous fossil woods (Gcm)

Pleistocene). This LUM type of old surface (thick hold of deciduous forest, Sal, and glimpses of gullies) are found in the blocks of Durgapur-Faridpur, Kanksa, Ausgram I and II, and the surrounding region of Durgapur, Panagarh, and Mankar. The eastward extension of LMU is found at Worgram (23°27′08″N and 87°46′59″ E), near south of Guskara town.

1.4.1.2 Sijua Morphostratigraphical Unit

The facies of hard, sticky, brownish to yellowing grey clays enriched with caliches (calcareous concretion) and small rounded ferruginous concretions is recognized as the Sijua Morphostratigraphical Unit (SMU). The SMU, undulatory surface, and terraces of older alluvium, were developed in between the Late Pleistocene and Early Holocene. Granulometric analysis reveals that the soils of SMU contain 4–47 % sand, 37–73 % silt, and 11–35 % clay, belonging to the silt loam and silty clay loam categories. The maximum thickness of this unit is 20 to 35 m, mostly covering the Khari River Basin. The SMU reflects that at 6–9 m depth, the clayey horizon (heavy suspended load) changes to sandy horizon (missed bedload) in which fine to medium brownish grey sun angular quartz, altered feldspar, and ferruginous concretion are observed. Detailed study reveals that SMU is represented by alternate caliche-rich and ferruginous concretion-rich zones with relative dominance of overbank fines (Fm, Fl, and Fsm). These sediments were formed in the very low fluvial regime of Damodar River (weak SWM) and fine-gradient drape deposits were formed in pools of standing water. The occurrences of clayey slit or silty clay (Fl) with pedogenic nodules signifies occasional slack water deposits (SWD) of high magnitude palaeofloods and postflood stability of lithofacies. The subsurface lithologue of Amarun is associated with six distinct lithofacies of SMU (Fig. 1.3b). The deep borehole of 146.0 m at Nawabhat (23°15′52″N, 87°50′07″E) on the SMU suggests that a thick layer of sticky clay (14.32 m bgl, below ground level) is overlain on the alternate yellowish sandy clay, fine sand, and medium sand (14.32–67.56 m bgl) and these are overlain on the greyish fine sand (67.56–108.96 m bgl) and greyish clay to sandy clay (108.46–146.0 m bgl). All these fluvial facies were

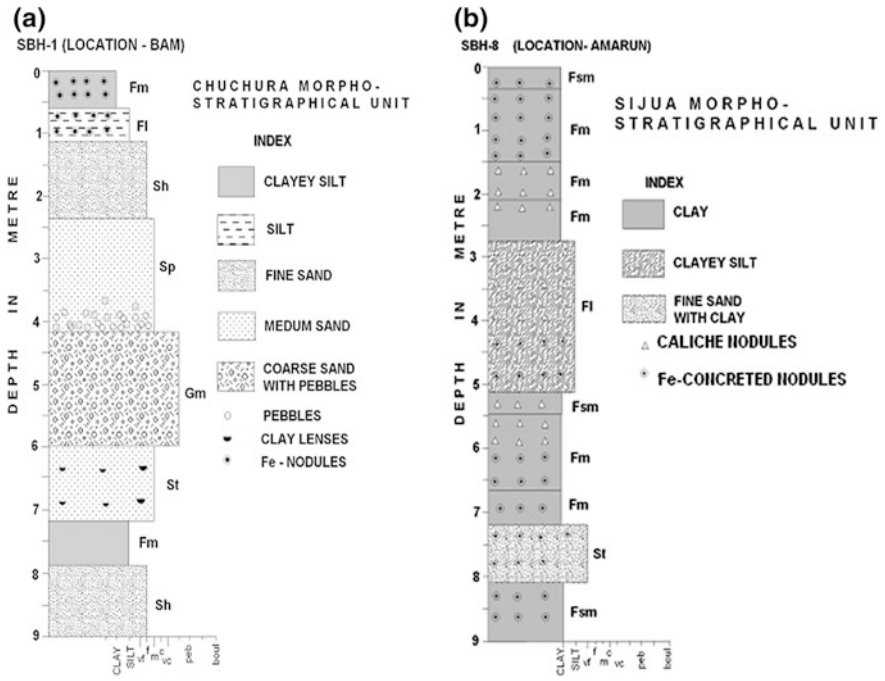

Fig. 1.3 **a** Distinct lithofacies of CMU at Bam, showing upward fining sequence, overbank deposits (Fm and Fl), coarse lag deposits of pebbles (Gm), channel fills (Sp and Sh), and ferruginous nodules of overbank palaeoflood deposits; and **b** occurrences of sticky clay and clayey slit (SMU) with caliches suggesting relatively semi-arid climate with occasional wet period deposition of iron nodules in between the Late Pleistocene and Early Holocene at Amarun (modified from Ghosh and Guchhait 2014)

deposited in very low energy waning flood with minor channel fills in between the Late Pleistocene and Early Holocene. Similarly at the section of Kamnara (north of Bardhaman town, Table 1.4) it has been found that the occurrence of Ft facies (at depths of 4.2–7.5 and 8.1–9.0 m) reflects fluvial fine deposition under suspension conditions with weak traction currents and development of pedogenic caliches under semi-arid conditions. At the top of that section (0–4.2 m depth) the massive development of waning flood deposits or overbank fine deposits (Fsm) was affected significantly by alternate warm–humid (presence of ferruginous concretions) and semi-arid (presence of caliches) climatic phases in the postdepositional period (within the Late Pleistocene to Early Holocene).

1.4.1.3 Chuchura Morphostratigraphical Unit

The Chuchura Morphostratigraphical Unit (CMU) is well exposed in the low-lying areas (adjoining riverbanks) from Rhondia to Paikpara where numerous

Table 1.4 Identified fluvial facies of SMU at Kamnara

Profile depth (m)	Lithological description
0–1.8	Light grey hard sticky clay with ferruginous patches, soft ferruginous concretions and fine fragments of caliches (Fm)
1.8–4.2	Greyish yellow hard sticky clay enriched with caliche up to 3 cm across
4.2–7.5	Brownish hard sticky clay mixed with fine sand, small caliche, ferruginous concretions, and kaolinized feldspar (Ft)
7.5–8.1	Light yellowish brown clayey sand (Fsm)
8.1–9.0	Brownish hard sticky clay mixed with fine sand, small caliche, and kaolinized feldspar (Ft)

geomorphic glimpses of palaeochannels, mature point bars, crevasse splay, back-swamps, and sinuous arrangements of water bodies are found. The CMU was developed in between the Early Holocene and Late Holocene. The possible OSL dating age of sediments (from B-horizon of soils) ranges from 3.6 to 5.44 ka in this region (Singh et al. 1998). The sediments are represented by the sparsely oxidized grey to brownish grey, micaceous silty clay, clayey silt, and sandy silt with Fe-concretions, grey to brownish grey fine to coarse sand locally with pebbles and gravels. Granulometric analysis reveals that the soils of SMU contain 5–42 % sand, 19–78 % silt, and 6–27 % clay, belonging to silt loam and silty clay loam soils. The borehole log on the CMU up to 115.8 m depth in Barsul (23°10′54″N, 87°57′51″E) area reveals clay and sandy clay from the top to 11.88 m bgl, followed downward by fine to coarse yellowish sand with occasional pebbles up to 90.6 m bgl and then by clay mixed with sand up to 115.8 m bgl. The lithosection of Bam (Fig. 1.3a) reflects that from 9.0 to 4.2 m depth an upward coarsening sequence (Fm–St–Gm; increasing fluvial regime, strong SWM) and from 4.2 m depth to the surface an upward fining sequence (Gm–Sp–Sh–Fl–Fm; decreasing fluvial regime, weak SWM) are observed. At the section of Baikunthapur, six lithofacies of CMU again reflect hydraulic differentiation and sedimentation under high and low energy floods (Table 1.5).

Table 1.5 Lithofacies of CMU at Baikunthapur

Profile depth (m)	Lithological description
0–3.3	Grey to light brownish sparsely oxidized sticky clay with brownish ferruginous patches and soft, dark rounded ferruginous concretions (Fm)
3.3–4.8	Brown more oxidized silty/sandy clay with unoxidized greyish patches with more ferruginous concretions (Fl)
4.8–6.0	Micaceous brown sandy silt mixed with clay (Ft)
6.0–6.6	Brownish yellow very fine sand mixed with clay (Sh)
6.6–8.7	Brownish yellow fine to medium sand (Sh)
8.7–9.0	Coarse pebbly brownish yellow sand with angular to subangular pebbles of quartz and feldspar with hard brown ferruginous rounded concretions (Gm)

1.4.1.4 Hooghly Morphostratigraphical Unit

The Hooghly Morphostratigraphical Unit (HMU) comprises recent sediments (active floodplain) on the present-day landforms of the Damodar River and has developed since the Late Holocene. The sediments of HMU are the aggregates of coarse- to medium-grained pale yellow to light grey sand mixed with brownish grey silt and the occasional presence of black clay or mud deposits. This type of sediment is defined as the active sediment (Faniran and Jeje 1983) which is transported by the stream flowing of flood: scour of the modern channel and the maximum grain size which the stream can competently transport at a flood stage. Hence, the upper flow regimes create horizontally stratified sand and lower flow regimes form trough cross-stratified grey sand, planar cross-stratified sand, ripple marks, and small-scale cross-stratification. In short, the sand-dominated HMU of the Damodar River has assemblages of interbedded slit–clay deposition (Fsc), dunes (St), sand waves, linguoid and transverse bars (Sh), ripple marks (Sr), and channel lag deposits (Gt).

1.5 Palaeoclimate and Climate Proxies of the Quaternary

Climatology, prior to the instrumental records of temperature, precipitation, and other weather elements is referred to as 'palaeoclimate' or past climate or ancient climate (Greek *Palaios* meaning ancient). Kale et al. (2010) suggest that the intensification of the monsoon climate during the Late Pleistocene to Early Holocene ($\sim$25 to 10 ka) had a dramatic and profound effect on the fluvial sedimentation and pedogenesis which are the invaluable fluvial archives of the floodplain, having great potentiality to explore our palaeoclimatic conditions. In the reconstruction of past climates the taken assumption is that the basic processes in the geoenvironments remain the same through time. Before going into palaeoclimatic discussion, a new fact has come to us that in contrast to the early twentieth century view of four Ice Ages, present research ($^{18}O/^{16}O$ isotopic ratios in the Foraminifera microfossils in sediments of deep oceans) reveals the occurrences of 50 Ice Ages (or glacial periods) and an equal number of intervening warmer periods (or interglacial periods) in the Indian subcontinents during the last 2.6 million years (Singhvi and Kale 2009). Therefore, those noticeable climate changes of the Quaternary may have direct or indirect impacts on the development of morphostratigraphic units and palaeopedogenesis of sediments in the DRB. The maximum information was collected from the fluvial archives of SMU and CMU using two important climate proxies of floodplain lithosections.

1.5.1 Climate Proxies

Reconstruction of past climatic events needs 'climate proxies' which are the physical, chemical, or biological attribute of the natural system enabling us to quantify the change in climate in the past (Singhvi and Kale 2009). Caliches and ferruginous concretions are two important climate proxies of fluvial archives which denote two different palaeoclimatic and pedogenic origins on the Damodar floodplain. These caliches show the number of nuclei represented either by quartz or muscovite around which growth of fibrous calcite crystals are seen. Other parts of the caliches are made up of carbonated clayey materials. On an average a single caliche contains 21.92 % Ca and 668 ppm of fluoride (F; Ghosh and Guchhait 2014). The microscopic morphology of Fe–Mn concretions reveals that they are either made up of fine limonitic concretion embedded within clayey materials or of a single concretion with a number of concentric layers. These concretions contain 20.04 % Fe, 4.98 % Mn, 756 ppm F, and 20 ppm arsenic (As). It is found that from core to rime SiO_2, Al_2O_3, and Fe_2O_3 increase from 1.75 to 20.66 %, 2.59 to 11.57 %, and 0.34 to 10.53 %, respectively (Ghosh and Guchhait 2014). Apart from chemical details, caliche is thin and calcareous bodies occur as crusts and nodules in the soils (as relocation of insoluble salts as nodules due to capillary action) which experience a tropical dry and semi-arid climate with a short wet season alternately for a considerable period. On the other side, the presence of Fe-nodules or mixed ferruginous concretions is associated with a strong tropical wet–dry seasonal regime or relatively warm–humid climate (favourable for the lateritization process and leaching).

1.5.1.1 Palaeoclimate of LMU (Palaeocene to Late Pleistocene)

In the history of plate drift through millions of years, those continents which travelled or had been travelled across tropics (30°N to 30°S) must bear the imprints of laterites and bauxites (Ghosh and Guchhait 2015; Kumar 1986). So the residual laterite profiles are the fossil type formed in past geological ages when climatic conditions were favourable for lateritization. The presence of LMU reflects a special palaeoclimatic condition of the tropics which differs a great deal from the palaeoclimates of SMU and CMU. It has now been shown that the occurrence of a ferricrete or laterite profile of tropical weathering of parent rocks reflects palaeoprevalence of the contrasted seasons (wet–dry) of a tropical climate, high temperature throughout the year (28°–35°C), annual average relative humidity of the air nearer to 60 %, annual rainfall lower than 1700 mm and long dry seasons during which a relatively low thermodynamic activity of water and atmospheric relative humidity decreases (McFarlane 1976; Tardy et al. 1991). That climatic condition of this region was favourable for lateritization from the Palaeocene to Late Pleistocene times and during that period the Indian Plate crossed the zone between 30°S and 30°N latitude (Ghosh and Guchhait 2015; Schmidt et al. 1983; Kumar 1986; Tardy et al. 1991).

1.5.1.2 Palaeoclimate of SMU (Late Pleistocene to Early Holocene)

The SMU lithosections of Attagarh, Beldanga, Birpur, Krishnapur, Kamnara, Vita, Nandra, and Amarun sites bear alternate glimpses of caliches and Fe-concretions in the facies of sticky clay, silty clay, and clayey silt. All caliche-rich facies represent the prevalence of a semi-arid tropical climate (dry phase) from the Late Pleistocene to Early Holocene with low stream power and pond deposits of waning palaeo-floods. The lithofacies containing Fe-nodules or concretions are the result of palaeopedogenesis of floodplain sediments with that time period in the warm–humid tropical climate (wet phase). The SMU lithosection of Attagarh reveals five distinct phases of climate changes (alternate semi-arid and warm–humid tropical climate) whereas six to seven climate changes are shown in the lithosections of Amarun and Beldanga (Figs. 1.3b and 1.4b; Table 1.6).

1.5.1.3 Palaeoclimate of CMU (Early to Late Holocene)

The CMU lithosections of Nari, Kandorsona, Balamhat, Bam, Kala Nabagram, Pamra, Sadhanpur, and Baikunthapur are represented through upward fining sediments with the occasional occurrence of Fe-nodules. At the section of Nari

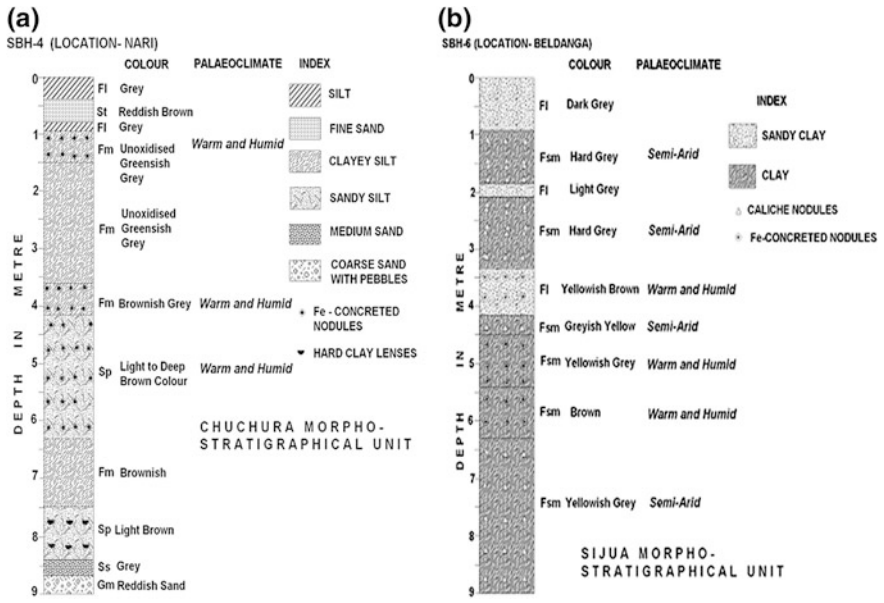

Fig. 1.4 **a** Identified lithofacies of CMU (at Nari) with iron nodules denoting three periods of relatively warm–humid climate in the Early–Middle Holocene: (i) 0.6–0.9 m (ii) 3.6–4.2 m, and (iii) 4.2–6.3 m; and **b** SMU nine alternate layers of caliches (semi-arid climate) and iron nodules (warm–humid climate) signifying six distinct phases of climate changes (Late Pleistocene–Early Holocene) at Beldanga (modified from Ghosh and Guchhait 2014)

Table 1.6 Facies architectures and evidence of climate changes in the SMU lithosection at Attagarh

Facies No	Depth (m)	Lithological description	Fluvial architecture	Palaeoclimate
FC 1	9.0–7.2	Reddish brown silty clay with Fe-nodules	Ft	Warm–humid
FC 2	7.2–6.0	Yellowish grey sticky clay with caliches transition with Fe-nodules at base	Fsm	Semi-arid
FC 3	6.0–5.4	Yellowish grey sticky clay with Fe-nodules	Fsm	Warm–humid
FC 4	5.4–3.6	Greenish grey hard clayey silt with caliches	Fsm	Semi-arid
FC 5	3.6–1.5	Greenish grey hard clayey silt with Fe-nodules	Ft	Warm–humid
FC 6	1.5–0	Brown grey clayey silt with Fe-nodules	Ft	Warm–humid

(Fig. 1.4a), three distinct oxidized facies of clayey silt (0.6–0.9 m bgl), clayey silt with globular ferruginous patches (3.6–4.2 m bgl), and sandy silt (4.2–6.3 m bgl) reflect three successive phases of relatively more warm–humid palaeoclimate in between the Early and Late Holocene. The base of all CMU lithosections (6–9 m bgl) comprises coarse sands, gravels, and pebbles which denote the braided pattern and lag deposits of the Damodar River in high flow regime in the Early–Middle Holocene. The upward fining sequence of Fsm, Fm, and Fl with Fe-nodules signifies a low flow regime and dominance of overbank deposition under a warm–humid tropical climate from the Middle to Late Holocene. Late Quaternary sediments of the Damodar floodplain show high smectite–kaolinite concentration and iron nodules during the Early Holocene period and this appears to reflect enhanced chemical weathering under warmer and more humid conditions.

1.5.2 Palaeoclimatic Reconstruction in the Damodar Floodplain

From the above study it is now understood that up to the Early Holocene ($\sim$11.5 to 9 kyear) the palaeoclimate of the Damodar floodplain was changed from semi-arid to a more warm–humid climatic condition with a high degree of pedogenesis in the stable environment. The alternate occurrences of big caliches (dry phase) and ferruginous nodules (wet phase) in the present humid to subhumid region of West Bengal indicate frequent but drastic change in the past climate during the Last Glacial Maximum, that is, around $\sim$18 to 14 ka, when SWM was very weak in the Peninsular India and lower Gangetic Plains. The presence of Fe-nodules in the CMU signifies that from the Early Holocene the palaeoclimate was transformed

from semi-arid to a more warm–humid tropical or monsoon climate with occasional SWD of extreme floods. On the basis of a literature review, the present sedimentological analysis and climate proxies give a brief reconstruction of palaeoclimate change or trend depicted here for the floodplain of the Damodar River, West Bengal (Table 1.7).

Table 1.7 Late quaternary palaeoclimatic reconstruction (~11.5 ka to present) in the Damodar floodplain

Period	Climate	Fluvial response and climate proxies
11,500 BP (before present)	Cool and dry	Fluvial aggradation; sticky clay, silt, and pedogenic caliches
11,500–8000 BP	Equable climate (Vedic period)	Snowmelt-fed Saraswati River existed; transition from fluvial aggradation to degradation
8000–7000 BP	Warm–humid with dominant seasonality (Ramayana period) (SWM started to strong)	Start of fluvial degradation with occasional flash floods; frequent overbank deposition; pedogenic iron nodules
7000–6000 BP	Warm–humid (Mahabharata period)	Frequent floods; strong fluvial degradation with presence of coarse sand and gravels; pedogenic iron nodules
6000–5000 BP	Cool and dry (SWM started to weak)	Frequent droughts; overbank deposition with sticky clay and caliches
5000–,000 BP	Warm–humid (Indus civilization)	Seasonal floods; pedogenic iron nodules with coarse sand
4000–3500 BP	Cool and dry (start of Jainism)	Frequent droughts; overbank deposition with sticky clay and caliches
3500–2600 BP	Warm–humid with dominant seasonality (Epic period and decline of Indus civilization)	Deasonal floods; start of valley incision; pedogenic iron nodules
2600–2000 BP	Cool and dry (Buddha–Ashoka period)	Frequent droughts; overbank deposition with sticky clay and caliches
2000–1400 BP	Warm–humid with short semi-arid phase	Deposition of fine sand and silt (slack water deposit); pedogenic iron nodules and caliches
1400–1100 BP	Cool and dry	Frequent droughts; overbank deposition with sticky clay, clayey silt and caliches
1100–750 BP	Mediaeval warm period	Frequent high-magnitude flash floods with pedogenic iron nodules
750–400 BP	Little ice age	Low fluvial degradation and increased aggradation
400–200 BP	Preindustrial	Frequent flash floods and lateral migration
200–Present	Anthropocene warm–humid seasonal extremes (wet–dry)	Infrequent high-magnitude flash floods, lateral migration, high sinuosity and overbank deposition of clay and silt

Source Ghosh and Guchhait (2014)

1.6 Conclusion

On the basis of the above analysis we have indentified four unique geological units of the Lower Damodar River Basin, viz., (1) Lalgarh (Palaeocene to Late Pleistocene), (2) Sijua (Late Plestocene to Early Holocene), (3) Chuchura (Early to Late Holocene), and (4) Hooghly (Late to Recent) morphostratigraphic units which are associated with the northwestern part of the Bengal Basin. The most important finding of this analysis is that from the Late Pleistocene to Early Holocene the fluvial activity (i.e. meandering nature) was reduced and was influenced more by the postglacial dry climate (yellowish to grey colour sediments and caliches) and the infrequent extreme floods. As these study sites of SMU are situated on the old elevated terraces of the Damodar and Khari Rivers, the stable topographically high surfaces received only overbank deposition in the water-logged condition. But in terminal Early Holocene the fluvial system was forced to enter a new phase of degradation (strong SWM) and cut down the surface of SMU to form CMU, with the ample supply of coarse sediments from the Chotanagpur Plateau. After crossing the lateritic *Rarh* upland (Middle–Late Pleistocene LMU) of Kanksa–Panagarh, the Damodar River system developed a fan-delta (older delta plain than the Bhagirathi–Hooghly Delta) in the western margin of the Bengal Basin where the River Damodar rotated its course clockwise or southerly (having the apex of the delta at Silla) shifting its previous mouth (present mouth of Khari River), 128 km to the south (Amta channel below Kolkata). The initial delta formation began $\sim$14 to 11 ka when the rising sea level led to backflooding of the low stand surface and the trapping of riverine sediments (coming from the west), an event marked by transition from alluvial sands or Pleistocene laterites to overlying mud. The recent lithofacies of HMU signify the active aggradational phase and lateral accretion of a floodplain. The frequent oscillation of thalweg and development and destruction of small in-channel bars denote an infrequent monsoonal flow and siltation of the active riverbed. The transition of CMU to HMU is leveled by overbank deposition of clay and silt, denoting waning flood deposits and relatively low energy floods in the Damodar River. Overall the climate proxies of LMU reflect a strong contrasted tropical wet–dry climate up to Late Pleistocene where the climate proxies of SMU indicate approximately six to seven climate changes (dry to wet) in between the Late Pleistocene and Early Holocene and the fluvial archives of CMU infrequently bear the imprints of a relatively more warm–humid climate. It is now found that the increased aridity occurred again $\sim$3.5 ka, but up to $\sim$2 ka the SWM again became much stronger than at present and the current climate condition was started from $\sim$2 ka to the present in this region of West Bengal.

Acknowledgements This research work is guided by Prof. Sanat Kumar Guchhait (Department of Geography, The University of Burdwan, West Bengal) who has made invaluable efforts, suggestions, and ideas to frame this work. The authors are very grateful to the Department of Geography, The University of Burdwan for providing the necessary facilities to undertake this work. The authors are also indebted to the Geological Survey of India (Eastern Region, Kolkata) for providing the geological expedition reports and data.

References

Acharyya SK, Shah BA (2007) Arsenic-contaminated groundwater from parts of Damodar fan-delta and west of Bhagirathi River, West Bengal, India: influence of fluvial geomorphology and quaternary morphostratigraphy. Environ Geol 52:489–501

Alam M et al (2003) An overview of the sedimentary geology of the Bengal Basin in relation to the regional tectonic framework and basin-fill history. Sed Geol 155:179–208

Babar Md, Snehal J (2014) Quaternary fluvial sedimentations of Sindphana River in Maharastra, India. Int Res J Geol Mining 4(4):116–121

Babar M et al (2012) Quaternary geology and geomorphology of Terna River Basin in west-central India. Quat Sci J 61(2):156–167

Bandyopadhayay S (2007) Evolution of the Ganga Brahmaputra Delta: a review. Geogr Rev India 69(3):235–268

Biswas A (1987) Laterities and lateritoids of Bengal. In: Datye VS, Diddee J, Jog SR, Patial C (eds) Exploration in the tropics. K.R. Dikshit Felicatiobn Committee, Pune, pp 157–167

Bridge JS (2003) Rivers and floodplains. Blackwell Publishing, Oxford

Das Gupta AB, Mukherjee B (2006) Geology of NW Bengal Basin. Geological Society of India, Bangalore

Faniran A, Jeje LK (1983) Humid tropical geomorphology. Longman, London

Ghosh S (2014) Palaeogeographic significance of ferruginous gravel lithofacies in the Ajay—Damodar Interfluve, West Bengal, India. Int J Geol Earth Environ Sci 4(3):81–100

Ghosh S, Guchhait SK (2014) Palaeoenvironmental significance of fluvial facies and archives of Late Quaternary deposits in the floodplain of Damodar River India. Arab J Geosci 7(10): 4145–4161

Ghosh S, Guchhait SK (2015) Characterization and evolution of primary and secondary laterites in northwestern Bengal Basin, West Bengal, India. J Palaeogeogr 4(2):203–230

Jain M, Tandon SK (2003) Quaternary alluvial stratigraphy and palaeoclimatic reconstruction at the Thar Margin. Curr Sci 84(8):1048–1055

Jain M, Bhatt SC (2004) Late Quaternary stratigraphic development in the Lower Luni, Mahi and Sabarmati river basins, western India. J Earth Syst Sci 113(3):453–471

Joshi VU, Kale VS (1997) Colluvial deposits in northwest Deccan, India: their significance in the interpretation of late quaternary history. J Quat Sci 12(5):391–403

Kale VS, Rajaguru SN (1987) Late quaternary alluvial history of north-western Deccan upland region. Nature 325:614–621

Kale VS et al (2004) Late Pleistocene—Holocene palaeohydrology of monsoon Asia. In: Kale VS, Gregory KJ, Joshi VU (eds) Progress in palaeohydrology. Geol Soc India, Bangalore, pp 403–417

Kale VS et al (2010) Palaeoflood records from upper Kaveri River, southern India: evidence for discrete floods during Holocene. Geochronometria 37:49–55

Kuehl SA et al (2005) The Ganges–Brahmaputra delta. In Gosian L, Bhattacharya J (eds) River deltas. SEPM, Tulsa, vol 83, pp 413–434

Kumar A (1986) Paleolatitudes and the age of Indian laterites. Paleogeogr Paleoclimatol Paleoecol 53:231–237

Kumar N et al (2004) Gravity signatures of accreted igneous layer beneath the eastern continental margin of India and adjoining Bengal Basin. In: 5th conferences and exposition on petroleum geophysics, pp 948–952

McFarlane MJ (1976) Laterite and landscape. Academic Press, London

Miall AD (1985) Architectural element analyses: a new method of analyses applied to fluvial deposits. Earth-Sci Rev 22:261–308

Miall AD (2006) The geology of fluvial deposits. Springer, New York

Miall AD (2014) Fluvial depositional systems. Springer, New York

Nichols G (2009) Sedimentology and stratigraphy. Wiley, New York

Ollier CD, Sheth HC (2008) The high Deccan duricrusts of India and their significance for the 'laterite' issue. J Earth Syst Sci 117(5):537–551

Rajaguru SN et al (1993) Quaternary fluvial systems in upland Maharastra. Curr Sci 64:817–821

Rajaguru SN et al (1994) A fresh look at the Quaternary litho- and bio-stratigraphy of a part of the central Narmada Valley, Narsinghpur district, Madhya Pradesh. In Dikshit KR, Kale VS, Kaul MN (eds) India: geomorphological diversity. Rawat Publication, Jaipiur, pp 435–452

Rajaguru SN et al (2011) Pleistocene climatic changes in western India: a geoarchaeological approach. http://www.tifr.res.in/~archaeo/FOP/…./Rajaguru%20climate.pdf. [27 November 2012]

Schmidt PW et al (1983) Magnetic ages of some Indian laterites. Palaeogeogr Palaeoclimatol Palaeoecol 44:185–202

Singh LP et al (1998) Evolution of the lower Gangetic Plain landforms and soils in West Bengal, India. Catena 33:75–104

Singhvi AK, Kale VS (2009) Palaeoclimatic studies in India: last Ice Age to the present. IGBP-WCRP-SCOPE-Report Ser 4:1–30

Sinha R, Sarkar S (2009) Climate-induced variability in the Late Pleistocene–Holocene fluvial and fluvio-deltaic successions in the Ganga Plains, India; a synthesis. Geomorphology 113:173–188

Sinha R et al (2005) Late Quaternary geology and alluvial stratigraphy of the Ganga basin. Himalayan Geol 26(1):223–240

Sridhar A (2008) Fluvial palaeohydrological studies in western India: a synthesis. Earth Sci India 1(1):21–29

Tardy Y et al (1991) Mineralogical composition and geographical distribution of African and Brazilian periatlantic laterites: the influence of continental drift and tropical palaeoclimates during the past 150 million years and implications for India and Australia. J Afr Earth Sci 12 (2):283–295

Tucker ME (1996) Sedimentary rocks in the field. Wiley, New York

Chapter 2
Lateritic Badland of Sinhati, Bankura, West Bengal: A Geomorphic Investigation

Ankan Aown and Nabendu Sekhar Kar

Abstract Located 4 km NW of Bishnupur town in the Sinhati area of Bankura district, a localized badland has developed in a north–south orientation over the Pleistocene lateritic sediments on the left bank of the River Birai, a tributary of the Dwarakeshwar River. The climatic condition of this region is ideal for development of lateritic badlands by water erosion. Three gully networks have been identified over this 50.8 ha area with dominance of lower-order streams indicating high erosional rates by overland flow and surface runoff. The mean bifurcation ratio is 4.1. A four-facet slope profile is developed here with a lateritic duricrust and mottled layer clearly representing deep weathering. The western section of the badland is more erosive than the eastern section. Typical micro- and mesoscale landforms were recognized, such as escarpment, cliff, duricrust, rills and gullies, gully fans, and so on. The traditional fish breeding practice by embanking gullies makes this badland the most revenue-earning site of the area, which marks it an exception against the general perception of nonproductive badlands. The indigenous technique of fish breeding also acts as an effective measure of restricting soil erosion which can be followed elsewhere. But increasing numbers of commercial fish-breeding farms, resulting from growing market demand, pose a threat of accelerated soil erosion at Sinhati.

Keywords Laterite Gully erosion · Badland · Duricrust · Soil erosion management

A. Aown · N.S. Kar (✉)
Department of Geography, University of Calcutta, 35, Ballygunj Circular Road, Kolkata 700019, India
e-mail: naba1224@gmail.com

B.C. Das et al. (eds.), *Neo-Thinking on Ganges-Brahmaputra Basin Geomorphology*, Springer Geography, DOI 10.1007/978-3-319-26443-1_2

2.1 Introduction

The western part of West Bengal can be divided into two distinct physiographic zones: the degraded part of the Chotanagpur Plateau in the west and plateau fringe fans in the east. These fans are comprised of old alluvium, transported by western tributaries of the Bhagirathi–Hugli River, which coalesces with the Ganga delta in the east (Bandyopadhyay et al. 2014). The major rivers flowing on this plain are the Dwarka, Ajoy, Mayurakshi, Damodar, Darakeshwar, Shilabati, and Kangsabati, among others. Lateritic badlands are common in this plateau fringe plain, traditionally known as the *Rarh Plain*. These low-level lateritic badlands are considered to have originated in situ over the unconsolidated secondary deposits from the high-level sources during the Pleistocene, and reworked later by subaerial weathering (Oldham 1939; Niyogi et al. 1968; Chakraborty 1970; Mallik and Niyogi 1972; Basu 1972; Niyogi and Mallik 1973; Chakrabarty 1985; Bandyopadhyay 1987, 1988; Mukhopadhyay 1992; Das and Bandyopadhyay 1995, 1996; Sen et al. 2004; Dey et al. 2009). Niyogi and Mallik (1973) identified this belt of laterite covering an area of 1000 km^{-2} running approximately NNE–SSW from Farakka through Kharagpur as the Worgram/Kharagpur belt which merges with the coastal laterite tract of Odissa. Ghosh and Majumdar (1981) alternatively suggested that the primary laterites in this belt, capping the alluvial deposits, were reworked and deposited as secondary laterites at a physiographically lower but stratigraphically upper part during the Middle to Late Pleistocene. Laterites are also found at higher levels in the western degraded plateau.

Badlands are barren lands with no or little vegetation cover, very rugged, inaccessible, and of very little or no economic value, developed by active rill and gullying by running water. Localised badlands in the districts of Puruliya, Bankura, Birbhum, and West Medinipur districts of West Bengal have been reported on the above-mentioned laterite belt by many scholars (Shome and Raychaudhuri 1960; Bhattacharya 1957; Goswami 1980; Biswas 1987; Bera and Bandyopadhyay 2013; Laha 2011). Extensive studies on evolution, development processes, channel and drainage character, slope character, and profile character have been carried out. The majority of the works are concentrated specifically on badlands Garhbeta of West Medinipur (Kar and Bandyopadhayay 1974; Bera 1996; Bandyopadhyay 1988; Das and Bandyopadhyay 1995, 1996; Sen et al. 2004; Dey et al. 2009) and Khoai of Birbhum district (Bandyopadhyay 1987; Mukhopadhyay 1992; Das and Bandyopadhyay 1996). Although several localized badlands are reported along the banks of various rivers in Bankura district, intensive study on the badlands of the district are rare.

Located 4 km NW of Bishnupur town in the Sinhati area of Bankura district, a localised badland is developed over the lateritic sediments on the left bank of the River Birai, a tributary of the Dwarakeshwar River. The present work aims to study the processes responsible for its development, analyse its profile and drainage character, and identify the typical landforms developed on it.

2.2 Database and Methodology

The Sinhati badland (23°05′16″N to 23°05′34″N and 87°16′6″E to 87°16′24″E) is situated on the left bank of the River Birai, a tributary of the Darakeshwar River. It falls under the Sinhati village of Ramsagar Gram Panchayat (local administration), located 4 km NW of Bishnupur town of Bankura district, West Bengal (Fig. 2.1).

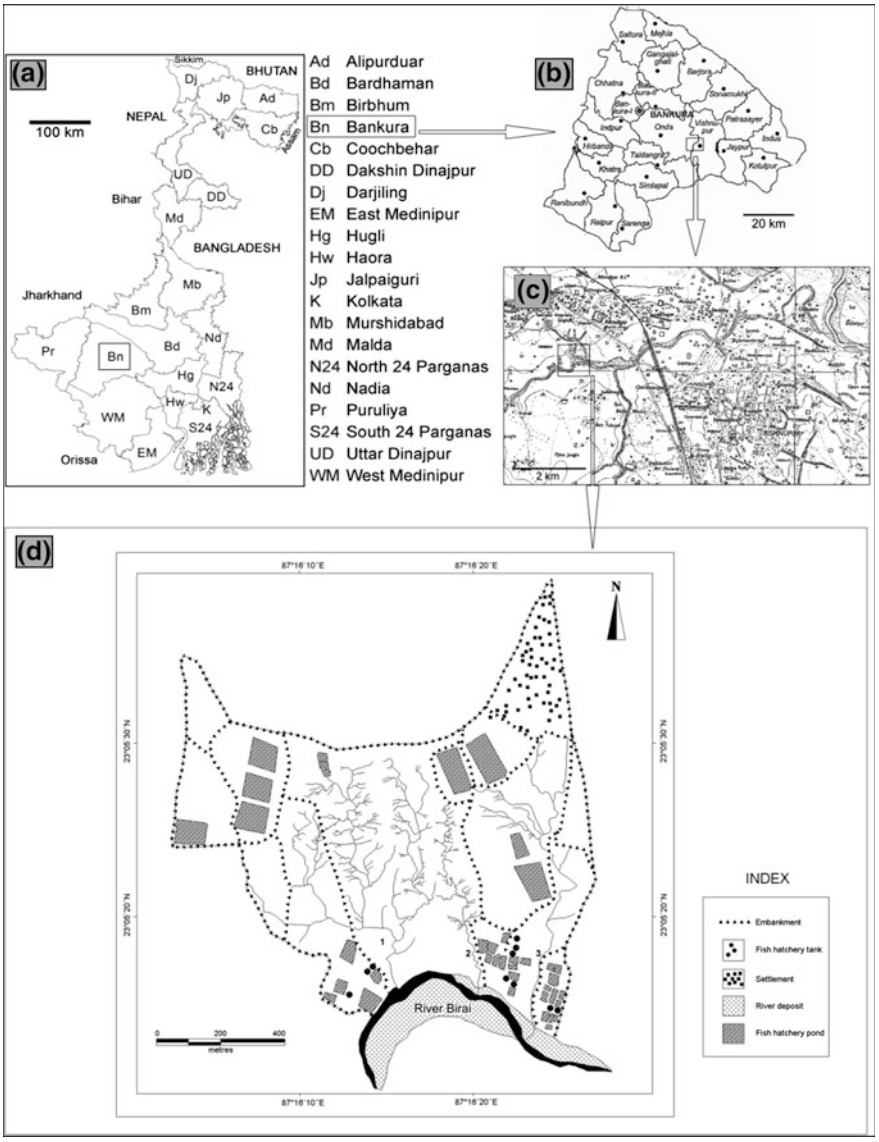

Fig. 2.1 Sinhati badland (**d**) is located 4 km NW of Bishnupur town (**c**) of Bankura district (**b**) of West Bengal (**a**). Three major gully networks annotated *1*, *2*, *3* in (**d**) are responsible for badland development

With active ravine and gully erosion over a lateritic escarpment facing the River Birai, a localised badland was formed in a north–south orientation. This badland covers only a small area of 50.8 ha and is in an early stage of development.

Secondary information on geology and formation of various lateritic badlands of the western part of West Bengal were collected and studied. For the base map, Survey of India topographical sheets (73 M/8 and 73 M/4 on 1:50,000 scale) surveyed in 1970–1972 and CNES/Astrium image (17 Feb 2014) downloaded from the Google Earth platform were used. Information on the geology of the area was obtained from a geological map of Bankura district, published by Geological Survey of India (GSI 2001) and meteorological data were collected from IMD (India Meteorological Department), Alipur office, Kolkata.

The ground survey was conducted using tape, clinometer, Abney level, and GPS (etrax 76csx) to study slope, gully side development, and profile character. Erosional intensity was measured following R.P.C. Morgan's method (1986; Morgan 2009); that is, number of first-order streams × length of the first-order streams per unit area. The mean bifurcation ratio was calculated after Strahler (1957). Various micro- and mesoscale landforms were identified also. Collected data were mapped using PCI Geomatica and Map Info software. Profiles were drawn with field data using Microsoft Excel.

2.3 Results and Discussion

2.3.1 Pluviometric Influence

The monthly average temperature data of 1971–2010 show that high temperature prevails more or less throughout the year in this area and monthly average rainfall data (1971–2010) shows that this region remains dry except the monsoon months (June–October) with 90 % of the annual rainfall (Fig. 2.2). This humid tropical monsoon climate is ideal for laterite development (Thomas 1974; Faniran and Jeje 1983; Battaglia et al. 2011). Short-spanning high-intensity monsoon rainfall over the bare lateritic surface of Sinhati, developed by indiscriminate forest cutting, is also favourable for the formation of badland topography.

Various kinds of water erosion are responsible for the formation of the badland, which are rain-splash, nonconcentrated flow such as sheet flow, and concentrated rill and gully erosion. Stream bank collapse, subsurface piping, slumping, and mass movements were also noticed.

Some morphometric exercises were done to map the intensity of pluviometric processes over the area. First, stream orders were identified following Strahler's law which clearly suggests active erosion by lower-order streams. The highest stream order was identified as fifth order (Fig. 2.3) and the mean bifurcation ratio was 4.1,

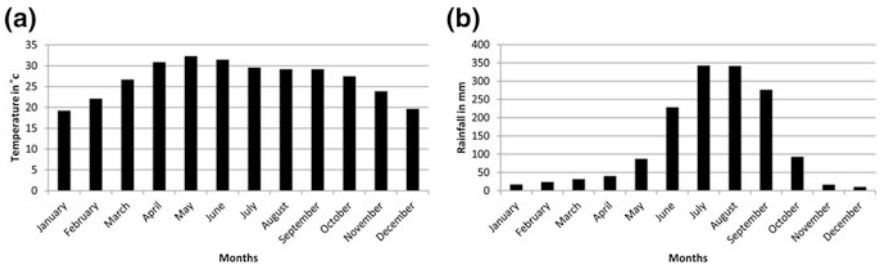

Fig. 2.2 Average (1971–2011) monthly temperature (**a**) and rainfall (**b**) trends of Sinhati are clearly related to the formation of lateritic horizon here (*source* India Meteorological Department)

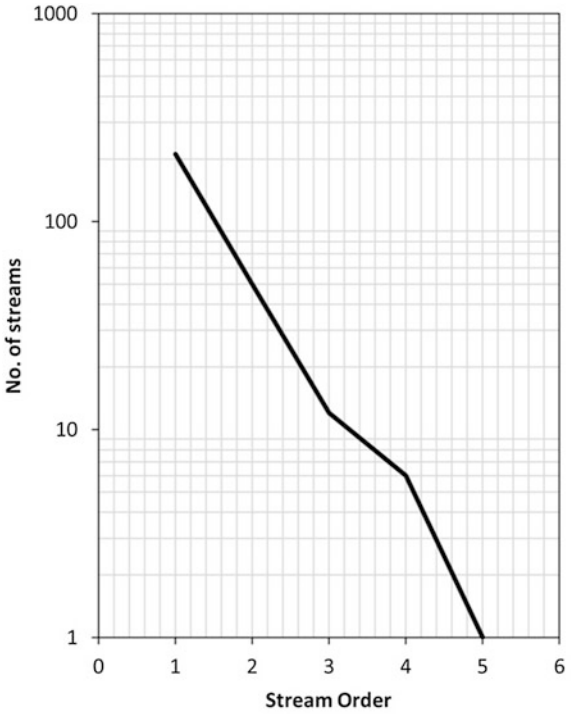

Fig. 2.3 Relation between stream order and number of streams clearly shows the dominance of lower-order streams indicating a high rate of erosion. Mean bifurcation ratio of gully networks of Sinhati is 4.1

which is very high for an area of 50.8 ha. Three major gullies (annotated 1, 2, and 3 in Figs. 2.1d and 2.4a) were identified in the region flowing north–south following the regional slope located in the eastern, middle, and western sections, respectively. The networks of gullies 1 and 2 were separated by a divide whereas gullies 2 and 3 were parted by an embankment built by locals. The natural badland development process of gully 3 was hampered by fish farming activities. Details of the gully network and gully side slope characters are shown on Tables 2.1, 2.2 and 2.3.

Table 2.1 Classification of Gullies at Sinhati Badland

Rill/gully type	Numbers	% of total gully network	Depth (m)	Average width (m)	Side slope (°)	Characteristics
Small	211	75	<1.5	<3	<10	Initial ephemeral channels, unstable and change courses with every shower; comparatively matured ones are distinct to the naked eye and relatively stable; occupy the zone of maximum erosion; headward erosion is prominent
Medium	66	24	1.5–3	3–7	10–30	Small rills coalesce or widen; channels are quite prominent and stable; during shower act as active transporter of sediments
Deep and narrow	3	1	>3	>7	>30	Most distinct and stable with high side slope; carry large amount of water and sediments during wet season

Table 2.2 Details of gully networks at Sinhati badland following Strahler's law of stream ordering (1957)

Gully network	Details	Stream orders				
		1st	2nd	3rd	4th	5th
Gully 1 (West)	Numbers	129	35	7	3	1
	Length (m)	45	12	6	3	12
Gully 2 (Middle)	Numbers	56	12	3	1	0
	Length (m)	12	56	3	3	0
Gully 3 (East)	Numbers	24	4	3	2	0
	Length (m)	11	2	2	10	0

Table 2.3 Gully side-wall types at Sinhati badland

Gully side wall type	Cause of development	Zone of occurrence
Sloping	Rain wash, creep, rill development	Northern midwestern part where small and medium gullies dominate
Vertical	Mass movement	Southern zone occupied by deep gullies

2.3.2 Slope and Profile Character

An east–west cross-section of the badland is shown in Fig. 2.4. From this section it is found that the deepest among the three gullies is gully 1 located on the western section of the area (Fig. 2.4b).

It was revealed from the erosional intensity map (Fig. 2.5) that the midwestern section of the Sinhati badland is most erosive. Sides of all three major gullies showed a four-facet profile comprising a top layer of hardened duricrustic materials (∼1 m) overlain by surficial soil, subrounded quartz pebbles, and loose pisoliths (murram) with diameter ranging between 0.3–2 mm. Below this layer a section of mottled clay and sand was found with orange patches (∼2 m) underlain by a thick facet (∼1.3 m) of pallid ash-white cemented materials of fine sand and clay. A dark layer of very fine (∼1 m) sand and clay was found below it (Table 2.4).

As recorded in a humid tropical environment (Young 1972; Thomas 1974; Faniran and Jeje 1983), the major processes of profile development are lateral erosion and parallel retreat of slopes. These processes are also active in the Sinhati badland. The eastern side of gully 3 was analysed (Fig. 2.4b) to discover the slope segment characteristics (Fig. 2.6).

2.3.3 Landforms

Denudation and deposition gave rise to different meso- and microscale landforms at Sinhati (Fig. 2.7).

Lateritic duricrust: Rock weathering and pedogenesis in a humid tropical climate result in the formation of duricrust. The duricrust of Sinhati, overlying the mottled and pallid horizons, signifies deep weathering (Fig. 2.7a).
Escarpment: An escarpment of ∼10 m height was formed on the left bank of River Birai due to bank erosion (Fig. 2.7b).
Cliff: Cliffs were formed here either by lateral erosion of gully side walls or mass movement (Fig. 2.7c).
Rills: Rills are typical features of badlands. Here intensive networks of rills show the initial signs of water erosion by overland flow and surface runoff (Fig. 2.7d).

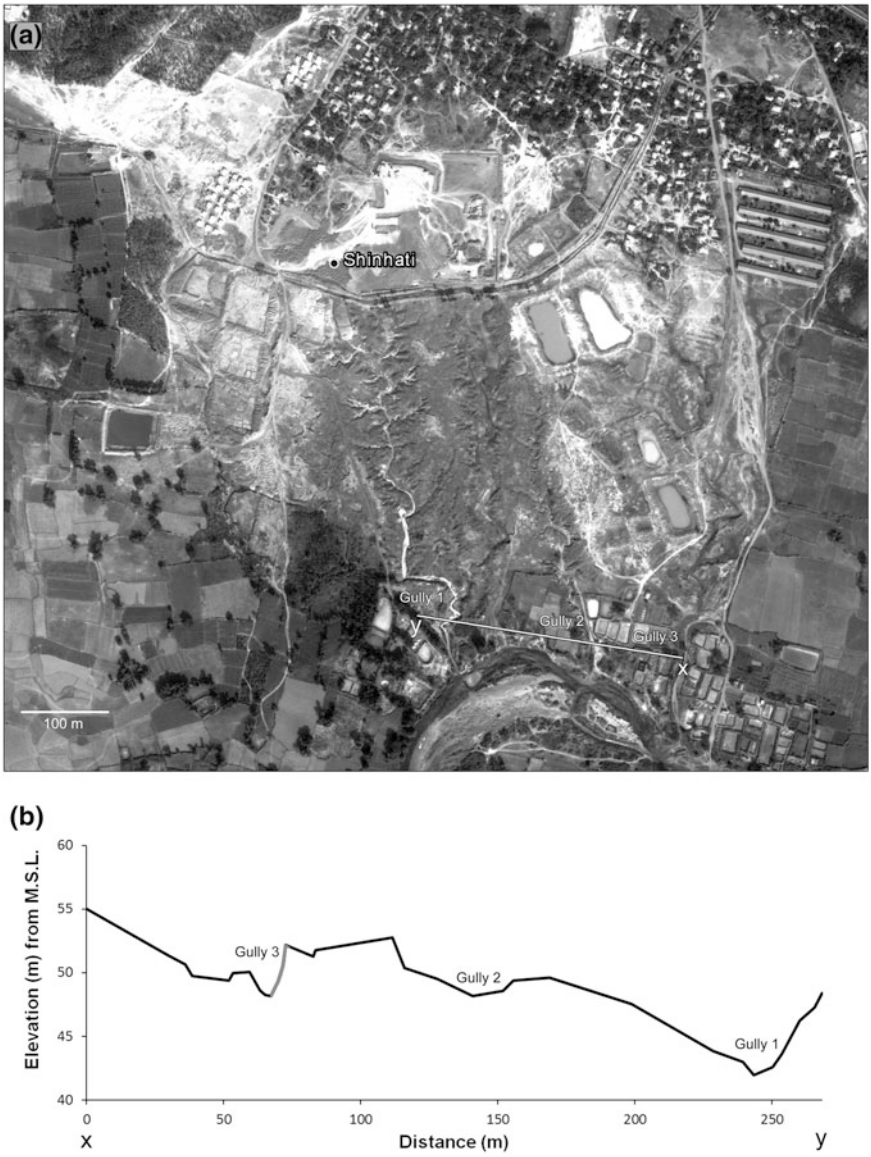

Fig. 2.4 CNES/Astrium image (17 February, 2014) downloaded from Google Earth platform shows the landscape of the area. A cross-profile (*xy*) is drawn with the help of Tape, Abney's level, and GPS shown in (**b**). Gully 3 (*ash colour* part of the section in **b**) side wall horizons are shown in Fig. 2.5

Table 2.4 Lateritic profile of Sinhati badland

Facet	Dominant process	Declinity (°)	Thickness (m)	Characteristics
Surficial soil, subrounded quartz pebbles and pisoliths	Disintegration by mechanical and chemical weathering, surface wash and overland flow.	85–90	~0.2	A surface cover of red soil eroded in many places. It is a weathered duricrust with pisoliths and subrounded quartz pebbles.
Duricrustic layer	Mechanical and chemical weathering. Head and lateral erosion		~1	Hardened layer of nodular duricrust containing iron concentration.
Mottled layer	Chemical and biological weathering, leaching	60–65	~2	A layer of fine sand and reddish mottled clay; partly cemented.
Pallid layer	Leaching, sidewall erosion	20–25	~1.3	An ash-white layer of cemented fine sand and clay.
Dark clay layer	Lateral erosion and basal deposition of eroded materials	10–15	~1	Greyish layer near the gully bed containing very fine sand and clay

Gullies: Three major defined gullies were identified in western (Fig. 2.7e), middle, and eastern sections, respectively (Figs. 2.1d and 2.4a). Average depth of the gullies from their beds is ~5 m.

Gully fan: All three gullies have produced gully fans where they meet the River Birai. The largest of them is created by Gully 1 (Fig. 2.7f) with a maximum width of 15.8 m.

2.3.4 Land Use and Management of Soil Erosion

The Sinhati badland is unique from the point of view of anthropogenic use (Fig. 2.1d). In general badlands are considered unproductive. But in the case of Sinhati, it is the most revenue-earning site of the area. This is the famous fish breeding ground of Bankura district. Fish hatchery ponds were built at the end of gullies by embanking them. During the monsoon season overland flow and surface runoff are stored here. These ponds also act as sediment catchponds. These ponds silt up with eroded materials within a cycle of 5–6 years. Then the fish breeders leave the silted ponds and build new ponds at the end of other newly formed gullies. It is a traditional practice here and quite effective in managing gully erosion.

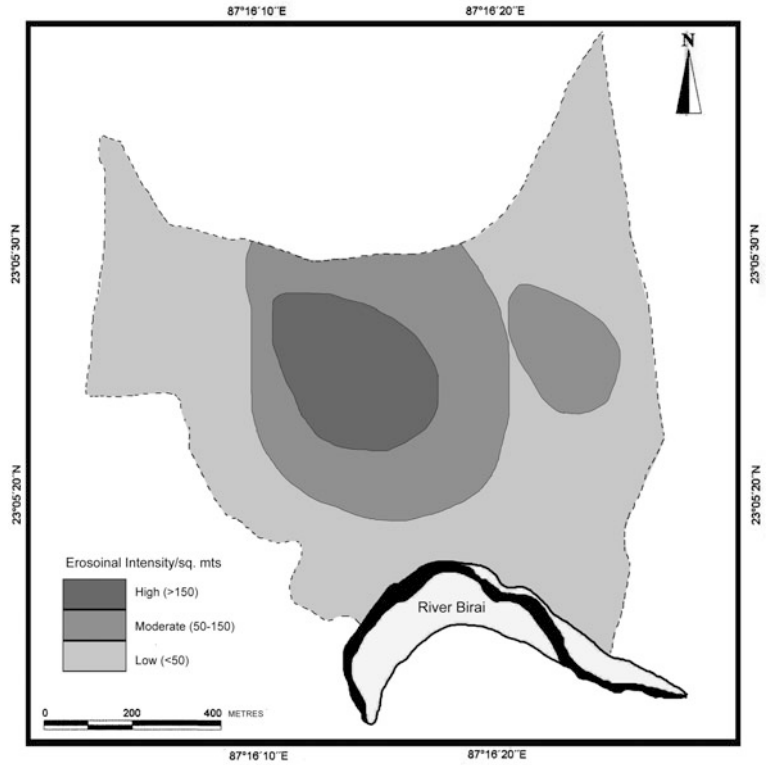

Fig. 2.5 Erosional intensity map of Sinhati Badland shows maximum intensity of erosion concentrating at north-midwestern section due to maximum density of small and medium sized gullies

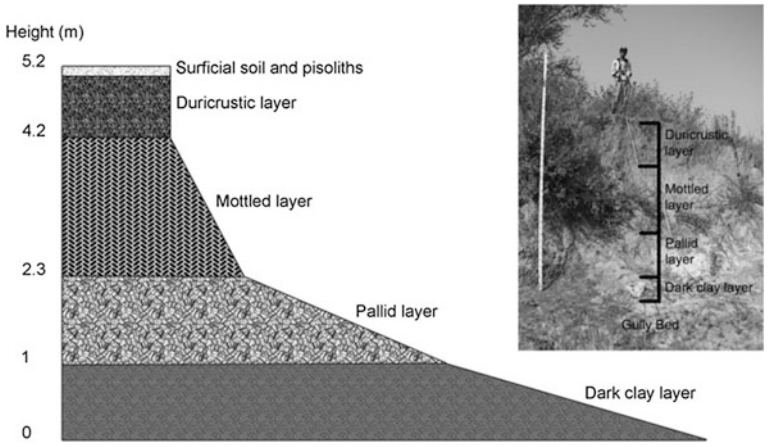

Fig. 2.6 Schematic sketch of eastern side wall of Gully 3 shown with the typical horizons formed over lateritic terrain of Sinhati. Heights indicative of thickness of horizons from local base level (*gully bed*)

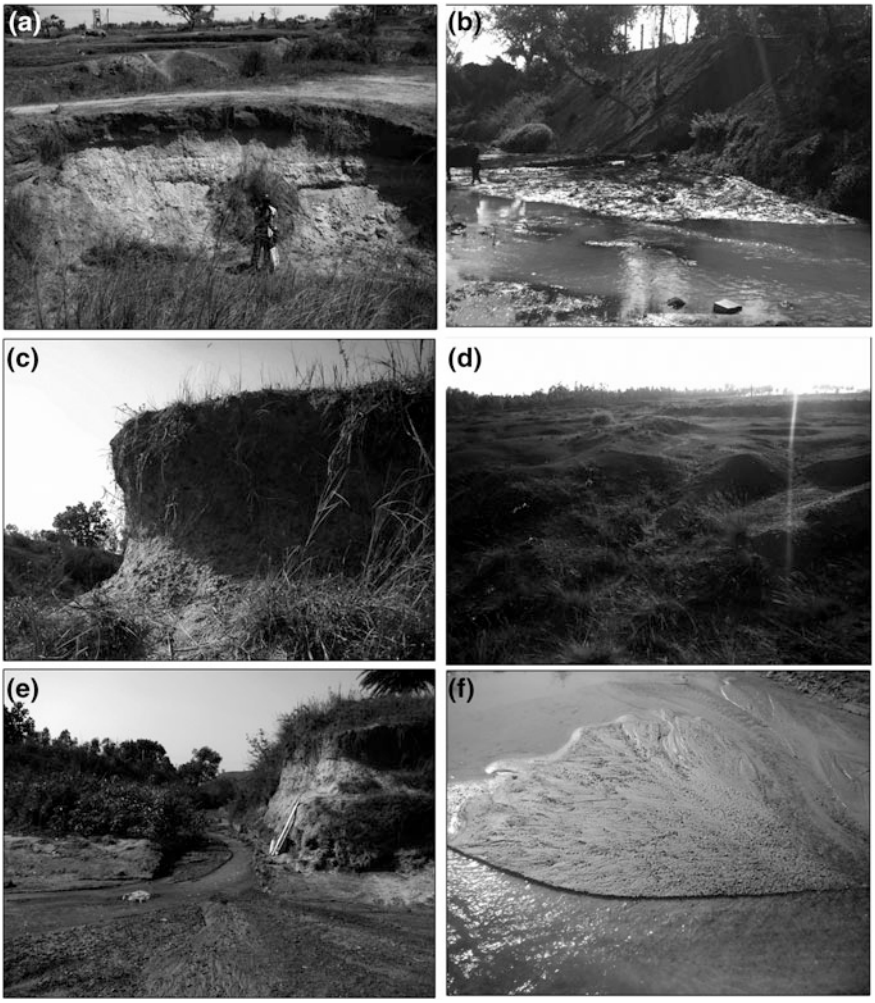

Fig. 2.7 Typical micro- and mesoscale landforms of Sinhati badland. **a** Laterite duricrust, **b** escarpment located on left bank of River Birai, **c** cliff formed by gully erosion, **d** rills, and **e** gully and **f** gully mud fan created by Gully 1

With increasing demand and commercialisation fish breeders are coming to this site and fish breeding practice migrates towards the head of the gullies (Fig. 2.8). This will lead to aggravated erosion of the badland and it should be restricted immediately.

As in the southern section near the River Birai, fish farms for their interest control and check soil loss; a management plan should be formulated by incorporating this traditional practice. Small check dams and bunds must be built at the source area of the gullies, that is, the northwest part where the maximum

Fig. 2.8 Increasing numbers of fish-breeding farms posing threat of accelerated soil erosion at Sinhati

concentration of rills is seen resulting in the maximum rate of corrosion. Mulching, plantation, and grass cover might be good options for restricting soil loss in this source area.

2.4 Concluding Note

Accelerated erosion in lateritic badlands is a major concern of soil erosion management in the tropical world. Various measures are taken for restricting erosion and increasing production of this type of lateritic terrain. Some are conventional techniques including construction of check dams and other sediment-catching structures or modern techniques such as extensive afforestation, biomatting, or chemical matting and the like, aimed at controlling accelerated erosion mainly for the development of agriculture. But in the case of Sinhati, the traditional sustainable practice of use of the badland as a very productive fish breeding ground serves as an operative soil erosion controlling technique. This gives us a new way of thinking about the management of badlands. Instead of cropping, badlands can also be used for other purposes.

References

Bandyopadhyay S (1987) Man-initiated gullying and slope formation in a Lateritic terrain at Santiniketan West Bengal. Geogr Rev India 49(4):21–26

Bandyopadhyay S (1988) Drainage Evolution in a Badland terrain at Gangani in Medinipur district, West Bengal. Geogr Rev India 50(3):10–20

Bandyopadhyay S et al (2014) River systems and water resources of West Bengal: a review. In: Vaidyanadhan R (ed) Rejuvenation of surface water resources of india: potential, problems and prospects. GeolSoc India, Bengaluru, Special Publication 3:63–84

Basu SR (1972) On the formation of a Shoal on the concave bank of Lateritic River Kopai, West Bengal. Geogr Rev India 34(3):287–297

Battaglia S et al (2011) Dynamic evolution of badlands in the Roglio basin (Tuscany, Italy).Catena 86:14–23

Bera S (1996) Remarks of paleoenvironment from the trace fossils from subsurface and outcrop tertiary-quaternary sediments of the western part of Bengal basin. J Geogr Env 1:1–15
Bera K, Bandyopadhyay J (2013) Prioritization of watershed using morphometric analysis through geoinformatics technology: a case study of Dungra Water Sub-Basin, West Bengal, India. Int J Adv Remote Sens GIS 2(1):1–8
Bhattacharya JC (1957) Erosion studies in the Lateritic areas of West Bengal. J Indian Soc Soil Sci 5:103–108
Biswas A (1987) Laterites and lateritoids of Bengal. In: Datye VS, Diddee J, Jog SR, Patil C (eds) Exploration in the tropics, Pune, pp 137–146
Chakrabarty B (1985) Geomorphic process—A case study of Mayurakshi Basin. In: Sen PK (ed) The conecpt and methods in geography, Institute of Geography, Burdwan University, pp 377–382
Chakraborty SC (1970) Some consideration on the evolution of physiography of Bengal. In: Chatterjee AB et al (eds) West Bengal. Geographical Institute, Presidency College, Calcutta, pp 16–29
Das K, Bandyopadhyay S (1995) Badland development over laterite duricrust. In: Jog SR (ed) Indian Geomorphology 1. Rawat Puplication, New Delhi, pp 31–42
Das K, Bandyopadhyay S (1996) Badland development in a Lateritic Terrain: Santiniketan, West Bengal. In: Jog SR (ed) Nat Geogr 31(1 and 2):87–103
Dey S et al (2009) Some regional indicators of the tertiary–quaternary geodynamics in the paleocoastal part of Bengal Basin (India). Rus Geol Geophys 50:884–894
Faniran A, Jeje LK (1983) Humid Tropical Geomorphology. Longman, London, pp 245–269
Ghosh RN, Majumdar S (1981) Neogene–quaternary sequence of Kasai Basin. In: Neogene–quaternary Field Conference, India, pp 63–73
Goswami AB (1980) Hydrology of lateritic terrain of Bankura and Medinipur districts. In: Proceedings of the international seminar on laterisation process, Trivandrum, India, pp 407–410
GSI: Geological Survey of India (2001) District resource map Bankura District (on 1: 250000 scale) Kolkata
Kar A, Bandyopadhyay MK (1974) Mechanism of Rills: an investigation in Micro-Geomophology (Garhbeta Badland). Geogr Rev India 36(3):204–215
Laha M (2011) Spatio-social impact of miniwatershed project at Bhalki, Bardhaman District, West Bengal. Wesleyan J Res 14(1):10–20
Mallick S, Niyogi D (1972) Some physical aspects of development of nodular laterites of West Bengal. Quat J Geol Metall Soc India 44(4):155–174
Morgan RPC (2009) Soil erosion and conservation. Wiley, London
Mukhopadhyay S (1992) Soil erosion in Kopai Basin, Birbhum. J Land Sys Ecol Stud 15(2):22–23
Niyogi D, Mallick S (1973) Quaternary laterite of West Bengal: it's geomorphology, stratigraphy and genesis. Quat J Geol Min Metal Soc India 45(4):155–174
Niyogi D et al (1968) A preliminary study of laterites of West Bengal. In: Seminar in proceedings of gomormhology and geotechnics of the lower Ganga Basin. Indian Institute of Technology, pp A81–A85
Oldham RD (1939) A manual of the geology of India and Burma (Revised and re-written by Pascoe EH), 3rd ed. (1964 reprint). Geological Survey of India, Calcutta, pp 1344–2130
Sen J et al (2004) Geomorphological investigation of badlands: a case study at Garhbeta, West Medinipur District, West Bengal, India. In: Singh S, Sharma HS, De SK (eds) Geomorphology and Environment. ACB Publication, Kolkata, pp 204–234
Shome KB, Raychaudhuri SP (1960) Rating of soils of India. Indian Agricultural Research Institute, Downloaded from www.New.dli.ernet.in/rawdataupload/uploads/insa/…/20005ad5_260.pdf. On 01.01.2015
Strahler AN (1957) Quantitative analysis of watershed geomorphology. Tran Am Geophys Union 38(6):913–920. doi:10.1029/tr038i006p00913
Thomas MF (1974) Tropical geomorphology. Macmillan, London, pp 49–82
Young A (1972) Slopes. Longman, New York, pp 198–201

Chapter 3
Analysis of Channel Asymmetry: A Different Perspective

Balai Chandra Das and Aznarul Islam

Abstract An attempt to measure channel asymmetry of a cross-sectional area of a river was perhaps taken first by Knighton (Quant Indices' Earth Surf Process Landf, 6:581–588, 1981). But his effort did not match his presumptions of keeping the index value within a fixed limit of 0 to 1, especially in his A_1 and A_2 measures. To overcome this and another genetic problem of those indices, this chapter presents alternative measures viz. A_w, A_a, and A_{wa} to the end. For the purpose, simple measures of trigonometry and mensuration, have been employed.

Keywords Asymmetry-Area ($\acute{A}$) · Bankfull width (w) · Channel centre line (L_c) · Channel median area line (L_m)

3.1 Introduction

Asymmetry may be the eternal essence of nature that keeps it dynamic. It is also true for the river channel cross-sectional form. About 90 % of channels are asymmetric (Leopold and Wolman 1960). Cross-sectional forms are asymmetric even in a straight channel (Majumder 2011) with successive bars of alternating pitch (Einstein and Shen 1964; Keller 1972). To measure the degree of asymmetry of a river channel cross-sectional form, Knighton (1981) formulated three indices. Of these three indices, the first (A^*) is very simple to measure the degree of asymmetry of river channel cross-sectional form. However, the second index (A_1) and third index (A_2) considered asymmetry in both directions, that is, horizontal and

B.C. Das (✉)
Department of Geography, Krishnagar Government College, Nadia 741101, India
e-mail: drbalaidaskgc@rediffmail.com

A. Islam
Department of Geography, Barasat Government College, Barasat,
Kolkata 700 124, West Bengal, India
e-mail: aznarulislam@gmail.com

B.C. Das et al. (eds.), *Neo-Thinking on Ganges-Brahmaputra Basin Geomorphology*, Springer Geography, DOI 10.1007/978-3-319-26443-1_3

vertical (Knighton 1981). In the case of horizontal symmetry, one half of the channel appears as a laterally inversed virtual image of other half (Gour and Gupta 1998) of optical physics. Thus a line on the reflection plane may be considered as a centre line of symmetry from which every point on the object and corresponding points on virtual images appear to be at equal distance. The centre line (Knighton 1981) of a cross-section therefore may be considered as a reference line of the measurement of symmetry of the channel. But in the case of vertical asymmetry, the reference line is not defined although the difference between mean depth and maximum depth is considered to be used. But what the expected mean depth of a channel with given cross-sectional area should be is not yet defined. With the words 'increasing vertical asymmetry' Knighton (1981) wanted to mean that the depth is increasing more and more than that of an expected mean depth. But it seems that vertical asymmetry is not possible at all. Therefore what is to be considered in designing an index of asymmetry of river channel cross-sections is simply 'area'. Because the cross-sectional form itself is a two-dimensional concept. Therefore the present chapter has incorporated areal asymmetry as the principal point of consideration and used some simple statistical tools to that end.

3.2 Derivation of Asymmetry Measures

As stated by Knighton (1981), the existence and significance of asymmetry have been studied in allied fields, from the viewpoints of both process action (Kranck 1972; Clifton 1976) and development (Sharp 1963; Tanner 1967; Kennedy 1976). Sharp (1963) defined asymmetry in wind ripple by length of shadow zone (Fig. 3.1a). Tanner (1967) and Reineck and Wunderlich's (1968) asymmetry index was the simple ratio of length of the horizontal projection of the stoss side to that of the lee side (Fig. 3.1b). The effort of Knighton (1981) in measuring channel asymmetry is

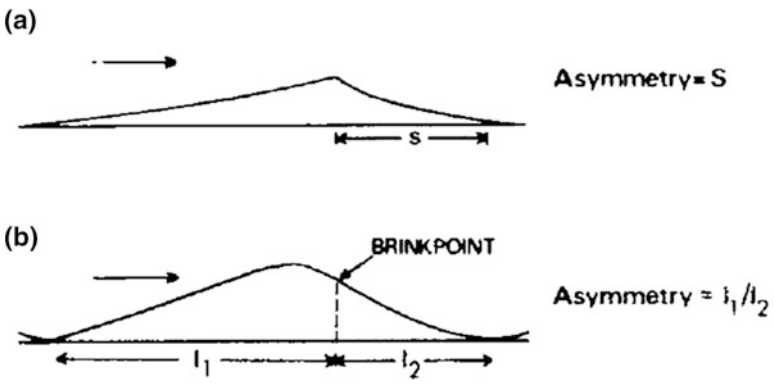

Fig. 3.1 Ripple asymmetry according to **a** Sharp (1963) and **b** Tanner (1967)

perhaps the best one till date. His asymmetry index $A^* = (A_l - A_r)/A$ seems better than two other indices by him. Channel cross-sectional form is a two-dimensional variable. But in indices A_1 and A_2, it seems that the influence of the vertical component has been nullified by the horizontal component. However, asymmetry measures introduced in this chapter are someway new and significant to the field.

An index of asymmetry should as far as possible fullfil certain basic requirements (Knighton 1981):

1. Extreme asymmetry should be expressed by the value '1'.
2. No asymmetry should be expressed by the value '0'.

The second measure in this chapter is the ratio of double asymmetry area ($2\acute{A}$) to the total bankfull area (A) of the channel. $\acute{A}$ is defined as the area between the channel centre line (L_c) and median area line (L_m). Bankfull width ($W = w_l + w_r$ and $w_l = w_r$) of the channel is defined as the horizontal length between the brinkpoint of the levee and high bank. The channel centre line (L_c) is a vertical line from the channel bed to the $W/2$ point separating w_l and w_r, and the median area line (L_m) is the vertical line from the channel bed which divides the cross-sectional area of the channel into two equal halves (Fig. 3.2). The width difference ($\acute{w}$) is the horizontal distance between L_c and L_m.

How far the channel is skewed to the left or right in terms of width can be measured by the simple equation:

$$A_w = (2\acute{w}/W) \tag{3.1}$$

It seems to be a clone of '$2x/w$' of Knighton's (1981) second equation. But Knighton defined 'x' as the horizontal distance between the centre line and the maximum depth line whereas '$\acute{w}$' is the horizontal distance in between the centre line and the median area line (Fig. 3.2).

This is done because, if we think about cases as shown in Figs. 3.3 and 3.4, we must face the problem of uncovering any asymmetry for the case in Fig. 3.4. Here,

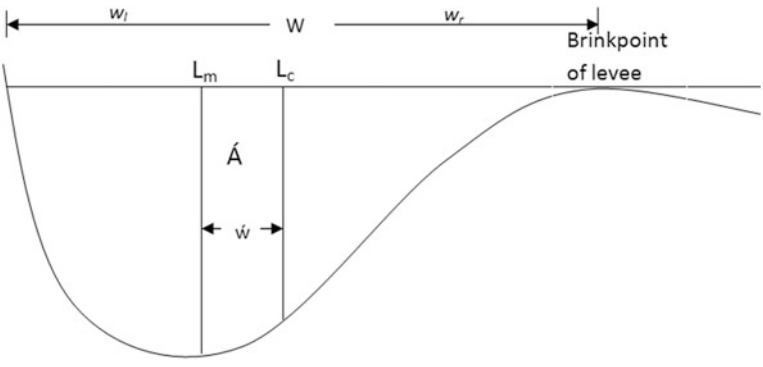

Fig. 3.2 Definition of parameters of an asymmetrical channel

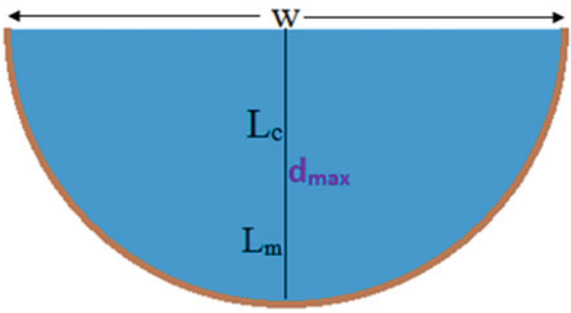

Fig. 3.3 Semicircular channel where L_c, L_m, and d_{max} are the same line and $2x = 0$

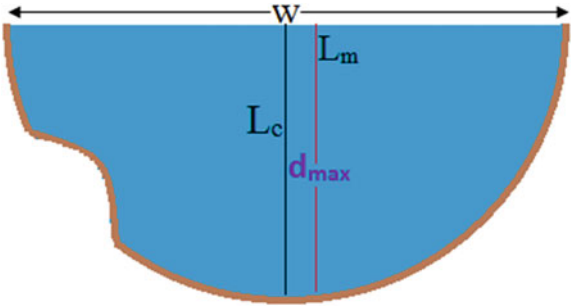

Fig. 3.4 Deformed semicircular channel where L_c, and d_{max} are the same line (*black*), so $2x = 0$; but L_m is a different line (*red*) and $2\acute{w} \neq 0$

the channel center line (L_c) and maximum depth line (d_{max}) are the same line. Hence there is no horizontal distance between L_c and d_{max}. Therefore, $2x = 0$. And $A_1 = \frac{2x}{w} \times \frac{d_{max}}{d} = 0$. If we employ $A_2 = \frac{2x}{w} \times \frac{d_{max}-d}{d}$, it will also produce '0' in both cases of Figs. 3.3 and 3.4. In Fig. 3.3, and in Fig. 3.4, $d_{max} > d$ and in both cases, $x = 0$. Therefore the difference between d_{max} and d has been nullified by the value $x = 0$ and showing both channels are similarly symmetrical.

But, if $A_w = (2\acute{w}/W)$ are employed, it will show no asymmetry for the case shown in Fig. 3.3 and in case of Fig. 3.4, it will produce some value of asymmetry which is $\neq 0$.

In this measure, if the value is '0', the channel is perfectly symmetrical and if it is 1, the channel is 100 % asymmetric in nature.

Asymmetry in width is not a complete measure of the cross-section of a river channel because the cross-section is a variable of two dimensions. Therefore area should be incorporated in the index of asymmetry. For the purpose, the asymmetry area ($\acute{A}$) is multiplied by 2 and result is divided by total area (A).

Therefore, asymmetry in area can be formulated as

$$A_a = \left(2\dot{A}/A\right) \tag{3.2}$$

It seems to be cloned from Knighton's A^* index because $A_a = (2\acute{A}/A) = (A_l - A_r)/A$. Only difference is that, in A*, signs (+, -) are considered which is absent in Aa. But this limitation can be overcome by considering Á as negative when L_c is to the left of the L_m and vise versa. But it is done so that one can calculate $\acute{A}$ from the cross-section from where the $\acute{w}$ is already calculated. However, if one directly subtracts Al from Ar, it will also give the same result because $2\acute{A}$ = absolute difference between A_l and A_r.

However, neither of the two equations separately can explain the degree of asymmetry of the channel in all possible terms. Equation (3.2) does not match with the dimension of cross-sectional area (two-dimensional). The second equation matches the two-dimensional variable of area.

But if the $\acute{A}$ is same for two different cross-sections with equal W but different ẃ (Fig. 3.5), then the second equation (A_a) will produce the same result for both cross-sections although there is a difference in width asymmetry (A_w) of the two cross-sections. Reversely, if the ẃ is the same for two cross-sections with equal w but different $\acute{A}$ (Fig. 3.6), then the first equation (A_w) will produce the same results for both cross-sections although there is a great difference in asymmetry of the areas (A_a) of the two cross-sections. To avoid the problem, the two equations can be amalgamated as

$$A_{wa} = (2\acute{w}/W) \times \left(2\acute{A}/A\right) \tag{3.3}$$

Therefore, incorporating both Eqs. (3.1) and (3.2), both measures of horizontal asymmetry and vertical peakedness are aptly amalgamated in a single equation (Eq. 3.3). Again, if the third equation of the present work and Knighton's A_1 and A_2 are to measure the degree of horizontal and vertical asymmetry of channels,

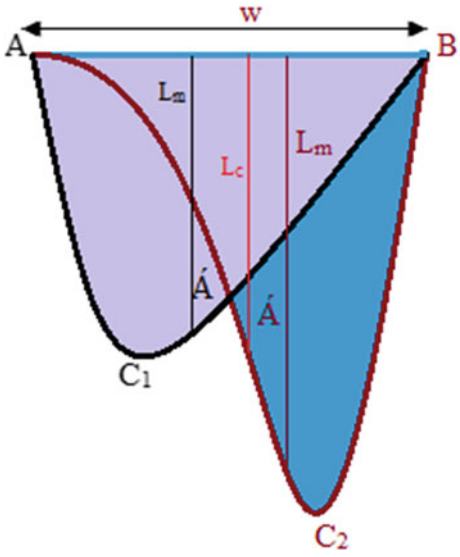

Fig. 3.5 Two cross-sections AC_1B and AC_2B with equal w but different $\acute{w}$

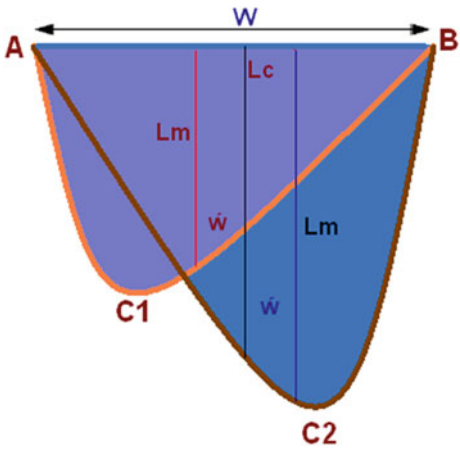

Fig. 3.6 Two cross-sections AC_1B and AC_2B with equal w and $\acute{w}$ but different $\acute{A}$

all these three measures are best suited for comparison among different channels. But if the degree of vertical asymmetry of a single cross-section is to be determined, then knowing the standard or ideal depth for a given cross-section is a precondition (Das 2014, 2015a, b; Das and Mukhopadhay 2015; Das and Islam 2015; Hickin 2004).

3.3 Discussion

The indices designed are based on a simple and basic consideration of trigonometry and mensuration. In the A_1 and A_2 measures of Knighton (1981), the first ratio and the second ratio of the equations do not give '0' simultaneously (Figs. 3.7 and 3.8). And the 'zero value' of one part may bring down the real numerical value of the other part to zero.

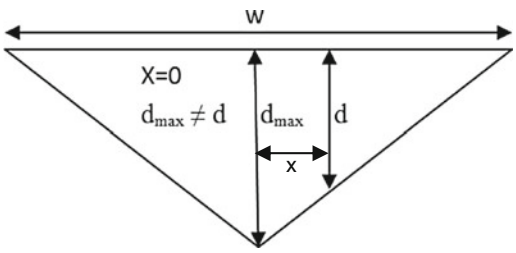

Fig. 3.7 Symmetrical triangular channel with $d \neq d_{max}$

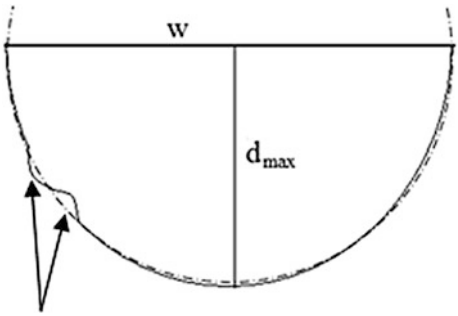

Fig. 3.8 Symmetrical semicircular with $d \neq d_{max}$

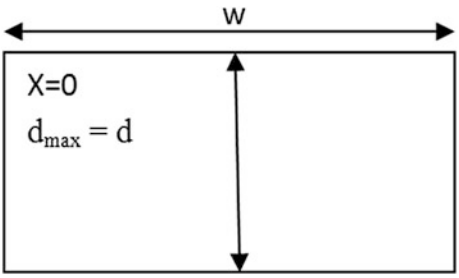

Fig. 3.9 Symmetrical rectangular with $d = d_{max}$

But in Eq. (3.3) of this chapter the first ratio and second ratio of the equation give '0' simultaneously (Figs. 3.3, 3.4 and 3.5) and no part is affected by the other (Fig. 3.9).

3.4 Testing of A^*, A_1, A_2 and A_w, A_a, A_{wa} on Natural Channel

Asymmetry of a number of cross-sections of a bankfull channel has been computed (Tables 3.1 and 3.2) based on a real river channel (River Jalangi in the district of Nadia, West Bengal, India) using indices by Knighton (1981) and indices designed in this chapter.

The correlation among the asymmetry indices depicts a very strong relation between $2x/w$ and A_1 and A_2 (Table 3.3). This apparent strength of the relationship is due to the consideration of the depth in all the cases. There has been a close association among these three indices of Knighton (1981) as appeared in the component plot derived from principal component analysis (PCA). Another group of indices consisting of A_w, A_a, or A^*, and A_{wa} are related strongly. These four indices have depicted a close association in the component plot. It is to mention that A_a is a cloned form of A^* but computed from different perspectives. Continuing from the case as stated in Fig. 3.4, it is to mention that $2x/w$, $A1$, and $A2$ are not able

Table 3.1 Channel Asymmetry Indices as per Present Chapter for Some Cross-Sections of Jalangi

C.S. No.	W (m)	$\acute{w}$ (m)	$2\acute{w}$ (m)	$A_{w\ =}\ 2\acute{w}/w$	$\acute{A}$ (m^2)	$2\acute{A}$ (m^2)	A (m^2)	$A_{a\ =}\ 2\acute{A}/A$	A_{wa}
1	144.43	12.00	24.00	0.17	132.56	265.12	917.35	0.29	0.05
2	142.00	1.60	3.20	0.02	6.64	13.28	1117.53	0.01	0.00
3	152.00	9.00	18.00	0.12	117.17	234.34	873.24	0.27	0.03
4	294.00	45.00	90.00	0.31	456.23	912.46	1319.24	0.69	0.21
5	206.00	21.00	42.00	0.20	369.33	738.66	1866.24	0.40	0.08
Mean	187.69	17.72	35.44	0.16	216.39	432.77	1218.72	0.33	0.07
SD	64.94	16.76	33.52	0.10	188.27	376.54	403.05	0.25	0.08
CV	0.35	0.95	0.95	0.64	0.87	0.87	0.33	0.74	1.10

Source Computed by the authors, 2015
For the present chapter, if A_a and A_w are:
<0.25, channel is considerably asymmetric
>0.25 but <0.5, channel is strongly asymmetric
>0.50, channel is very strongly asymmetric
And if:
A_{wa} < 0.0625, channel is considerably asymmetric
A_{wa} > 0.0625 but <0.25, channel is strongly asymmetric
A_{wa} > 0.25, channel is very strongly asymmetric

Table 3.2 Channel Asymmetry Indices of Knighton for the Same Cross-Sections of Jalangi

C.S. No.	X (m)	d_{max} (m)	W (m)	d (m)	$d_{max} - d$	$A_1 = 2x (d_{max})/d$	$A_2 = 2x (d_{max} - d)A$	$x/(w/2) = 2x/w$
1	45.00	12.90	144.43	6.35	6.55	1.27	0.64	0.62
2	2.00	14.80	142.00	7.87	6.93	0.05	0.02	0.03
3	7.00	13.78	152.00	5.74	8.03	0.22	0.13	0.09
4	32.00	14.12	294.00	4.49	9.63	0.69	0.47	0.22
5	23.00	17.75	206.00	9.06	8.69	0.44	0.21	0.22
Mean	109.00	73.35	938.43	33.51	39.83	2.66	1.47	1.18
SD	17.71	1.85	64.94	1.79	1.26	0.47	0.25	0.23
CV	0.16	0.03	0.07	0.05	0.03	0.18	0.17	0.19

Source Computed by the authors, 2015

to diagnose the asymmetry present in the cross-section. But A^* is capable of doing it. And A^* has a strong close relation with A_w, A_a, and A_{wa}, which means these equations are also as efficient as A^*. This asymmetry index A^* or A_a is the simplest and very significant in the domain of asymmetry analysis. The indices proposed in this chapter conform to the A^* of Knighton but not to A_1 and A_2 (Fig. 3.10).

Table 3.3 Correlation matrix for the asymmetry indices

		$2X/W$	A_w	A_a/A^*	A_{wa}	A_1	A_2
Correlation	$2X/W$	1.000	0.362	0.232	0.136	**0.974**	**0.903**
	A_w	0.362	1.000	0.989	**0.938**	**0.529**	**0.658**
	A_a	0.232	**0.989**	1.000	**0.957**	0.414	**0.563**
	A_{wa}	0.136	**0.938**	**0.957**	1.000	0.339	**0.514**
	A_1	**0.974**	**0.529**	0.414	0.339	1.000	**0.976**
	A_2	**0.903**	**0.658**	**0.563**	**0.514**	**0.976**	1.000

Source Computed by the Authors, 2015

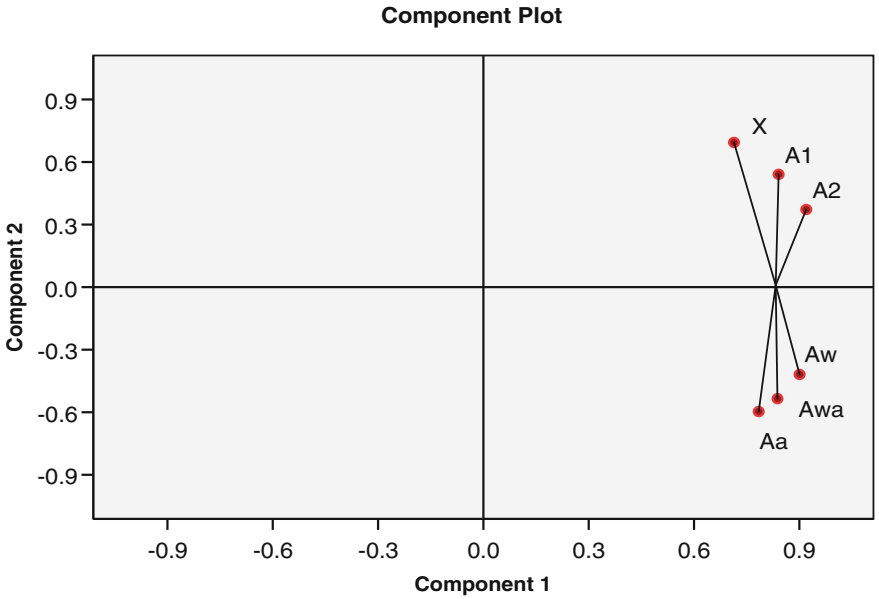

Fig. 3.10 Clustering of asymmetry indices. *Note X* in the component plot indicates $2x/w$

3.5 Conclusion

Asymmetry of different natural forms and processes has already been quantified and studied by different branches of natural science. Cross-sectional asymmetry of a river channel is a determinant of the alternate 'scour holes and meandering flow' of a river (Einstein and Shen 1964; Callander 1978). But asymmetry in a river channel before Knighton (1981) was found in the literature (Callander 1978) only. Therefore his effort is undoubtedly a benchmark in the field. Considering all the aspects of asymmetry indices, it can be concluded that A^* is a better index than A_1 and A_2 to the channel asymmetry where both vertical and horizontal dimensions are incorporated in a single variable of area. Moreover all the preconditions of an index

are maintained in this equation. Measures formulated in this chapter are free from technical problems and anonymity (explained earlier) which are present in Knighton's indices. Here all kinds of symmetrical channel are expressed as '0' and the extreme asymmetry is never exceeded by the value '1'.

References

Callander RA (1978) River meandering. Ann Rev Fluid Mech 10:129–158
Clifton HE (1976) Wave-formed sedimentary structures-a conceptual model. In: Davis RA, Ethington RL (eds) Beach and nearshore sedimentation, Society of Economic Palaeontologists and Mineralogists, Special Publication 24:126–148
Das BC (2014) Asymmetry of river channel cross-sections: a review. Int J Res Manag Sci Technol (E-) 2(3):15–18. Available at www.ijrmst.org (ISSN: 2321-3264)
Das BC (2015a) Modeling of most efficient channel form: a quantitative approach. Model Earth Syst Environ (ISSN 2363-6203). doi:10.1007/s40808-015-0013-6
Das BC (2015b) In search of ideal form-ratio of triangular channel. Stud Ubb Geogr ROMANIA 59(2):77
Das BC, Islam A (2015) Channel asymmetry of an Ox-Bow Lake: a different perspective. Int J Ecosys Sci Acad Pub (p-ISSN: 2165-8889, e-ISSN: 2165-8919)
Das BC, Mukhopadhay S (2015) Comparison of channel-form indices (C_fI) between lake and river channels. Int J Res Manag Sci Technol 3(3):60–63 (E-ISSN: 2321-3264)
Einstein HA, Shen HW (1964) A study of meandering in straight alluvial channels. J Geophys Res 69:5239–5247
Gour RK, Gupta SL (1998) Engineering physics. Dhanpat Rai Publications, Delhi
Hickin EJ (2004) River hydraulics and channel form. Wiley, Chichester, p 6.2
Keller EA (1972) Development of alluvial stream channels: a five-stage model. Geol Soc Am Bull 83:1531–1536
Kennedy BA (1976) Valley-side slopes and climate. In: Derbyshire E (ed) Geomorphology and climare. Chichester, Wiley, pp 171–202
Knighton AD (1981) Asymmetry of river channel cross-sections: part I. Quant Indices' Earth Surf Process Landf 6:581–588
Kranck K (1972) Tidal current control of sediment distribution in Northumberland Strait, Maritime Provinces. J Sedim Petrol 42:596–601
Leopold LB, Wolman MG (1960) River *meanders*. Geol Soc Am Bull 71:769–794
Majumder T (2011) Rajpat (in Bengali). Ananda, Kolkata
Sharp RP (1963) Wind ripples. J Geol 71:617–636
Tanner WF (1967) Ripple mark indices and their uses. Sedimentology 9:89–104
Wunderlich F, Reineck HE (1968) Zur Unterscheidung von asymmetrischen Oszillationsrippeln und Stromungsrippeln. Senckenbergiana Lethaea 49:321–345

Chapter 4
Present Geomorphic Categorization of Alluvial Channel Reaches Using Channel Dimensions and Geomatics in the Damodar River of West Bengal, India

Sandipan Ghosh

Abstract Quaternary to Recent floodplains and the channel bed of the Damodar River (West Bengal, India) are gradually formed by a complex interaction of fluvial processes and anthropogenic processes but their character and evolution are essentially the product of stream power, channel dimensions, and sediment character. The relation between a stream's ability to entrain and transport sediment and the erosional resistance of floodplain alluvium (that forms the channel boundary of the Damodar River) provides a basis of genetic classification of alluvial reaches and floodplains. The alluvial segment of the Damodar River, in between Rhondia (23° 22′08″N, 87°28′25″E) and Paikpara (23°00′58″N, 87°57′41″E), was selected as the study area to identify its special hydrogeomorphic individuality and multidimensionality. The pattern and configuration of the fluvial landscape of the Damodar was recognized using ASTER DEM, GIS analytical tools, channel dimensions, and multivariate statistics, treating each segment of channel and cross-sectional profile as a unit of geomorphic study. The analysis showed that the Damodar River (Rhondia to Bardhaman) was regarded as a bed-load channel with a medium-energy noncohesive floodplain upstream of the study area, and the downstream stretch (Basrsul to Paikpara) was identified as a mix-load channel with a low-energy cohesive floodplain. Multivariate statistical analysis categorized the study unit of the Damodar River into two parts: the upstream section of the river tended to braiding and lateral expansion, and the downstream section of the river tended to meandering and lateral confinement.

Keywords Channel dimension · Floodplain · Geomatics · Damodar river · ASTER · PCA

S. Ghosh (✉)
Department of Geography, Chandrapur College, Chandrapur, Bardhaman, West Bengal 713145, India
e-mail: sandipanghosh19@gmail.com

B.C. Das et al. (eds.), *Neo-Thinking on Ganges-Brahmaputra Basin Geomorphology*, Springer Geography, DOI 10.1007/978-3-319-26443-1_4

4.1 Introduction

Fluvial landscapes have been a source of fascination and inspiration for humans for thousands of years. Admiring the visual expressions of fluvial landforms, artists have striven to capture the essence of landscapes through paintings, prose, poetry, song, or other media, but they vary markedly from place to place as the landscapes are changed. On other side carrying a scientific understanding, the geomorphic enquiry of researchers entails the description and explanation of fluvial landscape forms, processes, and genesis in respect to space and time (Fryirs and Brierley 2013). Implicitly, it requires both a genetic understanding of the physics and mechanics of the process and an appreciation of the dynamic behaviour of landscapes as they evolve through time (Charlton 2008; Fryirs and Brierley 2013). The pattern or planform of a river can be considered at vastly variable scales, depending upon both the size of the river and the part of the fluvial system that is under consideration (Schumm 1985). In the hydrogeomorphic approach to fluvial study, an individual river or segment of a river can vary significantly downstream, changing its channel dimensions and pattern dramatically over a short distance. The most important fact about a segment of an alluvial river is that it is susceptible to major pattern change and to significant shifts in channel position as the alluvium is eroded, transported, and deposited and as the sediment load and water discharge alter (Schumm 1985). Reaches are singular because of the numerous variables acting that prevent a single variable, discharge, from dominating river morphology and behaviour (Leopold and Wolman 1960; Schumm 2005). The genetic classification of rivers and floodplains was developed by Schumm (1977, 1985), Nanson and Croke (1992), and Rosgen (1994). But except in India, these classification systems have been widely applied by researchers to identify the different reaches of rivers with their individuality. The classification of natural rivers has long been a goal of individuals working with rivers to define and understand the processes that influence the pattern and character of river systems (Rosgen 1994). Categorizing the reaches of a river we can (Schumm 1985; Rosgen 1994; Fryirs and Brierley 2013; Williams 1986; Garde 2006):

1. Predict a river's behaviour from its appearance
2. Develop specific hydraulic and sediment relations for a given morphological channel type and state
3. Provide a mechanism to extrapolate the site-specific character unique to fluvial dynamics
4. Provide a consistent and reproducible frame of reference to understand the multidimensionality of major components included in the fluvial systems

After more than 60 years of legacy it is expected that upstream reservoirs of the Damodar Valley Corporation (DVC), Durgapur barrage, Anderson weir, canals, and embankments have posed significant influence on the lower segment of the Damodar River which is notorious for monsoon floods in southern West Bengal. The annual changes in alluvial cross-sections and current status of channel dimensions may indicate the unique individuality of reaches which varies downstream. Dynamic

fluvial landscapes are so linked and sensitive that any changes in external and internal components can create a rapid response from the fluvial system (Sridhar 2007). Each response due to disturbance or management activity at one place and time may have off-site consequences over various timeframes (Fryirs and Brierley 2013). The pattern and configuration of the Damodar River can be derived from its composition (the kinds of elements it contains), its structure (how they are arranged and interplayed in space), and its behaviour (how it adjusts over time to various impulses for change). This chapter attempts to appraise how the fluvial features and channel dimensions fit together in the alluvial reaches of the Damodar River. Meaningful identification, classification, and description underpin effective explanation, providing a platform with which to make realistic predictions about likely future states.

4.2 Geographical Facets of Study Area

The river Damodar, historically known as the 'river of sorrow' or 'sorrow of Bengal' (Bhattacharyya 2011), was characterized by its annual occurrence of high magnitude floods (more than 10,000 m^3 s^{-1}) in the lower basin (i.e. southern West Bengal) till the pre-dam period (up to 1957; Sanyal et al. 2013). The Damodar River has good meteorological and hydrogeomorphic potentiality of extreme floods because its entire fan-shaped basin is situated in the major rainstorm zone and cyclone-affected region of the Bay of Bengal. The furious Damodar River originates from the Khamarpat Hill of the Chandwa CD Block (Palamau district, Jharkhand) and it is one of the longest east-flowing rivers (542 km length) of the Chotanagpur Plateau (Sen 1985; Chandra 2003; Bhattacharyya 2011). Downstream of Asansol the river crosses the hindrances of Durgapur Barrage and Anderson Weir, and after that it flows almost straight up to Barsul, traversing the laterite *Rarh* Plain (Early Pleistocene Litho-unit), the Sijua Litho-unit (Older Alluvium—Late Pleistocene to Early Holocene) and Chuchura Litho-unit (Newer Alluvium—Mid to Late Holocene) (Niyogi et al. 1970; Niyogi 1975; Bhattacharya and Dhar 2005). The straightness of course and low sinuosity of the lower Damodar are the direct result of three successive major faults: the Chotanagpur Foot-hill Fault, the Medinipur–Farraka Fault, and the Damodar Fault (Singh et al. 1998). Finally with an abrupt southerly bend near Palla (due to the Damodar Fault), below Paikpara it bifurcates into (1) the Kanki–Mundeswari and (2) the Damodar–Amta Channel and joins with the Hooghly River at Falta some 48.3 km south of Kolkata (Chandra 2003; Bhattacharyya 2011). For this sample study we have selected the lower segment of the Damodar (Fig. 4.1) in between Rhondia (Galsi I CD Block) and Paikpara (Jamalpur CD Block). The latitudinal extension of the selected area ranges from 22°00′ to 23°22′N and longitudinal extension varies from 87°28′ to 88°01′E. Under the DVC (Damodar Valley Corporation) and Lower Damodar Scheme of the IWD (Irrigation and Waterways Department, West Bengal), the entire downstream

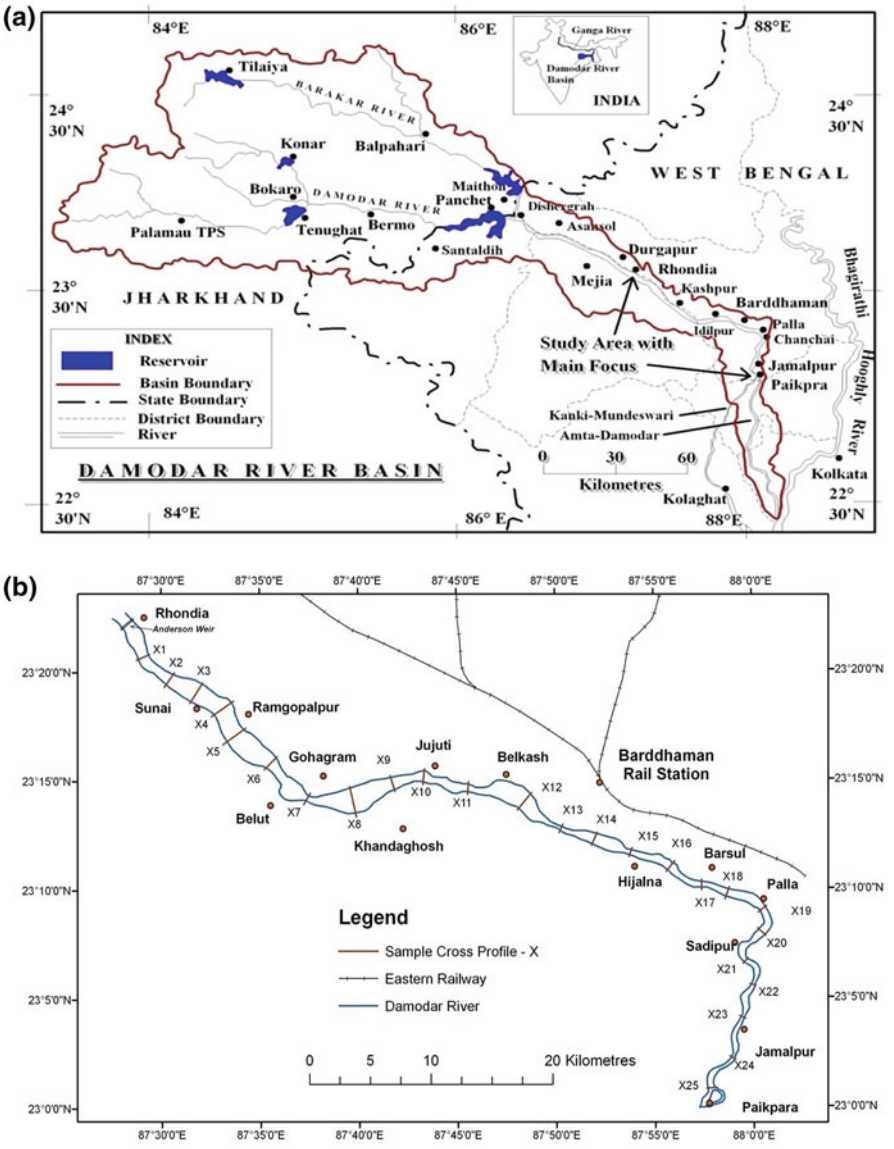

Fig. 4.1 **a** Location map of Damodar River Basin including area under study (after Ghosh and Guchhait 2014a, b), and **b** sample cross-sections (X1 to X25) across the Damodar River in between Rhondia and Paikpara

segment of the Damodar River is forced to transform from a natural channel to a 'reservoir channel' to manage recurrent floods (Sen 1991; Lahiri-Dutt 2006; Bhattacharyya 2011; Sanyal et al. 2013). The monsoon runoff of the Damodar and

Barakar catchments is managed by the large dams of Tilaiya, Konar, Maithon, Panchet, Durgapur Barrage, and Tenughta (Chandra 2003; IWD 2013).

4.3 Materials and Methods

Empirical observation of landforms is an approach by which researchers and scholars use their knowledge and experience to identify the assemblage of landforms or features that make up rivers, develop hypotheses to interpret the processes responsible for those landforms, determine how those features have adjusted and changed over time, and, finally, place this understanding in its spatial and temporal context (Fryirs and Brierley 2013). The long, continuous, up-to-date, and reliable hydrological records and geomorphic data are an indispensable part in the study of changing fluvial dynamics and flood risk assessment. In this context the constructivist (building block) approach to analysing the fluvial landscape is adopted here to assess the functionality of each part of the fluvial system relating to major channel dimensions and geometry. This 'bottom up approach' (Fryirs and Brierley 2013) synthesises the behaviour of fluvial components and evolution of landforms through systematic analysis of channel segments treating each reach as an individual unit of study (Fig. 4.2).

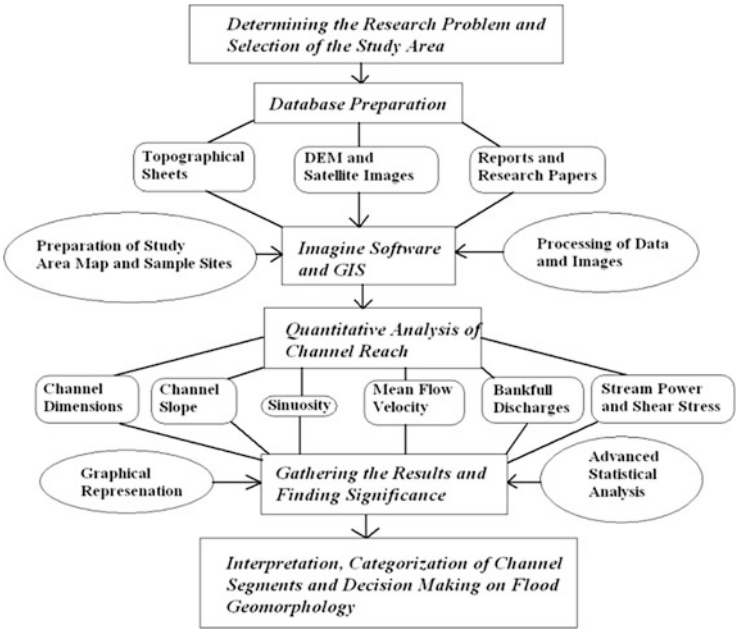

Fig. 4.2 Flowchart of methodology used in this study (after Ghosh and Guchhait 2014c)

Geomatics is an agglomeration of geospatial technologies which includes mainly spatial data, remote sensing, land surveying, cartography, GIS (geographic information system), global positioning system (GPS), and advanced geographical techniques in one forum to assess the practical problems. In this case the secondary hydrogeomorphic data and other geospatial information are mostly collected from the *Damodar Planning Atlas* (Chatterjee 1969), the book entitled *Lower Damodar River, India: Understanding the Human Role in Changing Fluvial Environment* (Bhattacharyya 2011), the official website of the Irrigation and Waterways Department of West Bengal, topographical sheets of R.F. 1: 50,000 (73 M/7, M/11, M/12, M/15, M/16, N/13, and 79 A/4) of Survey of India (SOI), ASTER data (2011), satellite images of IRS-P6 LISS IV (2008), Landsat ETM (2000), and Google Earth. The quantitative channel morphology is derived from the remotely sensed satellite data, *Advanced Spaceborne Thermal Emission and Reflection Radiometer* (ASTER), which has five remote sensory devices on board the Terra satellite launched into earth orbit by *National Aeronautics and Space Administration* (NASA) in 1999 (USGS; United States Geological Survey 2013). On 29 June 2009, the Global Digital Elevation Model (GDEM) of ASTER was released to the public having a spatial resolution of 30 m (USGS 2013). Here using processed ASTER DEM (digital elevation model) data of 2011 (http://earthexplorer.usgs.gov/), Global Mapper 14.2 software (using the technique of 3D path analysis and cut and fill volumes), and ArcGIS 9.3 software, we have taken 25 cross profiles,as representative ungauged sites of the Damodar River (Fig. 4.3), in between Anderson Weir, Rhondia (last water releasing controlled point) and Paikpara (bifurcation point, Damodar and Mundeswari). The main quantification of channel dimensions includes channel cross-sectional area (A_b), volume of channel reach in between two cross-sections (V_P), bankfull width (W_b), maximum depth (i.e. thalweg depth) of that profile (D_{max}), and width: depth ratio (W/D; Fig. 4.3). Alongside we have calculated the maximum width:depth ratio (W_b/D_{max}), sinuosity (Si), entrenchment ratio (ER), and channel slope (S). All morphological and statistical analysis was done towards the downstream segment from Rhondia to explain the variations with flow direction. As the river is seasonally dry or a single-thread channel in winter and summer, the ASTER data of December was very useful to study the channel-bed morphology (Fig. 4.4).

The empirical relationships (developed by Leeder 1973; Rotnicki 1983, Williams 1988; Pickup and Warner 1984; Kale et al. 2004) among channel dimensions, planform characteristics, and discharge have been compared and applied to derive the present hydrogeomorphic individuality of the controlled Damodar River. The important statistical techniques viz. mean, standard deviation, Pearson's product moment correlation, coefficient of determination, principal component analysis, Z-score, and so on (Mahmood 2007; Kothari 2009) were employed to derive a significant conclusion about the fluvial dynamics of an alluvial river.

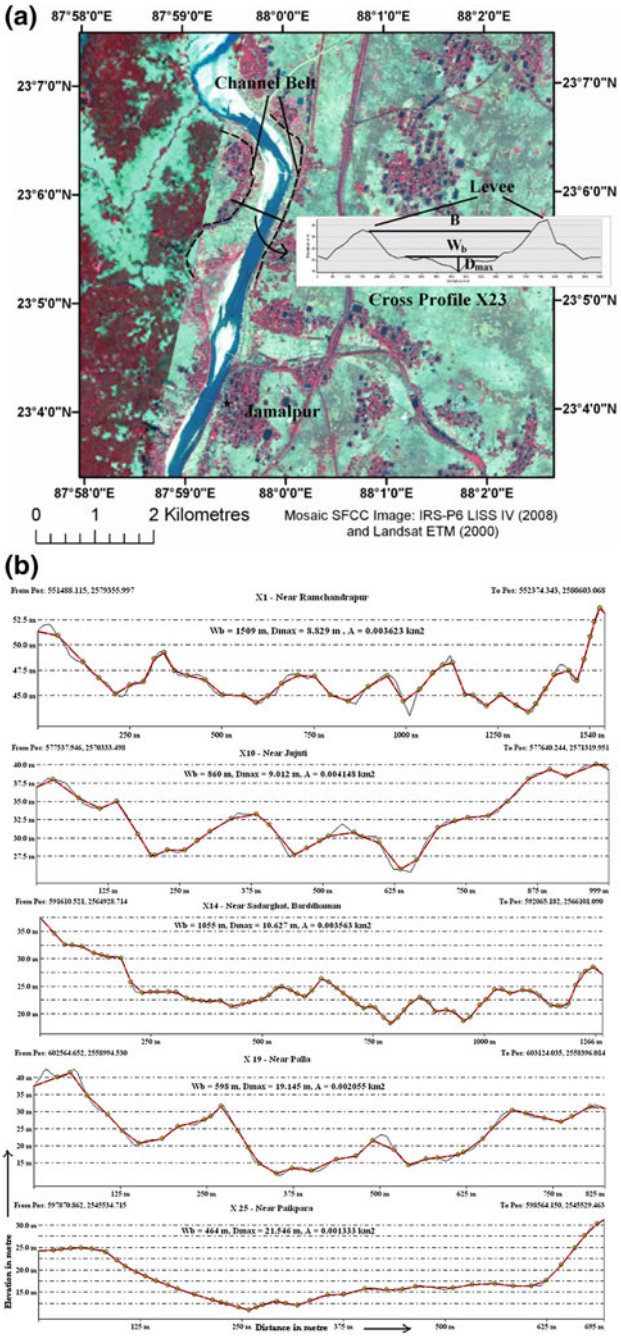

Fig. 4.3 **(a)** Sample estimation of channel dimensions at X23 using satellite image and ASTER cross-profile and (**b**) selected downstream cross-sectional profiles (X—distance in m and Y—elevation in m) of Damodar River at X1 (near Rhondia), X10 (near Jujuti), X14 (near Sadarghat, Bardhaman), X19 (near Palla), and X25 (near Paikpara)

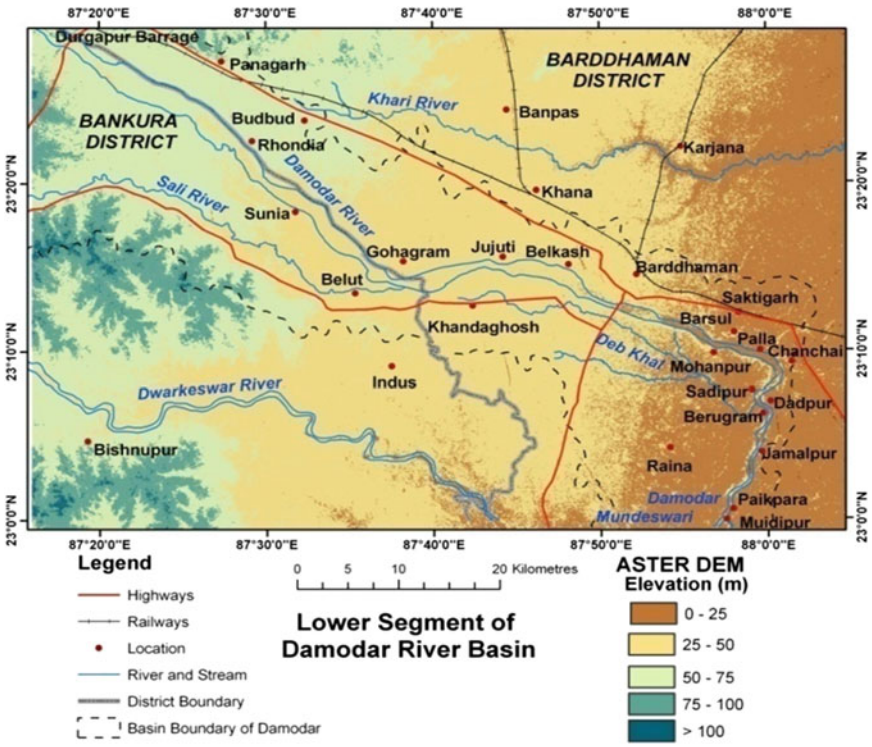

Fig. 4.4 Elevation map of study area prepared from ASTER DEM data (after Ghosh and Guchhait 2014c)

4.4 Results and Discussion

4.4.1 Empirical Classification and Categorization of Damodar River

Applying the classification system of Schumm (1985), the Damodar River (i.e. area under study) can be divided into two broad patterns:

1. The bed-load channel (pattern 5), Rhondia (23°22′08″N, 87°28′25″E) to Barsul (23°11′02″N, 87°57′56″E):

   - Bed-load channel with typical bars, braided stream.
   - Bars and thalweg shift within the unstable channel.
   - Sediment load and size are large.
   - Elongated mid-channel islands and mature point bars are developed and migrate through the channel.
   - Avulsion frequency is common.

- Flow velocity (V_c) and stream power (ω) are high and relative stability of channel bed is low.
- Channel shifting causes bank erosion.
- Sinuosity ranges from 1.0 to 1.05.
- Degree of braiding and anabranching is 35–65 %.
- Width: depth ratio is greater than 40.

2. The mix-load channel (pattern 2) Barsul to Paikpara (23°00′58″N, 87°57′41″E):

- The valley or channel belt is more or less straight, having a sinuous thalweg.
- Sinuosity index is nearer to 1.06–1.25 (confined meander).
- Relatively stable, small load of coarse sediment.
- Shifting of mid-channel bars and maturity of point bars.
- Banks are alternately exposed and protected by the alternate bars.
- Filling and scouring are common.
- Degree of braiding and anabranching is less than 5 %.
- Width:depth ratio is greater than 10 but less than 40.

Following Rosgen's (1994) classification of streams, the different segments of the Damodar River can be categorized on the basis of two broad levels:

1. The geomorphic characterization (level I): (1a) *D* type stream (braided broad channel) up to Hatsimul (23°12′17″N, 87°53′30″E) and (1b) *B* type stream (moderately entrenched narrow channel) up to Paikpara

(2) The morphological description (level II): (2a) *D*5 stream (high W_d/D_{max}, low Si, slight ER and moderate S) up to Hatsimul and (2b) *B*5 stream (very low W_d/D_{max}, moderate Si, high ER, and moderate S) up to Paikpara (5 denotes sand-dominated channel materials).

4.4.2 Genetic Classification of Damodar Floodplain

The floodplain is a strip of relatively smooth land bordering a stream and overflowing at a time of high water (Leopold et al. 1969). The Damodar River adjusts its hydraulic geometry and has built a surrounding floodplain since the Late Pleistocene in such a way as to produce a stable conduit for the transport of water and sediment. The relation between a stream's ability to entrain and transport sediment and the erosional resistance of floodplain alluvium that forms the channel boundary provides the basis for a genetic classification of floodplains. On the basis of the textural pattern of active floodplains, specific stream power, landforms, channel planform, aggradation, and degradation of the Damodar floodplain can be genetically categorized into two parts (Nanson and Croke 1992):

1. The medium energy (10–20 W m^{-2}) noncohesive floodplains from Rhondia to Barsul (tended to braided river floodplains, avulsion, overbank vertical

accretion, abandoned channel accretion, mature bars, lateral point bar accretion, high levees, backswamps, and dominance of coarse sand and gravels)
2. The low energy (<10 W m^{-2}) cohesive floodplains from Palla (23°17°38″N, 88° 01′00″E) to Paikpara (laterally stable single-channel floodplains, abundant silts, overbank clay with accretion organics, low levees, dominance of pools and riffles, and confined meandering).

As a result of both channel lateral movement (lateral accretion) and suspended load deposition (overbank deposition), the Damodar River bed and floodplain include the following two assemblages of Quaternary sedimentary facies (Leopold and Wolman 1957; Gregory and Walling 1973).

1. *Channel Bed Deposits*: Channel lag, point bars, longitudinal bars, channel fills facies
2. *Bank and Overbank Deposits*: Levees, backswamps, crevasse splays, and terrace facies

Through indentifying the fluvial features from the toposheets (1969–1974), ASTER DEM (2011), Landsat ETM image (2000), IRS-P6 LISS IV (2008), and Google Earth, a Quaternary floodplain map of the Damodar River was prepared to

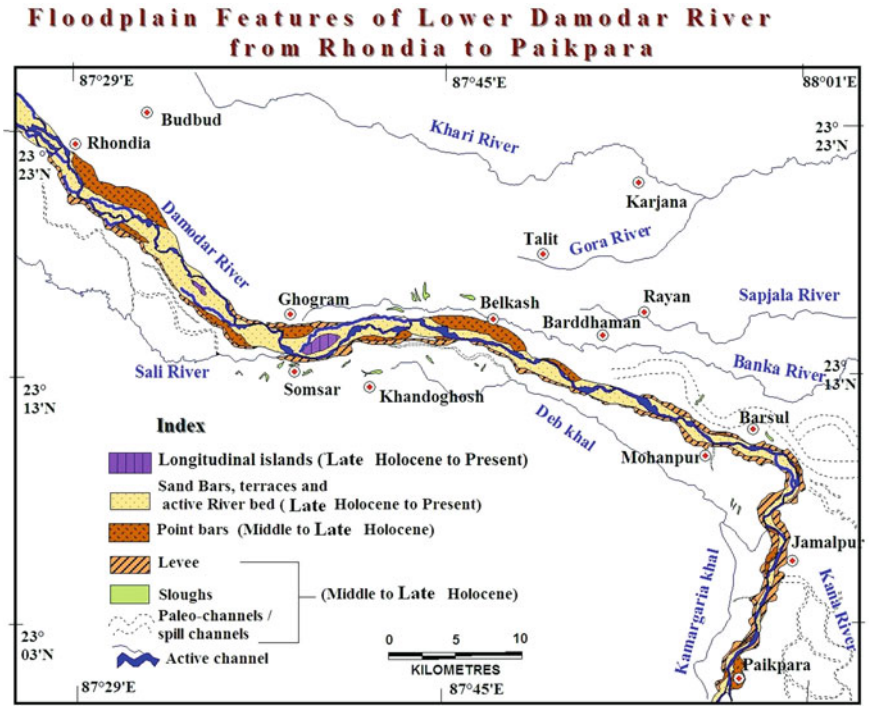

Fig. 4.5 Quaternary floodplain features of the lower Damodar River (Rhondia to Paikpara): the upper valley is dominated by elongated *point bars*, longitudinal islands, and terraces and the lower valley is dominated by *levee* and *palaeochannels* (after Ghosh and Guchhait 2014a)

depict the distinct association and location of floodplain geomorphic features (Fig. 4.5). It is evident that the longitudinal islands, sand bars, riverbed, and asymmetric terraces are associated with the depositional environment of the Late Holocene to the Present (~6 kyrs to the present) and the point bars, backswamps, levee, sloughs, palaeochannels, and spill channels were developed in the Middle Holocene to Late Holocene (~9 to 6 kyrs; Bhattacharya and Dhar 2005).

4.4.3 *Current Status of Channel Dimensions and Hydrogeomorphic Estimates*

The main channel dimensions include bankfull width, bankfull mean depth of channel, maximum depth of channel, bankfull cross-sectional area, channel width: depth ratio, and the like, which are widely used in the study of flood geomorphology, flood hydrology, and palaeofloods (Williams 1988). The empirical equations of fluvial hydrology and geomorphology (Table 4.1) have the potential to extract newfangled information which can be utilized in flood risk management. Therefore employing those equations the total analysis is subdivided into six parts: measurement and estimation of (1) channel dimensions, (2) channel slope, (3) sinuosity, (4) mean flow velocity, (5) stream power and shear stress, (6) potential volume of segment and discharge, and (7) annual maximum discharge (Table 4.1).

1. *Channel Dimensions*
   The bankfull stage is the critical stage of a particular section of the stream at which that stream first overflows its natural banks (Langbein and Iseri 1960). The bankfull width (W_b) is the maximum width of the lowest bank across the river. The analysis suggests that the Damodar River can be classified into two ideal segments: mean W_b of 1603 m (Rhondia to Hatsimul) and mean W_b of 617 m (Barsul to Paikpara). The highest sample W_b (1986 m) is observed at the cross-profile X3 (near Ramgopalpur) and lowest W_b (364 m) at profile X23 (near Jamalpur). The maximum depth (D_{max}) is the elevation difference between the lowest bank-top and thalweg at a cross-section of the river (Williams 1984). It has been noticed that the upper segments of the Damodar (with high W_b) are associated with low D_{max} (8–5 m) but after crossing Bardhaman have a high value up to Paikpara (12–30 m) following the tight valley alignment. Downstream of Palla (X19) the sudden increase of channel depth and also channel slope can be the result of neotectonic and topographic control over the reach. A north-to-south Damodar Fault (Singh et al. 1998) exists below this area, directing the southern shift of Damodar and fan-deltaic sedimentation. The bankfull cross-sectional areas (A_b) of 25 sample profiles across the Damodar River are directly measured from the ASTER DEM, using the 3D-path profiling tool of Global Mapper 14.2 software. Based on A_b data the study area can be divided into two broad segments: high and variable A_b (3500–6000 m^2) from Rhondia to Hatsimul, and low and least variable A_b (800–2100 m^2) from Barsul

Table 4.1 Empirical index and equations used in this study

Variables	Equations	Developed by
Entrenchment ratio	$ER = F_p/W_b$	Rosgen (1994)
Sinuosity index	$Si = L_T/L_D$	Friend and Sinha (1993)
Channel slope	$S = 0.0125\ Q_b^{-0.44}$	Leoplod and Wolman (1957)
Mean flow velocity	$V_C = R^{0.67}\ S_c^{0.50}/n$	Gauckler (1867) and Manning (1890)
Mean flow velocity	$V_C = (0.791/n)\ R^{2/3}\ S^{1/2} + 0.141$	Rotnicki (1983)
Bankfull discharge	$Q_b = 0.213\ A^{1.167}$	Pickup and Warner (1984)
Maximum peak discharge	$Q_{max} = 1.6\ (W_b^{1.56}/W_b/D_{max}^{0.66})$	Schumm (1972)
Maximum peak discharge	$Q_{max} = 0.56\ W_b^{1.46}$	Kale et al. (2004)
Stream power	$\omega = \gamma\ Q\ S/w = \tau \cdot V$	Kale (2003)
Shear stress	$\tau = \gamma\ R\ S$	Kale (2003)

to Paikpara. The wide A_b has the shape of a wide box with the undulation of the riverbed due to in-channel bars but the low A_b has an almost trapezoidal shape. The highest A_b (6360 m^2) is found at the X7 profile (near Gohagram) and lowest A_b (812 m^2) at the X22 profile (near Berugram). The width:depth ratio (W_b/D_{max}) is the important quotient of W_b and D_{max} of a particular channel cross-section (Table 4.2) which describes the shape factor of the reach (Rosgen 1994). As the downstream distance increased from Rhondia, the W_b/D_{max} (*y*-axis) of reaches declines significantly, carrying a linear growth function of distance (coefficient of determination, $R^2 = 0.753$). Up to Hatsimul (X15 profile) W_b/D_{max} varies from 67 to 202 signifying a high level of potential bankfull discharge, low competence to transport coarse sediments (high degree of braiding), and high expansion of the active channel belt. The highest W_b/D_{max} (202.32) is observed at the X3 profile (near Ramchandrapur) and the lowest (12.08) at the X23 profile (near Jamalpur). From Barsul (X16) to Paikpara (X25) the W_b/D_{max} declines abruptly from 53.86 to 21.53, signifying the narrowness of the channel, low level of bankfull discharge (i.e. high flood risk at threshold level), and relatively high competence to transport sediments in floods and increase boundary shear stress (i.e. high chance of bank shifts). A quantitative expression of the entrenchment ratio (ER, ratio of floodprone width F_p and bankfull width W_b) was developed by Rosgen (1994) to determine whether the river deeply incised or entrenched in the valley floor (vertical containment) or in the deposits feature. From Rhondia (X1) to Jujuti (X10) the average ER of 2.09 reflects a moderately to slightly entrenched channel because of the high flood-prone width with respect to the bankfull width. From Belkash (X11) to Barsul (X18) the average ER suddenly drops to 1.29, signifying the well-entrenched channel where F_p and W_b have not deviated very much in respect to each other.

Table 4.2 Dependency and interrelations among floodprone width (F_p), channel belt (B), mean annual bankfull discharge with two-year recurrence interval (Q_{max2}), volume of channel segment (V_p), and width: depth ratio (W_b/D_{max}) in the Damodar River

Sl. No.	X	Y	Established regression	Correlation coefficient (*r*)	*t*-Test result
1	W_b/D_{max}	F_p	$F_p = 101.9\ W_b/D_{max}^{0.659}$ $R^2 = 0.696$ SE = 2.942 log unit	0.765	In all cases calculated *t* is more than the tabulated *t* at 95 and 99 % significance level (two-tailed); so null hypothesis is rejected. There are significant relationships among the variables and *r* can be accepted in these channel segments
2		B	$B = 385.04\ W_b/D_{max}^{0.6818}$ $R^2 = 0.809$ SE = 3.461 log unit	0.797	
3		Q_{max2}	$ax = 147.4\ W_b/D_{max}^{0.411}$ $R^2 = 0.798$ SE = 2.012 log unit	−0.945	
4		V_p	$V_p = 70{,}384\ W_b/D_{max}^{0.610}$ $R^2 = 0.720$ SE = 6.65 log unit	0.664	

Note $Q_{max2} = 4.18\ A_b^{0.669}$, developed by Hodge and Tasker (1995) to estimate peak discharge for two-year recurrence interval; R^2 = coefficient of determination; SE = standard error of Y estimate on X; tabulated *t* value is 2.07 at 95 % level of significance and 2.82 at 99 % level of significance (degree of freedom = 25 − 2 = 23)

Again from Palla (X19) to Paikpara (X25) the average ER rises to 1.65, carrying evidence of moderate entrenchment.

2. *Channel Slope*
   The channel slope (S) can be determined by the elevation difference of the thalweg at two successive points and the distance between two points. The slope value is increased gradually as the W_b/D_{max} and Q_b are declined towards Paikpara, signifying the topographic control on valley alignment. The slope varies from 0.00036° to 0.00079° signifying the low channel competence to heavy load in flood stage. For that reason the high degree of braiding and aggradation is observed in between Durgapur and Belkash. With increasing downstream channel distance the W_b/D_{max} is radically reduced and the hydraulic sinuosity index (Mueller 1968) of the confined valley (i.e. high levee and embankments) is amplified more than the upstream section. However, the slope would be controlled by the Damodar Fault which can act as the extrinsic threshold to the fluvial system. From the analysis we have found that the

parameter of the channel slope (developed by Leopold and Wolman 1957) is driven by the major variables of the channels, viz., B, Si (i.e. sinuosity index), V_p, Q_{max}, Q_b, $\omega\ Q_{b,}$ and $\omega\ Q_{max,}$ respectively. On the other hand W_b, $W_b/D_{max,}$ and M significantly influence the degree of channel slope (Table 4.3).

3. *Channel Sinuosity*
   Channel sinuosity (Si) of a wide river is estimated as the ratio between channel thalweg length (L_T) and shortest distance between two cross-sections (L_D) using the satellite images and GIS (Friend and Sinha 1993; Rosgen 1994; Sinha and Friend 1994). The average sinuosity index of Damodar is 1.19 which signifies the almost straight river course with the topographic confinement and fault-guidance. Except for a few upper segments (X2, 3, 4, and 5) and lower segments (X20, 21, and 25) all other segments of Damodar are associated with Si less than 1.20.

4. *Mean Velocity*
   The accurate determination of mean velocity (V_C) is largely dependent on obtaining a valid and reliable measure of flow resistance (Khan and Tewari 2011). Applying the equations of mean flow velocity (Table 4.1) we have found that up to Barsul the potential V_C varies from 14 to 25 m s^{-1} whereas up to Paikpara it varies from 12 to 22 m s^{-1}. The hydraulic radius of Damodar ranges in between 2.2 to 3.4 m. The sections with high hydraulic radius (>2.8 m) and high wetted perimeter are associated with relatively high velocity in respect to the average coefficient of roughness (i.e. $n = 0.045$ for sandy bed) in this river.

5. *Stream Power and Shear Stress*
   Unit stream power (ω) and boundary shear stress (τ) are considered good measures of geomorphic effectiveness of peak discharges in the Damodar River (Kale 2003; Kale 1998). Calculations indicate that average estimated stream power of Q_b ($\omega\ Q_b$) varies from 6 to 8 W m^{-2} in between Rhondia and Hatsimul (X1 to X15 profiles) but it increases greatly from 9–12 W m^{-2}. Up to the X15 profile the average stream power of Q_{max} ($\omega\ Q_{max}$) varies from 10 to 16 W m^{-2}, but again it suddenly rises from 20 to 60 W m^{-2}. With respect to the high hydraulic radius and moderate slope the shear stress of upstream sections (X1 to X15 profiles) varies slightly from 7 to 10 N m^{-2}, but with increasing downstream distance it rises from 13 to 17 N m^{-2}, signifying high stress on bed and banks (i.e. risk of bank failure and avulsion).

6. *Potential Volume of Segment and Discharge*
   In between two sections the potential volume of segment (V_P) is calculated using the cut–fill volumes and trapezoidal rule (average end area rule; Basak 1994). Up to Barsul (X15) the average potential V_P is 14,731,000 m^3, whereas up to Paikpara it reduces to only 5,900,400 m^3. Bankfull discharge (Q_b) is the maximum amount of water which is carried by a specific channel before the

Table 4.3 Dependence and Independence of channel slope on percentage of fine materials, bankfull width, width: depth ratio, channel belt, sinuosity index, bankfull discharge, annual maximum discharge, segment volume, and stream power of Q_b and Q_{max} in the Damodar River

Sl. No.	X	Y	Established regression	Correlation coefficient (r)	t-Test result
1	M	S	$S = 0.0003\ M^{0.3408}$ $R^2 = 0.798$ SE = 0.0003 log unit	0.907	In all cases calculated t is more than the tabulated t at 95 and 99 % level of significance (two-tailed); so null hypothesis is rejected. There are significant relationships among the variables and r can be accepted in these channel segments
2	W_b		$S = 0.0132\ W_b^{-0.4979}$ $R^2 = 0.943$ SE = 0.0002 log unit	−0.865	
3	W_b/D_{max}		$S = 0.0016\ W_b/D_{max}^{-0.3156}$ $R^2 = 0.798$ SE = 1.58 log unit	−0.780	
4	S	B	$B = 0.0006\ S^{-2.084}$ $R^2 = 0.943$ SE = 3.39 log unit	−0.856	
5		Si	$Si = 1379\ S + 0.904$ $R^2 = 0.656$ SE = 3.304 log unit	0.834	
6		Q_b	$Q_b = 0.022\ S^{-1.48}$ $R^2 = 0.957$ SE = 2.824 log unit	−0.898	
7		Q_{max}	$Q_{max} = 0.2191\ S^{-1.28}$ $R^2 = 0.658$ SE = 3.304 log unit	−0.682	
8		V_p	$V_p = 9.165\ S^{-1.78}$ $R^2 = 0.763$ SE = 0.0002 log unit	−0.865	
9		$\omega\ Q_b$	$\omega\ Q_b = 1131\ S^{0.621}$ $R^2 = 0641$ SE = 0.136 log unit	0.756	
10		$\omega\ Q_{max}$	$\omega\ Q_{max} = 4.23\ e^{3.42\ S}$ $R^2 = 0.817$ SE = 0.734 log unit	0.916	

Note $W_b/D_{max} = 255\ M^{-1.08}$, developed by Schumm (1963), transformed this equation into log form with base 10 to find M; the final equation appeared as: $-1.08\ \log_{10} M = \log_{10} W_b/D_{max} - 2.406$

overflows and floods (Williams 1988). The analysis of bankfull discharge (i.e. annually observed in the active floodplain) suggests that the Damodar River can be classified into three important segments: (1) channel segment of Rhondia to Masjidpur (X1 to X11) with Q_b of 3312 to 4048 $m^3\ s^{-1}$, (2) channel segment of Belkash to Palla (X12 to X19) with Q_b of 2327 to 2428 $m^3\ s^{-1}$, and (3) channel segment of Habaspur to Paikpara (X20 to X25) with Q_b of 963 to 1274 $m^3\ s^{-1}$. We have found that up to the X15 profile the maximum monsoon discharge

Table 4.4 Estimated annual maximum discharge of Damodar River

Sl. No.	Equations	Developed by	Mean Q_{max} (m^3 s^{-1})	Maximum Q_{max} (m^3 s^{-1})	Minimum Q_{max} (m^3 s^{-1})
1	$Q_{max} = 1.6\ (W_b^{1.56}/W_b/D_{max}^{0.66})$	Schumm (1972)	5046	15,831	1311
2	$Q_{max} = 0.029\ W_b^{1.28}D_{max}^{1.10}$	Williams (1984)	5526	12,394	2160
3	$Q_{max} = 0.028\ W_b^{1.71}$	Kale et al. (2004)	6005	17,192	1016

(Q_{max}) varies greatly from 4130 to 17,190 m^3 s^{-1}, with mean of 8852 m^3 s^{-1}. After crossing Barsul, up to the X25 profile the Q_{max} is reduced from 2870 to 1066 m^3 s^{-1}, with a mean discharge of 1736 m^3 s^{-1}. Again applying equations (Table 4.1), the mean Q_{max} of X1–X15 ranges from 6232 to 6462 m^3 s^{-1}, whereas the mean Q_{max} of downstream sections varies from 2923 to 3675 m^3 s^{-1}.

7. *Annual Maximum Discharge*
Schumm (1972), Williams (1984, 1988), and Kale et al. (2004) presented the following formula for the calculation of annual peak flow using W_b and D_{max}. These nonlinear relations were already established in the study area with good significance level. Applying the equations (Table 4.4), we have found that up to the X15 profile the maximum monsoon discharge varies greatly from 4130 to 17,190 m^3 s^{-1}, with mean of 8852 m^3 s^{-1}. After crossing Barsul, up to the X25 profile, the Q_{max} is reduced from 2870 to 1066 m^3 s^{-1}, with mean of 1736 m^3 s^{-1}. Again applying the hydrologic equations, the mean Q_{max} of X1–X15 ranges from 6232 to 6462 m^3 s^{-1}, whereas the mean Q_{max} of downstream sections varies from 2923 to 3675 m^3 s^{-1}. This analysis directly reflects certain facts: (1) downstream reduction of bankfull width, cross-sectional area, and width:depth ratio (i.e. channel dimensions) decrease the limit of annual maximum discharge (Table 4.4) which can be safely accommodated by the channel, and (2) uncertainty of monsoon rainfall and tropical cyclones can create huge pressure on the river engineering structures because of lowering the safe limit to release excess water through the narrow and heavily silted lower Damodar.

4.4.4 *Relative Dominancy of Variables and Clustering of Channel Reaches*

It has been found that the geomorphic and hydrologic variables do not operate in isolation but rather as closely interlinked with each other, driving the fluvial system towards a dynamic metastable equilibrium. So a multivariate analysis seems to be

quite necessary to recognize the relative importance and dominancy of each variable with respect to the total system (Kothari 2009; Ghosh 2011; Ghosh and Bhattacharya 2012). To reduce the aforesaid number of variables or channel dimensions into a few factors or components, principal component analysis is employed here considering 17 variables of 25 sample sections. The importance of principal components (PC) is expressed as eigenvalues which signify the most effective components with increasing numbers of dominant variables and their role in the system functioning. Performing PCA we have extracted three principal components and cumulatively explained 88.13 % of total variance, having three eigenvalues of 10.42 (PC 1), 2.86 (PC 2), and 1.69 (PC 3), respectively (Table 4.5).

- **PC 1 (most important)**: Mainly bankfull area (A_b), bankfull width (W_b), width: depth ratio (W_b/D_{max}), channel belt (B), floodprone width (F_P), annual maximum discharge (Q_{max}), and bankfull discharge (Q_b) drive the fluvial system of the lower Damodar positively, whereas channel slope (S), percentage of silt-clay on bed and banks (M), shear stress, and stream power of Q_b and Q_{max} influence the same system in a negative direction (61.33 % of total variance).
- **PC 2 (medium important)**: Mainly Q_{max} and maximum channel depth (D_{max}) have high positive dominance where the hydraulic radius (R) and maximum flow velocity (V) stoutly influence the system in a negative direction (16.81 % of total variance).
- **PC 3 (least important)**: Principally channel planform dimensions (i.e. sinuosity index, Si, and entrenchment ratio, ER) receive highly positive importance (9.97 % of total variance).

The transformation of component values to component prinsscores (i.e. putting the value on space) we have found the reflection of each channel section based on the interplay of the aforesaid variables. The formula of finding each prinsscore in the first principal component loading can be defined as

$$\text{Prinsscore of profile X1} = \sum \left[V_i PC\,1 / \alpha_{PC\,1}^{0.5} \right]$$

where V_i are the actual values of variables (i = 1, 2, 3,…, *n*) in section X1, PC 1 are the component value of variables, and $\alpha_{PC\ 1}$ is the eigenvalue of PC 1. Calculating the prinsscores of PC 1 and PC 2 we have employed the *Z*-score to standardize the data and plotted the result in *x*, *y* coordinates to find the clustering. The main purpose of this discriminate analysis is to cluster the groups of channel segments which are discriminated from other groups and to recognize the maximum likelihood behaviour of hydrogeomorphic variables on sample sections. Two separate classes of channel reaches are categorized based on the cluster analysis (Fig. 4.6 and Table 4.6).

Table 4.5 Extraction of three principal components of selected variables of cross-sections and their relative dominance in the fluvial system

	A_b	Wb	D_{max}	W_b/D_{max}	B	F_p	ER	Si	S	R	Q_{max}	Q_b	V	M	τ	ω Q_b	ω Q_{max}
PC 1	**0.95**	**0.96**	−0.571	**0.892**	**0.95**	**0.83**	0.17	0.336	**−0.94**	−0.123	**0.73**	**0.95**	0.35	**−0.88**	**−0.96**	**−0.9**	**−0.88**
PC 2	0.123	0.254	**0.728**	−0.2	0.267	0.04	−0.22	0.065	0.136	**−0.64**	**0.59**	0.149	**−0.9**	0.36	−0.17	−0.316	0.42
PC 3	−0.13	−0.06	−0.074	0.1237	−0.06	0.47	**0.84**	**0.7**	0.183	−0.301	−0.22	−0.13	−0.07	0.131	0.037	−0.038	0.136

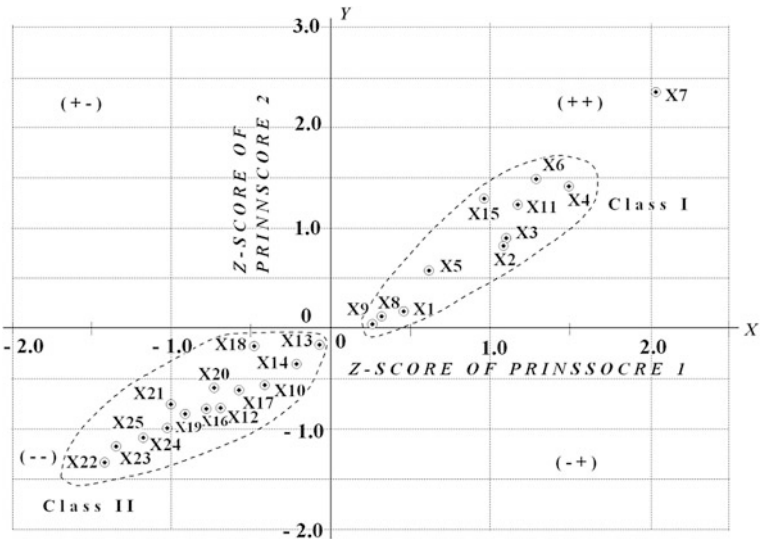

Fig. 4.6 Discriminate analysis showing two distinct clusters of channel reaches based on *Z*-scores of PC 1 and 2 components' prinsscores (after Ghosh and Guchhait 2014c)

Table 4.6 Categorization of Alluvial channel reaches on the basis of channel dimensions

Class I (tending to braiding and lateral expansion)	Class II (tending to meandering and lateral confinement)
Upstream sections of Damodar River (X1 to 6, X8, X9, X11, X15, including X7) show positive *Z*-scores based on the mutual interactions of channel dimensions and hydraulic parameters. The individuality or distinctiveness of this fluvial class is mainly associated with high A_b (3500–5500 m^2), high W_b (1400–2400 m), low D_{max} (8–15 m), high W_b/D_{max} (120–200), high B (>12,000 m), low ER (>1.4), low Si (<1.25), low S (<0.0004^0), high limit of Q_{max} (4500–9000 $m^3\ s^{-1}$), and Q_b (3000–5000 $m^3\ s^{-1}$), low τ (<9.5 N m^{-2}) and high ω of Q_{max} (10–13 W m^{-2})	Downstream sections of Damodar River (X10, X12–14, and X16–X25) demonstrate individuality based on the variables: low A_b (900–3000 m^2), low W_b (500–1200 m), high D_{max} (16–25 m), low W_b/D_{max} (20–100), low B (<1500 m), high ER (1.0–1.4), moderate Si (1.25–1.45), moderate S (0.0004^0–0.0007^0), low limit of Q_{max} (2200–4400 $m^3\ s^{-1}$), and Q_b (1000–3000 $m^3\ s^{-1}$), low τ (10–15 N m^{-2}), and high ω of Q_{max} (>15 W m^{-2})

4.5 Conclusion

The pattern or planform of the Damodar River is analysed here at very micro scale (cross-section of a reach), depending upon both the size of the river and the part of the fluvial system that is under consideration. It is now understood that river forms and fluvial processes evolved simultaneously and operate through mutual

adjustments towards self-stabilization in different alluvial reaches of the Damodar River. Categorization or classification of channel segments predicts the river's behaviour to internal and external factors and explains the current stage of morphological stability to affect channel discharge, aggradation, and degradation. DVC and IWD establish macro- to microcontrol measures of flood protection which range from deepening, widening, and straightening of the channel, jacketing the river with multilevel embankments, drainage diversion through canals, up to storing and releasing water through weir, sluices, barrage, and reservoirs. At present the Damodar River can be regarded as a 'controlled river' because its regular discharge, floods, sediment transport and deposition, and other fluvial behaviours are influenced and controlled by the engineering structures. The present landforms and channel dimensions of the Damodar River are products of the interplay between two master processes: quasi hydrogeomorphic processes, and anthropogenic interventions and land-utilization processes. The channel morphology of the Damodar River is significantly influenced by bankfull channel width, maximum channel depth, monsoon flood velocity, bankfull peak discharge, channel slope, sediment load, and boundary shear stress. A change in any one of these variables sets up a series of channel adjustments which lead to a change in the others, resulting in channel pattern alteration. Analysing the current hydrogeomorphic status of the lower Damodar River at the ungauged sites and treating each channel segment as an important fluvial unit, we have derived that with downstream increase of distance the Damodar River is tended from braiding (class I) to confined meandering pattern (class II) with significant loss of bankfull width, bankfull area, volume, and bankfull discharge which reflects an increasing vulnerability of flood risk. The classification of river and floodplain shows that the Damodar River can be regarded as a bed-load channel with a medium energy noncohesive floodplain upstream of the study area (Rhondia to Bardhaman) and the downstream stretch (Basrsul to Paikpara) can be identified as a mix-load channel with a low-energy cohesive floodplain.

References

Basak NN (1994) Surveying and leveling. Tata McGraw Hill, New Delhi

Bhattacharya AK, Dhar N (2005) A report on geo-environmental appraisal in Bardhaman urban agglomeration and its environment for sustainable developmental activities. Geological Survey of India, Eastern Region, Kolkata

Bhattacharyya K (2011) The Lower Damodar River, India: understanding the human role in changing fluvial environment. Springer, New York

Chandra S (2003) India: flood management—Damodar River Basin. Retrieved from www.apfm.info/pdf/case_studies/cs_india.pdfon 13th October, 2011 at 9:35 am

Charlton R (2008) Fundamentals of fluvial geomorphology. Routledge, London

Chatterjee SP (1969) Damodar valley planning atlas. NATMO, Calcutta

Friend PF, Sinha R (1993) Braiding and meandering parameters. In: Best JL, Bristow CS (eds) Braided rivers. Geological Society Special Publication, New York, pp 105–111 (No. 75)

Fryirs KA, Brierley GL (2013) Geomorphic analysis of river systems: an approach to reading the landscape. Blackwell Publishing, New York
Gauckler P (1867) Etudes Theoriques sur I'Ecoulement et le Mouvement des Eaux, Comptes Rendues de I'Academie des Sciences. Tome, Paris, pp 818–822
Garde RJ (2006) River morphology. New Age International Publishers, New Delhi
Ghosh S (2011) Determination of significant variables in the evolution of Sarujharna Basin of East Singhbhum. Jharkahand Practising Geogr 15(1):25–39
Ghosh S, Bhattacharya K (2012) Multivariate erosion risk assessment of lateritic badlands of Birbhum (West Bengal, India): a case study. J Earth Syst Sci 121(6):1441–1454
Ghosh S, Guchhait SK (2014a) Hydrogeomorphic variability due to dam constructions and emerging problems: a case study of Damodar River, West Bengal, India. Environ Dev Sustain 16(3):769–796
Ghosh S, Guchhait SK (2014b) Analyzing fluvial hydrological estimates and flood geomorphology from channel dimensions using ASTER DEM, GIS and statistics in the controlled Damodar River. India J Geomatics 8(2):232–245
Ghosh S, Guchhait SK (2014c) Palaeoenvironmental significance of fluvial facies and archives of late quaternary deposits in the floodplain of Damodar River. India Arab J Geosci 7(10):4145–4161
Gregory KJ, Walling DE (1973) Drainage basin form and process: a geomorphological approach. Edward Arnold, London
Hodge SA, Tasker GD (1995) Magnitude and frequency of floods in Arkansas. USGS Water Resource Investigations Report 95–4224:1–52
IWD (2013) Irrigation and Waterways Department Government of West Bengal. Daily River and Rain-gauge Data Section, http://wbiwd.gov.in/daily_river_rain_gauge_data.php
Kale VS (1998) Monsoon floods in India: a hydro-geomorphic perspective. In: Kale VS (ed) Flood Studies in India. Geological Society of India, Bangalore, pp 229–256
Kale VS (2003) Geomorphic effects of monsoon floods on Indian rivers. Nat Hazards 28:65–84
Kale VS et al (2004) Palaeohydrological reconstructions based on analysis of a palaeochannels and toba-ash associated alluvial sediments in the Deccan Trap Region, India. In: Kale VS, Gregory KJ, Joshi VU (eds) Progress in palaeohydrology: focus on monsoonal areas. Geological Society of India, Bangalore, pp 481–489
Khan ZA, Tewari RC (2011) Paleochannel and paleohydrology of a Middle Siwalik (Pliocene) fluvial system, northern India. J Earth Syst Sci 120(3):531–543
Kothari CR (2009) Research methodology. New Age International Publishers, New Delhi
Lahiri-Dutt K (2006) State and the community in water management case of the Damodar Valley Corporation, India. In: International symposium on community activities for the conservation of water environment—lessons learned from community activities, Institute for Global Environmental Strategies, Bangkok
Langbein WB, Iseri KT (1960) General introduction and hydrologic definitions. US Geol Surv Water-Supply Pap 1541-A:1–26
Leeder MR (1973) Fluviatile fining-upwards cycles and the magnitude of palaeochannels. Geol Mag 110:265–276
Leopold LB, Wolman MG (1957) River channel patterns: braided, meandering and straight. US Geol Surv Prof Pap 282-B:1–85
Leopold LB, Wolman WG (1960) River meanders. Geol Soc Am Bull 71(6):769–793
Leopold LB, Wolman MG, Miller JP (1969) Fluvial Processes in geomorphology. Eurasia Publishing House, New Delhi
Mahmood A (2007) Statistical methods in geographical studies. Rajesh Publications, New Delhi
Manning R (1891) On the flow of water in open channels and pipes. Trans Institution Civil Engineers Ireland 20:161–207
Mueller JR (1968) An introduction to the hydraulic and topographic sinuosity indexes. Ann Assoc Am Geogr 58(2):371–385
Nanson GC, Croke JC (1992) A genetic classification of floodplains. Geomorphology 4(6):459–486

Niyogi D (1975) Quaternary geology of the coastal plain in West Bengal and Orissa. Indian J Earth Sci 2:51–61
Niyogi D et al (1970) Geomorphic mapping in plains of West Bengal, India. In: Chatterjee SP, Das Gupta SP (eds) Selected paper on physical geography. 21st International Geographical Congress, vol 1. National Committee for Geography, Calcutta, pp 89–94
Pickup G, Warner RF (1984) Geomorphology of tropical rivers: channel adjustment to sediment load discharge in the fly and lower Purari, Papua New Guinea. Catena 5:19–41
Rosgen DL (1994) A classification of natural rivers. Catena 22:169–199
Rotnicki K (1983) Modelling past discharges of meandering rivers. In: Gregory KJ (ed) Background of palaeohydrology. Wiley, New York, pp 321–354
Sanyal J, Carbonneau P, Densmore AL (2013) Hydraulic routing of extreme floods in large ungauged river and the estimation of associated uncertainties: a case study of the Damodar River, India. Nat Hazards 66:1153–1177
Schumm SA (1963) A tentative classification of alluvial river channels. USGS Geol Surv Circular 477:1–10
Schumm SA (1972) Fluvialpalaeochannels. Mineral 16:98–107 (Spec Publ Soc Econ Paleontol)
Schumm SA (1977) The fluvial system. Wiley, New York
Schumm SA (1985) Patterns of alluvial rivers. Ann Rev Earth Planet Sci 13:5–27
Schumm SA (2005) River variability and complexity. Cambridge University Press, Cambridge
Sen PK (1985) The genesis of floods in the Lower Damodar catchment. In: Sen PK (ed) The concepts and methods in geography. The University of Burdwan, Burdwan, pp 71–85
Sen PK (1991) Flood hazards and river bank erosion in the lower Damodar Basin. In: Sharma HS (ed) Indian geomorphology. Concept Publishing Company, New Delhi, pp 95–108
Singh LP, Parkash B, Singhvi AK (1998) Evolution of the Lower Gangetic Plain landforms and soils in West Bengal, India. Catena 33:75–104
Sinha R, Friend PF (1994) River systems and their sediment flux, Indo-Gangetic plains, northern Bihar, India. Sedimentology 41:825–845
Sridhar A (2007) Discharge estimation from planform characters of the Shedhi River, Gujarat alluvial plain: present and past. J Earth Syst Sci 116(4):341–346
USGS (2013) United States Geological Survey Earth Explorer. http://earthexplorer.usgs.gov/
Williams GP (1984) Paleohydrologic equations for rivers. In: Costa JE, Fleisher PJ (eds) Developments and application of geomorphology. Springer, Berlin, pp 343–367
Williams GP (1986) River meanders and channel size. J Hydrol 88:147–164
Williams GP (1988) Paleofluvial estimates from dimensions of former channels and meanders. In: Baker VR, Kochel RC, Patton PC (eds) Flood geomorphology. Wiley, New York, pp 321–334

Chapter 5
An Enquiry into Fitting Natural Channel Shape to Geometric Shape: A Study on River Jalangi, India

Balai Chandra Das and Aznarul Islam

Abstract The cross-sectional form of a river channel is a two-dimensional variable. The average river channels tend to develop their channel cross-sectional form in such a way as to produce an approximate equilibrium between the channel and the load of water and sediment they transport. The cross-sectional form of a natural channel hardly can be epitomized by geometric instances. Yet all cross-sectional forms of channels may be grouped into three broad categories viz. triangular, circular, and rectangular. The present chapter formulates some mathematical devices to identify whether the cross-sectional form of the channel is either semicircular (most efficient of its kind) or equilateral triangular (most efficient of its kind) or rectangular with form ratio 2:1 (most efficient of its kind).

Keywords Channel shape · Width:depth ratio · Semicircular · Rectangular · Equilateral-Triangular

5.1 Introduction

May it be large, intermediate, or small (Church 1992), all cross-sectional forms of a natural stream channel are irregular in outline and locally variable (Knighton 1998). Commonly two groups of aspects are considered to describe channel cross-sectional form: channel size and channel shape. The former group includes width, mean depth, cross-sectional area, wetted perimeter, hydraulic radius, maximum depth, and bed width whereas the latter group of variables are width:depth ratio, maximum

B.C. Das (✉)
Department of Geography, Krishnagar Government College, Nadia 741101, India
e-mail: drbalaidaskgc@rediffmail.com

A. Islam
Department of Geography, Barasat Government College, Barasat, Kolkata 700 124, West Bengal
e-mail: aznarulislam@gmail.com

B.C. Das et al. (eds.), *Neo-Thinking on Ganges-Brahmaputra Basin Geomorphology*, Springer Geography, DOI 10.1007/978-3-319-26443-1_5

depth, mean depth ratio, channel asymmetry, bank slope, bed topography, and its resemblance to geometric shape. About 9/10 meandering channels' cross-sections are asymmetric (Leopold and Wolman 1960) and symmetry is assumed to be found at cross-over only (Knighton 1981) although cross-sectional asymmetry is found in so-called straight channels also (Einstein and Shen 1964; Keller 1972; Majumder 2011).

Decades have passed with the question remaining of whether a general physical principle governs channel form adjustment (e.g. Langbein and Leopold 1964; Yang 1976; Chang 1980; Jia 1990). Channel shape has its definite control over flow pattern and velocity distribution through a particular section normal to the direction of flow (Chow 1959). Critical flow depth, minimum specific energy, hydraulic diameter, with constant cross-sectional area are shape dependent (Chanson 2004). Magnitude of discharge and flow regime is also influenced by channel form (Harvey 1969; Stevens et al. 1975). Flow resistance of an open channel as well as closed pipe is greatly influenced by channel shape as it controls hydraulic radius (Das 2014, 2015; Henderson 1996). Variables of channel shape are used for channel classification (Rosgen 1994).

Channel shape on the other hand is controlled by driving variables and boundary conditions (Charlton 2008) and is primarily adjusted by bed and bank erosion (Charlton 2008), sediment storage (Nakamura and Swanson 1993), downed timber (Heede 1981), and lateral channel migration (Simon and Castro 2003). The width: depth ratio represents dominant measures of channel response (Simon 1992; Simon and Darby 1997; Richards 1982) and w:d alone does not define cross-sectional shape (Hey 1978). Change in base level has a great influence on channel shape which was expressed in the trapezoidal, gorge-like, cross-sectional form of channels of Og, Zeelim, and Arugot wadis due to lowering of the level of the Dead Sea (Bowman 2010). Form ratio w:d or w/d_{max} (Schumm 1960), section asymmetry a_l / a_r (Milne 1979), or channel asymmetry (Knighton 1981) regarding cross-sectional form give absolute measure. Although several geometric shapes of the channel have been identified (Chow 1959; Chanson 2004) most of them are artificial channels used for civil engineering purposes. In practice, a rectangular channel is very rarely found either as a natural or artificial channel for engineering purposes (Chanson 2004). Geometric shapes including trapezoidal, parabolic, egg-shaped, ovoid, semielliptical, U-shaped, catenary, horse-shoe, basket-handle, and others are somehow combinations of three basic geometric shapes: *triangular, circular, and rectangular*. Therefore, the effort in this chapter is to categorize the cross-sectional form of natural channels into the three basic forms of triangular, circular, and rectangular. However, the present chapter is related to the cross-sectional shape of the channel and aims to formulate devices to categorize cross-sectional shapes of river channels or to best fit the channel form with geometric figures such as a semicircle, equilateral triangle, or rectangle with width/depth ratio 2:1.

5.2 Materials and Methodology

5.2.1 Materials

For the study, 11 cross-sections of the River Jalangi were taken as materials for study (Fig. 5.1). Jalangi, one of the three Nadia Rivers (Majumder 1941, 1978, 1995; Garrett 1910; Hirst 1916), is a moribund distributary of the River Padma and tributary to the River Bhagirathi. Both the Rivers Bhagirathi and Jalangi join each other at Swarupganj opposite Nabadwip.

5.2.2 Measurement of Cross Sections

Measurement of channel cross-sections and computation were done by the Dumpy Level and its accessories. For measurement cross-sections, following principles (shown in Fig. 5.2) were followed.

'A' is the total cross-sectional area. Width (w) of the channel is extended up to the brinkpoint of the levee and the upper limit of the channel area is defined by a line extended from the brinkpoint of the levee towards the high bank. Maximum depth (d_{max}) of the channel is shown by the vertical line extended from the deepest point of the channel up to the horizontal line to denote the uppermost level of the bankfull channel (Knighton 1981).

5.2.3 Computation of Cross-Sectional Areas

Cross-sectional areas were calculated following the trapezoidal method. The whole cross-sectional area of the river channel has been divided into numbers of trapeziums. Then the area of the individual trapezium (A_T) has been computed with the help of the formula:

$$A_T = \frac{B+D}{2} * E$$

where B and D represent larger depth and smaller depth, respectively, and E represents the horizontal distance between B and D (Fig. 5.3).

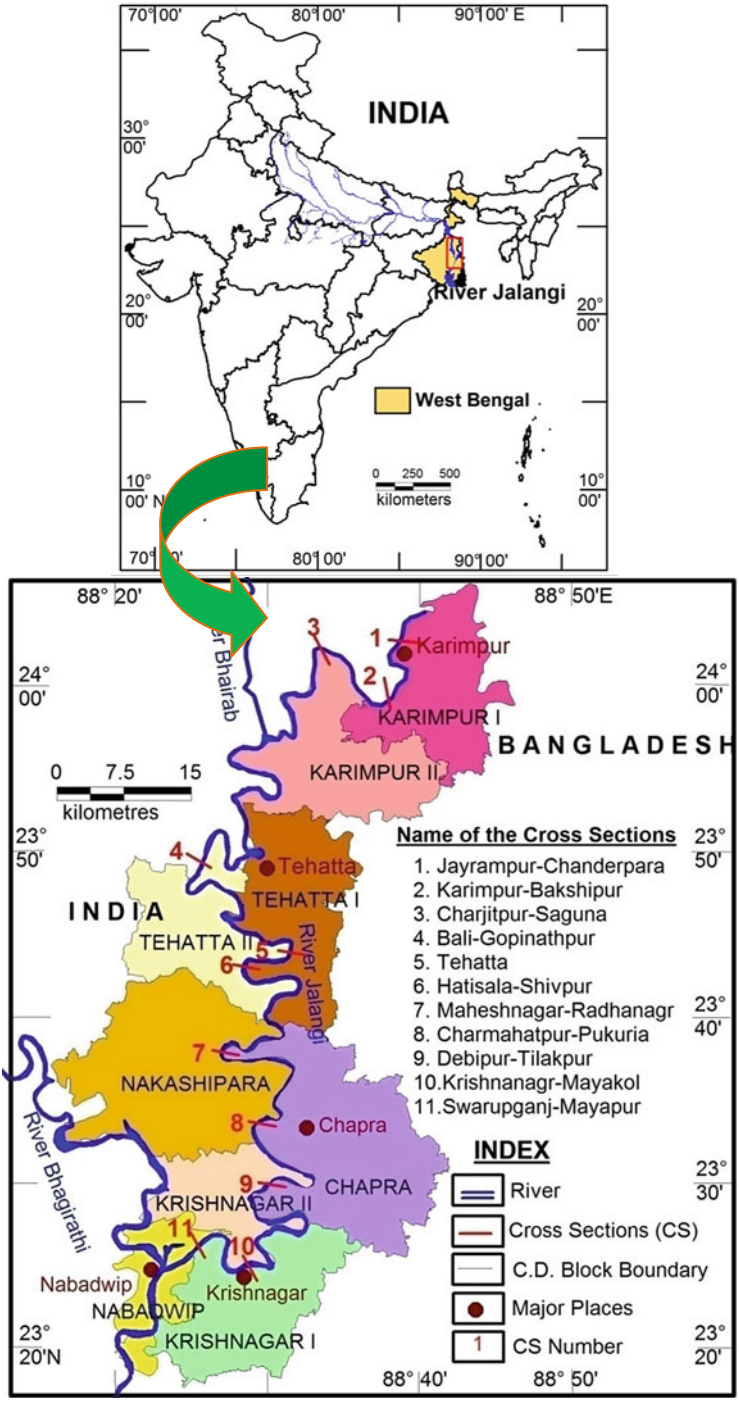

Fig. 5.1 Eleven cross-section sites on the River Jalangi

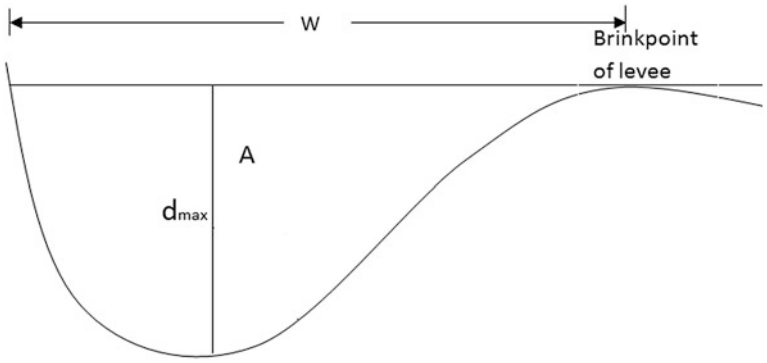

Fig. 5.2 Definitions of different parameters of a channel cross-section

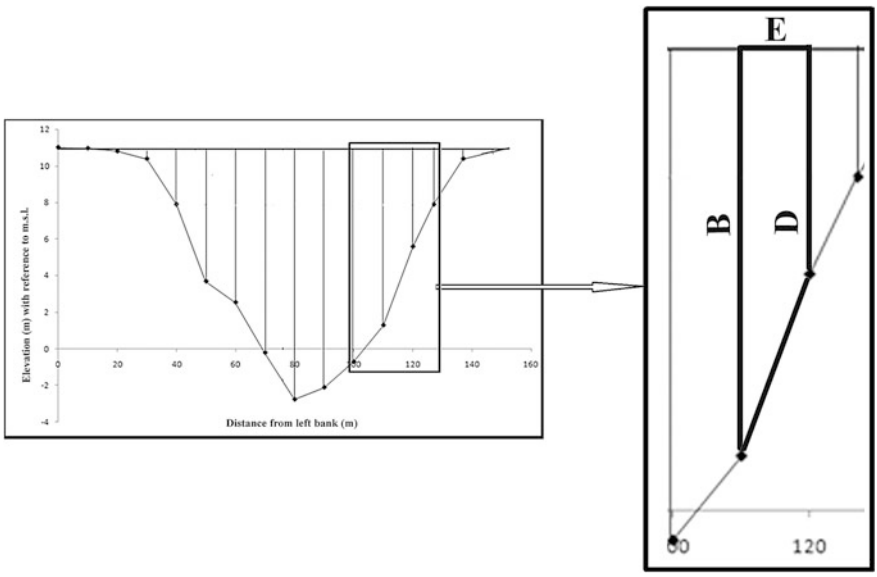

Fig. 5.3 Computation of cross-sectional area by trapezoidal method

5.2.4 Computation of Least Deviation Area

The deviation area is the area between lines of the observed channel shape and the ideal channel shape. Having a given cross-sectional area, the ideal channel shape may either be semicircular or equilateral triangular (Das 2015) or rectangular channel of a width:depth ratio 2:1 (Hickin 2004). The deviation area which is least out of three (between observed and semicircular, observed and equilateral triangular, and observed and rectangular) is the least deviation area (Fig. 5.4).

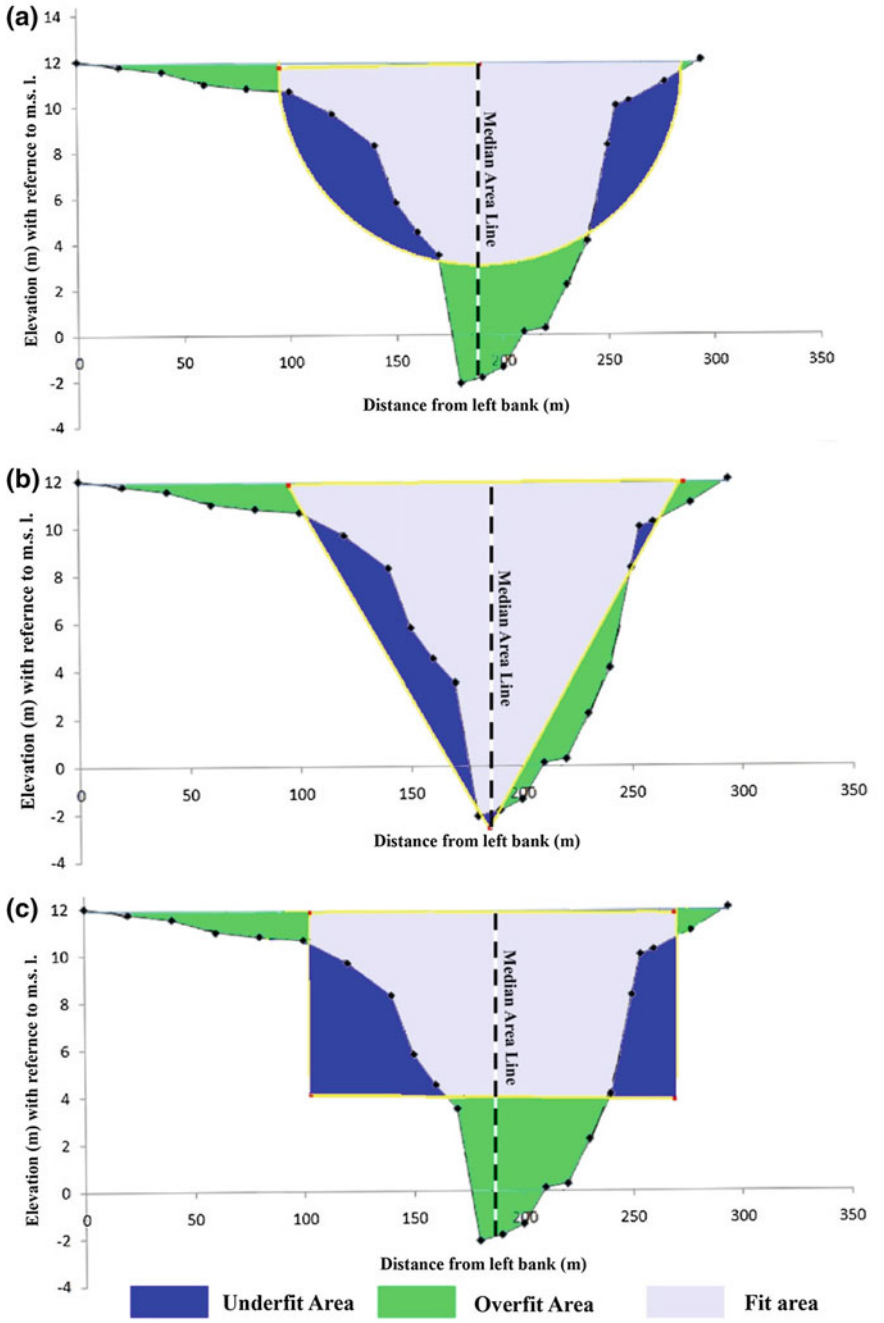

Fig. 5.4 Computation of least deviation cross-sectional area with reference to selected geometric shape: **a** semicircular, **b** equilateral triangular, **c** rectangular with ratio 2:1

The steps for calculating the least deviational area are as follows.

First: An equilateral triangle, rectangle, and semicircle have been drawn with the same area (A) as that of the observed cross-sections (CS) of the river. For drawing a semicircular channel, the radius (r) of the semicircle has been derived by the following formula.

$$r = 0.564\sqrt{A} \tag{5.1}$$

Similarly for drawing an equilateral triangular channel, one side of the triangle (s) has been derived by the following formula.

$$s = \frac{2\sqrt{A}}{\sqrt{3}} = 1.155\sqrt{A} \tag{5.2}$$

For drawing a rectangular channel, numerous combinations of width and depth are possible. Width:Depth ratio of the most efficient cross-section of rivers having the highest hydraulic radius with a given cross-sectional area (A) was calculated 2:1 by Hickin (2004). This ratio has been used to draw rectangular channel cross-sections.

$$\begin{aligned} A &= wd \\ w &= 2d, \end{aligned}$$

Therefore

$$\begin{aligned} 2d \times d &= A \\ \text{Or}, d &= \sqrt{\frac{A}{2}} \end{aligned} \tag{5.3}$$

Then: An equilateral triangle, rectangle, and semicircle have been superimposed on the observed profile. For superimposing the geometric figures (semicircular, equilateral triangular, and rectangular) on the observed profile, the median area line of the observed cross-section and median area lines of geometric figures were fused with each other so that it gave a single line view and could be used as a reference line.

Ultimately: The gap between the observed profile and the profiles of the equilateral triangle, rectangle, and semicircle gave deviational area for equilateral triangle, rectangle, and semicircle respectively. Out of the three geometric figures the one which has the least deviational area will be the best fit to the observed channel.

5.2.5 Channel Categorization Based on Least Deviation Area

If '0' is the theoretically possible lowest value of least deviation area, the channel is perfectly matched with that geometric figure; if it is less than 50 % (Table 5.3) of the total area of the channel, the channel shape is akin to that geometric shape, and if the deviation area crosses the 50 % (Table 5.3) area of the channel, the channel will be unclassified having maximum irregularity. Exactly 50 % deviation area seems to be a great deviation. But it includes both overfit area and underfit area (Fig. 5.4). If both the overfit and underfit areas are equal and the overfit area is superimposed over the underfit area, there will be a perfect match with the geometric shape. However, as both types of misfit areas are included, the real percentage of deviation should be half of the tabulated value. So half of the 50 % deviation area is 25 % and it is considered normal.

5.3 Results and Discussions

5.3.1 Nature of Channel Shape

Processes operating in the channel (Hancock et al. 1998), structure, bed and bank material, vegetation, land use, and hydraulics, all the internal variables along with external variables trigger channel shape. The cross-sectional form is stage dependent as it determines the processes of channel adjustment (Harvey and Anthony 1990). Channel shapes become rectangular as the stage goes down or width increases faster than depth in downstream and the cross-sectional form becomes increasingly rectangular (Sen 1993). It was found in present investigation that, out of 11 cross-Sections 4 cross-sections were semicircular (Tables 5.1 and 5.2), 5 were equilateral triangular and only 2 were rectangular in shape. That is, 36.4 % of the cross-sections of the river were semicircular and 45.5 % equilateral triangular in shape, but only 18.2 % were rectangular. Cross-Sections 1, 2, and 3 were drawn on the dead reach of the river. This reach from the closed off-take at Char Madhubona to Bhairab-Jalangi confluence at Moktarpur is literally dead and remains dry except during the rainy season. These three cross-sections represent an alternate arrangement of triangular and rectangular cross-sectional shapes. Cross-sections on crossovers are semicircular and on meander bent are triangular in shape. Cross-section numbers from 5 to 11 are on a relatively live channel. This reach maintains its flow through the off-take of the River Bhairab from River Padma (Ganges) during monsoon months and by seepage water during lean months. The sequence of riffles and pools is well expressed in this reach and in most cases cross-sections are semicircular at riffles and rectangular at pools. The eighth

Table 5.1 Cross-sectional area of the channel and derivation of magnitudes of geometric figures with same area

Cross-section number	Area in square metre	Radius for semicircular channel in metre ($0.798\sqrt{A}$)	Side for equilateral triangular channel in metre ($1.52\sqrt{A}$)	Width:depth ratio for rectangular channel (2:1)	
				Width (m)	Depth (m)
1	172.21	10.47	19.95	18.558556	9.27927799
2	453.66	17	32.37	30.1217529	15.0608765
3	30.11	4.38	8.34	7.76015464	3.88007732
4	568.9	19.03	36.25	33.7312911	16.8656456
5	524.78	18.28	34.82	32.3969134	16.1984567
6	860.22	23.4	44.58	41.478187	20.7390935
7	672.63	20.7	39.42	36.6777862	18.3388931
8	1016.32	25.44	48.46	45.084809	22.5424045
9	687.99	20.93	39.87	37.0942044	18.5471022
10	827.68	22.96	43.73	40.6861156	20.3430578
11	786.24	22.38	42.62	39.6545079	19.827254

Source Computed by the authors, 2015

Table 5.2 Calculation of deviational area

Cross-Section number	Deviational area in square metre			Best fit geometric figure (per minimum deviation area)
	For semicircle	For equilateral triangle	For rectangle (w/d ratio: 2:1)	
1	53.69	44.94	56.87	Equilateral triangular
2	162.15	212.10	140.51	Rectangular (2:1)
3	23.41	14.85	24.76	Equilateral triangular
4	115.25	196.65	198.17	Semicircular
5	144.77	83.63	191.24	Equilateral triangular
6	191.88	218.86	241.84	Semicircular
7	93.14	197.01	156.24	Semicircular
8	166.29	474.41	126.63	Rectangular (2:1)
9	177.24	267.22	179.93	Semicircular
10	288.23	221.13	376.67	Equilateral triangular
11	210.99	155.10	281.45	Equilateral triangular

Source Computed by the authors, 2015

cross-section is on a riffle where the bank and bed materials are dominated by sands as can be seen by the naked eye. Here, on a relatively horizontal surface having absolute relief of less than 12 m above sea level, lateral erosion and bank failure were accelerated by the presence of sandy bank and bed materials. For the whole

Table 5.3 Percentage in deviation area

Cross-section number	Deviation in area as % of total CS area			
	Semicircular channel	Equilateral triangular channel	Rectangular channel (W/D ratio: 2:1)	Least deviation area out of three
1	31.18	26.10	33.02	26.10
2	35.74	46.75	30.97	30.97
3	77.76	49.31	82.23	49.31
4	20.26	34.57	34.83	20.26
5	27.59	15.94	36.44	15.94
6	22.31	25.44	28.11	22.31
7	13.85	29.29	23.23	13.85
8	16.36	46.68	12.46	16.06
9	25.76	38.84	26.15	25.76
10	34.82	26.72	45.51	26.72
11	26.84	19.73	35.80	19.73
Mean	30.22	32.67	35.34	23.95
SD	17.24	11.41	17.70	10.20
CV	57.04	34.94	50.10	42.59

Source Computed by the authors, 2015

course of the river, the channel depths were increasing towards the lower reaches rather than in the upper reaches. That is why cross-sectional forms revealed a tendency of triangular shapes of channels with lower width: depth ratio towards downstream (Table 5.3).

As per results obtained from the minimum deviation method (Table 5.2), the equilateral triangular channel is more common than other forms because of the natural fluvial hydrodynamics. For the River Jalangi, most of the cross-sections are triangular although they have a high level of internal diversity when a more sophisticated approach involving the deviation area of equilateral triangle, rectangle, and semicircle and w:d ratio is embraced. This scenario has been assessed by multivariate techniques. The component plot derived from principal component analysis shows that the triangular channel has two distinct and distant groupings; one is located at the NE quadrant and the other is at the NW quadrant. Semicircular channels also have a similar positioning system. But the internal grouping on the basis of PC 1 and PC 2 dictates a relatively close association although containing two distinct but not distant groups. A close association between the semicircular and rectangular channel shapes has been observed in this study (Fig. 5.5).

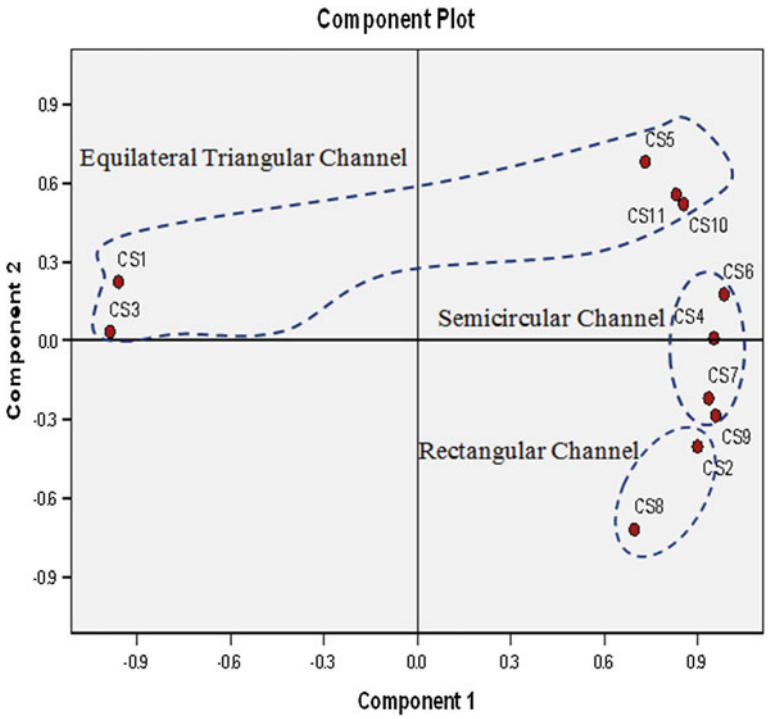

Fig. 5.5 Clustering of different channel shapes (Note: CS denotes cross-section number)

5.3.2 Channel Shape Vis-à-Vis Width:Depth Ratio

The width:depth or form ratio explains the channel shape. Hence analysis of the channel shape in relation to the form ratio is very significant. The form ratio variables were measured for 11 cross-sections of River Jalangi, India (Table 5.4).

The width:depth ratio is correlated with the different channel shapes, viz. semicircular, equilateral, triangular, and rectangular having w:d of 2:1. Generally the w:d ratio is negatively correlated with the deviation area (DA) computed from superimposition of different geometric figures on actual channel shapes. The higher the w:d, the lesser is the deviation area. A triangular channel in this regard portrays a weak correlation and insignificant relation (Table 5.5 and Fig. 5.6) whereas a semicircular channel has registered a moderately strong correlation and the relation is significant at a 95 % significance level. The rectangular channel having w:d of 2:1 is very strongly correlated with the w:d ratio and the relation is significant at a 98 % level. It implies that channel cross-sections are more triangular and semi-circular in shape than rectangular. Because DA decreases with increasing w:d ratio that means if the channel is wider, it is more fit with lesser DA. With a given cross-sectional area, a semicircular channel has the widest width. Equilateral

Table 5.4 Different variables of a cross-section

Cross-section number	Area (m^2)	Width (w) in metres	Mean depth (d) in metres	W:D ratio
1	172.21	116.64	1.48	79.00
2	453.66	181.01	2.51	72.22
3	30.11	47.12	0.64	73.74
4	568.90	135.00	4.21	32.04
5	524.78	98.72	5.32	18.57
6	860.22	134.20	6.41	20.94
7	672.63	117.22	5.74	20.43
8	1016.32	184.00	5.52	33.31
9	687.99	144.40	4.76	30.31
10	827.68	144.04	5.75	25.07
11	786.24	124.20	6.33	19.62
Average	600.07	129.69	4.42	38.66
SD	296.04	37.67	2.00	23.93
CV	49.33	29.04	45.16	61.89

Source Computed by the authors, 2015

Table 5.5 Correlation between width:depth ratio and ideal channel shape and their significance level

X	Y	'r'	r^2	Computed value of 't'	Tabulated value at 9 degrees of freedom	Remarks
Width: depth ratio	Semi-circular	−0.597	0.357	−2.235	1.83 (0.1); 2.26(0.05); 2.82(0.02); 3.25(.01); 4.78(0.001)	***H1 accepted at 95 %* level**
Width: depth ratio	Triangle	−0.396	0.156	−1.292		H0 accepted
Width: depth ratio	Rectangle	−0.722	0.522	−3.135		***H1 accepted at 98 %* level**
Width: depth ratio	Best fit	0.582	0.339	2.150		***H1 accepted at 90 %* level**
Semi-circle	Triangle	0.503	0.253	1.748		H0 accepted
Semi-circle	Rectangle	0.908	0.825	6.507		***H1 accepted at 99.9 %* level**
Semi-circle	Best fit	−0.008	0.000	−0.025		H0 accepted
Triangle	Rectangle	0.263	0.069	0.816		H0 accepted
Triangle	Best fit	0.172	0.030	0.524		H0 accepted
Rectangle	Best fit	−0.233	0.055	−0.720		H0 accepted

Source Computed by the Authors, 2015 (N.B. *H0* Null hypothesis and *H1* alternative hypothesis; bold italics in the Remarks column indicate significant relation at respective significance level)

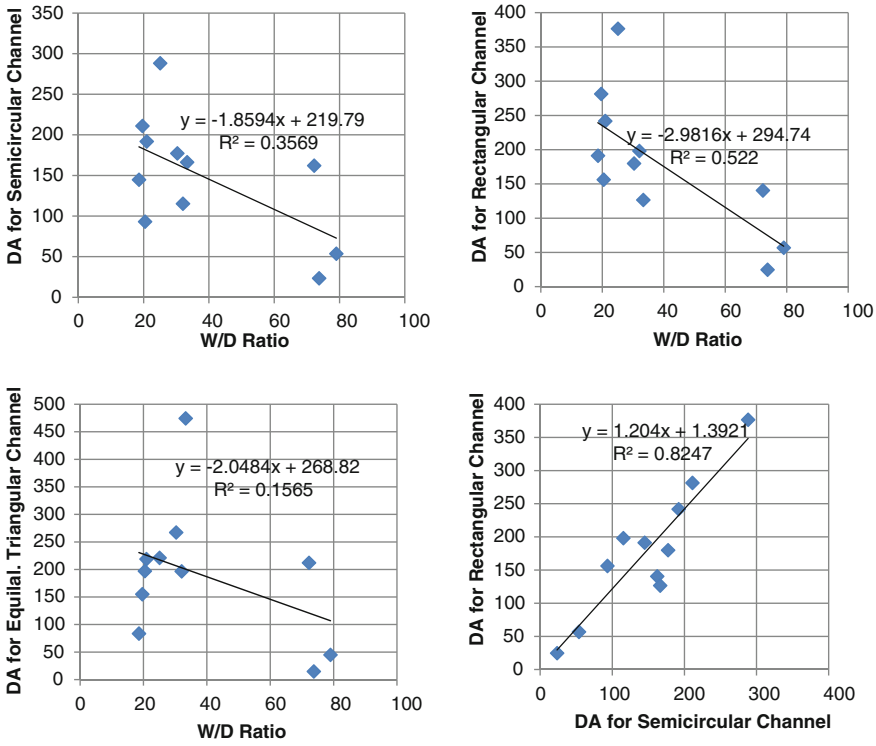

Fig. 5.6 Correlation between w:d ratio and DA for different channel shapes. *Note* DA denotes deviation area (sq.m)

triangular channels have more width than those of rectangular channels having w:d of 2:1.

With an increase in w:d ratio there will be a corresponding increase in the best fit value of DA (Tables 5.2 and 5.4, Fig. 5.7). In the present study the relation between the variables under consideration is significant at a 90 % significance level. The correlation between the different shapes in all possible combinations shows that except for the relation between semicircular shape and rectangular shape all other relations prove insignificant. The string correlation between the semicircular and the rectangular channel shapes proves that there is a close symmetry of the nature of the deviation area between the semicircle and rectangle. The naturality belongs to the principles of geometry.

Taking the variables viz. the w:d ratio and deviation area under triangular, semicircular, and rectangular and best fit curve, a PCA has been run. The component plot of the variables depicts that the selected 5 variables for 11 CS lie on or near the quadratic curve (Fig. 5.7). All the variables lie within the 95 % confidence level. There is a very strong quadratic correlation among the variables. The component location on the space shows a close association between the semicircular

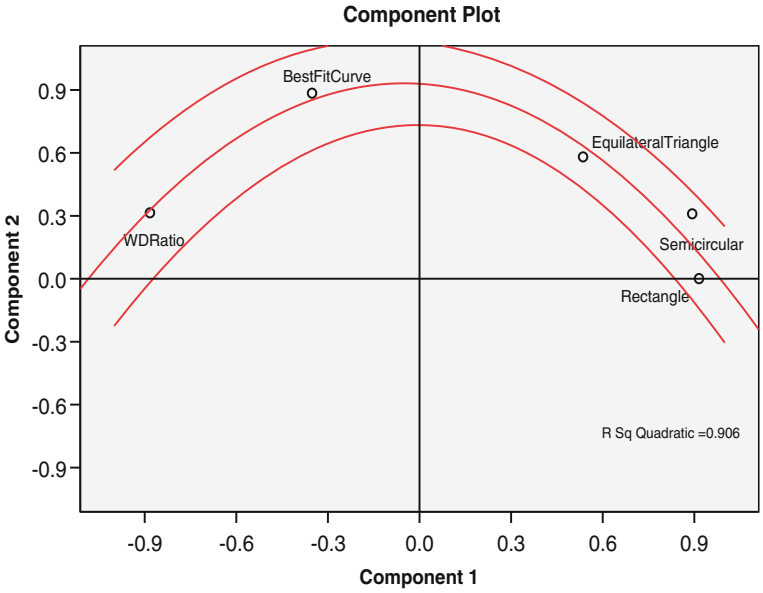

Fig. 5.7 Quadratic plot of the different channel shapes and w:d ratio

and rectangular channel shapes. The best fit curve is in distant association with the w:d ratio. Except for the best fit curve all other curves are located on the space diametrically opposite to that of the w:d ratio.

5.4 Conclusion

Channel shape is widely studied in different allied fields of river study as it has a definite control over flow pattern (Chow 1959). The channel form ratio (w:d) is the fundamental index of a channel shape. The ratio is inversely proportional to the silt-caly percentage of sediment (Schumm 1960). Hickin (1974) formulated the w:d ratio of a rectangular channel as 2:1. In general, shapes of channels appear in different geometrical shape including semicircular, triangular, rectangular, and trapezoidal, among others, in a different study (Chow 1959). This chapter tried to extend the radius of the sphere of the study of channel shapes. It provides tools for categorizing natural channel shapes to different groups of geometric figures to which the channel is the best fitted. The mean percentage of deviation area of these 11 cross-sections is less than 50 % (highest 49.31 %; Table 5.3) which implies that categorization of channels under different shapes is justified.

References

Bowman DTS (2010) Extreme rates of channel incision and shape evolution in response to a continuous, rapid base-level fall, the Dead Sea, Israel. Geomorphology 227–237
Chang HH (1980) Geometry of gravel streams. J Hydraul Div Am Soc Civil Eng 106 (HY9):1443–1456
Chanson H (2004) The hydraulics of open channel flow: an introduction, 2nd edn. Elsevier, Amsterdam, pp 44–46
Charlton Ro (2008) Fundamentals of fluvial geomorphology. Rutledge, New York, pp 4–7
Chow VT (1959) Open-channel hydrualics. McgrawHill Book Company, London
Church M (1992) Channel morphology and topology. In: Calow P, Petts GE (eds) The rivers handbook: hydrological and ecological principles. Blackwell, Oxford, pp 126–143
Das BC (2014) Asymmetry of river channel cross-sections: a review. Int J Res Manage Sci Technol (E-ISSN: 2321–3264) 2(3):15–18
Das BC (2015) Modeling of the most efficient channel form: a quantitative approach, modeling earth system and environment. Springer, New York
Einstein HA, Shen HW (1964) A study of meandering in straight alluvial channels. J Geophys Res 69:5239–5247
Garrett JHE (1910) Bengal District Gazetteer, Nadia, Bengal secretariat book depot, reprinted in 2001, p 14, 15, 26
Hancock GS et. al. (1998) Beyond power: bedrock incision process and form. In: Tinkler KJ, Wohl EE (Eds) Rivers over rock: fluvial processes in bedrock channels. Geophysical monograph series. American Geophysical Union, Washington DC, pp 35–60
Harvey AM (1969) Channel capacity and the adjustment of streams to hydrologic regime. J Hydrol 8:82–98
Harvey MD, Anthony DJ (1990) Stage-dependent cross-section adjustments in a meandering reach of fall river. Colorado Final Report. Final. Colorado: Geological Society of America, Bull, 1990
Heede BH (1981) Dynamics of selected mountains in the western United States of America. Zeitschriftfür Geomorphol 25:17–32
Henderson FM (1996) Open channel flow. Mac Millan Co., NewYork
Hey RD (1978) Determinate hydraulic geometry of river channels. J Hydraul Div 104 (HY4):365–379
Hickin EJ (1974) The development of meanders in natural river channels. Am J Sci 274:414–442
Hickin EJ (2004) River hydraulics and channel form. Wiley, Chichester, p 6.2
Hirst Major FC (1916) Report on the Nadia Rivers 1915, Bengal Secretariat Book Depot, pp 27–30
Jia Y (1990) Minimum froude number and the equilibrium of alluvial sand rivers. Earth Surf Process Land 15:199–209
Keller EA (1972) Development of alluvial stream channels: a five-stage model. Geol Soc Am Bull 83:1531–1536
Knighton AD (1981) Asymmetry of river channel cross-sections: part I. Quant Indices' Earth Surf Process Land 6:581–588
Knighton D (1998) Fluvial forms and processes a new perspective. Hodder Education, London, p 167
Langbein WB, Leopold LB (1964) Quasi-equilibrium state in channel morphology. Am J Sci 262:782–794
Leopold LB, Wolman MG (1960) River meanders. Geol Soc Am Bull 71:769–794
Majumder SC (1941) Rivers of the Bengal Delta. In: Biswas KR (Ed) 2001 Rivers of Bengal, Department of Higher Education, Government of West Bengal, p 17, 18, 54
Majumder D (1978) West Bengal District Gazetters Nadia. Government of West Bengal, p 5, 7, 16
Majumder S (1995) Sri Chaitanya Janmasthan Bitarka Tar Truti O Samadhan; Nabadwip, p 37
Majumder T (2011) Rajpat (in Bengali). Ananda, Kolkata

Milne JA (1979) The morphological relationships of bends in confined stream channels in upland Britain. In: Pitty AF (ed) Geographical approaches to fluvial processes. Geobooks, Norwich, pp 241–260

Nakamura F, Swanson FJ (1993) Effect of coarse woody debris on morphology and sediment storage of a mountain stream system in Western Oregon. Earth Surf Process Land 18:43–61

Richards K (1982) Rivers form and process in alluvial channels. Methuen & Co, New York, p 11

Rosgen DL (1994) A classification of natural rivers. Catena 22:169–199

Schumm SA (1960) The shape of alluvial channels in relation to sediment type, professional paper. U S Geol Surv 352B:17–30

Sen PK (1993) Geomorphological analysis of drainage basins. The University of Burdwan, Burdwan

Simon A (1992) Energy, time and channel evolution in catastrophically disturbed fluvial systems. (P. J. H, Ed.) Gemorphology 5:345–372

Simon A, Castro J (2003) Measurement and analysis of alluvial channel form. In: Kondolf GM, Piégay H (eds) Tools in fluvial geomorphology. Wiley, New York, pp 291–322

Simon AE, Darby S (1997) Process-form interactions in unstable sand bed river channels: a nuerical modelling approach. Geomorphology 21:85–106

Stevens MA et al (1975) Non-equilibrium river form. J Hydraul Div Am Soc Civ Eng 101 (HY5):557–566

Yang CT (1976) minimum unit stream power and fluvial hydraulics. J Hydraul Div Am Soc Civ Eng 102(HY7):919–934

Chapter 6
Effect of Longitudinal Disconnection on In-stream Bar Dynamics: A Study at Selected Road–Stream Crossings of Ajay River

Suvendu Roy and Abhay Sankar Sahu

Abstract Over the 1970–2010 periods, the effect of longitudinal disconnection was prominent around the road–stream crossings on the Ajay River of West Bengal. The crossings endorse significant changes on in-stream fluvial processes, for example, in-stream bar dynamics, thalweg wandering, and channel avulsion. The imbalanced condition of sediment delivery has induced a change of 87 and 61 % of the braiding index in the upstream and downstream reaches of a bridge-crossing at sample site I, respectively. The temporal aggradation of the river channel has been significantly illustrated from bar stability analysed using the Normalized Difference Vegetation Index (NDVI), flow height observation, and field verification. Unequal distribution of channel sinuosity, migration rate, and avulsion make a threat to the bridge stability associated with severe bank erosion.

Keywords Longitudinal disconnection · Braiding index · Bar dynamics · Bridge stability · NDVI · Bank erosion

6.1 Introduction

Rivers of the Lower Gangetic Plain are notable for their complex interaction with the increasing human population. An extended spectrum of direct and indirect human activities is continuously inducing change in the natural architecture of the alluvial rivers. The effect of road–stream crossing (bridge and culvert) is one of the important in-stream direct moderators of channel morphology (Norman 2006; Vermont Department of Fish and Wildlife 2009; Blanton and Marcus 2013), which

S. Roy (✉) · A.S. Sahu
Department of Geography, University of Kalyani, Kalyani Nadia-741235, India
e-mail: suvenduroy7@gmail.com

B.C. Das et al. (eds.), *Neo-Thinking on Ganges-Brahmaputra Basin Geomorphology*, Springer Geography, DOI 10.1007/978-3-319-26443-1_6

Table 6.1 Short- and long-term effects of highway, bridge, and/or culvert construction over the river channel on geomorphology and hydraulics (After FHWE 1990)

Immediate effects	Delayed effects
Increased flow velocity Contraction Local scour development Sediment removal from upstream and deposition in the immediate downstream Backwater effect Increased sediment yield in river water	Become straight planform of the channel downstream River incision or low entrenchment ratio Increase of the stream gradient Lowering of water level in the main channel, and negative change in the local base level of erosion of the tributary streams, increased channel bed gradient and erosional activities in the tributaries, and start of degradation of local area Instability of river bank and bridge/culvert

has recently been the focus of fluvio geomorphological research as a longitudinal disconnection in river channels. Road–stream crossings are necessary for land transport systems to cross waterways, but improperly designed crossing structures may cause alternation of stream geomorphology and create environmental harm for the stream habitat (Resh 2005; Wheeler et al. 2005; Merril and Gregory 2007; Bouska et al. 2010). The Federal Highway Administration or FHWE (1990) reported the significant general and local level effects of highway and bridge construction on fluvial geomorphology and hydraulics of river systems. This document has also categorized the total effects into two types: immediate and delayed effects on a river system (Table 6.1).

River connectivity varies in three spatial dimensions: lateral, longitudinal, and vertical (Amoros et al. 1987; Ward 1989; Blanton and Marcus 2009, 2014; Cong et al. 2014). Lateral connectivity induces a floodplain and channel relationship that helps to exchange energy and matter between these two platforms (Thoms 2003). Lateral disconnection could cause significant ecological damage, including loss of riparian forest, channel and floodplain habitat loss and/or simplification, and loss of richness and diversity for both terrestrial and aquatic species (Bravard et al. 1986; Ward and Stanford 1995; Blanton and Marcus 2009). Vertical connectivity refers to the surface–subsurface interaction of water, sediment, and nutrients (Brierley et al. 2006). Longitudinal connectivity, which is focused on in the present study, deals with upstream–downstream and tributary–trunk stream relationships (Cong et al. 2014). The longitudinal disconnection could negatively affect flow condition and sediment distribution in the river (Ward 1989; Wellman et al. 2000). Merril and Gregory (2007) documented the effect of road crossings on stream geomorphology and its biological behaviour with 14 stream crossings (six bridges and eight culverts) in North Carolina. Bouska et al. (2010) pointed out that water crossings act as partial or check dams within a channel and increase the riffle spacing, which affects fish passage. The backwater effect was also reported including changing local level in-stream geomorphology using Rosgen's (1994) stream classification model.

The role of road–stream crossing on the alternation of downstream channel width (Gregory and Brookes 1983; Roy 2013), flow velocity (Roy 2013), carrying capacity (Merril and Gregory 2007), inter-and intra-pool riffle spacing (Bouska et al. 2010), stream network (Jones et al. 2000), landslide and slope instability (Nelson and Martin 1981), lateral connectivity with floodplain (Blanton and Marcus 2009, 2014), and bridge pier-induced river hydraulics changes (Kothyari and RangaRaju 2001) have been well studied. However, the effect of longitudinal disconnection on in-stream bar dynamics is little explored. Bridge piers play a key role in the alternation of channel geomorphology as a longitudinal obstruction within the channel (Kothyari and RangaRaju 2001). These piers perform as dam structures and trap a large amount of sediment behind them, producing starved water downstream (Graf 1971; Ryan et al. 2014). Bridge piers have modified channel morphology by increasing flow velocities that generating greater flow turbulence (McKenney et al. 1995; Robert 2003; Wang et al. 2010; Roy 2013). In addition, these structures act as blockage for boulders and woody debris which directly influence in-stream sedimentation, development of bars, channel anabranching, planform geometry, and floodplain topography (Abbe and Montgomery 2003). Richardson and Richardson (1999) have recorded that during high flows a bed can degrade up to six metres and deep scour has been formed there. Due to bridge piers, local scour development can have a long-term impact on bed degradation and affect entire channel reaches (Simon and Johnson 1999). Grade and Kothyari (1998) have explained a mathematical mechanism of different shapes of bridge piers and their role in scour making.

At the regional level, Bhattacharya (1958) documented that bridge construction over the Rupnarayan River (for the Kolkata–Mumbai National Highway, West Bengal) with piers had induced heavy sedimentation, frequent flooding, and reduction of river navigability with significant loss of water passing capacity. According to Sing (1983), the construction of the bridge across the Gomti River modified the direction of channel flow and increased flow velocity which encouraged downstream erosion. Recently Roy (2013) in a micro-level study with a single road–stream crossing (bridge) on the Kunur River, West Bengal, observed that there is significant variation of channel geometry between upstream and downstream reaches of that crossing. It has been analysed that the connectivity structure of the megafan surface to predict the avulsion pathway of the August 2008 event demonstrated that the connectivity structure can serve as a predictive tool for postulating future avulsion pathways (Sinha et al. 2013). Kumar et al. (2014) presented an intensive GIS and field-based work on the two-dimensional (lateral and longitudinal) geomorphic connectivity over the Kosi megafan.

This present work tries to assess the effect of road–stream crossing on thalweg and in-stream bar dynamics and its consequence on bridge stability on the Ajay River.

6.2 Materials and Methods

6.2.1 Study Sites

Three sample bridge sites were selected for detailed investigation and mapping of the fluviogeomorphological changes due to the longitudinal obstruction created by bridge piers, abutments, and wingwalls. A five-km radius circular zone has been delineated from the centre of each site (Fig. 6.1). These three bridges play an important role in connecting two districts, Bardhaman in the south and Birbhum in the north on both sides of the Ajay River. The basic structural information of these bridges is listed in Table 6.2. For a comparative study between different segments of the Ajay River, a ~152 km reach from the confluence point (near Katwa) has been also investigated. The Ajay River flows here with an average slope of 0.036 m/m and sitewise slope varies from 0.048 m/m, 0.080 m/m, and 0.063 m/m for the sites 1, 2, and 3 respectively. During July to October, the average discharge of the Ajay is ~7000 cusec at Illambazar (Das and Biswas 1968). The average annual rainfall is approximately 1271 mm, however, sometimes this area faces torrential rainfall during the rainy season, for example, 369 mm rainfall within three days (18 to 20 September, 2000) and causing a devastating flood (Mukhopadhyay 2010). The uniform underlying geology of these sites (i.e. unoxidized Late Quaternary sediments of Diara Formation) consists of unconsolidated medium- to fine-grained pale yellow sands with minor light brown silt and grey to black clay porous in some point bar and channel bar deposits (Roy and Banerjee 1990).

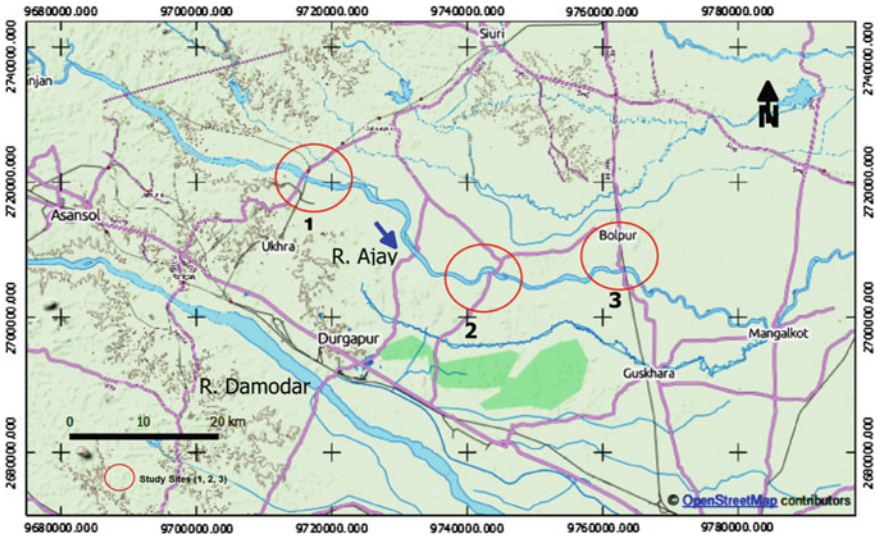

Fig. 6.1 Selected study sites (bridges) over the Lower Ajay River, West Bengal

Table 6.2 Structural characteristics of sample bridge sites

Site ID	Bridge site[a]	Road name	No. of piers within the channel	Length (m)	Span or width (m)
1	Pandaveswar (2)	NH 60 + Eastern Railway	14 (road); 14 (railway)	856 (road); 522 (railway)	10 (road); 11 (railway)
2	Illambazar (1)	SH 14	8 (road)	525.00 (road)	9.0 (road)
3	Bhedia (2)	NH 2B + Eastern Railway	29 (road); 29 (railway)	422 (road); 655 (railway)	10 (road); 10 (railway)

[a]Values in brackets indicate the number of bridges at a single site

6.2.2 *Extraction of Bars and Thalweg*

The stability of a bar depends upon the type of vegetation or level of biomass available on the deposited fluvial features (Brice 1964; Gurnell et al. 2009). Permanent vegetation or biomass turns bars into islands with the help of higher colonization of sediments (Bridge 2003; Gurnell et al. 2009). In the present work, the Normalized Difference Vegetation Index (NDVI) has been used for a temporal study about the growth of in-stream bars and islands. A Landsat series of satellite images (after transforming the bands from DN value to reflectance value) of the winter period for the years 1990, 2001, 2006, and 2015 (October to January) have been used for NDVI calculation, where the positive value >+0.20 was taken as permanent biomasses and negative value was taken as water bodies. The boundaries of bars and islands have been delineated based on the NDVI value (>+0.20) and thalweg of the Ajay River for these years are also delineated using negative NDVI values. The range of NDVI values has also been used for a qualitative interpretation of river depth and stability of bars.

6.2.3 *Delineation of Bank Bluff Lines*

With the basic rules of valley delineation by the Vermont Department of Fish and Wildlife (2009), Google Earth images (2015) are capitalized to delineate the bank bluff lines for the each bankside extended from five km upstream to five km downstream of the bridges. During this process, bankside tree line, vegetation types and pattern, land-use types, shape of cultivated fields, bedrock walls, and higher terraces using SRTM (Shuttle Radar Topographic Mission) DEM (Digital Elevation Model) generated a contour line at five m intervals; alluvial fan toes, man-made foot track, and so on are also followed.

6.2.4 Applied Fluviometric Indices

The degree of braiding in site 1 has been calculated using the braiding index as proposed by Brice (1960, 1964); that is, [(2 × sum length of bars or islands in a reach)/centerline reach length]. The sinuosity of thalweg lines has been estimated by a classical sinuosity index using the ratio of a long channel distance to the shortest path length (Leopold et al. 1964). Hawth's tool based (an extension in Arc GIS) flow turn angle of respective thalweg lines was calculated at every 1000 m interval. The interpretation of the flow turn angle should be integrated because certain changes in flow path, that is, thalweg lines may be the result of neotectonic influence or anthropogenic activities or both (Roy and Sahu 2015). The average migration rate (metre/year) of channel thalweg has also been calculated at 45 cross-section sites at about ~3 km intervals up to a confluence point. The temporal extensions were taken from 1973 to 1990, 1990 to 2001, and 2001 to 2015, respectively.

6.3 Result and Analysis

6.3.1 Dynamics of Channel Thalweg and Its Allocation

Extracted thalweg lines of the Ajay River for the last four decades show the shifting tendency of the thalweg is very frequent adjacent to the bridge sites (Fig. 6.2). With

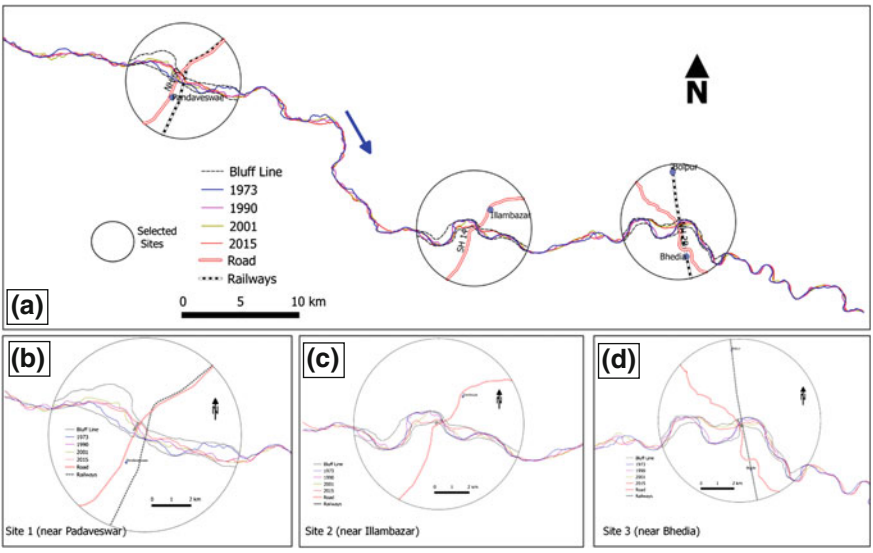

Fig. 6.2 Temporal changing pattern of Ajay River thalweg with special looks at three sample road–stream crossing sites

Table 6.3 Reachwise temporal variation of Thalweg Sinuosity index

Site Year	Site 1 (Pandaveswar)		Site 2 (Illambazar)		Site 3 (Bhedia)	
	Upstream	Downstream	Upstream	Downstream	Upstream	Downstream
1973	1.14	1.19	1.47	1.16	1.51	1.17
1990	1.21	1.10	1.51	1.18	1.48	1.20
2001	1.22	1.06	1.34	1.15	1.22	1.35
2006	1.14	1.05	1.25	1.10	1.23	1.14
2015	1.51	1.13	1.33	1.10	1.26	1.20
Average	1.24	1.11	1.38	1.14	1.34	1.21

respect to the other segments of the Lower Ajay River, thalweg lines in the upstream reach of each bridge site are highly wandering with an increasing sinuosity index (Table 6.3). The average sinuosities of upstream reaches are higher than downstream reaches for all three bridge sites. The lower sinuosity of the downstream area highlights the channel straightening due to increasing flow velocity, steep channel bed slope (McKenney et al. 1995; Robert 2003; Wang et al. 2010; Petrovszki et al. 2014), and lack of suspended sediment (Abbe and Montgomery 2003; Fryirs et al. 2007; Thompson et al. 2015). The higher sinuosity in the upstream area indicates the shifting of the active channel area due to sedimentation and progressive development of point bars (Williams 1986). Flow turn angles of three respective thalweg lines—1990, 2001, and 2015—reflect the role of the bridge structure on the alternation channel thalweg (Fig. 6.3a). Near sites 1 and 2, the turn angle of all three thalweg lines makes an approximately straighter pattern than found upstream, whereas near site 3 the turn angle abruptly increases more than upstream and downstream. Since 1973, the average thalweg fluctuation is also higher adjacent to the bridge sites (B) than other parts (Fig. 6.3b).

As seen in Figs. 6.2a–d and 6.3a, b, the wandering of the channel thalweg is directly associated with the allocation of road–stream crossing or bridge in particular for this work. According to Ramkumar et al. (2015), the in-stream geomorphological alternations are directly influenced by the thalweg instability. In these circumstances, the present study has focused on the in-stream bar dynamics at three sample bridge sites across the Ajay River.

6.3.2 Alternation of Bar Geomorphology at Sample Sites

6.3.2.1 Site I (Near Pandaveswar)

The braided segment of the Ajay River near Pandaveswar is clearly affected by road–stream crossing and it induces thalweg wandering (Fig. 6.2a) and flow pattern. Figure 6.4a–f shows the temporal decrease in braiding index which declines from 1.36 to 0.18 in the upstream and 0.82 to 0.31 in the downstream from 1990 to 2015.

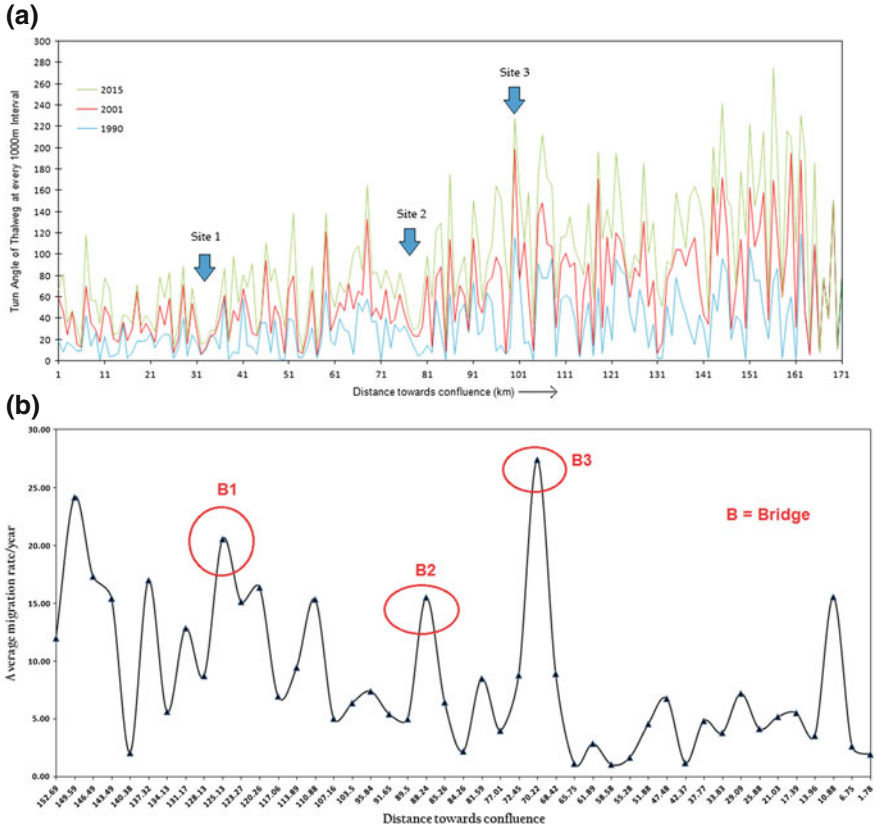

Fig. 6.3 **a** Flow turn angle (in degree) of thalweg lines at every 1000 m interval. **b** Average migration rate (m/y) of channel thalweg towards confluence point since 1973

Due to this declination, the Ajay River turns into a single thread channel from a multichannel river with the strong negative correlation between the sinuosity index and braiding index ($r = -0.91$ in the upstream and $r = -0.92$ in the downstream).

Since 1990, the negative range of NDVI (<0.00) is decreasing and it reduces the NDVI value of −0.41 to −0.14 between 1990 and 2015 because the temporal aggradation of the riverbed is increased due to huge sedimentation on the active channel bed. As a result, within this segment the cross-bar channels are enclosed day by day and it helps to assemble bars with the floodplain segment. Thereby, the Ajay River has lost its natural braiding pattern and is becoming a sinuous single channel (Gurnell et al. 2009). Nevertheless, the increasing range in positive value of NDVI (+0.28 to +0.68 from 1990 to 2015) suggests the temporal maturity of bars and islands with permanent vegetation. Although the maximum value of positive NDVI is high, the visual impression shows that the area of natural vegetation is low due to the transformation of the natural floodplain and stable island into the agricultural field and related encroachments of the Ajay River.

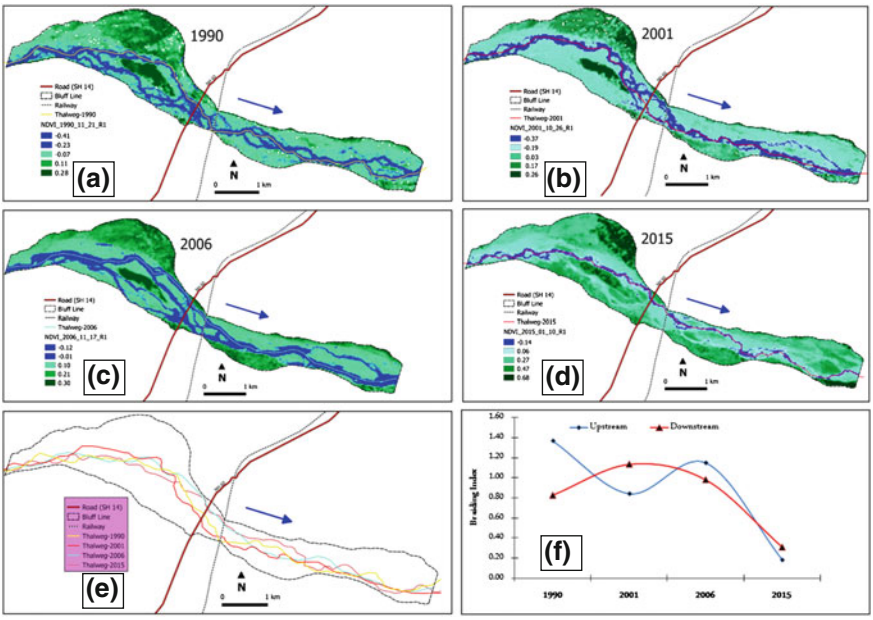

Fig. 6.4 a–f Multi-thread channel of Ajay River turns into single-thread channel near Pandaveswar segment due to river aggradation and associated decreasing braiding index

6.3.2.2 Site II (Near Illambazar)

The progressive growth of the point bar upstream of the Illambazar Bridge has been encountered using a temporal observation of satellite data (Landsat series of data for low water season, i.e. winter; Figs. 6.5a–f). Just immediately upstream of site 2, rapid erosion of a point bar generates a serious risk (viz., risks of basement loss, destruction of abutments and wing-walls of this bridge) for the collapse of bridge piers in the left bank. Due to local level longitudinal obstruction by bridge piers, the backwater effect induces the stacking of sedimented water upstream and encourages huge sedimentation. As a result, the highlighted point bar in the left bank of the upstream area extended its area from 1.01 to 1.46 km^2 from 1990 to 2015. Nevertheless, the right-side bar (it had 0.25 km^2 areal extension in 1990) in the immediate upstream of the crossing has totally vanished in 2015.

The growth of the upstream point bar towards downstream has forced a shift in the channel thalweg towards the south and accelerated the rate of bank erosion near the bridge abutments and wing walls. In the downstream, the mid-channel bar has lost its areal coverage from 2861 to 1960 m^2 from 1990 to 2015 and become a transverse circular bar from a longitudinal bar in shape. Similar to the previous site, the NDVI values also indicate the temporal maturity of bars with permanent healthy vegetation, but in terms of water depth analysis there is no radical change in negative NDVI values.

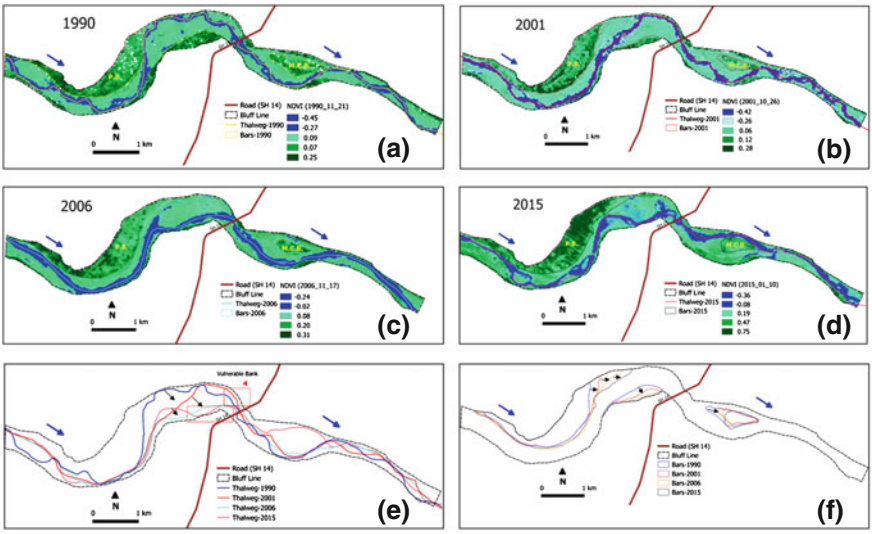

Fig. 6.5 Temporal alternation of in-stream geomorphology of Ajay River near Illambazar

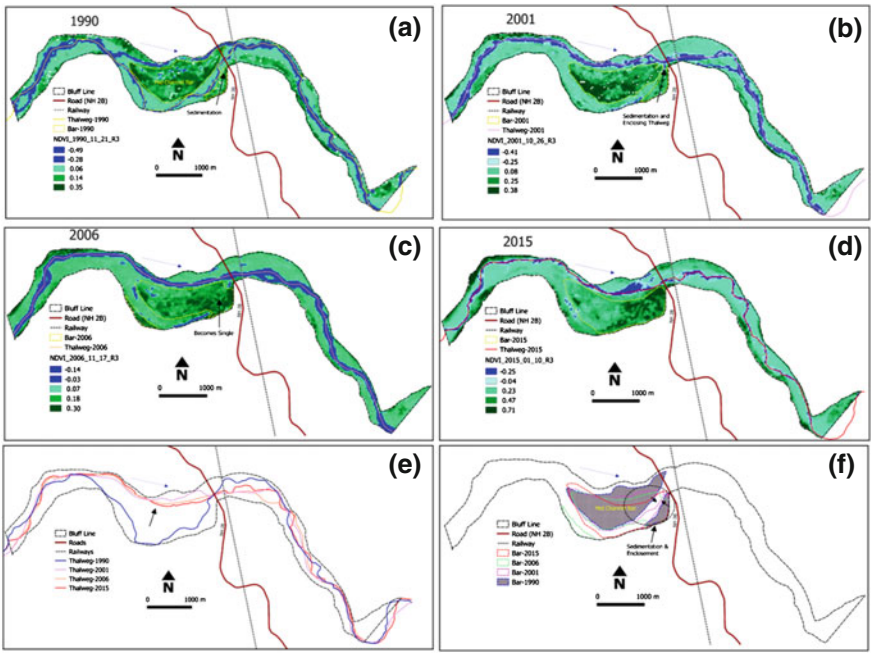

Fig. 6.6 Progressive transformation of mid-channel point bar into floodplain and channel shifting of Ajay River near Bhedia

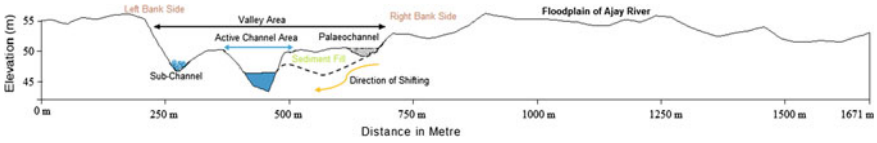

Fig. 6.7 Cross profile of the Ajay River Valley upstream of Bhedia Bridge

6.3.2.3 Site III (Near Bhedia)

Since 1990, the gradual transformation of the mid-channel point bar into the floodplain has been observed upstream of the Bhedia Bridge. It is assumed that initially the effect of backwater has helped to develop this mid-channel bar and the continuous sedimentation creates the present situation. The black arrow in Fig. 6.6a shows where the sedimentation starts due to the bridge and related to flow obstruction which helps to develop an expanding point bar just immediately upstream of the bridge structure. Due to the temporal expansion of both bars the cross-bar channel of this part has lost its dimension and is becoming an abandoned channel in 2006. With the continuous process of sedimentation during major floods of the Lower Ajay River Basin, the depression of this parafluvial zone is filled with sediments and it develops a continuous floodplain adjacent to the right bank of the Ajay River (Figs. 6.6a–f). As a result, the Ajay River channel shifts towards the north, and the left bank of this reach has faced the problem of bank erosion (Fig. 6.7).

6.4 Discussion

Fluvial discontinuities alter the longitudinal flux of water and sediment by storing, releasing, or changing the flow path of those materials (Burchsted et al. 2014). These can disrupt the progression of a river towards a graded system (Burchsted et al. 2014). Knowledge of the spatial and temporal trends of channel adjustment is important to protect and maintain bridge stability and transport connectivity. The very recent bridge cutoff in Darjeeling (near Mirik), India on 1 July, 2015 is also a result of channel instability and certain inflow of huge debris-accumulated water (ToI 2015). Over the Ajay–Damodar interfluve, there are many other examples of bridge failures following channel modification (Figs. 6.8a, b). Due to the frequent shifting of the Ajay's thalweg, the left bank of the Ajay River below Illambazar Bridge is also facing severe bank failure with a vertical fall of bedrock outcrops, that is, duricrust (Figs. 6.8c, d). As a result, the adjacent bridge pier is suspected to be under serious risk of collapse.

The temporal rising of the stream flow level at different gauge stations of the Lower Ajay River also support the gradual aggradation and rising of the channel bed (Fig. 6.9). Mukhopadhyay (2010) has reported the frequent and progressive

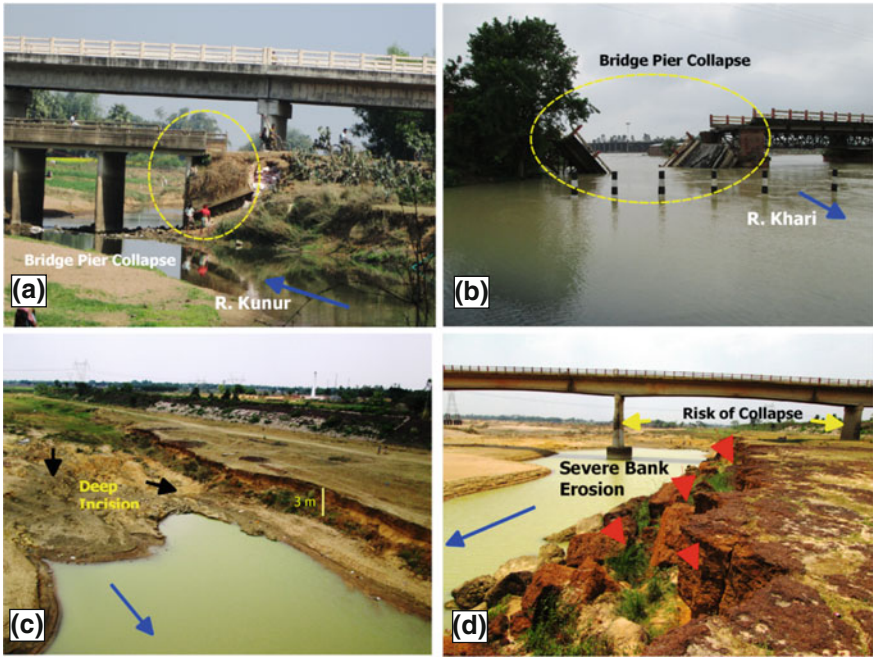

Fig. 6.8 **a**, **b** Typical examples of bridge cutoffs due to pier collapse; **c**, **d** deep channel incision and severe bank erosion of Ajay River is becoming a serious problem for bridge failure at Illambazar

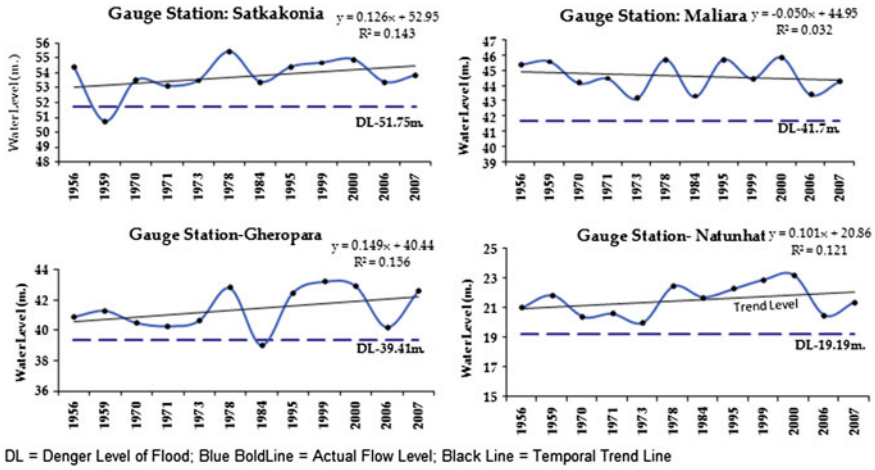

Fig. 6.9 Flow height of different gauge stations of the Lower Ajay River. *Source* Irrigation and Waterways Directorate, Mayurakshi South Canal Division, Govt. of West Bengal

nature of flood in the lower Ajay River Basin, where the rate of sand splay has also significantly increased due to riverbed rises and embankment breaching. The narrowing channel width of the Ajay River is also a serious cause of this situation (Mukhopadhyay 2010; Roy 2012; Roy and Sahu 2015), which may have an indirect effect on the bridge piers' instability and bank erosion.

According to Ramkumar et al. (2015), in-stream obstructions such as a dam or bridge helps the initial settling of sediment at a site and thereafter the settled sediments increase the friction with moving water, augmenting the settlement of sediment exponentially. With the continued and exacerbated sediment accumulation, the sediment layers rise near or above the water level and become the preferred regions of grass development. Similar processes may occur in the Ajay River by the bridge piers. In an experimental work, Coulthard (2005) showed that the presence of large and erosion-resistant plants within the channel (e.g. trees or shrubs) can

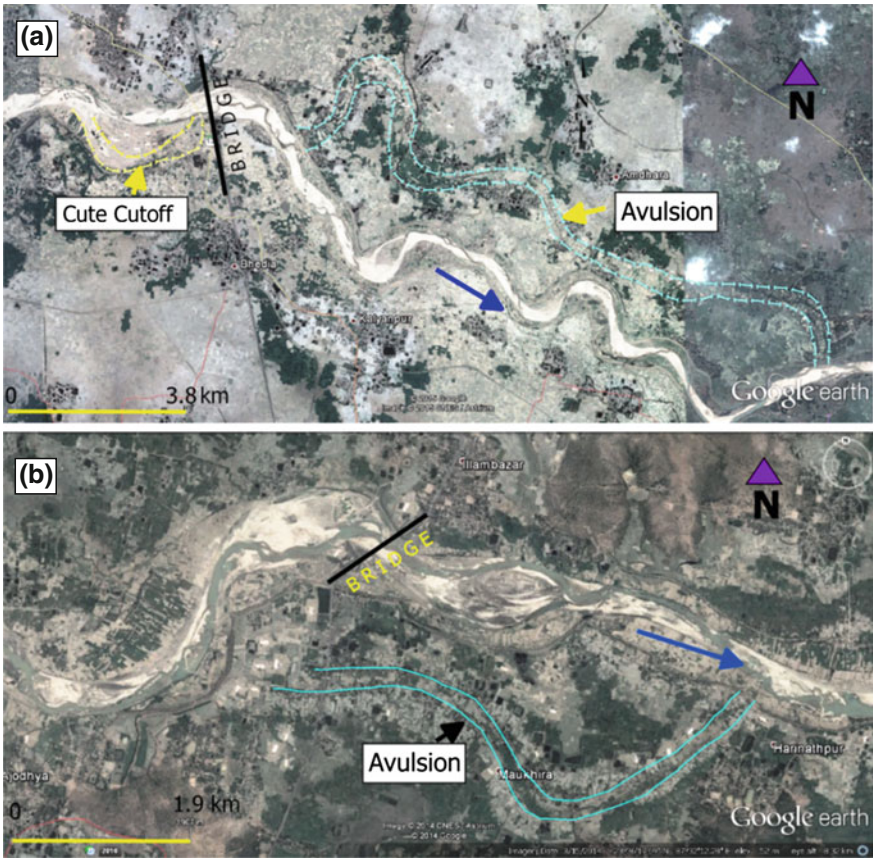

Fig. 6.10 Avulsion and cute cutoff of Ajay River adjacent to the road-stream crossings at **a** Bhedia and **b** Illambazar

have a significant impact on channel pattern and planform dynamics. Similarly, Hey and Thorne (1986) demonstrated that the widths of channels with densely vegetated banks were approximately 50 % narrower than similar but sparsely vegetated channels. Hupp and Osterkamp (1996) described how riparian vegetation is largely controlled by patterns of erosion and deposition along braided streams in the Great Plains area, and in channelized streams vegetation patterns were governed by cycles of degradation and aggradation. Jiongxin (1997) stated that channel width is the reflection of the channel boundary condition and this condition has strong control over the in-stream bar formation. According to FHWE (1990), in a sand-bed river, being adjacent to a bridge bed configuration can cause a threefold change in resistance of flow and a ten- to 15-fold change in concentration of bed sediment transport. In low-gradient higher-order streams obstruction of flow during high discharge may lead to local avulsion and overbank sedimentation on restricted areas of the floodplain (Gurnell and Gregory 1984), or to the development of chutes and meander cutoffs (Keller and Swanson 1979), as seen in the present study area (Figs. 6.10a, b).

6.5 Conclusion

Over the region, a complex interaction between stream network and transport infrastructure is captured from the examples of a bridge cutoff due to failure of piers, avulsions, dynamics in bar formation, frequent thalweg shifting, severe bank erosion, channel incision, temporal rising of flood flow height, and river aggradation, among others. Although the impact is at the local level, this type of study is essential for river engineering and development of a transport network while minimizing the possibility of bridge collapse. Further study helps to delimit the exact extension of bridge pier related problems in the upstream and downstream direction of a river channel with possible geomorphic changes. Upstream sedimentation and liquefying of the bank section are the major threats to bridge stability. Sustainable sand mining in the upstream reach and regular monitoring of delineated river reaches adjacent to the bridge site can help to manage the problems of bridge cutoff and bank erosion. Application of remote sensing and GIS has the potential to identify vulnerable bridge sites and monitor them rigorously, especially during the time of monsoon floods.

References

Abbe TB, Montgomery DR (2003) Patterns and processes of wood debris accumulation in the Queets river basin, Washington. Geomorphology 51:81–107

Amoros C, Roux A, Reygrobellet J, Bravad JP, Pautou G (1987) A method for applied ecological studies of fluvial hydro systems. Regulated Rivers Res Manage 1(1):17–36

Bhattacharya K (1958) BangladesherNad-Nadi o Parikalpana (in Bengali). Bidyadoya Library Ltd., Calcutta
Blanton P, Marcus WA (2009) Railroads, roads and lateral disconnection in the river landscapes of the continental United State. Geomorphology 122:212–227
Blanton P, Marcus WA (2013) Transportation infrastructure, river confinement, and impacts on floodplain and channel habitat, Yakima and Chehalis rivers, Washington, USA. Geomorphology 189:55–65
Blanton P, Marcus WA (2014) Roads, railroads, and floodplain fragmentation due to transportation infrastructure along Rivers. Ann Assoc Am Geogr 104(3):413–431
Bouska WW, Keane T, Paukert CP (2010) The effects of road crossings on prairie stream habitat and function. J Freshw Ecol 25(4):499–506
Bravard JP, Amoros C, Pautou G (1986) Impact of civil engineering works on the successions of communities in a fluvial system: a methodological and predictive approach applied to a section of the Upper Rhône River, France. Oikos 47(1):92–111
Brice JC (1960) Index for description of channel braiding. Bull Geol Soc Am 71:1833
Brice JC (1964) Channel patterns and terraces of the Loup Rivers in Nebraska. US Geol Surv Prof Pap 422D:1–41
Bridge JS (2003) Rivers and floodplains: forms, processes, and sedimentary records. Blackwell Publication, Oxford
Brierley G, Fryirs K, Jain V (2006) Landscape connectivity: the geographic basis of geomorphic applications. Area 38(2):165–174
Burchsted D, Daniels M, Wohl EE (2014) Introduction to the special issue on discontinuity of fluvial systems. Geomorphology 205:1–4
Cong W, Shiliang L, Li D, Qi L, Juejie Y (2014) Road lateral disconnection and crossing impacts in river landscape of Lancang River Valley in Yunnan Province China. Chin Geogr Sci 24 (1):28–38
Coulthard TJ (2005) Effects of vegetation on braided stream pattern and dynamics. Water Resour Res 41(W04003):1–9
Das S, Biswas AB (1968) Report on the groundwater investigation in parts of the Burdwan and Birbhum District, West Bengal. Unpublished Report, Geological Survey of India. Kolkata
Federal Highway Administration (1990) Manual for river environment conservation. Highways in the river environment (HIRE), Report No. FHWA-HI-90-016
Fryirs KA, Brierley GJ, Preston NJ, Kasai M (2007) Buffers, barriers and blankets: the (dis)connectivity of catchment-scale sediment cascades. Catena 70:49–67
Grade RJ, Kothyari UC (1998). Scour around bridge piers. PINSA 64(A) 4:569–580
Graf WH (1971) Hydraulics of sediment transport. McGraw-Hill, New Work
Gregory KJ, Brookes A (1983) Hydrogeomorphology downstream from bridges. Appl Geogr 3:145–159
Gurnell AM, Gregory KJ (1984) The influence of vegetation on stream channel processes. In: Burt TP, Walling DE (eds) Catchment experiments in fluvial geomorphology. Cambridge University Press, Cambridge, pp 515–535
Gurnell AM, Surian N, Zanoni L (2009) Multi-thread river channels: a perspective on changing European alpine river systems. Aquat Sci 71:253–265
Hey RD, Thorne CR (1986) Stable channels with mobile gravel beds. J Hydraul Eng 112:671–689
Hupp CR, Osterkamp WR (1996) Riparian vegetation and fluvial geomorphic processes. Geomorphology 14:277–295
Jiongxin X (1997) Evolution of mid-channel bars in a Braided River and complex response to reservoir construction: an example from the Middle Hanjiang River, China. Earth Surf Proc Land 22:953–965
Jones JA, Swanson FJ, Wemple BC, Synder KU (2000) Road effect on hydrology, geomorphology, and disturbance patches in stream network. Conserv Biol 14:76–85
Keller EA, Swanson FJ (1979) Effects of large organic material on channel form and process. Earth Surf Proc Land 4:361–380

Kothyari UC, RangaRaju KG (2001) Scour around spur dikes and bridge abutments. J Hydraul Res 39(4):367–374

Kumar R, Jain V, Babu GP, Sinha R (2014) Connectivity structure of the Kosimegafan and role of rail-road transport network. Geomorphology 227:73–86

Leopold LB, Wolman MG, Miller JP (1964) Fluvial processes in geomorphology. W.H. Freeman, San Francisco

McKenney R, Jacobson RB, Wetheimer RC (1995) Woody vegetation and channel morphogenesis in low gradient gravel-bed streams in the Ozark Plateaus, Missouri and Arkansas. Geomorphology 13:175–198

Merril MA, Gregory J (2007) The effects of culverts and bridges on stream geomorphology. In: Levine JF et al (eds) Technical Report (FHWA/NC/2006-15) on a comparison of the impacts of culverts versus bridges on stream habitat and Aquatic Fauna. NC State University and NC Museum of Natural Sciences, Raleigh, pp 15–45

Mukhopadhyay S (2010) A geo-environmental assessment of flood dynamics in lower Ajoy River including sand splay problem in Eastern India. Ethiop J Environ Stud Manage 3(2):99–110

Nelson JD, Martin JP (1981) Slope stability as related to stream hazards to bridges. In: Shen HW, Schumm SA, Nelson JD, Doehring DO, Skinner MM, Smith GL (eds) Methods for assessment of stream-related hazards to highways and bridges. FHWE/RD-80/160, U.S. Department of Transportation Washington, D.C., pp 87–143

Norman JR (2006) Effects of road-stream crossings on stream geomorphology and the movement of small bodied fishes in the Etowah River Basin, USA. Published Thesis of Master of Science, The University of Georgia, Athens, Georgia

Petrovszki J, Timar G, Molnar G (2014) Is sinuosity a function of slope and bankfull discharge?—a case study of the meandering rivers in the Pannonian Basin. Hydrol Earth Syst Sci Discuss 11:12271–12290

Ramkumar M, Kumaraswamy K, Arthur James R, Suresh M, Sugantha T, Jayaraj L, Mathiyalagan A, Saraswathi M, Shyamala J (2015) Sand mining, channel bar dynamics and sediment textural properties of the Kaveri River, South India: implications on flooding hazard and sustainability of the natural fluvial system. In: Ramkumar M, Kumaraswamy K, Mohanraj R (eds) Environmental management of River Basin ecosystems. Springer International Publishing, Switzerland, pp 283–318

Resh VH (2005) Stream crossings and the conservation of diadromous invertebrates in South Pacific island streams. Aquat Conserv Mar Freshw Ecosyst 15:313–317

Richardson EV, Richardson JR (1999) Determining contraction scour. In: Richardson EV, Lagasse PF (eds) Stream stability and scour at highway bridges. American Society of Engineers, pp 483–490

Robert A (2003) River processes. Arnold, London

Rosgen DL (1994) A classification of natural rivers. Catena 22:169–199

Roy S (2012) Spatial variation of floods in the lower Ajay River Basin, WestBengal: a geo-hydrological analysis. Int J Remote Sens GIS 1(2):132–143

Roy S (2013) The effect of road-stream crossing on river morphology and riverine aquatic lives: a case study in Kunur River Basin, West Bengal. Ethiop J Environ Stud Manage 6:835–845

Roy BC, Banerjee K (1990) Quaternary geological and geomorphological mapping in parts of Bardhaman and Bankura Districts(and preliminary assessment of sand deposits suitable for construction and other allied purposes). Published Report, Geological Survey of India, Eastern Region, Calcutta

Roy S, Sahu AS (2015) Quaternary tectonic control on channel morphology over sedimentary low land: a case study in the Ajay-Damodar interfluve of Eastern India. Geosci Front. doi:10.1016/j.gsf.2015.04.001

Ryan SE, Bishop EL, Daniels JM (2014) Influence of large wood on channel morphology and sediment storage in headwater mountain streams, fraser experimental forest, Colorado. Geomorphology 217:73–88

Simon A, Johnson PA (1999) Relative roles of long term channel adjustments processes and scour on the reliability of bridge foundations. In: Richardson EV, Lagasse PF (eds) Stream stability and scour at highway bridges. American Society of Civil Engineers, pp 151–165

Singh S (1983) Flood hazards and environmental degradation: a case study of the Gomti River. In: Singh LR (ed) Environmental management. Allahabad Geographical Society, Department of Geography, Allahabad University, pp 301–306

Sinha R, Gaurav K, Chandra S, Tandon SK (2013) Exploring the channel connectivity structure of the August 2008 avulsion belt of the Kosi River, India: application to flood risk assessment. Geology 41:1099–1102

The Times of India (2015) Heavy rainfall in Darjeeling trigger landslides, 36 killed—a news article. Kolkata, 2nd July, p 26

Thompson CJ, Fryirs K, Croke J (2015) The disconnected sediment conveyor belt: patterns of longitudinal and lateral erosion and deposition during a catastrophic flood in the Lockyer Valley, South East Queensland, Australia. River Res Appl doi:10.1002/rra.2897

Thoms MC (2003) Floodplain-river ecosystem: lateral connections and the implication of human interference. Geomorphology 56:335–349

Vermont Department of Fish and Wildlife (2009) Guidelines for the design of stream/road crossings for passage of aquatic organisms in Vermont. Vermont Fish & Wildlife Department, Vermont

Wang J, Edwards PJ, Goff WA (2010) Assessing changes to in-stream turbidity following construction of a forest road in West Virginia. TMDL 2010 Watershed Management to Improve Water Quality CD-ROM Proceedings, ASABE Publication Number 711P0710 cd

Ward JV (1989) The four-dimensional nature of lotic ecosystems. J North Am Benthological Soc 8 (1):2–8

Ward JV, Stanford JA (1995) Ecological connectivity in alluvial river ecosystems and its disruption by flow regulation. Regulated Rivers Res Manage 11(1):105–119

Wellman JC, Combs DL, Cook B (2000) Long-term impacts of bridge and culvert construction or replacement on fish communities and sediment characteristics of streams. J Freshw Ecol 15 (3):317–328

Wheeler PA, Angermeier PL, Rosenberger AE (2005) Impact of new highways and subsequent landscape urbanization on stream habitat and biota. Rev Fish Sci 13(3):141–164

Williams GP (1986) River meander and channel size. J Hydrol 88:147–164

Chapter 7
Causes of Flood Hazard in Murshidabad District of West Bengal: Victims' Perceptions

Swati Mollah

Abstract The flood is almost an annual phenomenon in Murshidabad district of West Bengal. Geographical location and socioeconomic diversity of the district deserve particular consideration in the matter of its sensitivity to flood risk. A number of factors contribute to the flood hazard in Murshidabad district. The study attempts to examine the causes of flood in the study area through the perceptions of the inhabitants living in 13 sample hamlets spread throughout the district. To quantify the rate of the responses of the inhabitants the RIDIT analysis method has been applied. It is found that victims' perceptions are subjective in terms of their past experience and the geographical location of their hamlets. The study also concludes that the geographical location of the hamlets plays the most noteworthy role in determining the perception of the inhabitants regarding the causes of flood in Murshidabad district.

Keywords Flood hazard · Flood risk · RIDIT analysis · Victims' perceptions · Murshidabad

7.1 Introduction

Extreme events in nature are determined by the principles of natural law but it is human perceptions of these events that turn them into disasters or resources. For exposed and vulnerable communities, the perception of natural risk is an essential link in the analysis of the human–environment coping relationship (Armas and Avram 2009). The perceptions of the causes of flood reveal people's knowledge of flooding and what needs to be done to ameliorate flood hazards (Agbola et al. 2012). It is necessary to understand how the residents perceive flood risk in their areas and what influences their consciousness towards preparedness against disaster. Because

S. Mollah (✉)
Department of Geography, Dumkal College, Basantapur, Murshidabad, West Bengal, India
e-mail: swatimollah@gmail.com

B.C. Das et al. (eds.), *Neo-Thinking on Ganges-Brahmaputra Basin Geomorphology*, Springer Geography, DOI 10.1007/978-3-319-26443-1_7

it is not possible that all people are so tolerant of flood risk in the areas where they live, it is important to identify the factors which affect the degree of acceptance of people to flood risk. In order to carry out early relief activities quickly in the event of a disaster, it is necessary to make local disaster prevention efforts. The people as well as the administrative authorities need to participate in actions and cooperate to protect their communities and have their efforts embedded in administrative planning. In order to promote local residents' involvement in disaster-prevention activities, a study needs to be conducted to identify the important factors of flood risk in their localities and their ranking in terms of their significance.

Communicating with people to learn about their current information, the basis of their decisions, and what information or government programs they desire, is a necessary step in lowering the social costs of floods. To design more effective communication, researchers need to learn more about how people think about floods and how much they know about the precipitating events and the protective actions they can take (Lave and Lave 1991). By failing to account for the additional people and property in the flood plain, experts conclude that the flood control program has not been effective (Platt 1986). No engineering structure can guarantee protection for people living in a flood plain. Recognizing this fact led social scientists to focus on people's decisions about location and protection (White 1945, 1964; Kates 1962).

One of the characteristics of recent flood disaster in Murshidabad district is that there is a huge economic loss including loss of livelihood, crops, livestock, housing, and so on, but the number of human casualties is less (IWD-GoWB 2009). The number of population affected and damages of croplands in different years due to flood have been shown in Fig. 7.1a, b. The people are not very equipped for this environmental extreme. One reason for people's lack of preparedness against flood disaster is the inappropriate perception of the flood risks in their locality. It has been shown in most studies on natural disaster that it is difficult for people to accept disaster risks appropriately (Slovic 1987). For example, people tend to perceive flood disasters as unavoidable periodic phenomena, not probable and random phenomena. Generally, people are rather inclined to believe that if a major flood disaster occurs in a certain year, then no major flood events are likely to come about in the near future. In addition, common people are tempted to assume that structures such as embankments and dams, being newly constructed, mean a total inhibition of disaster. It might be a strong point that such perceptions of people of natural disasters bear out people's recognition of flood risks in the study area. Thus the detailed study of the perceptions of local people regarding the causes of flood is a very significant approach to flood management in the study area.

There is no single source of flood in Murshidabad district but different parts of the district have different sources. The inhabitants from various parts share different kinds of perceptions regarding the cause of flood in their localities. The perception of victims about any environmental event is often influenced by a number of factors such as geographical location of the habitat, knowledge about the event, level of education, experience, and so on. Different communities have special responses to extreme events. Therefore the decision-making process necessarily calls for people's participation for efficient implementation of management policies. The

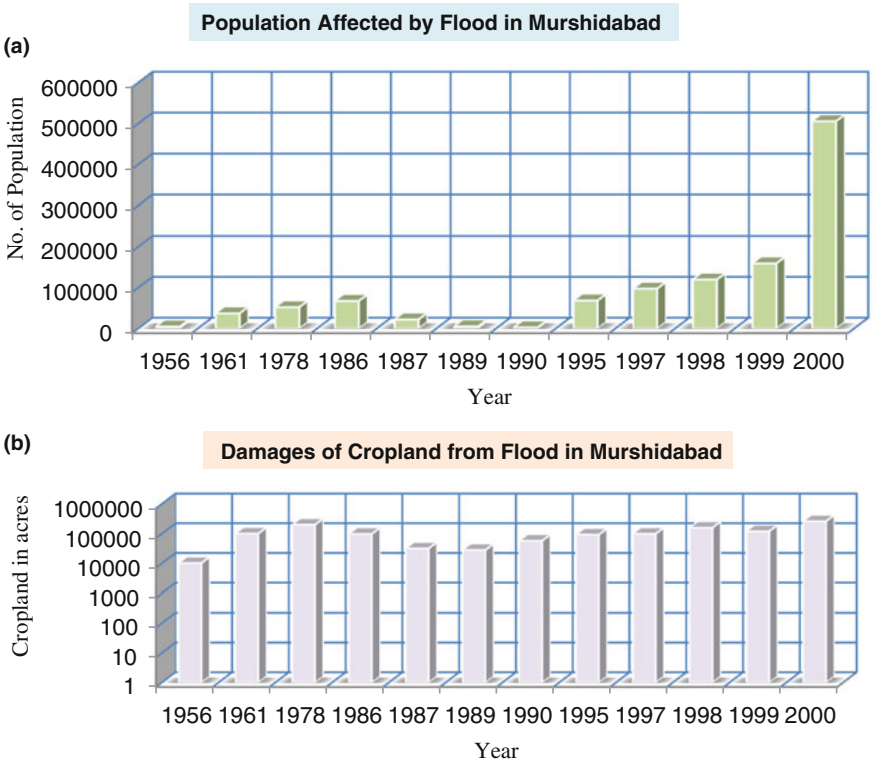

Fig. 7.1 **a** Population affected by flood in different years; **b** Damages of cropland from flood in different years; *Data Source* DRMS-GoWB (2009)

identification of commonly accorded apprehension of the flood hazard is the first step in a democratic process of formulating a flood-protection policy to be backed by the general public. More practice-oriented and experience-based local knowledge accumulated in flood prone areas' needs must be reconciled with a general expertise regarding flood issues. The effective ways of communicating the flood hazard message to the public, which are crucial for the efficacy of the participatory approach, have still been rather poorly explored.

7.2 Objectives

The study has the following objectives.

1. To analyse the causes of flood in the severely flood-affected hamlets of Murshidabad district
2. To assess the perceptions of the local inhabitants of the sample hamlets regarding the causes of flood in their localities

7.3 Study Area

Forming the apex of the Bengal Delta, Murshidabad district stretches between 23° 43′ to 24°50′N and 89°49′ to 88°46′E in the central part of West Bengal (Fig. 7.2). The district is a part of the Lower Gangetic Plain and is replete with rivers and stream channels. Its area is about 5324 km^2 and the total population of the district was 7,103,807 persons in 2011 (DCO-GoI 2011). As for its geographical situation, physiographic conditions, climatological characteristics, and socioeconomic peculiarity it deserves particular consideration in the matter of its susceptibility to flood.

Geomorphologically the district occupies the region between the River Padma (which roughly constitutes its eastern boundary) and the River Bhagirathi, the northernmost distributary of the Padma and several floodplains of the rivers (viz. Bansloi, Pagla, Dwaraka, Mayurakshi, and Babla Rivers) join the Bhagirathi on its west bank. About 54 % of the total geographical area of Murshidabad district is categorized as floodprone (Fig. 7.3a). Generally recurrent floods of the district are caused by spillage from the Padma, overflow from west bank tributaries of the Bhagirathi, sudden water release from the reservoir, and water-logging due to embankments along the feeder canal.

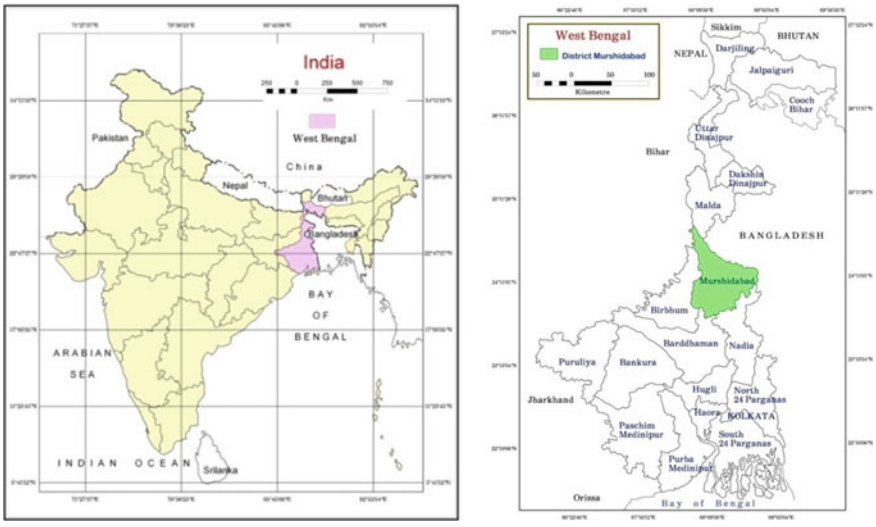

Fig. 7.2 Location of Murshidabad district in West Bengal

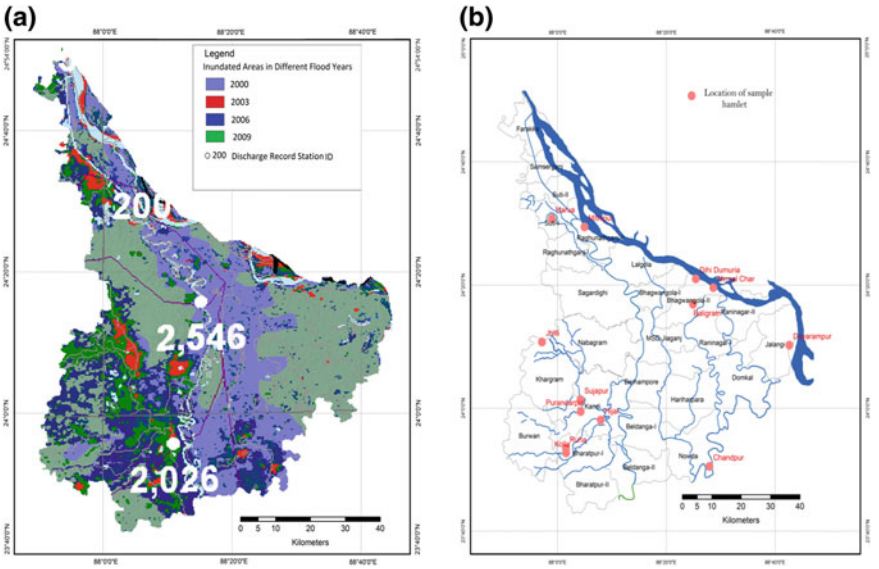

Fig. 7.3 (**a**-*left*; **b**-*right*) Flood affected areas of Murshidabad district during 2000–2010 (**a**) and locations of sample hamlets (**b**). *Source* **a** DFO and **b** prepared by the author

7.4 Methodology

This research work tries to examine the in-depth perceptions of the inhabitants about the causes of flood in their localities among the people living in the 13 sample flood-affected hamlets (Fig. 7.3b). The sampling procedure consisted of four steps. First, on the basis of purposive sampling, sample blocks were selected from the map showing flood-affected areas of Murshidabad district in the last decade (2000–2010) following the Dartmouth Flood Observatory Record. The sample villages were selected from the list of blockwise floodprone villages published by the Disaster Risk Management Section, Murshidabad, Government of West Bengal on the basis of percentages of floodprone areas following purposive sampling. Thirdly, sample hamlets from each sample village were selected randomly. In the final step for the selection of sample households a systematic sampling method was followed. The first household was selected randomly and the subsequent households of the sample village were selected at a fixed interval.

A questionnaire-based household survey was conducted and 604 respondents were surveyed. The respondents rated their perceptions by answering the question on a 5-point Likert scale, with 0 indicating least and 4 indicating most. They were asked to rate their flood-related perceptions in terms of causes of flood in their locality. The assessment of perceptions was done with the help of RIDIT analysis. Figure 7.4 shows the simple methodology of the study.

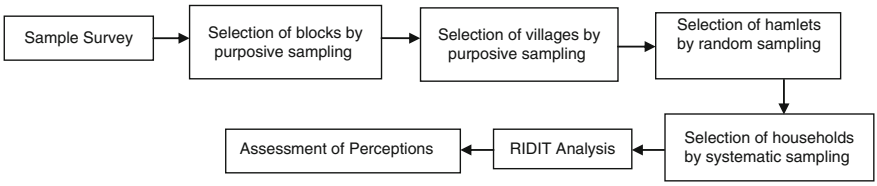

Fig. 7.4 Flowchart of methodology

7.4.1 RIDIT Analysis

The Likert scale is one of the tools used most often in social sciences to acquire data on human attitudes, perceptions, values, intentions, habits, and behavioural changes. RIDIT analysis is an important technique to be applied in the method to quantify the rate of responses.

Bross (1978) has suggested the use of RIDIT (relative to an identified distribution) analysis for data which are in ordered scale. The procedure is as follows. From a reference population with the same categories one determines a "RIDIT" or score for each category. This score for each category is the percentile rank of an item in the reference population and is equal to the number of items in all lower categories plus one-half the number of items in the subject category, all divided by the population size. Once the ridits for each category have been determined, they are taken as values of a dependent variable for the other (comparison) groups and the usual normal distribution family of statistics is applied (e.g. means, standard deviation, etc.).

The RIDIT method is as follows.

Frequency (f_j) for each category of responses is computed, where $j = 1,\ldots, n$

Midpoint accumulated frequency (F_j) for each category of responses is computed by

$$F_1 = \frac{1}{2} f_1 \tag{1}$$

$$F_j = \frac{1}{2} f_j + \sum_{k=1}^{j-1} f_k \tag{2}$$

where $j = 2,\ldots, n$.

Ridit value R_j for each category of responses in the reference dataset is computed by

$$R_j = \frac{F_j}{N} \tag{3}$$

where $j = 1,\ldots, n$.

N is the total number of responses from the Likert scale survey of interest.

Ridits and mean ridits for comparison datasets were computed. The comparison dataset is comprised of the frequencies of responses for each category of a Likert scale item.

$$r_{ij} = \frac{R_j \times \pi_{ij}}{\pi_i} \tag{4}$$

where $I = 1,\ldots, m$

π_{ij} is the frequency of category j for the ith scale item, and π_i is a short form for the summation of frequencies for scale item I across all categories; that is,

$$\pi_i = \sum_{k=1}^{n} \pi_{ik} \tag{5}$$

The mean ridit ρ_i for each Likert scale item is

$$\rho_i = \sum_{k=1}^{n} r_{tik} \tag{6}$$

The mean ridit for a group is the probability; a randomly selected individual from it has a value indicating greater severity or seriousness than a randomly selected individual from the standard group. If an item Y is selected at random from the reference population and an item X is selected at random from the comparison group, the mean ridit gives an estimate of $P(Y \leq X)$; that is, the probability of occurrence of Y is less than or equal to that of X. The mean ridit calculated for the reference population is always 0.5 by its definition. If the mean ridit for a comparison group is greater than 0.5, then more than half of the time a randomly selected subject from it will have a more extreme value than a randomly selected subject from the reference group. If a comparison group's mean ridit is less than 0.5, we would infer that its subjects tend to have less extreme values than the subjects of the reference group.

7.4.2 Sample Hamlets

Among the 604 households from 13 hamlets the average age of the respondent was 42 years. The youngest respondent was 25 years old, whereas the oldest one was 96. The proportion of male respondents (85.40 %) was much higher than that of female respondents of total respondents. Mostly, the male respondents were married (92.8 %) and the head of the household. Some 2.5 % of the respondents were widowed and very few respondents were single or separated. Generally, the respondents had a low level of education. About 28 % of the members of the

families completed primary school but only 11 % of them finished a secondary school course and 6 % completed high school.

A small fraction of them pursued vocational training or higher education (0.5 %) and more than 50 % of the members had not learnt how to read and write. The average household size was 6.29. The maximum household size in the sample was eight, and the minimum size was four. The gender rate was almost equally distributed. The average number of females and males in a household were 2.1 and 2.6, respectively. The respondents by and large were Muslims. Analysis of monthly income of the households showed that more than 56 % belonged to the less than Rs. 4000 monthly income group. This implies that a considerable proportion of households was very poor.

7.5 Results and Discussions

7.5.1 History of Flooding in the Study Area

In the years 1870, 1885, and 1890 the embankment, Lalitkuri, that had been built to guard against the spills over the left bank of the Bhagirathi breached and flooded the areas to the east of the Bhagirathi. In 1870 the flood washed away thousands of acres of paddy, both Aman and Aus varieties; the flood in 1885 rendered the areas submerged for two months, from August to September and it resulted in a high flow rate, 50,000 cusecs, when the River Jalangi flowed 8.8 m above the normal level; in 1890 it was a moderate incidence of flood compared to the above-mentioned. In 1904, 1907, 1924, 1931, 1933, and 1951 there were moderate floods in Murshidabad district

1956 The Dwarka River overflowed and destroyed many houses and 25 % of the total crops of the area; flood water remained for 6 days. The Padma destroyed 23 villages, affected 10,162 acres of arable land, 21,372 persons, and 4564 houses in the Bagri, as the river rose in spate.

1961 The Padma flooded 11 mouzas of Suti Police Station affecting 8569 acres of cropland, 21,879 persons, and 4466 houses. Lalgola, Bhagwangola, Raninagar, and Jalangi Police Station were equally affected. In total, 99,750 acres of cropland, 23,105 persons, and 36,868 houses were affected in 86 villages of 8 Police Stations.

1968 The Rivers Mayurakshi, Brahmani, Dwarka, and Gambhira occurred to be in spate simultaneously and overwhelmed the Kandi subdivision altogether. The floodwater rose 2.1 m above the normal level. The Bhagirathi and the Babla overflowed and submerged the adjacent floodplains at the same time. The flood affected one-third of the district.

1971 The Padma overflowed and flooded the contiguous basin areas; the Bhairab breached its embankments at several points and left the alongside tracts submerged affecting 86 villages. It was the second biggest flood next only to

that of 2000, in terms of both size and gravity of loss occurring in the century. To cope with the disaster military personnel had to be deployed and 236 relief camps provided for over one lakh homeless victims with food and accommodation.

1978 There commenced a devastating flood that lasted for 40 days (August and September). It ravaged 845 villages over 1300 km^2. The Afflux embankment broke down; the flood flows from the Padma and the Bhagirathi merged. The flood hit 21 out of 26 CD blocks of the district; it damaged 52,000 houses and washed away 75,000 ha croplands. The crop loss was estimated to be in 100 millions of rupees. That year the Kandi subdivision faced inundation on account of a postmonsoon flood spill from the Mayurakshi in October.

1987 This flood proved more devastating than the flood in 1978. Due to the overflow of the River Ganga the flood severely affected 23 blocks and four municipalities of the district. 31,532 hectares of land were inundated and crops worth Rs. 90 millions were damaged. It completely destroyed 10,483 houses and partially damaged 11,448 houses.

1989 To reconcile itself with a heavily sustained rain Tilpara Barrage discharged water at the rate of 19,000 cusec; that resulted in a flash flood releasing gushes of torrents that flooded Kandi subdivision entirely. This damaged some 7500 ha of crops. That year's flood also destroyed another 4000 ha of crops in Jalangi alongside the Padma.

1990 Although not as extensive in terms of space, it was a grievously devastating flood; Akheriganj in Bhagwangola II block was the worst hit area. At Salarpur Gram Panchayat alone the River Padma wiped out 2130 houses and 154 structures, schools, religious places, offices, shops, and so on. The huge quantum of floodwater had damaged the riparian households and croplands, causing displacement on a massive scale. It submerged 4000 km^2 of land. The scourge remains a vivid experience that still haunts the locals.

1995 The government spent Rs. 200 million to reinforce the embankment of the Padma. The rushing overflow of the Bhairab, however, heavily damaged a 1.2 km stretch of the embankment. Consequently on 11 June it flooded 70 villages and rendered 1 million people affected. The embankment of the Padma also breached at Bhagwangola II block.

1997 River bank of about 90 km across the Padma river eroded away and left 25 % of the poor people severely hit. The mighty stream flow of the Padma being barely 1 km removed from the Bhagirathi there could be a merger of the two flood flows to wash the entire tract down to Kolkata.

1998 Another devastating flood, on 6 September, hit 1.2 million people of 22 blocks in the district. A military contingent took over safeguarding the Afflux Embankment. The government extended succor, including over 20 million metric tons of food grain, to the helpless victims. Various NGOs joined hands in relief operations covering some five million flood-hit population.

1999 The cause of the dreaded flood of the year appeared to be the discharge from the reservoir of a fault. Over the period from 24 to 27 September, Tilpara Barrage, all persistently, released an improbable quantity of water. In addition to that it rained in torrents incessantly only to add to the blight; these two unleashed the furies of flood running across the district including the township of Bahrampur; the irrigation bunds in Kandi subdivision breached at several points. The flood completely affected Farakka, Suti I, Samserganj, and Raghunathganj II. It severely affected six municipalities and 221 gram panchayats; 13 people died; 2.3 million people were affected, and 70,200 houses fell in. In terms of rupees the loss of properties and crops was estimated at 5610 million.

2000 Flood occurred mainly due to overflow of water from the major rivers flowing through the district, sudden discharge of water from the dams, and riverbank erosion and continuous heavy rainfall from 18 to 21 September. The flood caused the deluge accompanied with innumerable breaches in the embankments and erosions of a catastrophic order: the mighty torrent washed away houses, human lives, livestock, crops, and whatever got in its way, playing terrific havoc with the ill-fated people. In all, 490,313 houses collapsed and 450,600 ha croplands were washed away. The loss of crops, livestock, and other properties was estimated to exceed Rs. 20,000 million. Six hundred human lives were lost.

2004 A combination of flood, erosion, storm, and downpour caused the affliction that affected 79,912 people living in 1563 villages and damaged some 22,746 houses; there was a crop loss estimated at Rs. 9745 million. Two people died.

2006 Twenty-six blocks, seven municipalities, and 1892 villages suffered flood and erosion, about 1.5 million people were affected, and 35,437 houses were completely damaged and 50,729 houses partly damaged. In all, 1,436,334 people were affected as were 74,476 ha of croplands. Eleven people died.

2007 The flood hit 26 blocks and 7 municipalities due to overflowing of the Rivers Dwarka, Brahmani, Mayurakshi, Bhagirathi, and their tributaries. The flood was caused by heavy rainfall recorded at 1622.60 mm followed by a discharge of water from different barrages. The highest discharge from Tilpara Barrage was 85,000 cusec on 15 August. There were 1310 villages entirely inundated with 556,995 people. In addition, 35 human lives were lost, 18,854 houses were fully damaged, and 33,062 houses were partly damaged. Agricultural lands with 38,058 ha of standing crops were totally damaged.

7.5.2 Flood Affected Villages of the Study Area

The field survey revealed the different aspects of the flood hazard in sample villages. It was found that the causes of flood were diverse for different villages due to their location. The environmental characteristics of the sample villages as revealed from the survey are described below.

Harua: This village is situated in the Suti I block of Murshidabad district. The River Pagla flows by the northern side of the village and a feeder canal lies to the east of the village. In the south of the village there is Bangsabati Beel. The approximate elevation of the village is 21.8 m. On account of its location the village suffers from inundation almost every year due to the drainage congestion resulting from obstruction by the feeder canal. The density of population of the village is 20 and the household density is 4 (number per hectare). About 15 % of the population belong to the Schedule Caste and the literacy rate is only 28.5 %.

Mithipur: This village is situated in the Raghunathganj II block of the district. It stands on the right bank of the River Ganga and the River Bhagirathi flows by the western side of the village. The approximate elevation of the village is 22 m. The village is affected by the Ganga erosion. The density of population of the village is 44 and the household density is 9 (number per hectare). About 15 % of the population belongs to the Schedule Caste and the literacy rate is 55 %.

Baligram: This village is situated in the Bhagwangola II block of Murshidabad district. The River Padma flows on the northern side of the village and the river Bhairab flows on the east. The approximate elevation of the village is 19.2 m. Due to its location the village experiences inundation almost every year due to overflow from the River Padma. The density of population of the village is 11 and the household density is 2 (number per hectare). The majority of the people belong to a minority population and literacy rate is 54 %.

DihiDumuria: This village is located on the island formed by the River Padma. The area is under the Bhagwangola II block of Murshidabad district. Due to its location the village is subject to severe riverbank erosion and consequent flood. The approximate elevation of the village is 16.6 m. The density of population of the village is only 2 and the household density is 0.3 (number per hectare). The literacy rate is 40 %.

Nirmal Char: This village is located on the island of the River Padma. The area is under the Bhagwangola II block of Murshidabad district. Due to its location the village suffers from severe riverbank erosion and consequent flood. The approximate elevation of the village is 16.6 m. The density of population of the village is only 2 and the household density is 0.4 (number per hectare). The literacy rate is only 32 %.

Dayarampur: This village is situated on the island of the River Padma. It falls under the Jalangi block of Murshidabad district. This village is situated on a comparatively stable river island which emerged many years ago. Due to its location the village is prone to riverbank erosion and inundation, but in the recent past no major flood has occurred in the village. The approximate elevation of the village is 19.4 m. The density of population of the village is only 16 and the

household density is 4 (number per hectare). The literacy rate is comparatively high at 60 %.

Jhilli: This village is situated in the Khargram block of the district. The River Dwarka flows on the eastern side of the village and a tributary of the River Dwarka flows on the south. The approximate elevation of the village is 18.8 m. The main flood-causing factor is overflow of the western tributaries of the River Bhagirathi. The density of population of the village is 7 and the household density is 2 (number per hectare). About 43 % of the population is Schedule Caste and the literacy rate is 46 %.

Sujapur: This is a village of the Khargram block in the district. The River Dwarka flows from north to south forming the eastern boundary of the village. A tributary of the River Dwarka flows from the western side and bounds the village in the southern part. One important feature of the village is that it is confined by embankment on all sides except the southern side where the tributary meets the River Dwarka. Thus there is drainage blockage aggravating the flood in the village. The approximate elevation of the village is 16.2 m. Flood occurs in the village due to overflow of the western tributaries of the River Bhagirathi and discharge from the Massanjore Dam. The density of population of the village is 3 and the household density is 0.5 (number per hectare). The village is totally inhabited by a Schedule Caste population and the literacy rate is 48 %.

Hijal: This village is situated in the Kandi block of the district. The River Dwarka flows on the eastern side of the village and the River Mayurakshi flows on the south. The approximate elevation of the village is 12.8 m. The village is situated in the lowland and has a saucer shape. Being a part of the HijalBeel area the village suffers from flood annually even in the event of little rainfall. Mainly the flood is caused by overflow of western tributaries of the River Bhagirathi. The density of population of the village is 3 and the household density is 0.6 (number per hectare). About 24 % of the population is Schedule Caste and the literacy rate is 41 %.

Purandarpur: This village falls in the Kandi block of the district. The River Dwarka flows on the northeast side of the village. The approximate elevation of the village is 13.7 m. The main flood-causing factor is overflow of western tributaries of the River Bhagirathi. The density of population of the village is 10 and the household density is 2 (number per hectare). The literacy rate of the village is 56 %.

Chandpur: This is a village situated in the Naoda block of the district. The River Jalangi bounds the village on the southern and eastern sides. The River Suti flows on the western side of the village. The approximate elevation of the village is 14.7 m. The main flood-causing factor is overflow of the River Jalangi and the drainage congestion at the confluence of the river Suti with the River Jalangi. The density of population of the village is 21 and the household density is 5 (number per hectare). The literacy rate of the village is 36 %.

Ruha: This village is situated in the Bharatpur I block of the district. The River Mayurakshi flows by the village on its southern skirt. The approximate elevation of the village is 18.7 m. Mainly the overflow of the western tributaries of the River Bhagirathi causes flood here. The density of population of the village is 10 and the household density is 2 (number per hectare). The Schedule Caste constitutes 30 % of the population and the literacy rate of the village is 57 %.

Kolla: This village is situated in the Bharatpur I block of the district. The village is bounded by the Mayurakshi on the northern side and the Kuye on the south. The approximate elevation of the village is 17.9 m. The main flood-causing factor is overflow of the western tributaries of the River Bhagirathi. The density of population of the village is 17 and the household density is 4 (number per hectare). The literacy rate of the village is 26 %.

7.5.3 Perception Analysis

The mean ridits of the perception of the flood-affected people regarding the causes of flood have been calculated. These values have been plotted in this part. The inference drawn from the value of the mean ridit can be presented as (Fleiss 1983)

When:

Mean ridit = >0.5: A parameter has some importance with reference to the overall perception level; the more the value of the mean ridit is above 0.5, the more significant the parameter is.
Mean ridit = 0: A parameter is perceived as irrelevant compared to the overall perception level, that is, the standard value.
Mean ridit ∼0.5: The significance of the parameter is close to that of the overall perception level, that is, the standard value.

Figure 7.5 represents the mean ridits of different sample hamlets in term of causes of flood in their locality. Two hamlets, Nirmal Char and DihiDumuria show

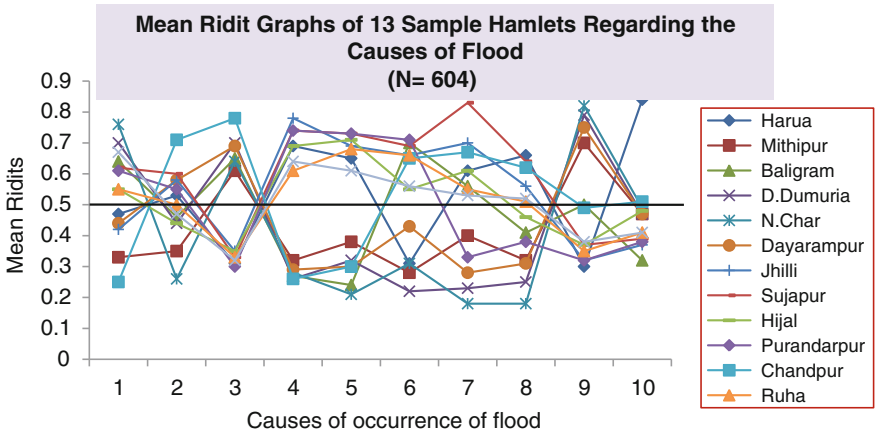

Fig. 7.5 Perceived causes of flood. *Source* Field survey, 2011 Notes: [*1* Work of God; *2* Incessant rainfall; *3* Overflow of the Ganga/Padma; *4* Overflow from western tributaries; *5* Sudden excess discharge from dam; *6* Breach of embankment; *7* Inadequate drainage system; *8* Nonmaintenance of drainage channels; *9* River bank erosion; *10* Obstruction from feeder canal]

very high probability (mean ridit 0.70 and 0.76, respectively) of perceiving flood as the work of God compared to the reference group. Kolla, Baligram, and Sujapur hamlets also have higher probability of responding positively to the aforesaid cause of flood. The rest of the villages ignore this cause as the significant factor of causes of flood in their locality compared to the reference population. Chandpur shows the highest probability (mean ridit 0.78) of accepting overflow of the Ganga/Padma causing the flood. To the other hamlets except Dayarampur, Jhilli, and Sujapur incessant rainfall stands insignificant for causing flood. For the hamlets Mithipur, Baligram, Nirmal Char, DihiDumuria, and Dayarampur the overflow of the Ganga/Padma is also a more significant cause of flood as compared to the reference population. Harua, Jhilli, Sujapur, Purandarpur, Ruha, and Kolla hamlets perceive overflow of western tributaries and sudden excess discharge from the dam to be more significant causes of flood in their locality. For all the hamlets except Harua, Mithipur, DihiDumuria, Nirmal Char, and Dayarampur breach of the embankment is a more significant cause of flood.

Sujapur hamlet presents the highest probability (mean ridit 0.83) of perceiving the inadequate drainage system as the cause of flood among the sample hamlets. Hamlets Harua, Baligram, Jhilli, Hijal, Chandpur, Ruha, and Kolla are more agreeable to that factor. Harua, Jhilli, Sujapur, Chandpur, Ruha, and Kolla show a higher probability of naming nonmaintenance of the drainage channel as the cause of flood. Nirmal Char has the highest mean ridit, 0.82 against the factor (i.e. riverbank erosion) as the cause of flood. The other three hamlets Mithipur, DihiDumuria, and Dayarampur perceive riverbank erosion is the more significant cause of flood in their locality. Only Harua hamlet shows the higher probability (mean ridit 0.83) of perceiving obstruction from the feeder canal as the cause of flood in their locality.

7.6 Conclusion

This analysis shows that all the stakeholders do not always share similar perceptions regarding flood hazard in their localities. Different societies within different hamlets have different perception levels. The sample survey also finds that academicians and experts are more likely to base their perceptions on statistics and probabilities, whereas laypersons are more subjective with respect to their past experience and knowledge about occurrence of flood in their locality. Their perceptions are influenced by their experiences, level of education, gender, socioeconomic development, geographical location, faiths, and the like. In this particular study perceptions regarding causes of flood are mainly governed by the location of the hamlets. The hamlets, situated in the western part of the district, perceive that the overflow of western tributaries and release of water from the dam are more significant causes of flood. On the other hand for the inhabitants located in the river islands (e.g. DihiDumuria and Nirmal Char) the main cause of flood is riverbank erosion. The villages situated in the eastern part of the district provide more weight

on overflow of the Ganga or Padma as a significant cause of flood. Only the village Harua due to its peculiar situation perceives the obstruction of the feeder canal as the major factor causing flood in their locality.

The management plans should also take care of a community's perceptions regarding the causes of flood hazard in their locality. A single plan alone cannot be suitable for all areas. Thus the policy makers should not overlook the ideas of local people with respect to their beliefs, experience, and knowledge.

References

Agbola BS et al (2012) The August 2011 flood in Ibadan, Nigeria: anthropogenic causes and consequences. Int J Disaster Risk Sci 3(4):207–217

Armas I, Avram E (2009) Perception of flood risk in Danube Delta, Romania. Nat Hazards 50:269–287

Bross IDJ (1978) Ridit analysis. Am J Epidemiol 107:263–264

Directorate of Census Operations, DOC (2011) District census handbook series-26 Part- XII-A. Directorate of Census Operations, Government of India, New Delhi

Fleiss JL (1983) Statistical methods for rates and proportions. Wiley, New York

Irrigation and Waterways Department, IWD (2009) Flood preparedness and management plan, 2009. IWD Disaster Risk Management Section Govt. of West Bengal, Kolkata

Kates RW (1962) Hazard and choice perception in flood plain management. University of Chicago, Chicago

Lave TR, Lave LB (1991) Public perception of the risks of floods: implications for communication. Risk Anal 11(2):255–267

Platt RH (1986) Floods and man: a geographer's agenda. In: Kates R, Burton I (eds) Geography, resources, and environment Volume II. University of Chicago, Chicago

Slovic P (1987) Perception of risk. Science 236:280–290

White GF (1945) Human adjustment to floods. University of Chicago, Chicago

White GF (1964) Choice of adjustment to floods. University of Chicago, Chicago

Chapter 8
Estimating Water Budget Through Water Balance Method in Alluvial Damodar Fan-Delta: A Study in Semi-critical Pandua Block of West Bengal

Arijit Majumder and Lakshmi Sivaramakrishnan

Abstract The water balance method is a bookkeeping procedure which estimates the balance between the inflow and outflow of water of the system. This method was developed by Thornthwaite in 1948 and was revised by himself and Mather in 1955. This method helps in identifying and estimating the natural water surplus and water deficit months of an area. There are 38 semi-critical blocks in West Bengal where there has been either a pre- or postmonsoon fall of static water level with respect to every preceding year. The Pandua block of Hugli District in West Bengal is a semi-critical block according to the CGWB but the area entirely lies in the alluvial Damodar fan-delta which is generally considered as highly potential for recharge. Hence the present study aims at estimating the water budget of the semi-critical Pandua block through the Thornthwaite and Mather water balance method to infer whether the study area is naturally a water surplus or water deficit block. Water surplus and water deficit months have been found based on precipitation, potential evapotranspiration, and actual evapotranspiration.

Keywords Water balance · Potential evapotranspiration · Actual evapotranspiration · Semi-critical block · Palaeochannels · Damodar fan-delta

A. Majumder (✉)
Department of Geography, Women's Christian College, Kolkata, India
e-mail: arijit.majumder83@gmail.com

L. Sivaramakrishnan
Department of Geography, Jadavpur University, Kolkata, India
e-mail: lakshmi.bu@gmail.com

B.C. Das et al. (eds.), *Neo-Thinking on Ganges-Brahmaputra Basin Geomorphology*, Springer Geography, DOI 10.1007/978-3-319-26443-1_8

8.1 Introduction

The water balance method is a bookkeeping procedure which estimates the balance between the inflow and outflow of water of the system (Kumar 2003). The present study deals with the water balance of the semi-critical Pandua block based on the Thornthwaite and Mather (TM) method. The method has been adopted to estimate whether this block is a water surplus block or a water deficit block under natural environmental conditions. This method was developed by Thornthwaite in 1948 and was revised by himself and Mather in 1955 (Black 2007). Thornthwaite's water balance technique is a comparative study of rainfall and evapotranspiration which plays a crucial role in many fields of earth science, especially agriculture and water resource development. This method uses air temperature as an index of the energy available for evapotranspiration assuming that the air temperature is correlated with integrated effects of net radiation and other controls of evapotranspiration and that the available energy is shared in fixed proportions between the heating of the atmosphere and evapotranspiration (Calvo 1986). Evaporation is a purely physical process depending mainly upon air temperature, although wind speed and humidity have some effect on the actual rate of transfer of water vapour from the ground to the atmosphere. Transpiration on the other hand is purely a biological process which takes place essentially during the period of sunshine but is governed by all the factors that determine evaporation (Rao and Subrahmanyam 1961). Because both evaporation and transpiration depend on air temperature, the early investigators considered temperature and precipitation for computation of the water budget required for climatic analysis of any arid or humid zone. Precipitation acts as the sole input into the system and the actual evapotranspiration is the output from the system which determines the water surplus or deficit of an area.

8.2 Area Under Study

The Pandua block of Hugli District in West Bengal is a semi-critical block and has been selected for the present study. The latitudinal extension of the area is 23°00′N–23°10′N and the longitudinal extension is 88°10′E–88°24′E. The area of the block is 280.07 km^2 as obtained by vectorisation of a block map of Pandua (Census of India 1961) in UTM projection and WGS84 datum. The area lies within the interfluve where the River Hugli flows in the east and the River Damodar in the west as shown in Fig. 8.1b. The area is a meander flood plain which represents the newer alluvium (National Bureau of Soil Survey and Land Use Planning 2001). The newer alluvium or the Holocene deposition is characteristically unoxidised and consists of sand, silt, and clay mainly deposited in fluvial settings (Acharyya 2005). Groundwater occurs within a thick zone of saturation under watertable condition in the entire Hugli District excepting a small portion to the west, beyond the River Darakeswar (Bhattacharjee 1982).

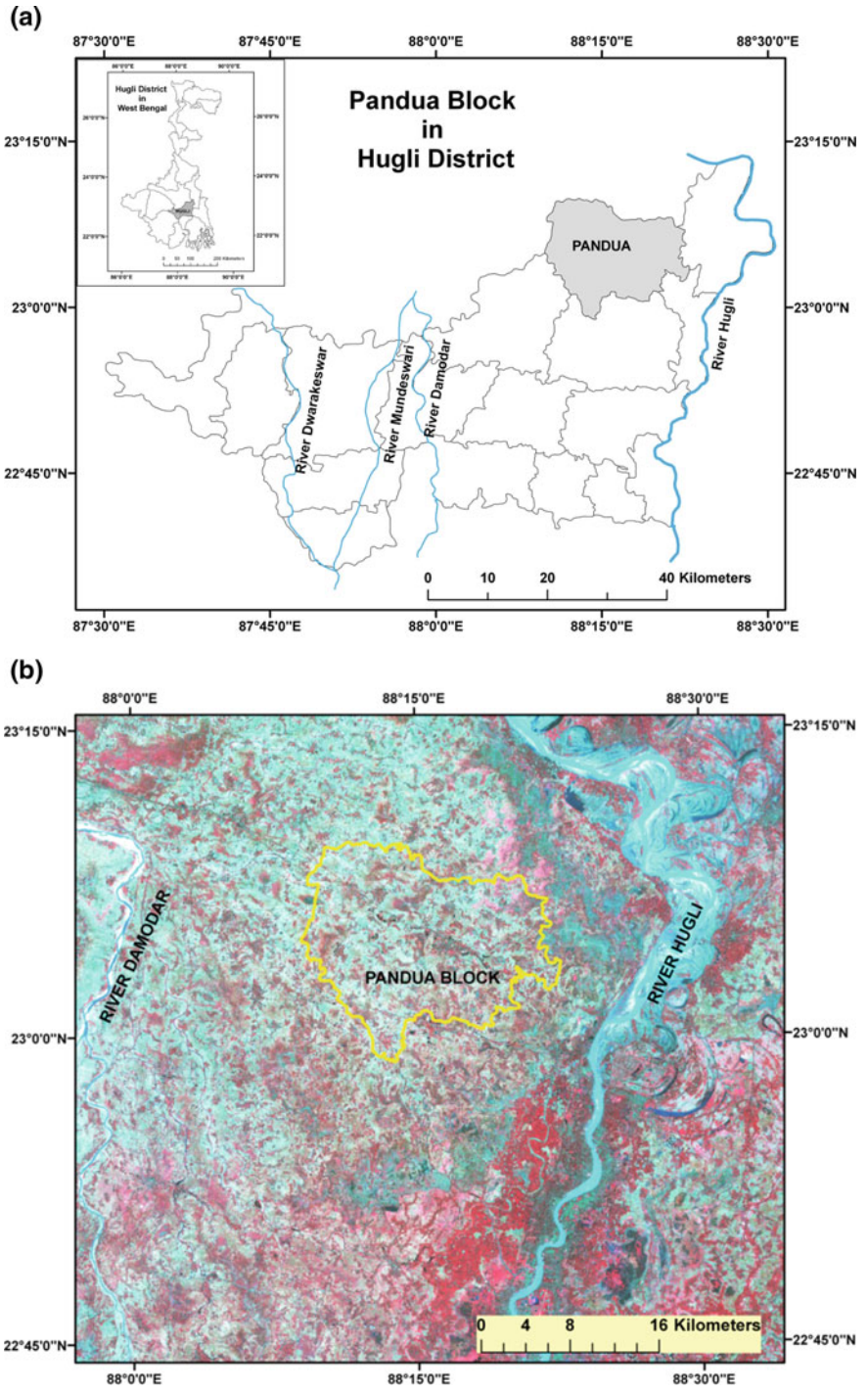

Fig. 8.1 **a** Location of study area. **b** FCC of LISS IV image of study area

8.2.1 Selection of the Area Under Study

The CGWB studied the status of 265 out of 341 blocks of West Bengal during 1994–2004. The study excluded Kolkata and the South 24 Parganas district. The CGWB categorized the blocks into safe, semi-critical, critical, and overexploited blocks on the basis of fall of groundwater level and stage of groundwater development. The CGWB reported that there has been a significant decline of groundwater level in some of the blocks and out of 341 blocks in West Bengal 38 blocks are categorized as in critical or semi-critical condition (Ray and Shekhar 2009). West Bengal has 37 semi-critical and 1 critical block based on the study of CGWB during 1994–2004 (Ray and Shekhar 2009) and all 38 blocks have been categorized as semi-critical as of March, 2009 (Central Ground Water Board 2011) where there has been either a pre- or postmonsoon fall of static water level with respect to every preceding year. The Pandua block of Hugli District in West Bengal is a semi-critical block according to the CGWB but the area lies entirely in the alluvial Damodar fan delta which is generally considered as having a high potential for recharge.

Thus this particular block has been selected for the study due to the irony of the following facts.

1. It is composed of unconsolidated Quaternary alluvium and hence considered highly conducive to groundwater recharge.
2. The block has been classified as a semi-critical block by the Central Ground Water Board (2011).
3. The fall of static water level (SWL) was more than 10 metres during last 40 years (according to data provided by SWID).
4. The total volumetric loss of groundwater from the aquifer system of Pandua amounts to more than 17,500 ham in the last 33 years (Majumder and Sivaramakrishnan 2013).

8.2.2 Geographical Facets of the Study Area

8.2.2.1 Geology

The Bengal Basin is a structural depression filled up by rivers during the last 150 million years (Bandyopadhyay 2007). The River Ganga brings a lot of sediment to the Bengal Basin through the Garo–Rajmahal gap. The rivers originating in the Chota–Nagpur plateau including the River Damodar and the River Ajay add to the sedimentation on the western side of the River Hugli, where the study area lies as shown in Fig. 8.2. The River Damodar after originating from the Chotanagpur plateau used to flow east to meet the River Hugli during the middle of the eighteenth century at the confluence point north of Kalna. Later the river started rotating, forming an obtuse angle with its vertex at Jamalpur and shifting its mouth

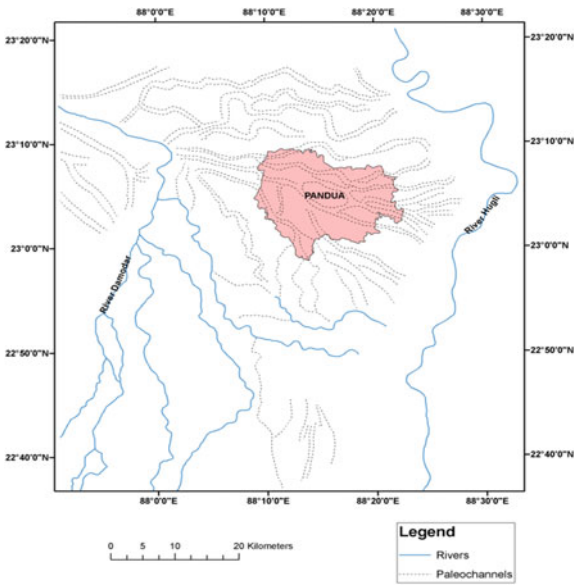

Fig. 8.2 Palaeochannels in the interfluve of River Damodar and River Hugli

128 km southwards to meet River Hugli at Garchumuk (Rudra 2010). In the process of shifting the river Damodar has formed two alluvial fans: the Memari fan trending east and the Tarakeswar fan trending south as shown in Fig. 8.2 (Acharyya and Shah 2006). The study area (i.e. the Pandua block of the Hugli district) lies entirely in the Memari fan. The map prepared by Mallick and Niyogi shows the presence of palaeochannels (Acharyya and Shah 2006) in the entire study area. The palaeochannel explains the huge deposits of sand and the characteristics of a meander flood plain.

8.2.2.2 Climate

The climate of this area is tropical humid type. The mean temperature is 26.2 °C as calculated on the basis of the last 30 years of data supplied by the Indian Meteorological Department. The maximum temperature is 30.20 °C which occurs in the month of May, and the minimum temperature is 18.54 °C in the month of January. The annual rainfall of the study area is 1530.4 mm. The maximum rainfall occurs in the month of July and amounts to 297.98 mm whereas the minimum rainfall occurs in the month of December and amounts to 6.87 mm. Most of the rainfall takes place in the months of June, July, August, and September, with 71.52 % of the rainfall occurring during these four months, and 88.38 % of the rainfall occurring during the months of May, June, July, August, September, and October. This signifies that 88.38 % of rainfall occurs during 6 months, that is, from May to October and 11.61 % of the rainfall occurs during the next six months.

8.3 Materials and Methods

The soil moisture balance method is a process of computing a balance sheet between the inflow and outflow of water in the unsaturated zone through natural processes (Mather 1974). The Thornthwaite and Mather method has been adopted to study the water balance of the study area. The main parameters required for the calculation of water balance based on the Thornthwaite and Mather method are precipitation and air temperature. This procedure allows estimating the potential evapotranspiration, accumulated potential water loss, soil moisture storage, actual evapotranspiration, and water deficit and water surplus (Dourado-Neto 2010). Precipitation is the only input into the system for calculating the water balance of an area. Monthly precipitation data have been collected from the Indian Meteorological Department (IMD) for the IMD station Bagati in Hugli district. The data have been collected for the period 1980–2008. There is no meteorological station within the study area. The IMD station lies at a distance of 5 km from the boundary of the block and at a distance of 20 km from the centroid of the block. Because the meteorological data are point data and it is not possible to collect weather data at each and every point, different mathematical models exist to convert the point data into raster data or spatially continuous data. According to A. Bhattacharya the rainfall data can be considered radially up to 30 km from a rain gauge station in the plains of West Bengal without much error (Ganguli 2010). Raghunath (2006) in his book Hydrology has stated that in the plains in India the rainfall data of one rain gauge station can be considered up to 520 km^2 at 10 % significance level. Beyond 25 km a Thessian polygon is adopted to convert several point data into spatially continuous data (Raghunath 2007). In as much as the centroid of the study area is within a distance of 20 km from the rain gauge station, rainfall data of the IMD station Bagati have been accepted to compute the water balance of the block. For calculating the monthly precipitation the mean monthly rainfall data for 29 years, that is, from 1980–2008, have been considered for calculation of water balance of the block.

8.3.1 Calculation of Potential Evapotranspiration

Potential evapotranspiration (PET) is the amount of water that would be evaporated under an optimal set of conditions, that is, having an unlimited supply of water (Bakundukize et al. 2011). There are several methods for computing the potential evapotranspiration, including Penman–Monteith equation, Hamon's equation, and Thornthwaite equation among others. In the Penman–Monteith equation the parameters required for estimating the potential evapotranspiration are net radiation at the crop surface, solar heat density, psychometric constant, mean air temperature, wind speed at 2 m height, saturation vapour pressure, actual vapour pressure, saturation vapour pressure deficit, and slope of the saturation vapour pressure curve.

Table 8.1 Estimating potential evapotranspiration (Thornthwaite and Mather)

Month	Temperature (°C)	i	I	a	PET (mm)
JAN	18.54	7.27	148.629	3.6688	36.02
FEB	22.00	9.42			67.42
MAR	26.53	12.51			134.01
APR	29.51	14.70			198.01
MAY	30.20	15.23			215.76
JUN	29.77	14.90			204.59
JUL	29.00	14.32			185.96
AUG	28.95	14.28			184.77
SEPT	28.72	14.11			179.37
OCT	27.53	13.24			153.65
NOV	23.81	10.62			90.16
DEC	19.82	8.04			45.97

Source IMD data, Station-Bagati (1980–2008), Hugli, West Bengal

This is one of the best methods for computing potential evapotranspiration and was used by Snyder and Eching in 2003 but the major drawback of this method is that it requires a wide variety of weather data which are not available at the IMD stations (Bakundukize et al. 2011). Hamon's formula requires only latitude for calculating the potential evapotranspiration. The latitude value is converted to day length, mean temperature, and hence the saturated vapour density (Bakundukize et al. 2011).

Thornthwaite's method is simple and has been widely used by investigators for computing potential evapotranspiration. This equation requires only temperature as the input data and has been used for the present study. Table 8.1 shows the computed values of potential evapotranspiration for all 12 months based on the Thornthwaite method. The Thornthwaite equation (Das et al. 2009) for estimating the PET can be expressed as

PET (mm) = 16 (10. T/I)a.
I = Heat index, is the sum of 12 month values of heat index i.
i = (T/5) 1.514.
$a = 0.000000675I^3 - 0.0000771I^2 + 0.01792I + 0.49239$.
T = Mean temperature of each month in degree Celsius.

8.3.2 Accumulated Potential Water Loss

The next step involves the calculation of the difference between the mean monthly precipitation and the potential evapotranspiration for each month. The potential water loss for a single month is when the potential evapotranspiration exceeds the precipitation. The cumulative loss for the preceeding months are calculated to find out the accumulated potential water loss (APWL) for each month.

8.3.3 Soil Moisture Storage

Soil moisture storage is defined as the total amount of water which is held by the plant root zone. The soil texture and the cropping pattern are the main factors that determine the soil storage. The rooting depth of the soil is directly proportional to the amount of water that can be held by the soil root zone. It means that the greater the crop rooting depth, the more water is stored in the soil zone and thus reduces the amount of water migrating beneath the zone to add as groundwater recharge. The maximum amount of water that can be held within the soil zone is referred to as field capacity (Sahai 2004). At field capacity the soil holds the water against the force of gravity. Conceptually the groundwater recharge does not commence until the moisture content exceeds the field capacity as it acts as the threshold limit. The water holding capacity at the root zone is obtained by multiplying the water content at the field capacity by the effective depth of the soil root zone. Table 8.2 shows the suggested values of the soil texture and the vegetation types prepared by Thornthwaite and Mather in 1957.

8.3.4 Change in Storage

Change in storage is the amount of water added or removed from the groundwater storage. It varies between zero to field capacity (Bakundukize et al. 2011), and is computed as the difference between the current month's soil moisture and the previous month's soil moisture. Water is added to the soil when precipitation exceeds potential evapotranspiration, whereas water is withdrawn from the soil when potential evapotranspiration is greater than precipitation. The excess water which is added to the soil over 200 mm is added as groundwater recharge.

8.3.5 Actual Evapotranspiration

Actual evapotranspiration is a function of available soil moisture, temperature, and humidity. Actual evapotranspiration takes place as long as there is availability of water for evaporation and moisture available for plants to transpire. It can thus be said that in dry months when potential evapotranspiration is greater than precipitation the moisture is not available to meet the evapotranspiration demand. Hence the actual evapotranspiration is less than the potential evapotranspiration due to lack of available moisture thus depleting the soil moisture storage. In the wet months when the precipitation is greater than potential evapotranspiration there is enough moisture available for evaporation and for plants to transpire water, hence the maximum actual evapotranspiration equals the potential evapotranspiration.

Table 8.2 Suggested values of water capacity at root zone

Vegetation	Soil texture	Water holding capacity (% volume) = water content at field capacity	Rooting depth (m)	Water capacity at root zone (CAP) (mm)
Shallow rooted crops (spinach, peas, beans, carrots, etc.)	Find sand	10	0.50	50
	Fine sandy loam	15	0.50	75
	Silty loam	20	0.62	125
	Clay loam	25	0.40	100
	Clay	30	0.25	75
Moderately rooted crops (corn, cereals, cotton, tobacco, etc.)	Find sand	10	0.75	75
	Fine sandy loam	15	1.00	150
	Silty loam	20	1.00	200
	Clay loam	25	0.80	200
	Clay	30	0.50	150
Deep rooted crops (alfalfa, pasture, grass, shrubs)	Find sand	10	1.00	100
	Fine sandy loam	15	1.00	150
	Silty loam	20	1.25	250
	Clay loam	25	1.00	250
	Clay	30	0.67	200
Orchards	Find sand	10	1.50	150
	Fine sandy loam	15	1.67	250
	Silty loam	20	1.50	300
	Clay loam	25	1.00	250
	Clay	30	0.67	200
Mature forest	Find sand	10	2.50	250
	Fine sandy loam	15	2.00	300
	Silty loam	20	2.00	400
	Clay loam	25	1.60	400
	Clay	30	1.17	350

Source Bakundukize et al. 2011 based on Thornthwaite and Mather

8.3.6 Water Deficit

Soil moisture deficit occurs when there is a lack of available moisture to be evaporated and transpired by plants. It means that the actual evapotranspiration is less than the potential evapotranspiration. Hence the soil moisture deficit is calculated as the difference between potential evapotranspiration and actual evapotranspiration (Bakundukize et al. 2011).

8.3.7 *Water Surplus*

Soil moisture surplus occurs when there is more water available than the actual evapotranspiration. It takes place when the precipitation is more than the computed potential evapotranspiration under the given circumstances. The water surplus is calculated as the difference between precipitation and actual evapotranspiration. The surplus water first reaches the field capacity and then the excess water, if any, adds to groundwater recharge.

8.4 Results and Discussions

It is clear from Table 8.2 that the main parameters required to calculate the water capacity at the root zone are soil texture and vegetation type of the study area. The soil type of the Pandua block is predominantly silty loam of the horal series (National Bureau of Soil Survey and Land Use Planning 2001). For determining the vegetation type of the Pandua block a remote sensing technique has been adopted. The LISS-IV image of 11 November, 2011 has been taken for the study area. The output spatial resolution of the LISS-IV image is 5 metres and the spectral resolution is three bands: green, red, and NIR. The block has been georeferenced in a Universal Transverse Mercators (UTM) projection and WGS84 datum as the coordinate system of the image. A subset of the image has been generated with the vector of the block boundary to get the image of the block area only. The raw image is then processed to get the standard false colour composite of the LISS-IV image of the Pandua block. Supervised classification of the image has been done using the maximum likelihood method. The subset image has been classified into six classes using Erdas Imagine 9.1 as shown in Fig. 8.3.

Table 8.3 shows the classification report of the study area based on the LISS-IV image of 11 November, 2011. According to the classification report the agricultural land is 17.13 % and the current agricultural fallow land is 72.05 %. Therefore it can be concluded that the total agricultural area amounts to 89 %. The high percentage of area under current agricultural fallow can be attributed to the fact that the classification has been done for the month of November, which is the period when *Aman* (rice cultivated during monsoon) has already been harvested and potato is yet to be sown. From the classification report it is clear that the predominant vegetation type of this area is moderately rooted crops. A primary field survey also suggests that rice and potato are the main staple crops of this area. Hence to determine the water capacity at the root zone the required parameters are moderately rooted crops and silty loamy soil. On the basis of Table 8.2 it can be deduced that the water holding capacity at the root zone is 200 mm. The statement that the water holding capacity at the root zone is 200 mm means that when the water in the root zone exceeds 200 mm, that is, the field capacity, only then can it add as groundwater recharge.

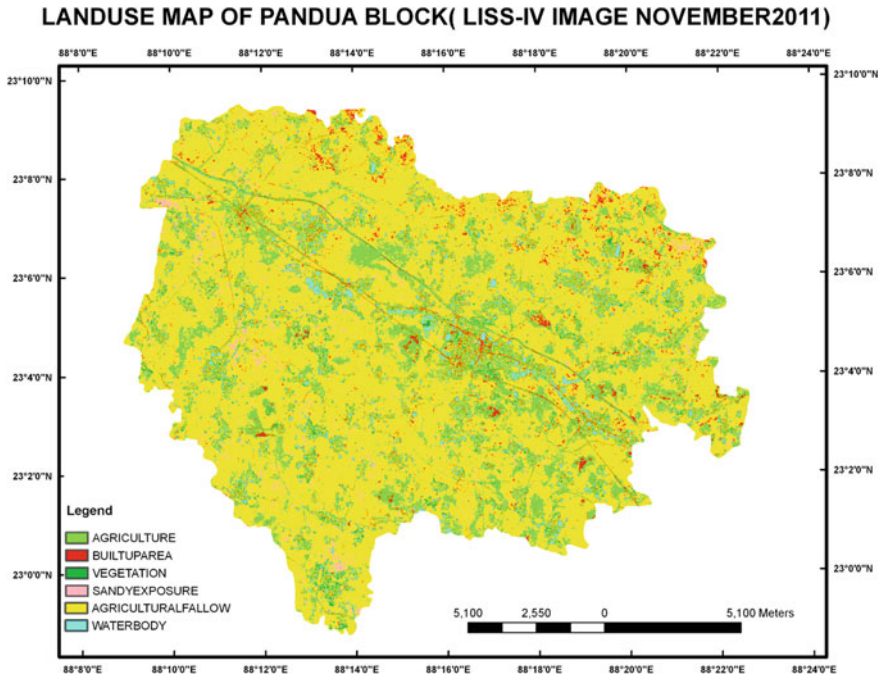

Fig. 8.3 Supervised classification image of Pandua block

It is also to be remembered that the soil moisture storage is a function of the accumulated potential water loss (APWL) in accordance with Thornthwaite and Mather's 1957 table (Subrahmanyam 1982), where the values of the soil moisture storage are plotted as corresponding values of APWL. The soil moisture storage values increase till they reach the field capacity which is 200 mm after which the excess water is added as groundwater recharge.

Potential evapotranspiration required for the computation of water balance of the Pandua block has been calculated in Table 8.1. The water holding capacity at the root zone has also been found in accordance with soil texture and analysis of the LISS-IV image of the block. The water holding capacity at the root zone is found to be 200 mm.

From Table 8.4 it is to be noted that only four months (i.e. June, July, August, and September) are water surplus and the rest are water deficit months. The surplus water is available after the actual evapotranspiration has occurred. Hence, the surplus water is either available for soil moisture storage, generates runoff, or adds as groundwater recharge.

Table 8.3 Image classification report of Pandua block

Land use type	Area in square kilometres	Area in percentage
Agriculture	47.98	17.13
Agricultural fallow	201.80	72.05
Vegetation	6.02	2.15
Sandy exposure	6.38	2.28
Water body	7.55	2.69
Built-up area	10.35	3.70
Total	280.07	100.00

Source Supervised classification of LISS IV image

8.5 Conclusion

The Thornthwaite and Mather method of water balance is a comparison of rainfall and evapotranspiration in a particular area. From the calculation of water balance of the Pandua block it can be inferred that the amount of rainfall exceeds the actual evapotranspiration in the months of June, July, August, and September (Table 8.4). The total rainfall in the study area is 1530.4 mm and the surplus water in the system amounts to 339.8 mm. The surplus water, 339.8 mm, results from the summation of water surplus in the system in the above-mentioned months. The surplus water first satisfies the soil moisture storage and then adds as groundwater recharge or generates run-off. The water holding capacity at the root zone in the study area is 200 mm which is achieved in the month of July and continues till the month of September. The storage is 88 mm in the month of June and is 200 mm in the

Table 8.4 Calculation of water balance (TM method) of the Pandua block

Month	Rainfall (P) (mm)	PET (mm)	P—PET (mm)	APWL (mm)	Storage (mm)	Change in storage (mm)	AET (mm)	Water deficit (mm)	Water surplus (mm)
Jan	14.1	36	−21.9	152	93	−11	25.1	10.9	
Feb	30	67.4	−37.5	190	76	−17	57	10.4	
Mar	41.4	134	−92.6	282.1	48	−28	69.4	64.6	
Apr	63.2	198	−134.8	416.9	25	−23	96.2	101.8	
May	127.1	215.8	−88.6	505.5	16	−9	136.1	79.7	
Jun	276.6	204.6	72		88	72	204.6		72
Jul	298	186	112		200	112	186		112
Aug	262.3	184.8	77.5		200	0	184.8		77.5
Sept	257.7	179.4	78.3		200	0	179.4		78.3
Oct	130.9	153.9	−23	23	178	−22	152.9	1	
Nov	22.2	90.2	−68	91	126	−52	74.2	16	
Dec	6.9	46	−39.1	130	104	−22	28.9	17.1	

Source Calculated by the author

months of July, August, and September. This signifies that the surplus water in the months of June and July is required to satisfy the soil moisture storage in the study area. Therefore the surplus water in the months of August and September either adds as groundwater recharge or generates runoff. October is almost a balanced month in terms of soil moisture inasmuch as the potential evapotranspiration almost equals the actual evapotranspiration. The actual evapotranspiration exceeds the rainfall in the months November, December, January, February, March, April, and May which makes them water deficit months. These water deficit months require irrigation facilities for agricultural practice in the study area. April is the month of maximum water deficit whereas the excess water adds to the system in the months of August and September. Finally it can be concluded that the soil moisture storage is saturated in the month of July and thus there is excess water in the system in the months of August and September which adds as groundwater recharge or generates runoff. Therefore the Pandua block is a water excess block with respect to its soil moisture budget.

References

Acharyya SK (2005) Arsenic levels in groundwater from quartenary alluvium in Ganga plain and the Bengal basin, Indian subcontinent: insights into influence of stratigraphy. Gondwana Res 8 (1):55–66

Acharyya SK, Shah BA (2006) Arsenic-contaminated groundwater from parts of Damodar fan-delta and west of Bhagirathi River, West Bengal, India: influence of fluvial geomorphology and Quaternary morphostratigraphy. Environ Geol 52:489–501

Bakundukize C et al (2011) Estimation of groundwater recharge in Burgesera Region (Burundi) using soil moisture budget approach. Geol Belg 14:85–102

Bandyopadhyay S (2007) Evolution of the Ganga Brahmaputra delta: a review. Geogr Rev India 69(3):235–268

Bhattacharjee BK (1982) Rainfall-recharge correlation; a method for evaluating potential groundwater. In: Proceedings of exeter symposium on improvements of methods of long term prediction of variations in groundwater resources and regimes due to human activity IAHS Publication 136, pp 161–167

Black EP (2007) Revisiting the Thornthwaite and mather water balance. J Am Water Resour Assoc 43(6):1604–1605

Calvo CJ (1986) An evaluation of Thornthwaite's water balance technique in predicting stream runoff in Costa Rica. Hydrol Sci 31(1):51–60

Census of India (1961) District census handbook, Hooghly. Directorate of Census Operations, West Bengal

Central Ground Water Board (2011) Dynamic ground water resources of India. Ministry of Water Resources, Government of India, Faridabad

Das Y et al (2009) Energy and water balance studies in the boundary layer over Delhi (India). Contrib Geophys Geodesy 32(9):163–185

Dourado-Neto D (2010) General procedure to initialize the cyclic soil water balance by the Thornthwaite and Mather method. Sci Agrricola 67(1):87–95

Ganguli M (2010) Water balance of Chinsurah-Hooghly, West Bengal. Indian J Landscape Syst Ecol Stud 597–604

Kumar CP (2003) Estimation of groundwater recharge using soil moisture balance approach. J Soil Water Conserv 2:53–58

Majumder A, Sivaramakrishnan L (2013) Computation of loss of groundwater storage during 1975–2008: a study in Pandua block of Hugli district, West Bengal. Int J Curr Res 5 (8):2351–2355

Mather JR (1974) Climatology: fundamentals and applications. McGrawhill, New Delhi

National Bureau of Soil Survey and Landuse Planning (2001) Soils of Hugli District for optimising land use. Indian Council of Agricultural Research, Nagpur

Raghunath HM (2006) Hydrology. New Age International (P) Limited, New Delhi

Raghunath HM (2007) Ground water. New Age International (P) Limited, New Delhi

Rao BS, Subrahmanyam VP (1961) A climatic study of arid zones in Central Deccan. Retrieved 7 June 2012

Ray A, Shekhar S (2009) Ground water issues and development strategies in West Bengal. Bhujal News 24(1):1–17

Rudra K (2010) Banglar nadikatha. Sahitya Sansad, Kolkata

Sahai VN (2004) Fundamentals of soil. Kalyani Publishers, Kolkata

Subrahmanyam VP (1982) Water balance and its applications. Andhra University Press, Visakhapatnam

Chapter 9
Can We Treat Dug-Well Water Level as Groundwater Level?

Malay Ganguli

Abstract Water lies beneath the surface of the earth broadly in two zones, saturated and unsaturated. The uppermost level of the saturated zone is called the groundwater level. This level is controlled by hydrogeological setup and human interference. The groundwater system is more complicated in alluvium than a hard rock hydrogeological setup. In an alluvium setup where thick clay belongs to the uppermost layer, a dug-well water level is never synonymous with groundwater level. The present chapter is an argument to establish that the water level of a dug well cannot be treated as the groundwater level in an area where thick clay lies on the earth surface. The water comes into the dug well either from soil seepage or from direct rainfall. This water level is directly influenced by the surrounding pond water. The present work is an attempt to look into how groundwater level and dug-water level exist in the study area distinctively. The investigation has been done on Chandernagore Municipal Corporation (CMC) and Hooghly–Chinsurah Municipality (HCM), two class-I cities of West Bengal. The supporting database is mainly primary; however, a secondary database has also been used for the better reflection of the work. The samples have been selected purposively from CMC and HCM.

Keywords Dug-well water level · Ground water level · Clay layer · Seepage · Aquifer

9.1 Introduction

Water is a natural resource which occurs in different modes in our earth system. Water lies beneath the surface of the earth broadly in two zones, saturated and unsaturated. The uppermost level of the saturated zone is called the groundwater

M. Ganguli (✉)
Centre for Policy Research, New Delhi 110021, India
e-mail: malayganguli@gmail.com

B.C. Das et al. (eds.), *Neo-Thinking on Ganges-Brahmaputra Basin Geomorphology*, Springer Geography, DOI 10.1007/978-3-319-26443-1_9

level. Water in the saturated zone is the only underground water that supplies wells and springs and is the only water to which the name groundwater is correctly applied (Heath 2004). Groundwater is the largest source of fresh water on the planet (Raghunath 2006). The groundwater system is more complicated in alluvium than that of the hard rock hydrogeological setup. In alluvium groundwater mostly belongs to a leaky aquifer system. A clay layer divides the upper and lower aquifer systems (Mathur 1969; Sing 1983). The groundwater level of a particular place is defined by the total input and output of water in that system with respect to time. The groundwater level is also called the static water level if the water level is not affected by any pumping operation. The static water level refers to the elevation or level of the water table in a well when the pump is not operating (http://www.groundwater.org/gi/gwglossary.html.). The water level in a dug well may be analogous to groundwater level and also may not be. This is mainly controlled by the hydrogeological setup of the concerned area. The contour water level map was measured in the dug wells at Patna for both for pre- and postmonsoon periods (Maitra and Ghosh 1992). Water levels encountered in a deep aquifer that indicate a piezometric surface of the deep confined aquifer are different from the phreatic surface in the dug wells (Maitra and Ghosh 1992). The water level depth of Meerut district, Uttar Pradesh, is recorded from open shallow masonry wells (Mathur 1969). However, the dug-well water level and groundwater levels exist separately in Chandernagore Municipal Corporation (CMC) and in Hooghly–Chinsurah Municipality (HCM).

CMC and HCM are two class-I cities of West Bengal which are situated in the easternmost part of Hooghly District. The geographical location of the study area is 22° 50′ 08″N–22° 56′ 42″N and 88° 18′ 16″E–88° 24′ 40″E (Fig. 9.1). Hooghly district is located in the Western part of the Bengal Basin, which is directly formed by the alluvium brought by the River Ganga and its tributaries and distributaries.

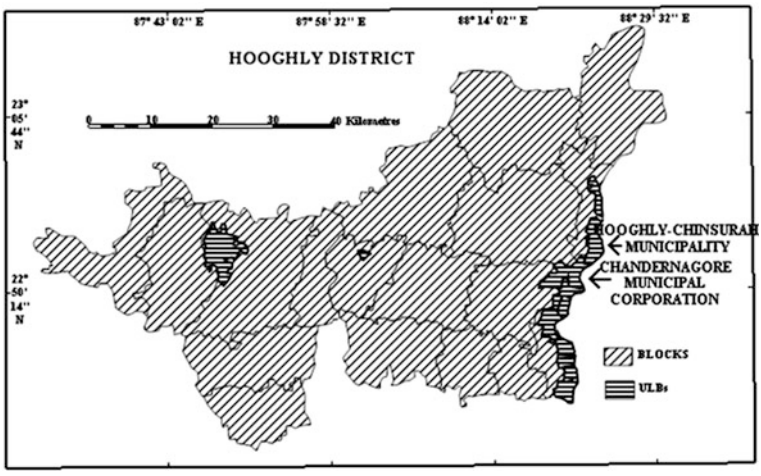

Fig. 9.1 Location map

Archaean crystalline basement, Gondwana sediments, and Rajmahal volcanic of the Mesozoic age cover this part of the Bengal Basin to the west and northwest. The district is covered by a huge thickness of Quaternary alluvium underlain by Tertiary and Mesozoic formations (Biswas 1959). The Indo-Gangetic alluvial plain is characterized by regionally extensive and highly productive multiaquifer systems (Rangachari et al. 2012). The main composition of the alluvium is clay, silt, and sand with different gradations. Clay is the dominant geological material on the surface of the area. The occurrence of clay bed is very common at the upper part of the geological succession in the twin city of Calcutta–Howrah (Sikdar 2008). Sand layers occur as a single aquifer system, overlain by a clay layer with a varying thickness of 20–50 m in the South Ganga Plain of Bihar (Saha et al. 2008). The main source of water of both the cities (CMC and HCM) is groundwater. Being located on a newer alluvium zone the area is also facing a declining trend of the static water table. Ram and Bilas (2010) have shown that overexploitation of groundwater results in a decline of groundwater level in the Chanduali district of Uttar Pradesh. The groundwater crisis has been alarming over the years in India (Shankar et al. 2011). The thick clay layer offers a great opportunity to the area to have numerous numbers of ponds and also dug wells. Here, the dug-well water level is not significantly affected by the declining static water level trend in CMC and in HCM.

The present research work is an attempt to look into how the groundwater level and dug-water level exist in the study area distinctively. The chapter is an argument to establish that the water level of a dug well cannot be treated as the groundwater level in an area where thick clay lies on the earth's surface.

9.2 Database and Methodology

The present study is mainly based on a primary database which has also been shaped by some secondary data sources. The primary data regarding the water level of dug wells has been collected purposively based on their geographical locations from CMC and HCM. The water level depth is measured from the ground surface. There are 33 wards in CMC and 30 wards in HCM. Two samples (i.e. dug wells) from each ward have been selected. Therefore, the total number of samples chosen from CMC is 64 (except ward no. 27 which is not in the present study). However, there are a few wards in HCM where only one dug well has been found from each ward. Therefore, the total number of samples is 51 in HCM. Including both cities, the number of samples is (64 + 51) 115 for the study done in the pre- and post-monsoon season of 2011. The secondary database regarding the static water level has been provided by the State Water Investigation Directorate (SWID), West Bengal, and also by the water departments of the concerned cities. The lithological studies of the area have been done based on the lithologs of different bore wells of the area.

9.3 Dug-Well Water Level

The water level of a dug well was not the same all over the area. The water-level depth was measured in the premonsoon (April) and postmonsoon (November) seasons of 2011. Each and every sample was studied during the pre- and post-monsoon to measure the depth minutely which helps to get the net available water resource from dug wells. The water is available year-round. The water levels of dug wells of the area were directly influenced by the amount of precipitated rainfall over the area, surrounding pond water, domestic withdrawal of water, and also evapo-transpiration, as the watertable lies in the root zone of local vegetation mainly in the postmonsoon season. The minimum and maximum depths of the premonsoon water level of CMC was 0.8 metre below ground level (mbgl) and 4.8 mbgl, respectively. The minimum and maximum postmonsoon water levels of CMC were 0.3 and 2.7 mbgl. The average depths of pre- and postmonsoon water levels were 1.8 and 0.9 mbgl in CMC. The average fluctuation of the watertable was 0.9 m in CMC in 2011. The premonsoon water level (CV = 45 %) was less consistent than the postmonsoon water level (CV = 38 %) over CMC. The watertable fluctuation varied over the area with remarkable range. The range of water level fluctuation was 0.2–3.7 mbgl. The depth of the bottom of the well differed from place to place. The highest depth was recorded as 9.4 mbgl and the lowest depth was recorded as 3.3 mbgl in CMC. Depth of wells helps to estimate the volume of water within the well. The average depth of the bottom of wells in CMC is 6.09 mbgl. Therefore, a well can hold 2777.27 l (2.777 cumec) of water maximum on an average. The minimum depth of the water level during premonsoon has been recorded in the central part of CMC which was 1.06–2.06 mbgl. The maximum water level depth has been recorded in the southwestern part of CMC as 4.06–4.54 mbgl (Fig. 9.2).

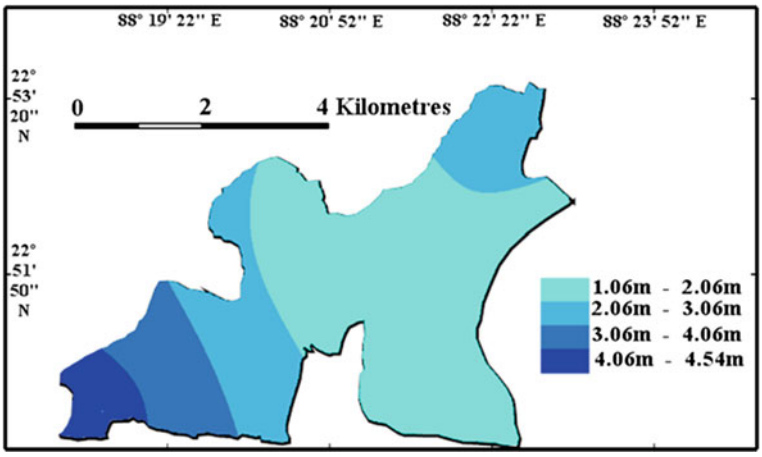

Fig. 9.2 Premonsoon water level of dug well of CMC, 2011

It was observed that most of the area of CMC is occupied by the minimum depth zone range. The maximum depth zone is least in terms of surface coverage area of CMC. The water level depth increases from the central to north and southwestern parts of CMC. During postmonsoon, most of the area of CMC belongs to the shallow water level zone having a depth of 0.75–1.25 mbgl. The maximum depth has been found in the northeastern part of the area having a depth of 2.25–2.72 mbgl. The maximum depth zone covers a very small part of the area. The watertable depth increases toward the northeastern part of CMC (Fig. 9.3).

From the above discussion it is clear that the pattern of water level depth is almost the reverse between the pre- and postmonsoon periods which increases the water level between fluctuation zones. The depth range is lower in the postmonsoon water level than the premonsoon water level in CMC. Therefore, we get four zones of water level in pre- and postmonsoon periods, however, the interval is 0.5 m in postmonsoon and 1 m in premonsoon season over the area. Therefore, the gradient is maximum in the premonsoon season rather than the postmonsoon season.

The minimum and maximum depth of the premonsoon water level in HCM is 1.1 and 4.0 mbgl, respectively. The average depth of the premonsoon water level is 2.26 mbgl which is more than that of CMC. The minimum and maximum depths of the postmonsoon water level are 0.5 and 2.3 mbgl, respectively. The average depth of the postmonsoon water level is 1.18 mbgl which is also more than that of CMC. The average fluctuation of the pre- and postmonsoon water level is 1.08 m. The average depth of surface soil and clay is 27.5 m from the surface. Therefore, the pre- and postmonsoon water level belongs to the surface soil and clay. The maximum depth zone covers the northern and southernmost part of HCM having a depth of 3.36–3.93 mbgl during the premonsoon period. The shallow depth zone

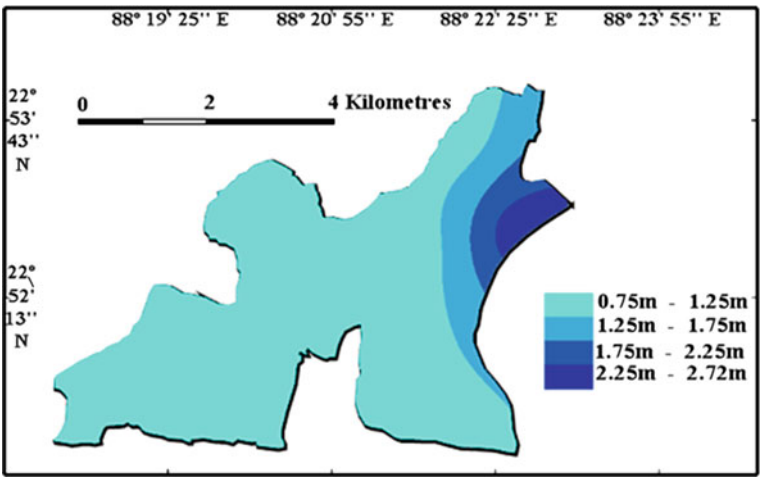

Fig. 9.3 Postmonsoon water level of dug well of CMC, 2011

covers the south-central part of the area having a depth of 1.36–2.36 mbgl. The water level depth also increases from south-central to north and south in HCM during premonsoon (Fig. 9.4).

The maximum depth zone having a depth of 1.95–1.96 mbgl covers the northern part and southernmost area of HCM during the postmonsoon period. The south-central part is covered with a shallow depth zone having a depth of 0.45–0.95 mbgl. Therefore, the water level depth increases from south-central to north and south in HCM during postmonsoon (Fig. 9.5).

The range of water level gradient during pre- and postmonsoon is lower in HCM than CMC. The average depth of the bottom of a well is 5.65 mbgl, which is less than CMC. Therefore, the water-holding capacity of a well is 2576.61 l (2.5766 cumec) maximum on an average in HCM.

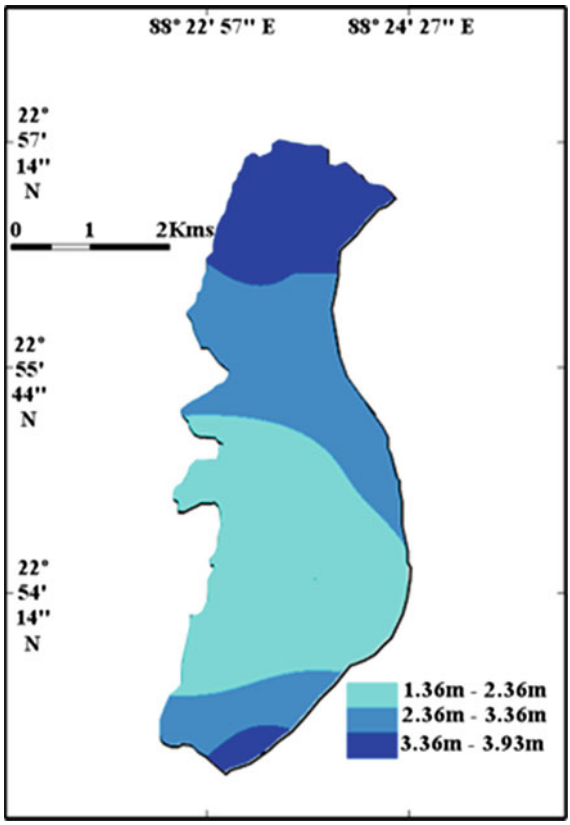

Fig. 9.4 Premonsoon water level of dug well of HCM, 2011

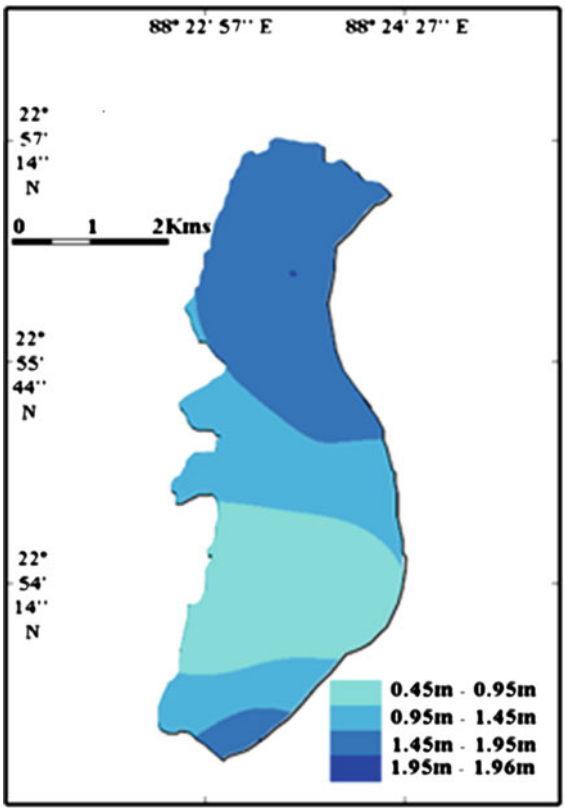

Fig. 9.5 Postmonsoon water level of dug well of HCM, 2011

9.4 Groundwater Level

The groundwater level indicates the uppermost water level of the saturated zone. The groundwater level is treated as a static water level when the level is not influenced by any pumping operation. Generally, it is stated that the groundwater level in an unconfined aquifer is synonymous with a piezometric surface. However, in a confined aquifer a piezometric surface may or may not be analogous to groundwater level. The groundwater level or static water level belongs to the study area much below the water level of a dug well. Here, the groundwater level represents the piezometric surface. The trend of the groundwater level has been declining over the years (Fig. 9.6). The static water level of CMC and HCM show that the premonsoon levels were 11.50 and 8.57 mbgl in 1995 which increased to 16.53 and 15.09 mbgl, respectively, in 2011 (Table 9.1). It was found that the groundwater of CMC and HCM are recharged not by the amount of rainfall the area itself gains, but rather mainly from the surrounding rural areas.

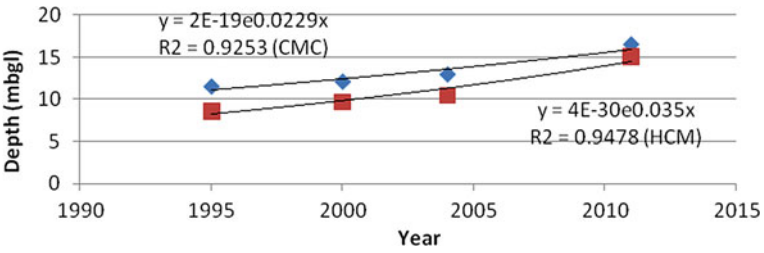

Fig. 9.6 Temporal premonsoon static water levels

Table 9.1 Premonsoon static water level of the study area

Year	Water level of CMC (mbgl)	Water level of HCM (mbgl)
1995	11.50	8.57
2000	12.08	9.70
2004	12.95	10.48
2011	16.53	15.09

Source SWID, West Bengal and Water Supply Dept. of the cities

9.5 Results and Discussion

It is clear from the above discussion that there is a prominent difference between the water level of a dug well and the static water level in CMC and in HCM (Fig. 9.7). Generally, it was found that the water level of a dug well is mainly influenced by rainwater of the area and also by surrounding ponds. Water is available year-round. Many dug wells are used year-round with sufficient water withdrawal. However, these dug wells never go dry because they get a constant water supply from the

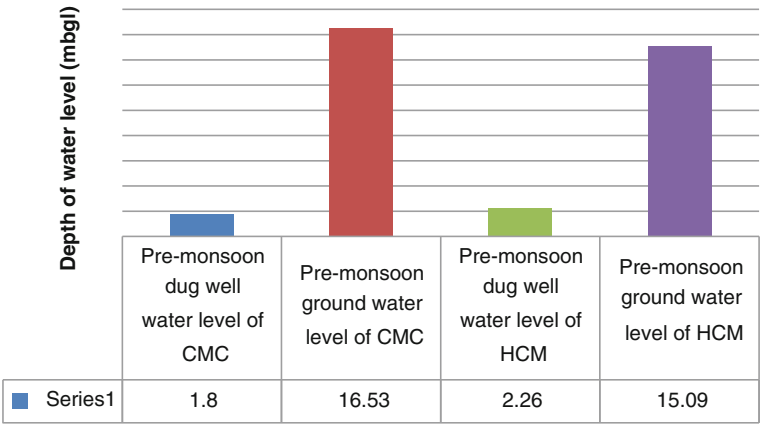

Fig. 9.7 Premonsoon water level of dug well and ground water, 2011

surrounding ponds which enters the well through soil seepage. There are huge numbers of different sized ponds in the study area. The average depth of surface soil and clay from the surface is 27.5 m which has been derived from the lithological logs of the area. With the increase of depth, the nature of the clay also changes. Higher depth means higher pressure which compacts the material. In the clay layer, within the dug well water level zones permit water to come into the well from the surrounding ponds. However, this clay behaves like an aquitard below a certain depth in the area (Datta 2007; Ganguli 2011). Clay is more compressible than other geological materials in an alluvium environment. Clayey materials are highly compressible (Todd 2006). The bulk modulus of compression is the minimum in clay (Raghunath 2006). The thick clay layer on the top does not allow pond water or dug-well water to reach the static water level. Otherwise there was little chance of a declining static water level. It was estimated from the field survey that the amount of annual renewable surface water (water in different sized ponds) amounts to 896.40 ha m in CMC and 497.88 ha m in HCM (2011). This huge amount of renewable water keeps dug wells from going dry year-round by keeping a constant supply. It was observed from the field survey (2011) that much building construction is done using water from dug wells in the study area because of the year-round constant availability of water in the dug wells.

Therefore, water in dug wells comes through soil seepage and directly from rainwater. It is not the groundwater of an aquifer. However, in other hydrogeological setups the water level in a dug well is an indicator of the static water level. Generally, the water level of a dug well and of groundwater is the same where high permeable material exists on the surface to the depth of the aquifer. In that case both water levels respond equally.

9.6 Conclusion

The depth of the water level of a dug well is much above the static water level of the area. The static water level indicates the piezometric surface which is directly connected to the aquifer system of the area. This difference in the depth of the dug-well water level and static water level is observed mainly because of a thick clay layer on the top. The average depth of the surface soil and clay is around 27.5 m from the surface. Clay helps to create a huge number of ponds and to separate the water level of dug wells from the groundwater level of the area. Therefore, it is established that we cannot treat the dug-well water level as the groundwater level where a thick clay layer exists on the surface.

Acknowledgments The author is highly grateful to the Council of Scientific and Industrial Research (CSIR) for funding support and also to the State Water Investigation Directorate, West Bengal and to the Water Supply Departments of CMC and of HCM for providing relevant data and information.

References

Biswas (1959) http://www.cgwb.gov.in. Accessed 5 July 2012
Datta S (2007) Hydrogeology and ground water resources of Hugli district, a report published by Central Ground Water Board, Kolkata, West Bengal
Ganguli M (2011) Ground water withdrawal and land subsidence: a study of singur Block, West Bengal, India. Int J Geomat Geosci 2(2):465–471
Heath R (2004) Basic ground-water hydrology. USGS Water Supply Paper, USGS. http://www.usgs.gov/. Accessed 7 Mar 2011
http://www.groundwater.org/gi/gwglossary.html. Accessed 15 July 2012
Maitra M, Ghosh N (1992) Groundwater management—an application. Ashish Publishing House, New Delhi
Mathur R (1969) A study in the ground water hydrology of the Meerut District, Uttar Pradesh. Banaras Hindu University, Varanasi, India
Raghunath H (2006) Ground water. New Age International (P) Limited, New Delhi
Raghunath H (2009) Hydrology principles, analysis, design. New Age International (P) Limited, New Delhi
Ram R, Bilas R (2010) Groundwater management in Chandauli district, UP: a case study. Natl Geogr J India 56:93–100
Rangachari R et al (2012) Water resources development scenario in India. Central Water Commission, Ministry of Water Resources, Government of India. New Delhi
Saha D et al (2008) The aquifer system and evaluation of its hydraulic parameters in parts of South Ganga Plain, Bihar. In: Das S (ed) Hydrogeological Research in India, Geological Survey of India, Bangalore, pp 165–186
Shankar P et al (2011, January 8) Indian's groundwater challenge and the way forward. Econ Polit Wkly XLVI(2):37–44. http://www.cgwb.gov.in. Accessed 20 Mar 2011
Sikdar P (2008) Geology of the quaternary aquifers of the twin city of Calcutta-Howrah. In: Das S (ed) Hydrogeological Research in India. Geological Survey of India, Banglore, pp 107–125
Sing U (1983) Assessment and prospects of water resources in Eastern UP, Banaras. The National Geographical Society of India, Varanasi
Todd D (2006) Groundwater hydrology. Wiley Dreamtech India (p) Ltd, New Delhi

Chapter 10
Utilisation Prospects of Bapung Coal, Meghalaya, Northeast India

Manabendra Nath

Abstract Bapung coal in the Jaintia Hills of Meghalaya is important with respect to its quality. The unique physico-chemical composition (low ash, high volatiles, and hydrogen content) of the coal exhibits better utilisation prospects. The coal has low ash content (1.5–2.8 %) but high organic sulphur (2.44–3.64 %), which is intimately intermingled with the coal. The coal can be used in blends (10–15 %) with Gondwana coal (high ash, low sulphur) which is now practiced in the Bengal–Jharkhand region for producing metallurgical coke for steel plants. The high reactive content (vitrinite and liptinite, 83.7 %) of this coal improves the overall composition of Gondwana coal with high inert content; it is suitable for stream-raising and gasification. The low temperature carbonization (LTC) of coal yields coke—595 to 689 kg, tar—109 to 136 lt, liquor—51 to 77 lt, and gas—97.5 to 130.6 cubic-metre per tonne for coal. The quality of the coke is not good and found to be non-caking. The LTC tar can be more readily converted in one stage to petroleum oil due to its high hydrogen content (5.13–5.70 %).

Keywords Bapung · Coal · Low ash · Sulphur · Metallurgical coke · Utilisation · Prospects

10.1 Introduction

The coalfields of Meghalaya are located far away from the main producing Gondwana Basin of the country. The coal-bearing formations are understood to have been deposited on a platform basin under stable shelf conditions along the periphery of the Shillong plateau.

The first report of the occurrence of coal in Meghalaya was made by Medlicoot (1868). This was followed by Mallet (1875), La Touche (1889), Bose (1904), Evans

M. Nath (✉)
Department of Geology, G.C. College, Silchar 788004, Assam, India
e-mail: manabendra.nath@rediffmail.com

B.C. Das et al. (eds.), *Neo-Thinking on Ganges-Brahmaputra Basin Geomorphology*, Springer Geography, DOI 10.1007/978-3-319-26443-1_10

(1932), Ghosh (1940, 1964), Goswami and Das (1965), Chakraborty and Bhattacharyya (1969), and Raja Rao (1981). The coal deposits of Meghalaya have been studied by a number of workers from time to time. A mention may be made of the contributions of Ahmed (1971), Ahmed and Bora (1981), Ahmed and Bharali (1983), Bora and Ahmed (1983), Ahmed (1996), and Singh and Singh (2000).

The coal deposits of Meghalaya (along with Bapung in the Jaintia Hills of Meghalaya) have been studied from time to time with respect to their petrographic and chemical characteristics but the earlier studies lack a systematic approach.

The Bapung coalfield is located in the Jaintia Hills, Meghalaya at a distance of 90 km from Shillong (Figs. 10.1 and 10.2). The mining town Ladrymbai of this coalfield is on the Jowai–Badarpur Road. The area is bounded by latitudes 25°22′ N–25°25′N and longitudes 92°18′E–92°21′E.

In the present study an effort has been made to carry out a detailed petrographic and geochemical study of a large number of samples from all the coal seams measuring one metre in thickness. The main objective of this study is to focus on the utilisation prospects of the coal (based on different geochemical and carbonisation studies) formed on a platform basin under stable self conditions.

In the Jaintia Hills the Jaintia Group of rocks (Eocene age) lie uncomfortably over the Archaean gneisses and granites. The Lakadong sandstone member of the Shella Formation (Jaintia Group) is exposed in the Bapung Coalfield. It comprises chiefly sandstones and shales of varying nature and houses three coal seams (Fig. 10.3).

There are three coal seams in the area. The thickness of the coal seams ranges from 0.5 m to 1.00 m and the bottom seam is thicker than the other two seams. The seams are persistent in nature and frequently associated with carbonaceous shales. The coal seams along with the interseam rocks have a general strike in the NE–SW direction with a common southerly dip of 4°–5°.

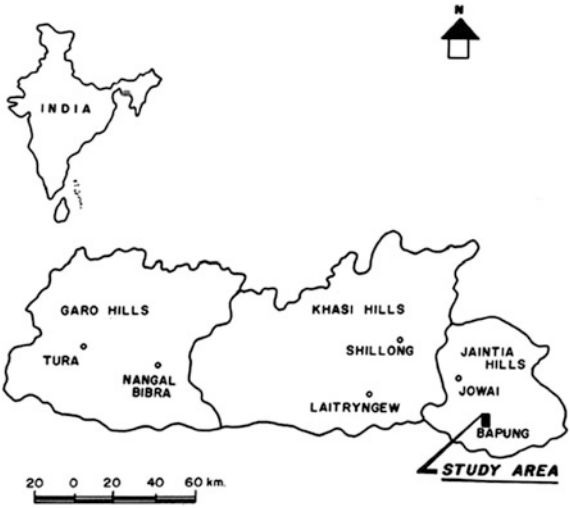

Fig. 10.1 Location map of Bapung coalfield

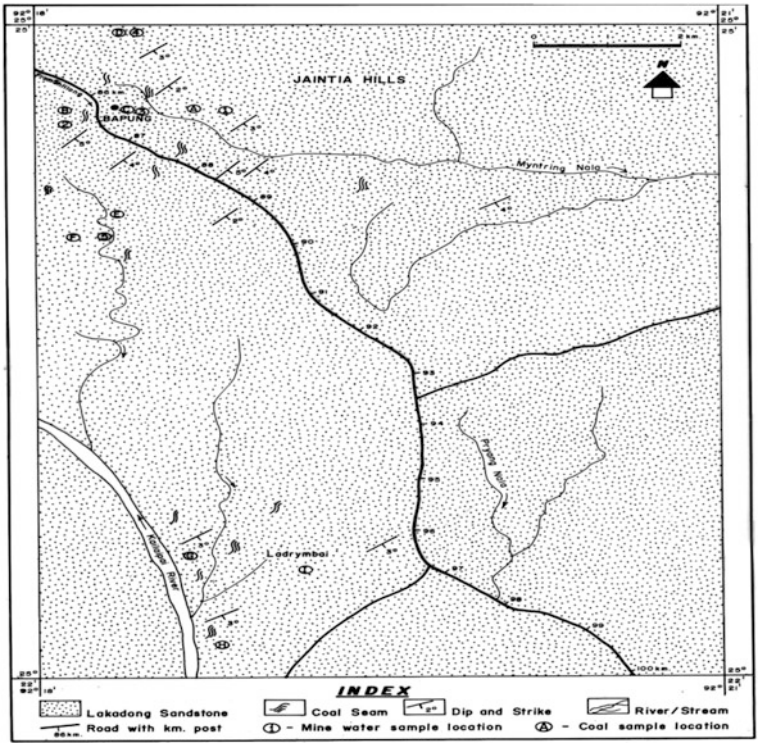

Fig. 10.2 Geological map of the area around Bapung

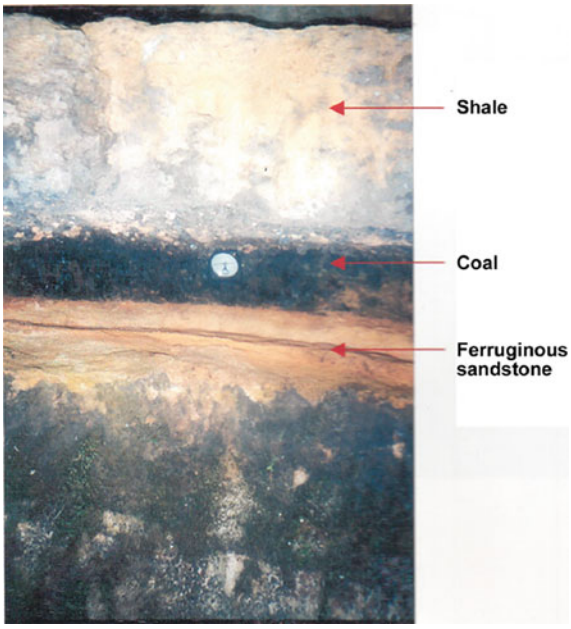

Fig. 10.3 A typical coal seam developed in the Bapung area interbedded with sandstone at the *bottom* and shale at the *top*

The coal lacks banded structure and appears to be entirely made up of vitrain. The lustre ranges from glossy to dull. The coal breaks with cubical fracture. But, the hard ones break with subconchoidal to conchoidal fracture. Most of the coals, when exposed to the sun, are found to be friable and disintegrate into small chips. Sometimes very thin pyrite bands are observed in the seams. On weathering, they show a tendency of breaking parallel to the bedding plane.

10.2 Materials and Methods

10.2.1 Chemical Composition

A total of nine channel samples collected from the field were first air dried to remove the free moisture. The samples were then taken for coning and quartering and the portions selected were crushed and sieved through a 211 micron sieve and stored in airtight glass bottles. In the laboratory, proximate and ultimate analyses (Figs. 10.4 and 10.5) were carried out following the Indian Standard Specification

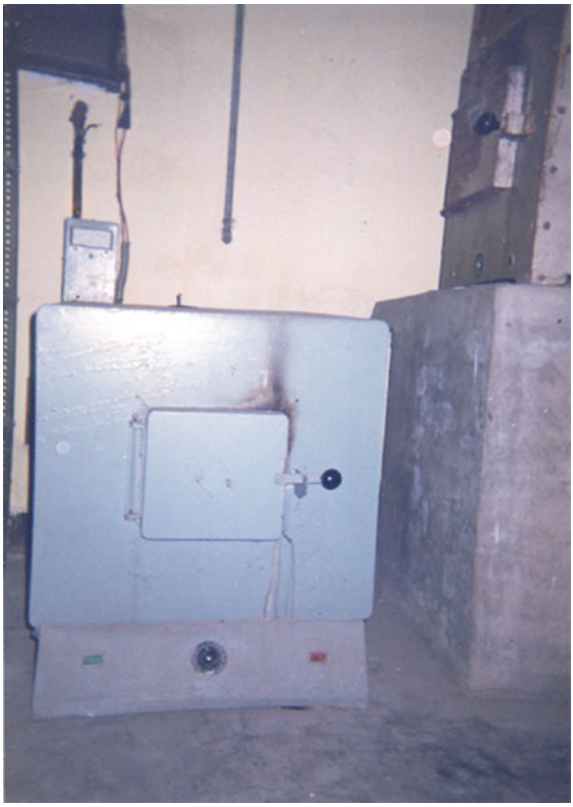

Fig. 10.4 Determination of moisture content instrument (muffles furnace)

Fig. 10.5 Determination of ash content instrument

[ISI; 1350; Pt I, 1969; IS; 1350, Pt IV/ Sect I; 1974; IS: 1350, Pt III, 1969; IS: 1350 (part IV/ Sec. 2) 1975].

10.2.2 Determination of the Calorific Value by Bomb Calorimeter

The calorific value of Bapung coal was determined in the laboratory with a bomb calorimeter. 1 gram of coal was burnt in an atmosphere of oxygen under a pressure of about 25 atmospheres. The coal inside the bomb was ignited electrically. The bomb was placed in 0.5 cc water. The heat produced was absorbed in the water, and the rise in water temperature after the combustion was measured with a Beckmann thermometer.

10.2.3 Petrographic Composition

Polished blocks prepared from the channel samples were studied under reflected light with an oil-immersion objective using a Leitz microscope. Quantitative petrography was carried out with an electric point counter attached to a mechanical stage of the microscope. Individual macerals were counted and finally computed to corresponding groups.

10.2.4 Low-Temperature Carbonisation

The low-temperature carbonisation (Fig. 10.6) of coal was done at a temperature of 600 °C to determine the coke, tar, liquor, and gas yield of the coal. In the experiment 20 gram of coal were kept in a silica retort with an asbestos plug and the silica retort was inserted into the hot furnace. The retort was connected with a receiver to collect the tar and liquid products of carbonisation. The receiver was kept in an ice bath to cool the vapours coming out of the silica retort, which was connected to a gas-collecting bottle filled with water. The pressure inside the gas-collecting bottle was always kept equal to the atmospheric pressure. Gases released from the silica retort during carbonisation were collected in the bottle replacing the water. After keeping coals in the retort and fitting every apparatus properly, the temperature of the furnace was steadily increased at a rate of 5 °C′ min to a constant temperature of 600 °C and this temperature was kept for one hour. The separated gases were collected in the gas-collecting bottle; tars were collected in the receiver and cokes were left in the silica retort. The nature of the coke was determined by correlating it with photographs of some standard types.

Fig. 10.6 Low-temperature carbonisation (LTC) instrument

10.3 Results and Discussion

10.3.1 Chemical Composition

The results of the chemical analysis of Bapung coal are presented in Table 10.1.

Bottom seam: The results of proximate analysis (air-dried basis) show that the moisture content of bottom coal ranges from I.5 to 1.9 %, ash from 2.2 to 2.8 %, and volatile matter from 41.20 to 44.20 %. The ultimate constituents (air-dried basis) such as carbon range from 72.89 to 75.02 %, hydrogen from 5.39 to 5.70 %, nitrogen from 1.79 to 2.80 %, oxygen from 8.1 to 10.53 %, and organic sulphur from 3.47 to 3.64 %.
Middle seam: The middle seam coals show a range of moisture content from 1.7 to 2.0 %, ash from 1.6 to 2.7 %, and volatile matter from 40.10 to 44.70 % (air-dried). In the ultimate composition (air-dried basis) the carbon content ranges from 71.36 to 73.34 %, hydrogen from 5.13 to 5.55 %, nitrogen from 2.1 to 2.71 %, oxygen from 10.89 to 13.46 %, and organic sulphur from 2.44 to 3.42 %.
Top seam: The moisture content of coals of the top seam ranges from 1.6 to 2.1 %, ash from 1.5 to 2.7 %, and volatile matter from 42.15 to 45.25 % (air-dried). In the ultimate analysis (air-dried basis) the carbon content ranges from 74.28 to 75.67 %, hydrogen from 5.62 to 5.86 %, nitrogen from 1.32 to 2.56 %, oxygen from 8.99 to 10.57 %, and organic sulphur from 3.14 to 3.37 %.

Table 10.1 Results of proximate and ultimate analysis (on air-dried basis) of Bapung coal

Particulars		Channel samples, Bapung coal (in weight %)								
Seam		Bottom			Middle			Top		
Sample No.		CC3	CC6	CC9	CC2	CC5	CC8	CC1	CC4	CC7
Moisture		1.9	1.8	1.5	2	1.7	1.8	1.8	2.1	1.6
Ash		2.8	2.4	2.2	1.6	2.7	2.4	1.5	2.7	1.5
Volatile matter		41.20	44.25	42.75	40.25	44.70	40.10	42.15	45.25	43.70
Fixed carbon		54.10	51.55	53.55	56.15	50.90	55.70	54.55	49.95	53.20
Carbon		75.02	72.89	74.56	71.36	73.34	72.02	74.28	74.58	75.67
Hydrogen		5.39	5.70	5.57	5.13	5.14	5.55	5.62	5.86	5.65
Nitrogen		2.80	1.79	2.72	2.71	2.11	2.10	2.56	1.68	1.32
Oxygen		8.1	9.34	10.53	13.46	12.74	10.89	10.57	10.24	8.99
Sulphur	Total	4.45	4.27	3.58	4.25	3.76	4.40	4.11	4.31	4.38
	Sulphate	0.43	0.42	0.50	0.45	0.46	0.54	0.41	0.52	0.57
	Pyritic	0.55	0.68	0.64	0.42	0.45	0.72	0.34	0.38	0.48
	Organic	3.47	3.57	3.64	3.38	2.44	3.43	3.36	3.14	3.37

Source Gauhati University Laboratory Analysis, 2013

10.3.2 Calorific Composition

The calorific value of coal is determined in the laboratory using the bomb calorimeter. Air-dried samples of coal liberate 6712.8–7592.5 cal/gm (12083.04–13583.88 BThU/lb) calorific value (Table 10.2).

The bottom seam yields 6712.8–7461.9 cal/gm (12,083.04–13,431.42 BThU/lb), middle seam 6809.2–7546.6 cal/gm (12,256.56–13,583.88 BThU/lb), and the top seam 7254.6–7474.7 cl/pg (13,058.28–13,454.46 BThU/lb).

10.3.3 Petrographic Composition

The macerals of all three groups—vitrinite, liptinite, and inertinite—have been indentified in the Bapung coal (Table 10.3). The macerals of the vitrinite group were dominantly represented by collotelinite (structureless vitrinite). The macerals of the liptinite group present were sporinite and resinite. The macerals of the inertinite group present were fusinite, semifusinite, and funginite. Pyrite was the most dominant mineral matter of these coals.

The vitrinite content ranges from 80.05 to 82.62 % in the bottom seam, 78.05 to 82.02 % in the middle seam, and 76.50 to 81.76 % in the top seam (84.53 to 86.11 % in the bottom seam, 81.51 to 84.73 % in the middle seam, and 79.25 to 87.26 % in the top seam, mineral matter free, mmf basis; Tables 10.3 and 10.4).

The concentration of liptinite is meager. It ranges from 1.25 to 2.95 % in the bottom seam, 1.28 to 1.70 % in the middle seam, and 1.27 to 3.25 % in the top seam (1.29 to 3.13 % in the bottom seam, 1.34 to 1.76 % in the middle seam, and 1.31 to 3.47 % in the top seam, mmf basis; Tables 10.3 and 10.4).

Table 10.2 Calorific value of Bapung coal on air-dried basis (determined in bomb calorimeter)

Sample No.	Cal/gm	BThU/lb
Bottom seam		
CC3	7461.9	13431.42
CC6	6712.8	12083.04
CC9	7341.2	13214.16
Middle seam		
CC2	6809.2	12256.56
CC5	7106.3	12791.34
CC8	7546.6	13583.88
Top seam		
CC1	7254.6	13058.28
CC4	7474.7	13454346
CC7	7390.8	13303.44

Source Gauhati University Laboratory Analysis, 2013

Table 10.3 Petrographic composition of Bapung Coal (in percent)

Sample No.	Vitrinite	Liptinite	Inertinite	Mineral matter
Bottom seam				
CC3	80.05	2.95	11.40	5.60
CC6	82.62	2.16	11.17	4.05
CC9	81.86	1.25	13.73	3.16
Middle seam				
CC2	78.25	1.52	14.73	5.50
CC5	78.05	1.28	16.42	4.25
CC8	82.02	1.70	13.08	3.20
Top seam				
CC1	81.76	3.25	8.69	6.30
CC4	77.35	1.27	18.08	3.30
CC7	76.50	1.98	18.05	3.47

Source Gauhati University Laboratory Analysis, 2013

Table 10.4 Petrographic composition (visible mineral matter-free basis, percent)

Sample No.	Vitrinite	Liptinite	Inertinite
Bottom seam			
CC3	84.79	3.13	12.08
CC6	86.11	2.25	11.64
CC9	84.53	1.29	14.18
Middle seam			
CC2	82.80	1.61	15.59
CC5	81.51	1.34	17.15
CC8	84.73	1.76	13.51
Top seam			
CC1	87.26	3.47	9.27
CC4	79.99	1.31	18.69
CC7	79.25	2.05	18.69

Source Gauhati University Laboratory Analysis, 2013

Inertinite is moderate in its concentration and ranges from 11.17 to 13.73 % in the bottom seam, 13.08 to 16.42 % in the middle seam, and 8.69 to 18.08 % in top seam (11.64 to 14.18 % in the bottom seam, 13.51 to 17.15 % in the middle seam, and 9.27 to 1869 % in the top seam, mmf basis; Tables 10.3 and 10.4).

The content of the mineral matter varies from 3.16 to 5.60 % in the bottom seam, 3.20 to 5.60 % in the middle seam, and 3.30 to 6.30 % in the top seam (Table 10.3).

10.3.4 Carbonisation Assay of Bapung Coal at Low Temperature

The results of a low-temperature Gray King Assay at 600 °C of Bapung coal are given in Table 10.5.

The coal yields 595–689 kg of coke per tonne of coal in air-dried basis. Tar yields range from 109 to 136 litres per tonne of coal, liquor yields ranges from 51 to 77 litres per tonne of coal**,** and gas yields from 97.5 to 130.6 cubic metres per tonne of coal (at normal pressure and temperature) in air-dried basis. The coke formed resembles types A and B of the standard figure of Francis (1961) indicating non-caking character.

The bottom seam of the area yields more coke (665–690 kg) compared to the top (595–660 kg) and middle (630–675 kg) seams. The coke formed from the bottom seam resembles type B of the standard figure of Francis. The middle seam yields coke, which does not swell in carbonisation, and resembles type A. The top seam also shows type A of the standard figure.

Table 10.5 Low-temperature carbonisation products of the Bapung coal

Sample No.	Coke in kilogram	Tar in litre	Liquor in litre	Gas in cubic metre	Coke type
	In per tonnes of coal	In per tonnes of coal	In per tonnes of coal	In per tonnes of coal	
CC1 (top seam)	660	122	61	97.5	A
CC2 (middle seam)	675	127	58	105.2	A
CC3 (bottom seam)	690	129	60	101.5	B
CC4 (top seam)	595	110	51	113.3	A
CC5 (middle seam)	630	131	57	121.5	B
CC6 (bottom seam)	665	135	65	123.6	B
CC7 (top seam)	646	109	67	130.6	A
CC8 (middle seam)	672	122	71	125.5	A
CC9 (bottom seam)	689	136	77	127.3	B

10.3.5 Relation with Ash

The lower the ash content (Table 10.1) of the coal is, the higher is the yield of coke and tar (Table 10.5). The ash content of this coal varies from 1.5 to 2.8 % and it can be used in blends (10–15 %) with Gondwana coal (high ash, low sulphur) of Bengal–Jharkhand for producing metallurgical coke for steel plants.

10.3.6 Relation with Macerals During Carbonisation

During carbonisation, the reactive constituents (vitrinite + liptinite) present in the coal first soften and then harden in a solid mass called coke. The inertinite groups of macerals remain more or less unchanged during the process. The ultimate strength of the resultant coke produced after carbonisation depends on the relative proportion of the reactive and inert components as well as the rank of the coal which controls the quality of the plastic mass that binds the coke (Crelling and Russell 1980).

10.3.7 Utilisation and Prospects

The Bapung coal can be used for thermal plants, the gas industry, and domestic purposes. As the coal contains low ash content (1.5–2.8 %), the yield of coke and tar is more. Low-temperature carbonisation tar can be more easily converted in one stage to liquid fuels due to its high hydrogen content. The gas and liquor may be used as sources of fuels, fertiliser, and other industries.

10.4 Conclusion

From the study it can be concluded that with low ash (1.5–2.8 %) and high calorific value [6712.8–7546.6 cal/gm (12083.04 to 13583.88 BThU/lb)] the Bapung coal exhibits better utilisation prospects. But the high sulphur content (2.44–3.64 %, organic form) and the non-caking quality make the coal very unsuitable for the conventional coke-making industry. Moreover, the high percentage of organic sulphur in the total sulphur stands as an uncrossable barrier in desulphurisation of the coal (Ahmed and Rahim 1993). Thus, unless an economically viable desulphurisation technique is developed, the Bapung coal along with other northeast Indian coals cannot be used for metallurgical purposes in the conventional way. But blending with high-ash Indian Gondwana coal exhibits a very fine caking quality with low sulphur content; its high ash content decreases the calorific value of the

cokes. Thus, blending of Tertiary coals of Bapung coalfield containing low ash content with Gondwana coals containing high ash content increases the calorific value of the coke produced, as overall ash percentage is reduced considerably in the process.

Although the Bapung coal is not used for making metallurgical coke, low-temperature carbonisation of this coal can be done to produce diverse types of coal by-products. A wide range of hydrocarbons can be obtained from the tar and liquor contents produced in carbonisation. Low-temperature carbonisation tars can be more easily converted in one stage to liquid fuels due to the high hydrogen content (Lahiri 1966).

A part of production is locally used as domestic fuel after producing soft coke by open stack burning. The major part is supplied to Assam and Bangladesh for use in brick fields and other industries. As the Bapung coal is the bituminous type having a high amount of volatiles (above 40 %), it is suitable for steam-raising and gasification.

Acknowledgements The author expresses his sincere thanks to the Head of the Department of Geological Sciences, Gauhati University for providing the necessary facilities. The author also expresses his sincere gratitude to the reviewer for constructive suggestions in modifying the present chapter.

References

Ahmed M (1971) Petrochemical study of coal, Litryngew coalfield, K & J Hills, Assam. J Geol Soc 1:15–20

Ahmed M (1996) Petrography and rank of Tertiary coal, Bapung coalfield, Jaintia Hills, Meghalaya. J Geosci I:21–27

Ahmed M, Bharali D (1983) Petrographic characters of Tertiary Coal, Nangalbibra, West Daranggiri Coalfield. In: Proceedings of the fifth Indian geophyto-logical conference, Lucknow., Spl. Publ. 1984, pp 242, 245

Ahmed M, Bora JP (1981) Geochemistry of Tertiary coal, Bapung coalfield, Jaintia Hills, Meghalaya. J Assam Sci Soc 24(2):9–10

Ahmed M, Rahimm A (1993) Desulphurisation of Eocene cola by chemical means, Jaintia Hills, Meghalaya. In: Proceedings of the international congress coal science, Banff, Canada, vz, pp 81–84

Bora AK, Ahmed M (1983) Occurrence of pyrite nodules in the Bapung coalfield, Jaintia Hills, Meghalaya, India. Quart J Geol Min Met Soc 55:99–100

Bose PN (1904) Report on the Um Rileng coal beds. Geol Surv India Rec 31(1):1–52

Chakraborty SN, Bhattacharyya U(1969) Report on geology and coal resources of central part of the Mawlong-Shella Coalfield, United Khasi and Jaintia Hills, Meghalaya, geological survey of India, unpublished report

Crelling C et al (1980) Principles and applications of coal petrology, short course, E No. 8.

Evans P (1932) Exclamatory notes to accompany a table showing the Tertiary succession in Assam. Trans Miner Geol Met Inst Ind 27:168–248

Francis W (1961) Coal, its formation and composition. Edward Arnold Ltd., London, pp 806

Ghosh AMN (1940) Stratigraphical position of the Cherra sandstone, Assam, India. Rec Geol Surv 75:1–19

Ghosh TK (1964) On Tertiary coal from Daraggiri, Assam Q.J., India. Geol Soc 36:91–92
Goswami AC, Das MK (1965). Detailed Mapping of the Cherrapunji Plateau. United Khasi & Jaintia Hills district, Assam. Geological survey of India, unpublished report
IS: 1350 (Part I) (1969) Methods of Test for coal and coke, Pt I Proximate analysis. Indian Standard Institution, New Delhi
IS: 1350 (Part III) (1969) Methods of Test for coal and coke, Pt III Determination of Sulphur. Indian Standard Institution, New Delhi
IS: 1350 (Part IV/Sec I) (1974) Methods of Test for coal and coke, Pt IV ultimate analysis, Section I Determination of Carbon & Hydrogen. Indian Standard Institution, New Delhi
IS: 1350 (Part IV/Sec 2) (1975) Methods of Test for coal and coke, Pt IV ultimate analysis, Section 2 Determination of Nitrogen. Indian Standard Institution, New Delhi
La Touche THD (1889) Report on Cherrapunji Coalfields. Geological survey of India, Rec. 22 (Pt-3), 167–171
Lahiri A (1966) A review of possibilities of conversion of coal to oil in India. Oil Commentary, vol IV, No. 7–8, pp 10–16
Mallet FR (1875). Note on coals recently found near Moflong, Khasi Hills. Geol Surv Ind. Rec 18 (Pt-3):65–92
Medlicott HB (1868), Coals in Garo Hills. Geol Surv Ind Rec 1 (Pt-1):1–22
Raja Rao CS (1981) Coalfields in India, coalfields in northeastern India. Geol Surv Ind Bull Ser A 45(1):75
Singh MP, Singh AK (2000) Petrographic characteristics and Depositional conditions of Eocene coals of Plat form Basins, Meghalaya, India. Int J Coal Geol 42:315–356

Chapter 11
Depletion of Water Level and Environmental Threat in Urban Areas: A Case Study of Kolkata and Salt Lake City, West Bengal

Mahua Bardhan

Abstract Kolkata City's water supply is dependent on both surface water sources from the river Hooghly and groundwater sources. A large part of the Kolkata Metropolitan Area (KMA) is currently served by groundwater pumped up from an aquifer deep below the city. The city draws water from the aquifers more rapidly than they can recharge themselves. The adjacent town of Salt Lake City covering an area of 12.35 km^2 was a conglomerate of several salt lakes 50 years back. Though planned as a satellite town, the water level is also decreasing fast due to overuse of groundwater at the rate of 20 cm/year. Therefore the objectives of this study are to find the reason for depletion of the water level, depict the present piezometric level in both Kolkata and Salt Lake City, identify the threat of land subsidence and arsenic contamination already begun in the area and classify the areawise subsidence rate to assume the future threat. The methodology followed in this chapter is mainly the analysis of the secondary data related to the temporal change of groundwater level, counting the land subsidence rate, and so on. The result shows that the city's water level has receded by 7–11 m between 1958 and 2003, especially in some areas of both north and south Kolkata. In around 30 % of the city area the level comes close to or falls below the clay layer which is ideal for subsidence and in some areas subsidence ranges from 10 to 14 mm a year creating high-risk zones. The remedial measures are given in the form of groundwater recharge by rainwater harvesting and mandatory installation of rooftop harvesting in Kolkata and Salt Lake along with improvement of the chemical quality of the water.

Keywords Groundwater · Subsidence · Contamination · Piezometric level · Risk zone

M. Bardhan (✉)
Department of Geography, Netaji Satabarshiki Mahavidyalaya, North 24 Parganas, West Bengal, India
e-mail: mahua_4440@yahoo.co.in

B.C. Das et al. (eds.), *Neo-Thinking on Ganges-Brahmaputra Basin Geomorphology*, Springer Geography, DOI 10.1007/978-3-319-26443-1_11

11.1 Introduction

Groundwater plays a very important role in meeting the water demand of Indian cities. There are three types of situations: (i) where the entire water supply is met from surface water, (ii) where the entire water supply is met from ground water, and (iii) where there is a mixed supply, a combination of both. Generally mixed water use is popular in most cities and in the study areas also. However, in recent decades an increasing population, neglecting the existing water harvesting and storage structures, and obstruction of the water supply channels by people and also by urban planners due to ill-planned urbanisation, have resulted in encroachment and dysfunction of natural drainage.

A large part of the Kolkata metropolitan area (KMA) is currently served by groundwater pumped up from an aquifer deep below the city. The domestic water supply is provided mainly from the Hooghly River through the Tala pumping station and the Garden Reach pumping station. In spite of these surface water sources a huge amount of water is drawn from the groundwater aquifers below Kolkata. The population growth of Kolkata City is increasing rapidly which also enhances the demand for groundwater in the city and ultimately imposes stress on the groundwater regime in the area. This exploitation is so huge that permanent depletion of the water level has occurred in the groundwater of Kolkata (Mishra 2011). The city is drawing water from the aquifers more rapidly than they can recharge themselves. The groundwater level in Kolkata is below 10 mbgl (metres below ground level) during the postmonsoon season and it reaches about 20 mbgl during the premonsoon season (Rajmohan and Prathapar 2013). The groundwater depth ranges from 3.34 to 16.32 mbgl in premonsoon. It is true for its satellite town Salt Lake also where the water level is reducing rapidly due to overexploitation on a regular basis. But estimation of groundwater resources is not possible due to paucity of data as the aerial extension of the aquifer cannot be determined because of cover by urban agglomeration.

11.2 Objectives of Study

The present study tries to explain the following objectives.

1. To find out the reason for depletion of present groundwater level in Kolkata and adjacent areas
2. To detect the environmental threat especially associated with land subsidence due to groundwater depletion
3. To analyse the deteriorating quality of groundwater and arsenic contamination in the city and related health problems
4. To assess the reduction of the piezometric level over time and place
5. To suggest suitable measures for recharging groundwater and its sustainable use

11.3 Database and Methodology

The study is mainly based on secondary data collected from Central Ground Water Board (CGWB), Public Health Engineering (PHE), Bidhannagar Municipality, Kolkata Municipal Corporation (KMC), and State Water Investigation Directorate (SWID), related to water level, groundwater extraction, and arsenic contamination etc. and these were mapped in GIS software such as Arc GIS and MapInfo to show the picture of groundwater level in the cities. Field checking was done in some selected wards and blocks for the primary survey.

The methodology followed in this chapter was prefield, field, and postfield study, and the analysis of data related to the temporal change of groundwater level, counting land subsidence rate, arsenic concentration, and so on. The analysis was done in two parts. First, data collected from secondary sources were used to find the consequences of overexploitation of groundwater (land subduction and arsenic contamination in different parts of the city) and secondly the data were used to create maps of various aspects of the environmental issues related to water reduction in the city. Some maps were also referenced to show the geomorphological and hydrological condition of Kolkata.

A digital elevation model and contour map (5 and 10 m contour) of the city were prepared on the basis of the ground elevation data, spot height, and GPS survey at certain points. Based on the data of the arsenic level in groundwater in each ward of KMC, the arsenic contamination map was prepared. The surface map was generated by referencing the Kolkata Metropolitan Development Authority (KMDA) map, followed by digitization and modification in software. Based on the locational data on saline and fresh water level, the groundwater map was prepared. All these maps were helpful for the analysis of the present groundwater scenario in the city. Based on the collected data about the piezometric level in different parts a zonation was done to classify the areas.

11.4 The Study Area

Kolkata is a metropolitan city with 187.33 km^2 area comprising of 144 wards and 15 boroughs. With a population of 4,496,694 (2011) and density of 24,252 persons/km^2, the growth rate of Kolkata City is 17,305 people per year (Census 2011). The population growth of Kolkata City is increasing rapidly which also enhances the demand for groundwater in the city and ultimately imposes stress on the groundwater regime in the area. The study area was the lower deltaic plain of the Ganga–Bhagirathi Basin. Hooghly is the main river and drainage system. Several canals including Bagjola, Beliaghata, Circular, Adiganga, and Tallynala, among others cover a large area and these are the main drainage channels. The soil is mainly younger alluvial of silt clay to clay type. Groundwater is generally monitored through wells of the CGWB. There are 21 monitoring wells (12 tube

wells and 9 piezometres, as of 31 November, 2007, KMC, WB) in the city. Monsoon rainfall is the main recharge source of groundwater. It rains mainly from June to September and the annual rainfall of the KMC area is 1647 mm (2006).

The water supply for the KMC area comprises the conjunctive use of treated surface water of the Hooghly River and tapping of groundwater by deep tube wells and hand tube wells. The KMC area is situated on the unconsolidated sediment of the lower Bengal delta. Typically these sediments comprise a number of successions of clay, silt, and sand and their mixtures in different proportions. KMC owned 264 large diametre (203 mm) tube wells fitted with 20 hp submersible pumps and 10,000 number small diametre (40 mm) tube wells fitted with hand pumps, which were operating in the KMC area as of December, 2006. Withdrawal from a large dip tube well was about 112.5 MLD (million litres per day) and a hand pump fitted

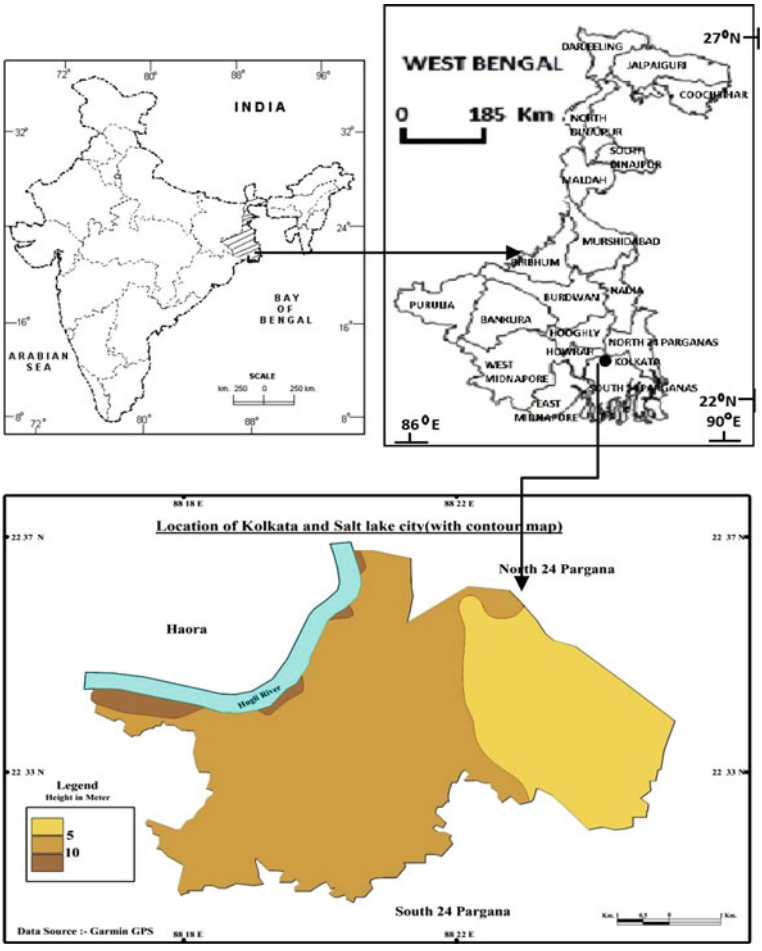

Fig. 11.1 Location of the study area

small diametre tube well was 21.4 MLD. In addition to KMC-owned tube wells, there were 5831 privately owned small diametre (101 mm) tube wells.

Physiographically Kolkata and the surrounding area represent a typical deltaic flat plain with elevation ranging between 4 and 6 m. The location map along with the contour map (Fig. 11.1) of Kolkata shows that the area has an average height of 5–10 m above sea level and Salt Lake is lower than the city as it has an average height of less than 5 m and is mainly covered by wetlands in eastern part. The slope of the land hence is from west to east.

Other studies also show high land near the Hooghly River and also along the Adiganga channel. The surface is gently sloping towards the east and southeast and forms low-lying areas in the east which transgress into the saline lakes or east Kolkata wetlands. Salt Lake City (also known as Bidhannagar) is adjacent to Kolkata and is a satellite township of it lying at the northeastern part of the metropolis, covering an area of 12.35 km^2 in a low-lying saucer-shaped basin and a conglomerate of several salt lakes. It has an added area of 21.5 km^2 which is part of the East Kolkata wetlands. The town has 25 wards and 74 blocks (Now under Bidhannagar Municipal Corporation and administrative boundaries are under change) with a population of 215,000 (Although planned as a satellite town the water level is also decreasing fast due to overuse of groundwater with a rate of 20 cm/year. There are two piezometric wells in Salt Lake: one at the CGWB office at Sector V and another one are at IA Park, Sector 3. Both wells show depletion in water level in the last 20 years due to overuse. These are mainly confined aquifer.

11.5 Geomorphology and Hydrogeology of Kolkata and Surrounding Area

Kolkata forms a part of the lower deltaic plains of the Ganga–Bhagirathi River system. It is a typical deltaic flat land with surface elevation ranging between 3.5 to 6 m above mean sea level. Younger levee, deltaic plain, interdistributory marsh, paleochannels, and younger levee adjacent to the River Hooghly and older levee on both sides of the old Adi Ganga are the important geomorphological units present in the area. It is very difficult to identify the different geomorphological units in Kolkata due to the urbanisation and absence of exposure of surface materials in many areas. Satellite data do not reveal the detailed geomorphic features apart from the pattern of settlements.

In and around Kolkata, in addition to the top clay layer, another 20–30 m thick clay layer occurs at around 150 m depth, the thickness of which increases to 50–60 m farther south. It is underlain by an alternating sequence of sand and clay layers down to a depth of about 300 m. In parts of the delta and riverine flood plains, the intervening clay layers may be absent, connecting the aquifers at depth and providing avenues for polluted groundwater to migrate deeper. This complex phenomenon seems to be responsible for the variation in arsenic content in groundwater on tapping

the same aquifer within a short distance in the delta and flood plain deposits. At Thakurpukur and Garia in the south, this water level is 10 mbgl and at the southern fringes of Kolkata the depth is 6 mbgl. This indicates that groundwater is flowing from south and southwest Kolkata to south-central Kolkata.

The geomorphological map (Fig. 11.2) and panel diagram (Fig. 11.3) indicate that there are two regionally extensive clay beds throughout the KMC area within the depth of 400 mbgl. The depth of occurrence of the basal clay bed varies from place to place but in general it occurs from 300 to 450 mbgl and the depth gradually decreases southward. The top clay bed of 10 to more than 60 m thick occurs above the entire alluvium sequence from the ground surface in the KMC area.

Thin lenses of very fine grain sand and silt in the silt clay layer also occur above the top clay layer at some places around Ballyganj, Tollyganj, Tijola, Dhakuria, Kasba, Santoshpur, Garia, Behala, Barisha, and Thakurpur in the swampy lands. The thickness of these sand and silt layers varies from place to place. In the levee deposits along the bank of River Hooghly lenses of fine to coarse grained sand are also present above the top clay bed at some places (Mishra 2011). The hydrogeological map (Fig. 11.4) depicts the aquifer conditions in the KMC area. The groundwater yield prospect is 90–120 m^3/h. From a general hydrogeologic point of view, the sediments have been categorized as aquifer (sand and gravel) and aquitard (clay). The first or uppermost aquifer is about 10–20 m thick on average. The

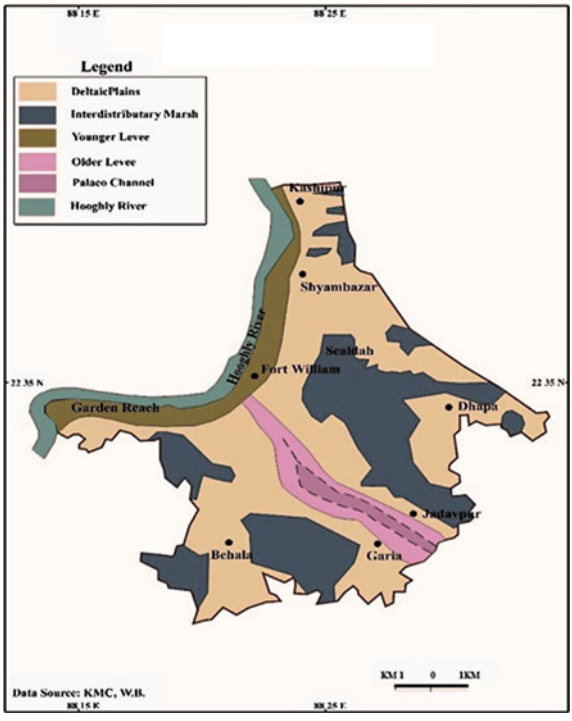

Fig. 11.2 Geomorphological map of KMC area based on Remote Sensing

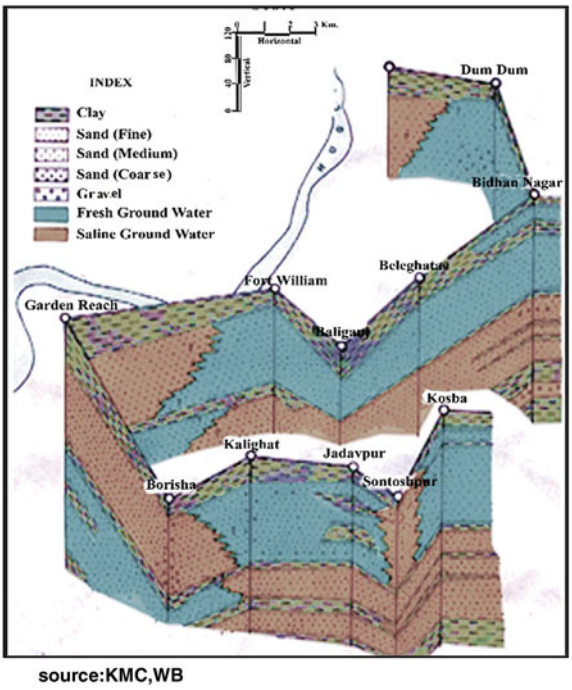

Fig. 11.3 Subsurface disposition of aquifers in Kolkata Municipal Corporation area. *Source* KMC, WB

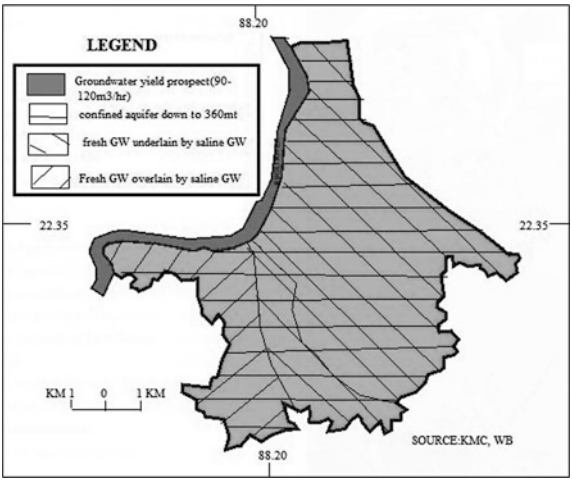

Fig. 11.4 Hydrogeological map of KMC

material is essentially fine sand. Most houses in the Bansdroni and Garia areas lift water from this zone. The second aquifer occurs between the depths of 65 and 120 m and this aquifer is about 30–50 m thick. This is the most potential and most exploited aquifer of Kolkata (Sengupta 2009).

11.6 Depletion of Groundwater Level

Due to heavy exploitation of groundwater a major change has occurred in the water level condition of Kolkata. This extraction has led to the development of a 6–8 m conical depression in central and south-central Kolkata. This trough has reversed the natural direction of groundwater flow towards the Bay of Bengal. Instead, polluted water flowing in from all directions has been collecting in this depression. Investigations conducted in Kolkata for the last 20 years reflect an alarming depletion of the piezometric level. At present the piezometric level is 14–16 mbgl in the Alipur, Babughat, Ballygunge, Kalighat, and Park Circus areas, whereas in the Bansdroni and surrounding areas this level is 9–11 m deep. At Garia and surrounding areas the piezometric level is between 8 and 10 mbgl. In the north the Baguihati, Sinthi, and Beleghata areas have the premonsoon water level of 12–14 mbgl, whereas in Dumdum and the surrounding area this level is from 10 to 12 mbgl. The piezometric level is at a depth of 6–10 m below sea level on average. During the postmonsoon period the piezometric level rises to the tune of 1–1.5 m in Alipur and about 2 m in Bansdroni and Garia and in north Kolkata and Dumdum (Sengupta 2009). Of the places, for example, the Park Circus and Tollygunge rate of pumping water is very high, whereas in some places the pumping rate is very low from where water flows outward in and around these places.

In Salt Lake the groundwater level is comparatively high due to infiltration from the water bodies in and around that area.

Dynamic Groundwater Resources and Issues in Kolkata (computed from Rajmohan and Prathapar 2013)

- Net annual replenishable groundwater resource (Mm3), 2004: 74.46
- Annual groundwater draft (Mm3): 111.40
- Allocation of groundwater for domestic and industrial use (for 25-year calculation; mm 3): 116.96
- Groundwater issue: Declining groundwater level, seawater intrusion, and As contamination

It is clear from Tables 11.1, 11.2, and 11.3 that from 1986 till 2006, that is, in 20 years, the number of deep and shallow tube wells in the KMC area have increased in number (though deep tube wells have reduced from 1998) but demand for drinking water increased due to the pressure of the population. The shallow wells are used for domestic purposes whereas the deep wells are used as the source of potable water in the city. But total extraction of groundwater has increased drastically as per the demand from 121.5 to 144.3 ml per day which reduces the

Table 11.1 Aquifer properties in Kolkata (2006)

Average annual rainfall	GW bearing formation	Water fluctuation level (mbgl)		Discharge (m^3/h)	Storativity (s)	Transmittivity (m^2/day)
		Premonsoon	Postmonsoon			
1647 mm	Quarternary alluviam	12.09–19.59	10.72–15.42	25.99–70.60	33×10^{-3} to 20×10^{-3}	2065–2276

Source Rajmohon and Pratapadhar (compiled from GWI Booklet, KMC 2007)

Table 11.2 Piezometriclevel of groundwater in Kolkata and Salt Lake

Present piezometric level (m)	Area
16–18	Salt Lake
14–16	Alipur, Babughat, Ballyganj, Kalighat, Park Circus
9–11	Banshdroni
8–10	Garia and surrounding area
12–14	Baguihati, Sinthi, Beleghata
10–12	Dumdum

Source Computed from Sengupta (2009) and CGWB, 2010

Table 11.3 Yearwise groundwater extraction from tube well in KMC area

Year	No. ground water structures (KMC owned)		Total groundwater withdrawn (million litres per day)
	Deep tube well	Shallow tube well (hand pump fitted)	
1986	232	5000	121.50
1991	285	10,500	184.95
1993	308	11,877	202.72
1998	325	12,000	209.70
2006	264	10,000	144.30

Source GWI Booklet, KMC (2007)

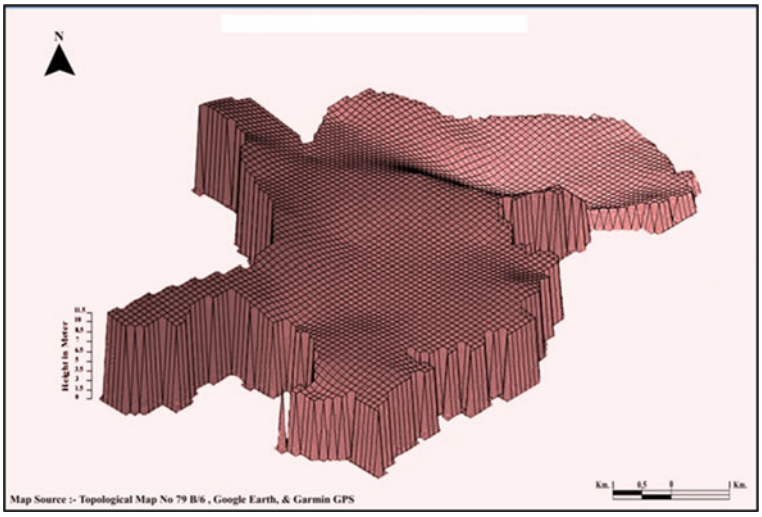

Fig. 11.5 Digital elevation model of Kolkata and Salt Lake city

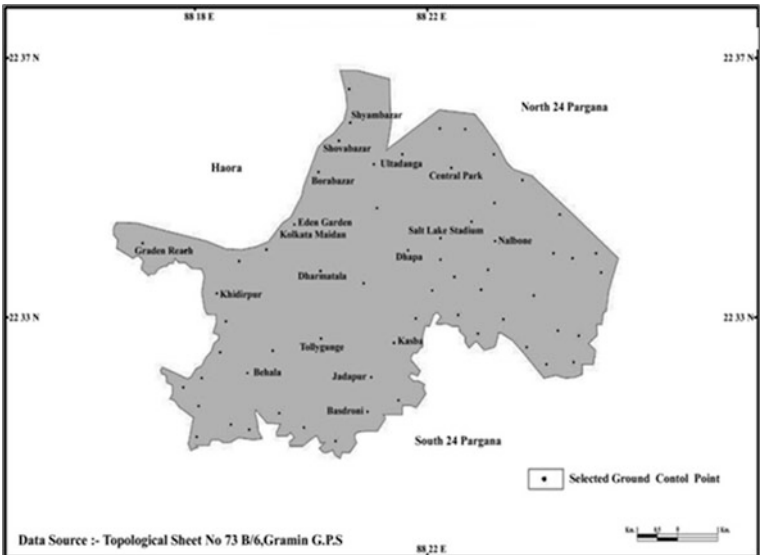

Fig. 11.6 Ground control point of Kolkata and Salt Lake city

water level and leads to various environmental problems. The metropolitan authority supplies 1209 MLD through a pipeline of which 1096 MLD is treated surface water and the rest is groundwater. About one-sixth of Kolkata's water supply is dependent on groundwater.

The digital elevation model (Fig. 11.5) with the help of the reference ground control point map (Fig. 11.6) shows that the slope of the land is from west to east; that is, earlier before setting up the Salt Lake satellite town the wastewater and surface water drained through the channels present here towards Salt Lake and the East Kolkata wetland. But after setting up the town, the flow was restricted. Hence waterlogging in both cities is common in monsoon especially in Salt Lake town for the last five to six years.

Due to heavy exploitation of groundwater a major change has occurred in the water level condition of Kolkata. Investigations conducted in Kolkata for the last 20 years reflect an alarming depletion of piezometric level in different places (Table 11.2).

The groundwater map (Fig. 11.7) shows that there is a thick clay layer under the surface of Kolkata and surrounding areas and after that an alternative layer of fresh and saline water is found. In most places saline water is beneath the fresh water, but in Salt Lake the saline water level dominates and there is an absence of fresh water which indicates that the area was a part of the moribund river delta in recent history with a connection to the Bay of Bengal. Sengupta (2009) shows that groundwater movement in areas of flat topography in the Bengal Basin may be mostly vertical and lateral flow may be limited to the local scale. Surface water and groundwater

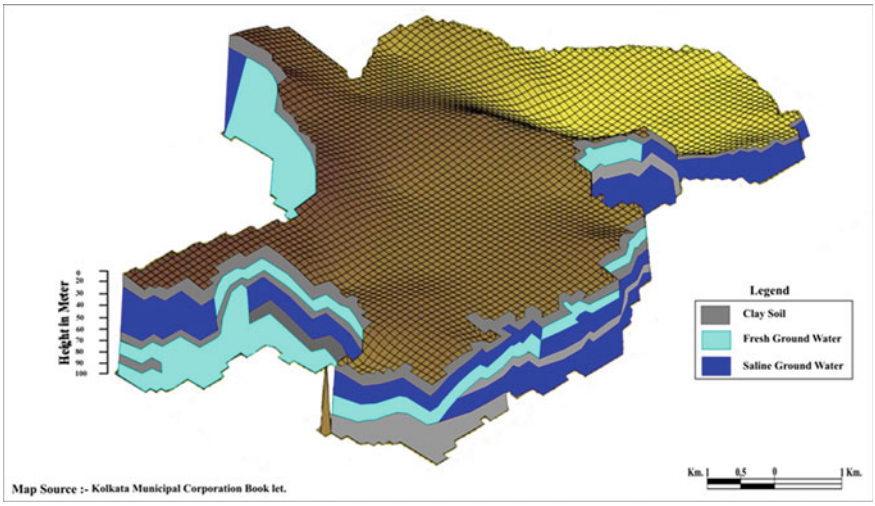

Fig. 11.7 Groundwater level of Kolkata and Salt Lake city

Fig. 11.8 Surface road network of Kolkata and Salt Lake city

interaction generally occurs within local flow systems. Bhagirathi–Hooghly is a losing stream along most of its length and recharges the shallow aquifers.

Construction of high rises and the growing pressure of the population reduce the water level by more and more extraction per day. The average building height of Kolkata City varies from 5 to 15 m, excluding a few 10–20 storied high-rise buildings scattered in the city centre, and newly developed commercial and residential clusters (EMP Bypass). Only a small quantity of rainwater reaches up to the aquifer because a large surface of the city has buildings, concrete roads, and so on (Fig. 11.8). The city has not enough parks and open spaces or green and vegetative cover and the permeability of the soil of thick fine silty clay type in most of the city is poor.

11.7 Environmental Problems Due to Depletion of Groundwater Level

There are several environmental and ecological problems observed in the study area due to depletion of water level. But as most of the city's need is fulfilled by purifying the river water the effect on human health is still not obvious. Arsenic contamination and land subsidence are the two most important environmental threats in this area. The intermediate aquifer usually shows arsenic contamination. At a greater depth, aquifer arsenic may not be present at the beginning but may become contaminated in the course of time.

11.7.1 Problem of Land Subsidence

Recent research shows that the land subsidence rate has been increasing in Kolkata and the eastern part for the last 44 years (Bhattacharya and Kumar 2012). Bhattacharya (2011) shows that the top 30 m of subsurface soil stratification in Kolkata generally indicates softer clayey soil in the first 15 m and relatively stiffer soil between 15 and 30 m. The continuously reducing piezometric level in different parts of Kolkata indicates an average subsidence rate of 7.5 mm/year. The rate of subsidence is based on linear and logarithmic theory which shows the compressibility of the clayey layers will be less because of the increasing overburden pressure. Sahu and Sikdar (2011) mapped different subsidence zones of the area (Fig. 11.9) from a very high to very low subsidence rate (Fig. 11.10; Tables 11.4, 11.5 and 11.6).

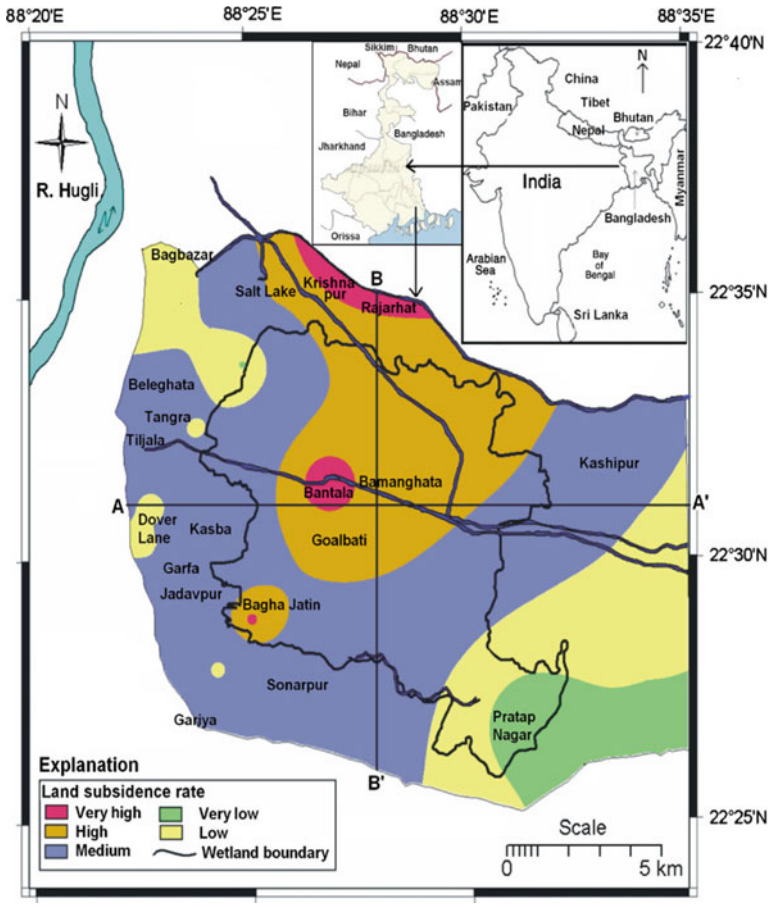

Fig. 11.9 Subsidence zones of the study area (*source* Sahu and Sikdar 2011)

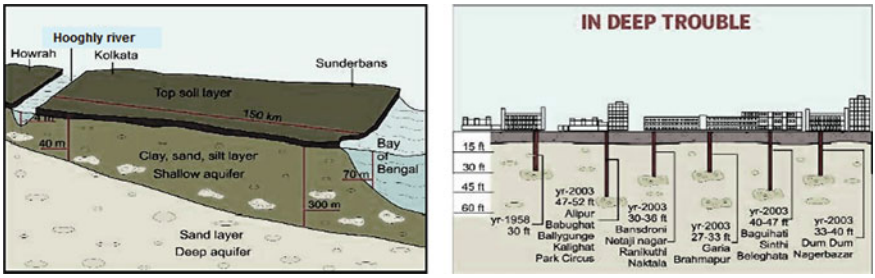

Fig. 11.10 Situation of aquifer in Hooghly River and groundwater level in selected areas (*source* Times of India, June 13, 2013)

Table 11.4 Stratification of normal Calcutta deposit (Dastidar and Ghosh 1967)

Stratum	Depth (m)	Description	Coefficient of volume compressibility *mv* (cm^2/kg)
I	0–5	Firm grey silty clay	0.014
II	5–15	Soft grey clay with wood stumps	0.04
III	15–20	Bluish grey clay with kankar	0.01
IV	20–25	Laminated brown clay, silt	0.01
V	25–30	Stiff mottled grey and yellow clay with kankar	0.01
VI	>30	Mottled silty clay laminated with parting of golden brown silty sand	

Table 11.5 Land subsidence in different places of Kolkata

Place	Piezometric level below ground		Subsidence in 44 years	Subsidence rate (mm/year)
	1956	2000		
Tangra	4.94	13.94	32.864	7.47
Baguihati	2.63	12.13	33.112	7.525
EMP bypass (near Salt Lake)	2.5	12.5	57.182	13
Ultodanga (near Salt Lake)	2.05	11.05	80.23	18.23

Source: Computed from Bhattacharya (2011)

Table 11.6 Classification of land subsidence rate

Land subsidence rate (mm/year)	Class
>20	Very high
15–20	High
10–15	Medium
5–10	Low
0–5	Very low

Source: Sahu and Sikdar (2011)

This study along with maps and data indicates the threat of possible land subsidence due to unrestricted groundwater abstraction in the KMC, Salt Lake, and EKW (East Kolkata wetland) areas. Data analysis from 1956 to 2000 shows that in 44 years places including Tangra, Baguihati, Salt Lake, and Ultodanga have land subsidence of approximately 7–19 mm/year (Bhattacharya and Kumar 2012; Sahu and Sikdar 2011). It was also found that Salt Lake is subsiding more than Kolkata as it was built by filling up the wetlands with sand and silt from Hooghly. It comes under the high-risk zone of land subsidence. It was also found that a medium-range earthquake can cause subsidence of the whole town. Therefore it is more vulnerable to the future land subsidence hazard. Because all of Kolkata is more or less

Table 11.7 Recent subsidence in the city

Date	Place	Suspected reasons
3 September, 2014	Dhakuria bridge	Gap in road pitch layer
12 September, 2014	Shayambazar	Break in the brick structure in sewage pipe
21 September, 2014	Chetla	Subsidence of tube well pipe
21 October, 2014	CR avenue	Activities of rats
22 October, 2014	Ultodanga	Failure of sewage pipe
23 October, 2014	Sovabazar	Leakage of Ganga water pipe
28 October, 2014	Armherst street	Collapsing brick structure of pipeline

Source: Ei Samai, Bengali Newspaper, 29/10/2014

uniformly subsiding, no visible ground crack or collapse of buildings or structures have been reported. But recently separate incidences of road subsidence due to various reasons have been reported (Table 11.7).

An attempt had been made primarily to identify the subsiding areas in Kolkata during 1992–1998. According to Chatterjee et al. (2007) due to overdrafting of groundwater under a confined aquifer condition, the potential land subsidence phenomenon has been reported by many researchers and by the local media. In a confined aquifer overextraction causes lowering of peizometric pressure, which results in the development of tensional forces in the overlying confining layer and material. Consequently compaction of this overlying confining layer material takes place and land subsidence occurs. In Kolkata the presence of a thick surface clay layer with an average thickness of more than 40 m (up to 60–70 m at places) over the aquifer sand layer raises a question of the probability and doubtfulness of land subsidence.

11.8 Arsenic Contamination—Another Environmental Threat

Apart from the land subsidence threat, a direct effect of overuse of groundwater is arsenic contamination of drinking water. Arsenic is a naturally occurring trace element found in rocks, soils, and the water in contact with them. Arsenic has been recognized as a toxic element and is considered a human health hazard.

As per the Bureau of Indian Standards (BIS) for drinking water (BIS 1991 and subsequent modifications), the maximum permissible limit of arsenic concentration in groundwater is 0.01 mg/l. The occurrences of arsenic in groundwater beyond the permissible limit (>0.05 mg/l) has been shown on the maps as water quality hot spots set up in West Bengal which recommended 0.05 mg/l as the permissible limit based on an earlier BIS Standard. The present drinking water demand in Kolkata is around 1262 million litres per day (MLD).

A 2002 study by the CGWB found traces of toxic elements such as chromium and cobalt in the shallow aquifers. The tanneries in east Kolkata are also culprits, discharging effluents into the wetlands and agricultural fields, which leach into the groundwater. In many places, the water is brackish and contains excessive amounts of iron, as in Jodhpur Park in south Kolkata or Salt Lake in the east.

Of the 144 wards that the city is divided into, as many as 77 have 'high levels' of arsenic in the groundwater, as shown in a study by the School of Environmental Studies (SOES) of Jadavpur University. In 32 of these 77 wards, the arsenic level is 'dangerously high,' and traces of the deadly metalloid were found in samples drawn from 32 more wards, but the level was within permissible limits. SOES has analysed 3626 samples from hand tube well water for arsenic from 100 out of 144 administrative wards in Kolkata. In 65 wards, tube wells had arsenic concentrations above 10 lg/L and in 30 wards above 50 lg/L. Their analysis showed out of 734 KMC wells 121 (16.5 %) had arsenic above 10 lg/L, 26 (3.6 %) above 50 lg/L, and only 2 (0.2 %) above 300 lg/L (CGWB 2010; Fig. 11.11). The study showed that the southern part of Kolkata City is more contaminated than the northern and central parts. It is alarming in places such as Sithi, Barangar, and Chitpur in north Kolkata and many places in south Kolkata. SWID surveyed 31 areas out of which 9

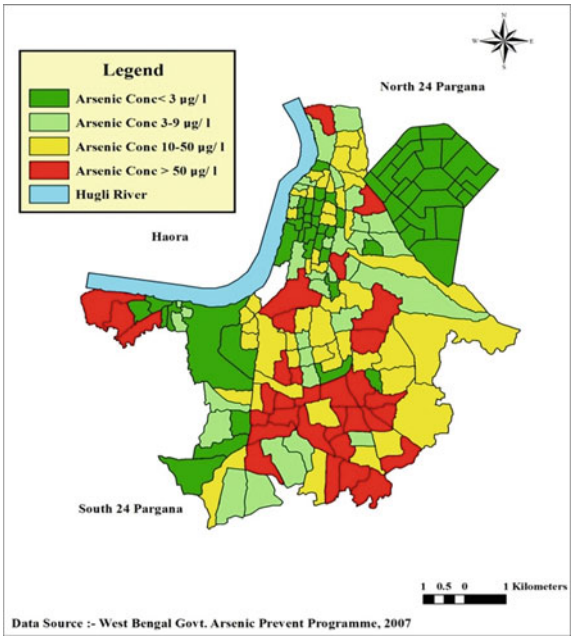

Fig. 11.11 Arsenic affected areas of Kolkata and Salt Lake city

Table 11.8 Arsenic concentration in KMC

Depth (m)	Arsenic (μg/l)
20	>50
100	10–50
100–300	<10

Source Computed from CGWB Report, 2010

have arsenic levels over the permissible limit and another 11 areas are also at risk (Table 11.8).

Chronic arsenic poisoning, which stems from long-term exposure through drinking water, could cause a wide variety of diseases, including cancer of the skin, lungs, kidney, and urinary bladder. Cancer, though, is a late phenomenon and usually takes more than 10 years to develop, according to the World Health Organization (WHO). In Kolkata arsenic enters the human body through vegetables, rice, milk, meat, and so on.

11.9 Findings of the Study

1. Development of the aquifers of Kolkata City has not yet received any serious attention of the planning agencies, as the problem deserves. Tube wells fitted with hand- or electric-driven pumps have been installed haphazardly as per local requirements without giving any consideration to the potentiality of the aquifers.
2. Due to the presence of a thick clay layer at the top of the sediment in the KMC area, there is no direct groundwater recharge. The surface area is covered by roads and built-up areas which also hinder groundwater seepage.
3. Groundwater pollution mainly arises from external sources in the city for anthropogenic reasons. Groundwater quality from deep tube wells shows high concentrations of chlorides and the chemical composition is not satisfactory, but free of bacterial contamination. In some wards of the city, the groundwater has been found to contain impermissible amounts of arsenic, lead, and cadmium. Iron content is also high (more than 5.7 mg/l) in the Salt Lake, Rajabajar, and Tiljala areas.
4. Due to increasing demand of the population, water stress has become acute leading to overuse of groundwater and reducing the piezometric level. Decline of yields of tube wells may also be related to choking of slots of strainers and improper spacing of tube wells resulting in interference of depression cones.
5. In the eastern part of KMC (Tangra-Topsia) toxic materials are found in excess of 0.01 mg/l in the shallow aquifers within 20 mbgl. Leather industries are present in that area. Effluents from the tanneries are causing serious environmental hazards.
6. Groundwater tapped in open wells in the Ballygunge, Tollygunge, Dhakuria, Kasba, Garia, and Behala areas in marshy land is hydraulically connected to the surface water bodies such as ponds, drains, and the like.

7. Sporadic occurrence of arsenic in groundwater in excess of permissible limits is found in many places, especially in the wards of the south and southeast regions. Deep tube wells which were earlier supplying good water have now been affected.
8. There are no water charges levied in the city. Moreover, 40 % of the piped treated river water is wasted through leaking public taps which leads to water shortages. Rainwater harvesting is mandated only for very large buildings and there is no attempt to popularize it to save water.

11.10 Suggestions and Management Plan for Sustainable Use of Groundwater

Different scholars and scientists have suggested remedies for the problem of overexploitation of groundwater in Kolkata. Among them Sahu and Sikdar (2011) gave the management plan shown in Table 11.9.

Table 11.9 Management plan for zones with different subsidence zones and groundwater potential

Groundwater potential	Very high to high	Medium	Poor to very poor
Excellent to good	GW abstraction should be minimized and treated surface water supply to be introduced along with roof-top rainwater harvesting	Some groundwater abstraction possible	Further groundwater abstraction possible
Medium	GW abstraction should be minimized and treated surface water supply to be introduced along with roof-top rainwater harvesting and artificial recharge	Some groundwater abstraction possible	Further groundwater abstraction possible
Poor to very poor	GW abstraction should be minimized and treated surface water supply to be introduced along with roof-top rainwater harvesting and artificial recharge	Status quo to be maintained	GW abstraction should be minimized and treated surface water supply to be introduced along with roof-top rainwater harvesting

Other suggestions recommended by the researcher are:

1. A development plan, if implemented properly in particular areas, will help in changing the present 'closed' groundwater flow system to the earlier '*open*' *flow* system by influx of fresh water from the north of the city.
2. Improvement in operation *and maintenance of the water supply system*, reduction in wastage of water through leakage and illegal tapping can solve the issue.
3. The century-old Kolkata drainage system is undergoing a change. As it has developed a number of cracks in different spots, it should be *modernized* quickly to improve the surface water flow.
4. *Reducing stress over the groundwater* resource is the need of the hour. In addition to increasing the dependency on surface water, recharge of the Hooghly River should be adopted.
5. There is a bright future for *rainwater harvesting* in this city. This will reduce the stress on ground and surface water and will help to control further decline of the water level.
6. *Roof-top harvesting and artificial recharge of groundwater* must be adopted in central and south Kolkata and in Salt Lake also as it is still not mandatory for all construction. It is only done at Bidhannagar Municipal building and Bidhannagar college building.
7. Regular *monitoring of the quality of groundwater* is to be done systematically. This will help to understand the change in groundwater quality and to identify the tube wells affected by arsenic or any other chemical and/or biogenic contamination.
8. Groundwater from open wells, wherever present, may be used for domestic purposes after *proper treatment*. Further groundwater exploitation is to be restricted.
9. *Reducing wastage of water* can be effective and recycling wastewater for urban gardening, urinal flushing, and so on, can be tertiary treatment of water for city dwellers to save water from wastage.

11.11 Conclusion

It can be concluded from the study that the piezometric level of Kolkata and Salt Lake is reducing rapidly due to the overuse of groundwater which leads to the threat of land subsidence. Already cracks and subsidence have been observed in some major points of the city. It is also clear from the study that the land subsidence rate is higher in the eastern region of Kolkata than other areas. Steady depletion of groundwater is not only turning the city subsidence-prone, it is also exposing Kolkata to earthquake risks. In addition, the drinking water is arsenic-contaminated in almost 77 out of 144 wards of south and southeast Kolkata due to high pollution from different sources, although the adjacent town of Salt Lake has not faced such a problem yet.

The stress on the urban water supply is likely to increase further to keep pace with rapid urbanization. If proper measures are not taken immediately, a further scenario could be more leaks. As the water level and quality both are going down, it is necessary to go deeper to find safe drinking water. Therefore rigorous groundwater monitoring on a regular basis is needed for tracking the water table depletion and deterioration of water quality.

Acknowledgements The author is thankful to Kolkata Municipal Corporation, Bidhannagar Municipality, and the Central Groundwater Board (Salt Lake) for their cooperation to complete this work.

References

Bhattacharya A (2011) Land subsidence in Kolkata due to groundwater depletion. EJGE 6:1415–1428

Bhattacharya A, Kumar D (2012) Land subsidence in East Kolkata. IOSR J Eng 2(3):408–413

Bureau of Applied Economics & Statistics (2004) Govt. of West Bengal, Kolkata District statistical hand book, Kolkata

Central Ground Water Board (2010) Ground water quality in shallow aquifers of India, Ministry of water resources, Govt of India, Faridabad, pp 10–12

Central Ground Water Board (2012) Ground Water Year Book, India 2011–12, Ministry of Water Resources, Govt of India, Faridabad

Chatterji GC, Biswas AB, Basu S, Niyogi BN (1964) Geology and ground water resources of the greater Calcutta metropolitan area, West Bengal. Bull Geol Surv India, Ser B21:150

Chatterjee RS et al (2007) Assessment of land subsidence phenomenon in Kolkata city India using satellite based D In SAR technique. Curr Sci 93(1):85–93

Dastidar AG, Ghosh P (1967) A study of subsoil conditions of Calcutta. J Civ Eng Div Inst Eng (India) 48(3):692–714

Groundwater Information Booklet (2007) KMC, Govt of West Bengal

Ground water Levels in different localities of Kolkata, April (2000), State Water Investigation Directorate (SWID), West Bengal, India

Kolkata City Population, Census of India (2011) Govt of India

Kolkata Metropolitan Development Authority (KMDA), West Bengal, India (2000): Lithological logs of boreholes (132 numbers.) over the entire KMDA area of Kolkata

Kolkata's groundwater a cocktail of toxic waste. Hindustan Times, 4 Sept 2012

Mishra AK (2011) Hydrogeological study in KMC area with special reference to declining of piezometric level through ground water development, pp 115–123

Mishra T (2011) Kolkata city, West Bengal in Ground water scenario in major cities of India. CGWB, Ministry of Water Resources, Govt of India

Rajmohan N, Prathapar SA (2013) Hydrogeology of the Eastern Ganges Basin: an overview, International Water Management Institute (IWMI) working paper 157, Colombo, 42 p, 13–18

Sahu P, Sikdar P (2011) Threat of land subsidence n Kolkata city and East Kolkata Wetlands, WestBengal, India. J Earth Sci 120(3):435–446

Sengupta PK (2009) Groundwater in Kolkata—an overview of spatial distribution pattern of chemical parameters. Centre for study of Earth Science, Jadavpur

Index

B.C. Das et al. (eds.), *Neo-Thinking on Ganges-Brahmaputra Basin Geomorphology*, Springer Geography, DOI 10.1007/978-3-319-26443-1